ABSOLUTE AND RELATIVE MOTION SATELLITE THEORIES FOR ZONAL AND TESSERAL GRAVITATIONAL HARMONICS

A Dissertation

by

BHARAT MAHAJAN

Submitted to the Office of Graduate and Professional Studies of
Texas A&M University
in partial fulfillment of the requirements for the degree of

DOCTOR OF PHILOSOPHY

Chair of Committee,	Srinivas R. Vadali
Co-Chair of Committee,	Kyle T. Alfriend
Committee Members,	John E. Hurtado
	Igor Zelenko
Head of Department,	Rodney Browersox

May 2018

Major Subject: Aerospace Engineering

ABSTRACT

In 1959, Dirk Brouwer pioneered the use of the Hamiltonian perturbation methods for constructing artificial satellite theories with effects due to nonspherical gravitational perturbations included. His solution specifically accounted for the effects of the first few zonal spherical harmonics. However, the development of a closed-form (in the eccentricity) satellite theory that accounts for any arbitrary spherical harmonic perturbation remains a challenge to this day. In the present work, the author has obtained novel solutions for the absolute and relative motion of artificial satellites (*absolute motion* in this work refers to the motion relative to the central gravitational body) for an arbitrary zonal or tesseral spherical harmonic by using Hamiltonian perturbation methods, without resorting to expansions in either the eccentricity or the small ratio of the satellite's mean motion and the angular velocity of the central body. First, generalized closed-form expressions for the secular, long-period, and short-period variations of the equinoctial orbital elements due to an arbitrary zonal harmonic are derived, along with the explicit expressions for the first six zonal harmonics. Next, similar closed-form expressions are obtained for the sectorial and tesseral (collectively referred to as tesserals henceforth) harmonics by using a new approach for the exact Delaunay normalization of the perturbed Keplerian Hamiltonian. This approach reduces the solution for the tesseral periodic perturbations to quadratures. It is shown that the existing approximate approaches for the normalization of the tesseral problem, such as the method of relegation, can be derived from the proposed exact solution. Moreover, the exact solution for the periodic variations due to the tesseral harmonics produces a unified artificial satellite theory for the sub-synchronous and super-synchronous orbit regimes without any singularities for the resonant orbits. The closed-form theories developed for the absolute motion are then used to develop analytic solutions in the form of state transition matrices for the satellite relative motion near a perturbed elliptic reference orbit. The expressions for differential equinoctial orbital elements for establishing a general circular orbit type satellite formation are also derived to avoid singularities for the equatorial and circular reference orbits. In order to negate the along-track drifts in satellite formations, an ana-

lytic expression for the differential semimajor axis is derived by taking into account the secular effects due to all the zonal harmonics. The potential applications of the proposed satellite theories range from fuel-efficient guidance and control algorithms, formation design, faster trade and parametric studies to catalog maintenance, conjunction analysis, and covariance propagation for space situational awareness. Two specific applications, one for solving a perturbed multiple revolution Lambert's problem and the other for rapid nonlinear propagation of orbit uncertainties using point clouds, are also given. The theories presented in this work are implemented for computer simulations in a software tool. The simulation results validated the accuracy of these theories and demonstrated their effectiveness for various space situational awareness applications.

DEDICATION

To my grandfather Tara C. Gupta, whose fascinating stories about WW-II pilots and their “close encounters” piqued a young kid’s curiosity about the heavens above, although he continued to believe his grandmother went to Heaven and became one of those stars.

ACKNOWLEDGMENTS

"The mind uses its faculty for creativity only when experience forces it to do so."

-Henri Poincaré

I feel lucky to have the opportunity to learn from the experience and wisdom of two great advisers, Drs. Rao Vadali and Terry Alfriend. In the past five years, I enjoyed the best of both worlds. I often feel amazed at Dr. Vadali's clear insight into any research problem that comes my way, and Dr. Alfriend's knack for providing instant answers using his many (almost mysterious) rules of thumb. I would like to thank both of them for their mentorship and supporting me at every step of this journey.

I would also like to thank Drs. John Hurtado and Igor Zelenko for serving on my committee, and reviewing my dissertation.

I am grateful to my colleagues and friends, Drs. Kirk Johnson, Hui Yan, Kohei Fujimoto, and Inkwan Park, for all the discussions and idea exchanges we had. A few more names deserve mention for being my mentors over the years: Drs. Hank Pernicka and S. N. Balakrishnan, Ankur Gupta from my undergraduate days, and Vaibhav Khanduja from my time in Hewlett-Packard. And my friends for all the *good* times, you know who you are.

A special thanks to my mother, Shashi, for learning LaTeX and offering me her help in typesetting the equations for this dissertation. I might start using this catchphrase from now on: My mom knows LaTeX, how about yours!

Looking back, it was surely an odyssey of ten years since my baccalaureate, including my time in the industry and all the scheming to go back to school. I wouldn't have come this far *if not for you*: Renu, Ravi, and Shashi (the three sisters, the three mothers, and literally, my three very first teachers).

CONTRIBUTORS AND FUNDING SOURCES

Contributors

This work was supported by a dissertation committee consisting of Professors Srinivas R. Vadali (advisor), Kyle T. Alfriend (co-advisor) and John E. Hurtado of the Department of Aerospace Engineering, and Professor Igor Zelenko of the Department of Mathematics. All the work conducted for the dissertation was completed by the author independently.

Funding Sources

The author's graduate study was supported by Air Force Research Lab (AFRL) contract No. FA9453-13-C-0202 along with teaching assistantships from the Department of Aerospace Engineering.

NOMENCLATURE

AST	Artificial Satellite Theories
GCO	General Circular Orbit
PCO	Projected Circular Orbit
GA-STM	Gim-Alfriend State Transition Matrix
RM-STM	Relative Motion State Transition Matrix (Φ)
MC	Monte Carlo
PRINCE	Perturbation Relegation In New Canonical Elements
PBJ	Poisson Bracket Jacobian
(A, B)	Poisson Bracket of A and B
LVLH	Local Vertical Local Horizontal
RSS	Root Sum Square
U	Gravitational potential energy
V	Gravitational potential
$\mathcal{H}$	Hamiltonian
$\mathcal{K}$	Transformed (or averaged) Hamiltonian
S	Generating function for canonical transformations
$\mathcal{W}$	Generating function for Lie-series based near-identity canonical transformations
t	Time
C	Direction cosine matrix
Σ	Geometric transformation matrix
ϕ_m	Differential mean state transition matrix

D_{SP}	Differential long-period to short-period transformation matrix
D_{LP}	Differential mean to long-period transformation matrix
D	Differential mean to osculating transformation matrix ($= D_{SP}D_{LP}$)
μ	Gravitational parameter
n	Spherical harmonic degree
m	Spherical harmonic order
ϕ	Latitude (planetocentric)
λ	Longitude (planetocentric)
θ	Greenwich sidereal time
R_e	Radius of the central body (Earth)
w_E	Rotational speed of the central body (Earth)
P_n	Legendre polynomial of degree n
J_n	Zonal harmonic coefficient of degree n
C_{nm}	Spherical harmonic coefficient of degree n and order m
S_{nm}	Spherical harmonic coefficient of degree n and order m
r	radial distance
$\tilde{n}$	Mean motion
p	Semilatus rectum
a	Semimajor axis
e	Eccentricity
i	Inclination
h (also Ω)	Right ascension of the ascending node
g (also ω)	Argument of periapsis
l	Mean anomaly

f	True anomaly
Λ	Mean longitude (l+g+h)
Ψ	True longitude (f+g+h)
ϑ	True argument of latitude (f+g)
η	$\sqrt{1-e^2}$
si	$\sin i$
ci	$\cos i$
p_1	$\tan\left(\frac{i}{2}\right)\cos(h)$
p_2	$\tan\left(\frac{i}{2}\right)\sin(h)$
q_1	$e\,\cos(g+h)$
q_2	$e\,\sin(g+h)$
$[x, y, z]$	Curviliear coordinate vector in the radial, along-track, and cross-track directions
$\mathbb{Z}$	Set of all integers

TABLE OF CONTENTS

Page

LIST OF FIGURES

FIGURE Page

LIST OF TABLES

TABLE Page

1. INTRODUCTION AND LITERATURE REVIEW

1.1 Introduction

The dawn of artificial satellite theories can be traced back to the planetary theories. Much before the advent of the space age, perturbation methods were the staples in celestial mechanics for predicting the motions of the planetary bodies and in some cases, proving their existence, namely Neptune. With the launch of Sputnik 1 in 1957, there was a new need to accurately predict the motion of an artificial satellite in an arbitrary orbit, being perturbed chiefly by the nonspherical gravitational effects of Earth and the atmospheric drag. Conventional planetary theories derived using the perturbation methods assumed small orbital eccentricity and the inclination. Moreover, the long-period dynamics of the nodal and apsidal lines in these theories were essentially treated along with the secular dynamics due to the very long time scales involved. For the artificial satellites, however, these time scales are much shorter and as a result, new strategies were needed to treat the long-period dynamics as purely periodic effects using trigonometric series rather than the power series used in the planetary theories.

An important motivation behind the development of the artificial satellite theories in previous decades was in geodesy for estimating the parameters of Earth's nonuniform gravitational field. By observing the variations in the orbital elements of the artificial satellites caused by the nonuniform gravitational field, the parameters characterizing the field can be computed. Although, fast off-the-shelf numerical orbit propagators are widely available today, artificial satellite theories built using perturbation methods have not lost their significance. They are indispensable for many tasks required for space situational awareness, such as catalog maintenance, orbit uncertainty predictions, conjunction analysis, etc., and more generally, for guidance and control, proximity operations, and perturbed relative motion propagation. The development of satellite theories that maintain long-term prediction accuracy under the effects of various perturbations such as nonspherical gravitational effects, atmospheric drag, solar radiation pressure, third-body perturbations, etc. remains an

active area of research to this day.

The focus of this work is specifically on developing an artificial satellite theory for zonal, sectorial, and tesseral gravitational harmonics and its utilization for formulating the analytic solutions for the perturbed satellite relative motion. The two primary goals behind this work are: develop a second-order theory in a generalized form valid for an arbitrary spherical harmonic and compute the solutions in closed-form, without resorting to expansions in either the eccentricity or ratio of the mean-motion to the angular velocity of the central body. The achievement of these two goals would ensure that the analytic solutions developed are compact in size, easily computable, and at the same time, are suitable for propagating the absolute and relative motion (*absolute motion* in this work refers to the motion relative to the central gravitational body) of satellites in arbitrary elliptic orbits. Dependence on special software such as Poisson Series Processors to manipulate large expressions for a specific spherical harmonic is avoided in this work and any off-the-shelf general purpose symbolic computation software should suffice, if need be.

1.2 Literature Review

This section gives a review of the past research on various aspects of artificial satellite theories, including the canonical perturbation methods, nonspherical gravitational perturbations in the form of the spherical harmonics, atmospheric drag effects, third-body perturbations, the critical inclination singularity, and the resonance effects due to the tesseral and sectorial harmonics. Additionally, the past research into the utilization of these satellite theories for developing analytic solutions for the perturbed relative motion of the artificial satellites is also discussed. An effort is made to discuss significant contributions made in the past dealing with each of these aspects. However, considering the vast amount of the existing literature on these subjects, the author makes no claim to include each and every deserving contribution in this survey. The literature review is divided into the time periods based on the author's opinion of the pioneering work that was presented in the beginning of that period. In some cases, closely related works are grouped together despite having significant time period between their publications.

1.2.1 Satellite Theories for Nonspherical Gravitational Perturbations

1.2.1.1 Before 1959

A few other methods existed before Brouwer's well-known work on the use of canonical perturbation methods for constructing the artificial satellite theories (AST) in 1959 (much after he computed Titan's mass using Hill's method as a student [2] in 1924). A general perturbation theory for the rectangular coordinates using the variation of elements in the canonical form was proposed by Brouwer in 1944 [3] (later modified by Musen in 1966 [4]). Using a method similar to the one used in the Hill*-Brown† lunar theory, Brouwer provided a solution, correct up to third order in the eccentricity, for the orbital motion of a particle of negligible mass influenced by a spheroidal central body [5]. His motivation for this work came from a celestial mechanics problem: the motion of Jupiter's fifth satellite, which is affected more by the non-sphericity of the planet than the third-body perturbations. His approach of retaining the spherical harmonic coefficients as algebraic quantities in the expressions (to be determined separately from the observational data) rather than explicitly specifying the mass distribution parameters in the theory, would become a standard approach later on. The physicist and astronomer Lyman Spitzer also published a paper on the perturbations of an artificial satellite's orbit, in which he included third-body perturbation effects as well [6]. In 1956, Blitzer et al. used a Lindstedt-Poincare type method to compute a first-order perturbation solution for the spherical coordinates of an artificial satellite affected by an oblate Earth, valid for near-circular orbits [7]. They anticipated that the analytical solutions for the variations of the pericenter and the line of nodes could be used to estimate the oblateness coefficient of Earth by making observations of the soon-to-be launched artificial satellites. Meanwhile, King-Hele considered the problem of predicting the orbits of an artificial satellite perturbed by the atmospheric drag, in his first paper [8] with many to come later on this subject.

Before Sputnik 1 was launched in 1957, a compilation of the various papers, edited by Van Allen, on the applications of the artificial satellites was published, in Chapter 1 of which Davis

*http://www.phys-astro.sonoma.edu/BruceMedalists/Hill/index.html
†http://www.phys-astro.sonoma.edu/BruceMedalists/Brown/index.html

et al. considered the effects of the major perturbations, the oblateness and the atmospheric drag, on the satellite orbits [9]. In 1958, Sterne applied the conventional Hamilton-Jacobi theory in an astronomically unconventional way (his exact words) to compute an exact analytical solution of a Hamiltonian that included a major portion of the oblateness effects [10]. His pioneering work was based on an important observation that the Hamilton-Jacobi equation in the spherical coordinates for the Hamiltonian

$$\mathcal{H} = \frac{1}{2}\left(p_r^2 + \frac{p_\lambda^2}{r^2\cos^2\phi} + \frac{p_\phi^2}{r^2}\right) + V_1(r) + \frac{1}{r^2}V_2(\phi) \tag{1.1}$$

is separable and can be solved exactly. In the above equation, r, λ, and ϕ are the radial distance, the planetocentric right ascension (or longitude), and the planetocentric declination with respect to the planet's equator (or latitude), respectively; p_r, p_λ, and p_ϕ are the corresponding conjugate momenta; and V_1 and V_2 are arbitrary functions of r and ϕ, respectively. The exact solution S to the Hamilton-Jacobi equation corresponding to the above Hamiltonian is:

$$S = \int \frac{N}{r}\,\mathrm{d}r + \int M\,\mathrm{d}\phi + \alpha_3\,\lambda, \tag{1.2}$$

where

$$N^2 = 2r^2\alpha_1 - 2r^2V_1(r) - \alpha_2^2,$$

$$M^2 = \alpha_2^2 - \alpha_3^2\sec^2\phi - 2V_2(\phi),$$

and α_1, α_2, and α_3 are the canonical constants. Sterne showed that the actual Hamiltonian with the oblateness effects can be expressed in the form given in Eq. 1.1 with the residual considered as the perturbation Hamiltonian. In case of the equatorial orbits, this residual vanishes. The exact solution of the zeroth-order Hamiltonian was expressed in terms of the elliptic integrals. An important significance of this work was that the zeroth-order exact solution described an *intermediary* orbit that included the first-order secular part of the oblateness effects and geometrically, can be thought

of as an ellipse precessing nonuniformly about the two fixed axes. An intermediary must include the first-order secular effects due to a perturbation, and desirably some second-order secular effects too. The three fundamental frequencies associated with the intermediary are the anomalistic, nodical or draconic, and sidereal. The anomalistic frequency corresponds to one full vibration of r, the nodical frequency is associated with the time necessary for a particular angle, analogous to the argument of the declination in an ordinary elliptic orbit referred to the equator, to increase by 2π, and the sidereal frequency is associated with the time necessary for λ to increase by 2π. In case of the Keplerian ellipse, all three frequencies are equal. Garfinkel improved upon Sterne's solution by choosing a slightly different form of the zeroth-order Hamiltonian, which resulted in all the secular perturbations of the pericenter and the node line in the intermediary orbit, and simultaneously a reduction in the number of the elliptic integrals required in the exact solution [11]. Brouwer, employing the Hill-Brown method, provided an improvement of his earlier solution valid for near-circular orbits with arbitrary inclination [12]. Remarkably, he computed a second-order solution of the variational orbit including the contributions of the first two even zonal spherical harmonics. The analytical solution had small divisors near the critical inclination, which Brouwer anticipated that they could be removed from his theory using Delaunay's normalization method (which turned out to be not true later on). He also pointed out that a modification of Delaunay's method by von Zeipel* could provide significant advantages. It is reported that von Zeipel himself gave credit for this method to Poincaré [13], nevertheless von Zeipel contributed important modifications of the original Poincaré's method, and they are described in Chapter 3 of Reference [14]. A first-order theory for the secular effects due to the oblateness of Earth by an approximate integration of the Lagrange planetary equations was also presented by Izsak [15]. A fourth-order analytical solution for the oblateness effects directly in the spherical coordinates of an artificial satellite was derived by King-Hele by assuming the eccentricity as a first-order and the oblateness parameter as a second-order quantity [16].

*http://www.astro.uu.se/history/zeipel.html

1.2.1.2 1959-1965: The von Zeipel Method Era

The year 1959 is arguably the most prolific year for the development of artificial satellite theories. Four different approaches for constructing the satellite theories applicable in Earth's gravitational field were published in the literature, with three of them appearing in the same issue (no. 64) of The Astronomical Journal. Chronologically, the papers were received in the order: Vinti, Garfinkel, Brouwer, and Kozai. A clear distinction emerged between the two major approaches to account for the non-sphericity of the central body in the satellite theories during this time: the Brouwer-Kozai type methods with a two-body ellipse as the unperturbed orbit, and the Vinti-Garfinkel type methods with an intermediary orbit as the unperturbed solution that included either complete or a portion of the oblateness effects in exact form.

Vinti's method facilitated the most accurate satellite theory in principle as it provided an exact solution for the second zonal harmonic perturbation, also called the main problem of the AST [17, 18]. It also accounts for a portion of the higher zonal harmonics in the exact solution. Unlike Sterne's use of the spherical coordinates, Vinti showed that the Hamilton-Jacobi equation is completely separable in the oblate spheroidal coordinates for a potential function of an axially symmetric body, which is a solution of Laplace's equation. This solution, when expanded in spherical harmonics, can represent the gravitational potential field due to any oblate central body by matching the three arbitrary constants present in the solution to the amplitudes of the zeroth, first, and second zonal harmonic. The amplitudes of the higher zonal harmonics are then all fixed. It is noted that for this special case of the gravitational potential, the critical inclination singularity disappears. Izsak expressed the exact solution of Vinti in an explicit form using the Fourier series in a certain parameter (related to the oblateness parameter) up to order two [19, 20]. Later, Vinti formulated a simpler explicit solution using the complete elliptic integrals of the first and second kind only, which included the secular terms exactly and the periodic terms up to second order. While the orbital elements introduced by Izsak in his explicit solution of Vinti's theory could only be found numerically from the initial conditions, Vinti proposed a new set of orbital elements that may be computed from the initial conditions analytically [21, 22]. The explicit solution of Vinti's

problem showed that the orbits perturbed by the oblateness effect have two apoapsides at the two nodes and the two periapsides at the highest and lowest points of the orbit above and below the equatorial plane [23]. It can be shown that the problem of an artificial satellite in the gravitational field of an oblate central body is equivalent to the integrable problem of the two fixed centers, known also as Euler's problem, situated at purely imaginary distances from one another [24]. This analogy between the two problems was also independently discovered around the same time by the researchers in the former Soviet Union [25]. In one instance, Aksenov et al. showed that the potential corresponding to Euler's problem of the two fixed centers can be generalized to resemble Vinti's potential and proposed more convenient transformations for formulating the solution of Vinti's problem [26].

Garfinkel extended his earlier work, in which he solved the Hamilton-Jacobi equation in spherical coordinates for the secular portion of the second zonal harmonic. He applied von Zeipel's canonical perturbation method to account for the residual part of the second zonal harmonic along with the fourth zonal harmonic [27]. The benefit of the intermediary, compared to Brouwer's unperturbed elliptic orbit, shows up in the relative smaller magnitudes of the secular variations at second order. This results in superior accuracy in the calculated positions. Garfinkel noted that the singularities in his theory near the critical inclination disappeared for either circular orbits or if the condition $J_4 + J_2^2 = 0$ is satisfied, which is a characteristic of Vinti's potential.

The credit for the first use of von Zeipel's perturbation method (henceforth referred to as the von Zeipel method) in AST goes to Brouwer, as acknowledged by Garfinkel. The von Zeipel method is a modification of Delaunay's method and removes all the periodic terms from a Hamiltonian using a single canonical transformation instead of the multiple transformations (almost 500) as originally employed by Delaunay in his lunar theory [14]. Using the von Zeipel method, Brouwer showed that the artificial satellite theories can be constructed in closed-form without first expanding the perturbing Hamiltonian in powers of the eccentricity (although it may have been suggested to Brouwer by Garfinkel first). Prior to his work, the perturbation theories for predicting the motion of celestial bodies relied on the expansions of the perturbations in powers of the eccentricity for eliminating

the short-period terms from the Hamiltonian. Exact or closed-form in the eccentricity theories are better suited for propagation of artificial satellites or space debris with moderate to high values of the orbital eccentricity. Additionally, avoiding the eccentricity expansions results in a more compact theory. Brouwer's theory included the secular variations up to second order, short-periodic and long-periodic variations of the Delaunay elements up to first order for the zonal harmonics up to degree five [28]. In Brouwer's theory, the unperturbed orbit is a Keplerian ellipse as opposed to the intermediaries of Sterne, Garfinkel, and Vinti. The singularities near the critical inclination are also present in Brouwer's theory. In the same year, Kozai developed a theory by separating the secular, short-periodic and long-periodic terms from the disturbing potential and then computed the corresponding variations of the orbital elements using Lagrange's planetary equations. With this approach, Kozai computed secular variations up to second order and the periodic variations up to first order. An interesting account of Brouwer and Kozai with regards to their 1959 papers on artificial satellite theories is given by Kozai himself*. A comparison between the theories of Brouwer and Vinti for accuracy and speed is given in Reference [29], in which the conclusion was drawn that Vinti's theory is faster and more accurate than Brouwer's theory. However, due to its simplicity (in part because of the lack of any elliptic integrals in the solutions), Brouwer's theory is comparatively easier to implement as well as to extend for incorporating various perturbations.

Following the seminal works of Brouwer and others in 1959, numerous satellite theories were developed in a quest to achieve improved accuracy and wider applicability, with mostly using either the von Zeipel-Brouwer method or the Sterne-Garfinkel method with non-Keplerian intermediary orbits (relatively fewer publications focused on Vinti's theory in later years). In a different approach, Kaula formulated an elegant theory for the periodic variations of the classical orbital elements due to an arbitrary spherical harmonic, including the tesseral harmonics, by an approximate analytic integration of Lagrange's planetary equations [30]. While a few preceded Kaula for solving this problem, Kaula's solution was simpler and included second-order effects additionally. His theory was computed by first expressing the complete nonspherical gravitational potential in terms

*https://www.aip.org/history-programs/niels-bohr-library/oral-histories/24816

of the classical orbital elements of the satellite and the Greenwich sidereal time using the series expansions in powers of the eccentricity. Kaula's theory provides the generalized expressions for the orbital element variations due to an arbitrary spherical harmonic. The motivation behind the development of Kaula's theory was to numerically estimate the spherical harmonic coefficients by using optical observations of the artificial satellites. Kozai extended Brouwer's theory to order two for the periodic effects and to order three for the secular effects due to J_2-J_8 zonal harmonics, using the von Zeipel method [31]. Breakwell and Vagners devised a technique for the first-order Brouwer-type theories to keep the in-track position error levels at the second order with the aid of the energy integral [32]. Lyddane reformulated Brouwer's theory in terms of the Poincaré elements to remove singularities for the equatorial and circular orbits [33].

On the suggestion of Brouwer, Hori applied the von Zeipel method to compute a first-order analytical theory for a hyperbolic artificial satellite that included the oblateness effects, which was also valid for any inclination [34]. A noteworthy difference from the elliptic case lies in the fact that there is no such distinction between secular, long-period and short-period terms in the oblateness potential, which affects the choice of the integration constants that are added to the first-order generating function. The corresponding satellite theory for the hyperbolic orbits in the gravitational field due to Vinti's potential is given by Lang [35]. For elliptic orbits, Musen used Hansen's perturbation method to formulate a numerical theory for the oblateness effects on the rotation of the orbit plane (small effects) and the motion of a satellite in that rotating orbit plane (larger effects), separately [36]. Izsak noted that the von Zeipel method can be used to compute the short-periodic variations of the canonical polar-nodal variables directly, without first computing the variations of the elements [37]. Garfinkel and McAllister extended their previous theory of the main problem of the artificial satellite to include the secular and long-periodic effects of all the higher zonal harmonics using the von Zeipel method [38, 39]. They expressed the generalized expressions for the secular and long-periodic variations of the Delaunay elements in a compact form using the associated Legendre polynomials in the eccentricity and the inclination, which also provided the benefit of the recursive formulation for some of these expressions. The singularities present in the

expressions for the circular and equatorial orbits were removed by computing the similar formulae for the variations of the coordinates. Further, Garfinkel computed the long-periodic variations due to the tesseral and sectorial spherical harmonics (henceforth collectively referred to as the tesseral harmonics) for the sub-synchronous orbits using the von Zeipel method [40, 41]. He used the eccentricity expansions to express the tesseral potential function (compare it to Kaula's potential in Reference [42], Chapter 3) in terms of the Delaunay elements and then separated the long-periodic part of the potential that does not depend on the mean anomaly [43]. Interestingly, Garfinkel solved the partial differential equation for the long-periodic generating function (including the m-daily contributions), resulting from the application of the von Zeipel method, using the method of characteristics.

After the initial work on intermediaries by Sterne, Vinti, and Garfinkel, a much simpler intermediary compared to the earlier (see [10, 11]), which enabled the construction of efficient second-order theories, was proposed by Aksnes [44]. In another novel approach, Cid and Lahulla proposed the construction of intermediaries using a near-identity contact transformation (called as elimination of the argument of latitude) instead of splitting the original Hamiltonian into integrable and non-integrable parts [45, 46]. They used the von Zeipel method to construct the generator of the transformation. The intermediaries computed with the help of a near-identity contact transformation applied to the main problem are referred to as natural intermediaries by Deprit. He proved that the intermediary of Cid and Lahulla is, in essence, the result of the averaging of that part of the perturbation that makes no direct contribution to the secular and long-period effects; in other words its average with respect to the mean anomaly is zero [47]. Since the intermediary of Cid and Lahulla is obtained by simply removing the terms containing the argument of latitude from the main problem, it is considered as a type of intermediaries known as radial intermediaries as opposed to the zonal intermediaries of Sterne, Garfinkel, and Aksnes. Given the gravitational potential for the main problem:

$$V = -\frac{\mu}{r} + J_2 \frac{\mu R_e^2}{r^3} \left(-\frac{1}{2} + \frac{3}{2} \sin^2 \phi \right), \tag{1.3}$$

Table 1.1: The zonal intermediaries.

Intermediary	c_1	c_2	c_3	c_4	Elliptic Integrals	Secular Effects
Sterne	$1/p$	$\frac{1}{2}\sin^2 i$	0	$-\frac{1}{6}P_2(\cos i)$	4	$\mathcal{O}(J_2)$
Garfinkel	$1/p$	$\cos^2 i$	$\frac{(1-e^2)^{1/2}P_2(\cos i)}{2p^2}$	0	2	$\mathcal{O}(J_2^2)$
Aksnes	$1/p$	$1/3$	0	0	3	$\mathcal{O}(J_2)$

the various zonal intermediaries can be defined with the help of the following representation of V, in which the integrable part V_0 enables the separation of the Hamilton-Jacobi equation in spherical coordinates [48]:

$$V = V_0 + V_1, \tag{1.4}$$

where

$$V_0 = -\frac{\mu}{r} + 3J_2\mu R_e^2 \left(\frac{c_1}{2r^2} \left(\sin^2\phi - c_2 \right) + \frac{c_3}{r} + \frac{c_4}{r^3} \right),$$

$$V_1 = 3J_2\mu R_e^2 \left(-\frac{c_1}{2r^2} \left(\sin^2\phi - c_2 \right) - \frac{c_3}{r} - \frac{1}{r^3} \left(c_4 - \frac{1}{6} + \frac{1}{2}\sin^2\phi \right) \right).$$

The values of the four parameters along with the number of elliptic integrals involved and order of the secular effects incorporated are given for the zonal intermediaries of Sterne, Garfinkel, and Aksnes (see References [48, 49]) in Table 1.1. The four parameters in the intermediaries of Sterne and Garfinkel are considered constants, whereas in case of Aksnes' intermediary, the parameter c_1 is considered a dynamic variable. Aksnes chose his intermediary by nullifying the secular part of V_1. This crucial distinction simplifies the construction of higher-order theories using the intermediary of Aksnes. Vinti's intermediary provides an exact solution for the complete potential $V_0 + V_1$. One disadvantage of the zonal intermediaries compared to the natural ones is that their solutions involve the elliptic integrals.

Breakwell and Pringle [50], and Deprit [51] independently applied the von Zeipel method

to normalize a Hamiltonian of a particle near the triangular points of the restricted three-body problem. They recognized the limitations of the von Zeipel method due to the dependence of the short-period averaged Hamiltonian on the mixed variables. Schechter, on the suggestion of Breakwell, solved this problem by carrying out a near-identity transformation (precursor to the Lie-series based transformations) to express the short-period averaged Hamiltonian entirely in terms of the new canonical variables [52]. A good review of the progress made in various Celestial Mechanics problems including the artificial satellite theories up to 1963 is provided by Brouwer [53, 54]. Some important works on the von Zeipel method that extended and compared it with other perturbation methods are given in References [4, 55, 56, 57].

1.2.1.3 1966-1980: Lie-Series Methods Era

The generating function for the periodic perturbations computed using the von Zeipel method is a function of the mixed (old and new) variables, resulting in the transformation equations in an implicit form. In 1966, Hori formulated a new theory of canonical transformations using Lie-series expansion, which avoided the inconvenience of the presence of the mixed variables in the generating function [58, 59]. Additionally, the resulting transformation equations are canonically invariant and provided a general procedure to compute expansion of an arbitrary function of the old variables in terms of the new variables. This distinction between the explicit and implicit transformations is due to the fact that the canonical transformation employed in Hori's method is truly a near-identity transformation compared to the more general contact transformation of the von Zeipel method [14]. An extension of Hori's method for time-dependent Hamiltonian systems along with a recursive formulation to generate the perturbation equations, is provided by Mersman [60]. An equivalent theory of canonical perturbations to Hori's method was presented by Deprit using Lie-transforms, in which the generating function itself is a function of the small parameter [61]. Like Hori's method, Deprit's method also provides the explicit form of the transformation equations. Kamel provided a general recursive and simpler formulation of Deprit's method [62, 63] (for different perspectives on Deprit's method, see [64, 65]). In Deprit's algorithm, an assumption is made with regards to the generating function being dependent on the same small parameter that

specifies the strength of the perturbation. As discussed by Mersman [60], this assumption is not made in Hori's algorithm, which results in a simpler theory especially for constructing the inverse transformation. An insightful discussion on the construction of the near-identity transformations using Lie-series methods and Hori's technique of performing the Delaunay normalizations in any set of the canonical elements, not necessarily action-angle variables, using the so called Hori's kernel is given in Reference [14]. Campbell and Jefferys provided the explicit relations between the Hori and Deprit generating function up to sixth order [66]. The equivalence between the von Zeipel and Deprit's Lie-transform based method using an order-independent method was proved by Shniad [67]. Hori compared his theory with the von Zeipel method and showed that up to second order, both theories produce the same canonical transformations [68, 69]. And the equivalence between all the three methods as well as the recurrence relations for constructing the generating functions of each were established by Mersman [70, 71] and another unified treatment is given by Kirchgraber [72]. Using Kamel's technique [73], Hori provided an extension of his original method to the non-canonical systems [74] and a more general method for treating non-canonical systems using any canonical perturbation method was presented by Choi and Tapley [75]. A more recent extension of Hori's method to include dissipative dynamical systems is given by Baenas et al. [76]. Stern provided a technique for constructing explicit canonical transformations in case of the von Zeipel method, thus removing its major limitation [77]. Another extension of the von Zeipel method to slowly (or adiabatically) perturbed systems was also proposed by Stern [78]. A more recent work on removing all the major limitations of the von Zeipel method compared to Lie-series based methods is presented by Deprit and Deprit [13].

Eckstein et al. presented a perturbation technique to compute the higher-order terms by using an integral of motion for the time history of the satellite motion as a function of an angular variable, after the geometry of the orbit has been obtained [79]. Aksnes first used the von Zeipel method to extend his earlier work on the exact solution of an intermediary orbit, and computed second-order secular variations and first-order periodic variations due to the first five zonal harmonics using the expansions in the eccentricity [80]. Aksnes claimed that his solution remains valid at

the critical inclination, but this is doubtful as his long-period variations does have the angular rate of the moving apsidal line in the denominator. Later using Hori's method and Hill's variables (also known as the polar-nodal or Whittaker variables), Aksnes computed a complete second-order theory for the first four zonal harmonics starting from his intermediary orbit, without relying on the eccentricity expansions [81]. Aksnes also derived Brouwer's theory completely in terms of Hill's variables to show that expressions are more compact and involve simpler computations in case of Hill's variables [82]. Aksnes' intermediary was further refined by Deprit and Richardson [83]. It is known that Hill's variables are not completely defined for the equatorial orbits. Cefola proposed the use of the nonsingular equinoctial elements to construct the satellite theories [84]. It is noted that the mixed-secular terms can arise in perturbed intermediaries if the Delaunay elements are used to define the non-degenerate intermediary, which can be avoided by the use of the *natural* elements similar to the ones used in Vinti's theory [85]. Using the symbolic computations on a computer and the Lie-transform based perturbation method, Deprit and Rom computed a Brouwer-type theory for the main problem with secular, short-periodic, and long-periodic variations included up to third order [86]. They incorrectly concluded that the second-order periodic variations cannot be computed without using the expansions in powers of the eccentricity (see Kozai solution [87]), which was later corrected by Aksnes in his note [88]. Vinti's theory was extended to the universal variables by Getchell [89] and a reformulation of Vinti's theory in extended phase space is given by Alfriend et al. [90].

An application of Brouwer theory to determine the time epochs corresponding to a satellite's arrival at its periapsis, apoapsis, the two nodes, and the point of maximum and minimum geodetic sublatitude points using a recursive algorithm is given by Gordon [91]. Kamel and Tibbitts provided the algorithms for computing the orbit node locations given the various requirements on the inclination using a satellite theory with oblateness and luni-solar effects included [92]. A hybrid method to combine the efficient analytical satellite theories with the more accurate but less efficient numerical integration methods is proposed by Alfriend and Velez [93]. An artificial satellite theory with the zonal and tesseral harmonics and luni-solar perturbations along with resonance

effects is derived in nonsingular variables using the eccentricity expansions by Giacaglia [94]. A method similar to Kaula was adopted by Cefola [95] and Giacaglia [94] by expressing the tesseral potential in terms of the equinoctial elements. McClain provided averaged equations of motion for tesseral harmonics in case of the non-resonant as well as resonant orbits by using Cefola's tesseral potential [96]. Cefola and McClain computed the short-period generating function in a recursive form using the generalized method of averaging [97]. Their work was further extended by Proulx et al. for computing a recursive semi-analytic theory including the first-order tesseral short-period variations of the equinoctial elements [98]. All of the work done by Cefola and his colleagues in 1970s and 1980s culminated into the Draper Semianalytic Satellite Theory (DSST), which includes the analytic models of the zonal and tesseral harmonic perturbations including the resonant tesseral effects, third-body luni-solar perturbations, atmospheric drag effects using empirical density models, solar radiation pressure, and solid Earth tides [99, 100]. Kinoshita used Hori's method to expand the original perturbation Hamiltonian for J_2-J_4 harmonics in eccentricity up to $O(e^6)$, and computed the short and long-period variations up to order three and secular effects up to order four [101]. Hoots reformulated the Brouwer-Lyddane theory in terms a new set of nonsingular variables, which requires fewer computations to compute position and velocity and also avoids one solution of Kepler's equation [102].

In 1970, a new canonical theory of dynamical systems in the extended phase space using KS (Kustaanheimo-Stiefel) regularizing transformation was proposed by Scheifele. A time-dependent Hamiltonian system can be converted into a homogeneous system by augmenting the Hamiltonian with the time and energy states. Scheifele proposed generalized canonical transformations in the extended phase space to include the transformation of the independent variable as well as the transformations to augment the number of states. He applied this formalism to the perturbed Kepler problem by doing a transformation of the independent variable time to introduce a new set of eight canonical elements [103, 104]. When either the true anomaly or the eccentric anomaly is chosen as the independent variable, a set of elements with geometrical interpretation similar to the conventional Delaunay elements can be derived and are called as Delaunay-similar elements.

Using the conventional definition of the Poincare canonical elements, a set of completely nonsingular Poincare-similar elements can also be derived (e.g., see [105]). Further performing the KS-transformation of the canonical system produces a set of ten canonical elements for the completely regularized perturbed Kepler problem. Scheifele and Graf constructed an analytical satellite theory for the main problem and 24-hour satellite problem using the eight Delaunay-similar elements including the true anomaly [106]. Their first-order analytic theory had accuracy comparable to the conventional second-order satellite theories and additionally, the expressions are significantly more compact. Deprit later showed that the canonical transformation of Scheifele to make the true anomaly a coordinate, is an extension of Hill's transformation from six-dimensional phase space of Hill's variables to an eight-dimensional manifold with time and energy providing the two extra dimensions [107]. A discussion on the regularization of the artificial satellite theories and their benefits is given by Saari [108].

1.2.1.4 1981-present: Special Canonical Transformations Era

The Hamiltonian corresponding to the main problem of the AST can be normalized up to order two without using the eccentricity expansions as shown by Kozai and others [31, 88]. Higher-order normalizations in closed-form in the eccentricity are made feasible by a special canonical transformation, known as the elimination of the parallax, introduced by Deprit in 1981. The specialty of this canonical transformation that makes it distinct, is that it does not normalize the Hamiltonian directly, rather transforms the Hamiltonian into a simpler form. After that simplification, the Hamiltonian can be normalized in closed-form in the eccentricity using the conventional transformations with additional benefits of producing a more compact theory. Later, more canonical transformations were also discovered to provide further simplifications of the perturbed Hamiltonian for performing the Delaunay normalizations in closed-form.

Deprit introduced the elimination of the parallax transformation using the polar-nodal variables to remove the short-period variations that cause torsion in the apsidal frame through the argument of latitude angle [49, 109]. The transformed Hamiltonian system contains short-period effects only due to the irregularities of the equation of the center, which are separated by the subsequent

Delaunay normalizations. The polar-nodal variables are the canonical elements defined as the set (r, $f+g$, h, $\dot{r}$, G, H), with the last three elements being the conjugate of the first three. In the polar-nodal variables, the Keplerian Hamiltonian $\mathcal{H}_0$ (which can also be obtained from the Hamiltonian in Cartesian variables using Whittaker transformation, see [110]) is given as follows:

$$\mathcal{H}_0 = \frac{1}{2}\left(\dot{r}^2 + \frac{G^2}{r^2}\right) - \frac{\mu}{r}. \tag{1.5}$$

Deprit defined the following three state functions:

$$p = \frac{G^2}{\mu}, \tag{1.6}$$

$$C = G\left(\frac{1}{r} - \frac{1}{p}\right)\cos\vartheta + \dot{r}\sin\vartheta \tag{1.7}$$

$$= \frac{G}{p}e\cos g, \tag{1.8}$$

$$S = G\left(\frac{1}{r} - \frac{1}{p}\right)\sin\vartheta - \dot{r}\cos\vartheta \tag{1.9}$$

$$= \frac{G}{p}e\sin g, \tag{1.10}$$

where ϑ is the true argument of the latitude. The Lie-derivatives of the above functions in a Keplerian flow are identically zero, which can be easily verified when the Poisson brackets are evaluated in terms of the Delaunay elements. Therefore, the Lie-derivative of any function $\mathcal{W}(p, C, S, \vartheta)$ dependent on the three state variables in addition to ϑ is obtained using the chain rule as shown below:

$$\mathcal{L}_{\mathcal{H}_0}\mathcal{W}(p, C, S, \vartheta) = (\mathcal{H}_0, \mathcal{W}) \tag{1.11}$$

$$= (\mathcal{H}_0, p)\frac{\partial\mathcal{W}}{\partial p} + (\mathcal{H}_0, C)\frac{\partial\mathcal{W}}{\partial C} + (\mathcal{H}_0, S)\frac{\partial\mathcal{W}}{\partial S} + (\mathcal{H}_0, u)\frac{\partial\mathcal{W}}{\partial u} \tag{1.12}$$

$$= \frac{G}{r^2}\frac{\partial\mathcal{W}}{\partial\vartheta}, \tag{1.13}$$

where $(\_,\_)$ represents a Poisson bracket. The significance of the above result is that the partial derivatives of the three state functions can be ignored when computing the Lie derivatives. In order to carry out the elimination of the parallax transformation, the parallactic term $(a/r)^n$ in the perturbation Hamiltonian $\mathcal{H}_1$ is reduced to $(a/r)^2$ and any appearance of the $\dot{r}$ is removed by expressing the Hamiltonian in terms of the state functions using the following relations:

$$\frac{1}{r} = \frac{1}{p}\left(1 + \frac{p\,C}{G}\cos\vartheta + \frac{p\,S}{G}\sin\vartheta\right), \tag{1.14}$$

$$\dot{r} = C\sin\vartheta - S\cos\vartheta. \tag{1.15}$$

The first-order homological equation that must be solved for the new Hamiltonian $\mathcal{K}$ and the generating function $\mathcal{W}$ for this near-identity transformation (see Section 2.1.2), is

$$\mathcal{K}_1 = \mathcal{L}_{\mathcal{H}_0}\mathcal{W}_1 + \mathcal{H}_1, \tag{1.16}$$

$$= \frac{G}{r^2}\frac{\partial\mathcal{W}_1}{\partial\vartheta} + \frac{G^2}{r^2}\bar{\mathcal{H}}_1, \tag{1.17}$$

where

$$\bar{\mathcal{H}}_1 \equiv \frac{r^2}{G^2}\mathcal{H}_1.$$

The transformed first-order Hamiltonian term $\mathcal{K}_1$ is chosen to include all the terms in $\bar{\mathcal{H}}_1$ that are not an explicit function of ϑ, although they can have an implicit dependence on ϑ through C and S state functions. The first-order generating function term $\mathcal{W}_1$ is then computed using a simple quadrature considering C and S independent of ϑ. A simpler treatment of the elimination of the parallax transformation in terms of the Delaunay elements is given by Lara et at. [111, 112]. In Delaunay elements, the first-order homological equation is given as

$$\mathcal{K}_1 = \frac{\partial \mathcal{H}_0}{\partial L}\frac{\partial \mathcal{W}_1}{\partial l} + \mathcal{H}_1. \tag{1.18}$$

The parallactic terms r^{-n} in $\mathcal{H}_1$ are reduced to r^{-2} using the following identity:

$$r^{-n} = r^{-2}\left(\frac{1 + e\cos f}{a\eta}\right)^{n-2}, \quad n > 2.$$

Then $\mathcal{K}_1$ is chosen by selecting all the terms of $\mathcal{H}_1$ that do not depend explicitly on the true anomaly f. The remaining periodic terms are integrated by quadrature to obtain $\mathcal{W}_1$. It is noted that the new Hamiltonian $\mathcal{K}_1$ also contains short-periodic terms in addition to the secular and long-periodic terms due to the presence of r. The same procedure of reducing the parallactic terms and separating the terms that do not depend explicitly on ϑ or f is repeated to obtain the higher-order terms for $\mathcal{K}$ and $\mathcal{W}$.

Using the elimination of the parallax type special canonical transformations, Deprit introduced a new way of finding intermediaries, which he referred to as natural intermediaries [49]. A natural intermediary corresponds to an integrable Hamiltonian that includes a part of the first-order perturbation and is obtained from the original non-integrable Hamiltonian by applying a near-identity canonical transformation. The new Hamiltonian only needs to be integrable and not necessarily separable in order to obtain a natural intermediary. It is noted that a Hamiltonian that can be transformed into quasi-Keplerian form, is separable. Deprit showed that the common intermediaries of Sterne, Garfinkel, Aksnes, and Cid-Lahulla can be obtained from applying different near-identity transformations to the Hamiltonian for the main problem [49, 83]. Additionally, he proposed a new radial intermediary that results from applying the elimination of the parallax transformation to the main problem [49, 110]. The solution of this radial intermediary, similar to the one by Cid-Lahulla, do not involve elliptic integrals. Using the elimination of the parallax transformation, Coffey and Deprit computed a very compact third-order solution in closed-form in the eccentricity for the main problem of the artificial satellite theory [113].

Another canonical transformation, the elimination of the perigee, to simplify the Hamiltonian and produce more compact satellite theories is proposed by Alfriend and Coffey using the polar-nodal variables [114]. The elimination of the perigee transformation is carried out after applying the elimination of the parallax transformation. All the long-period terms that are functions of the perigee are removed from the Hamiltonian to choose the new transformed Hamiltonian. The remaining terms are integrated to compute the generating function for the elimination of the perigee transformation. Its reformulation in terms of the Delaunay elements is given by Lara et at. [112]. Cid et al. utilized Deprit's perturbation method along with the elimination of the perigee to obtain an improved version of the original intermediary of Cid and Lahulla that incorporated all of the zonal harmonics [115]. They also linearized their radial intermediary with the help of a Sundman-type regularization.

Breiter considered all the zonal harmonics as first-order perturbations and computed an analytic solution up to order two for an arbitrary high degree of the potential using the eccentricity expansions [116]. A distinct feature of Breiter's solution was the inclusion of the first-order secular effects of all the zonal harmonics in the zeroth-order Hamiltonian, which makes the zeroth-order solution an intermediary orbit. Additionally, Breiter carried out a single transformation to eliminate the short-period and long-period terms from the original Hamiltonian together, and used a Runge-Kutta based numerical scheme to compute the resulting periodic variations. Saedeleer computed the generalized analytic formulae for the first-order averaged Hamiltonian and the short-period generating function for an arbitrary zonal harmonic [117]. Recently, Lara presented a reformulation of the Brouwer theory in terms of Hill's variables [118] and a comparison between Deprit's intermediary orbit and the Brouwer theory [119].

The majority of the literature since 1959 on artificial satellite theories is focused on including the effects of the zonal harmonic perturbations. In relatively few cases, the analytic expressions for the periodic variations of the orbital elements due to the tesseral harmonics are computed using the eccentricity expansions as discussed earlier [42, 40, 41, 99, 94, 120, 96, 97, 98]. A closed-form solution for the short-period effects due to the tesseral harmonics is yet to be found. Coffey

and Alfriend used two separate Lie-type transformations to construct a satellite theory for the tesseral harmonics [121]. The first transformation was similar to the elimination of the parallax transformation, which was performed in closed form in the eccentricity, and it produced a simpler intermediate Hamiltonian. The second transformation completed the Delaunay normalization by expanding the intermediate Hamiltonian in powers of the eccentricity. It was acknowledged by Coffey and Alfriend that no closed-form normalization of this problem is known to exist. The first transformation of Coffey and Alfriend can be seen as a precursor to the method of relegation that can be used to perform the Delaunay normalization of the tesseral perturbation Hamiltonian without using the typical eccentricity expansions. Wnuk utilized Hori's perturbation method to normalize a more efficient form of the tesseral disturbing function compared to Kaula's formulation (see [42], Chapter 3) and computed analytic expressions for the second-order short-periodic variations due to an arbitrary tesseral harmonic [122]. He further computed the third-order short-periodic variations due to coupling between the second zonal harmonic and the tesseral harmonics [123]. Wnuk retained the general form of the eccentricity function in his explicit expressions for the short-period effects rather than using its series expansion in order to evaluate it separately for a given value of the eccentricity. These infinite series expansion of the eccentricity function in powers of the eccentricity is given in Kaula [42] (Chapter 3).

The methods that use the eccentricity expansions for the Delaunay normalization of the tesseral Hamiltonian, contain singularities in the form of small divisors near the resonance conditions. These singularities arise when the true anomaly in the disturbing function is expanded in powers of the eccentricity, which additionally degrades the accuracy of the theory for elliptic orbits with medium to high values of the eccentricity. It is known that the series expansion of the true anomaly diverges for high values of the eccentricity. The technique that comes close to providing a closed-form (in the eccentricity) normalization of the tesseral Hamiltonian is the method of relegation [124, 125]. This method successively reduces the magnitude of the perturbation Hamiltonian by scaling it with a small multiplier with the help of the canonical transformations. After a sufficient number of iterations, the perturbation Hamiltonian is deemed small enough to be safely

ignored. Segerman and Coffey applied the method of relegation to the Delaunay normalization of the tesseral Hamiltonian [126]. Their results showed that the method of relegation generated large number of terms in multiple transformations corresponding to each iteration for normalizing the tesseral Hamiltonian. In addition, two different flavors of the relegation method are required for sub-synchronous and super-synchronous orbit regimes, resulting in two separate theories. While the relegation method avoids the eccentricity expansions, its convergence properties restrict the method to small eccentricities in most cases as discussed in References [127, 128]. An alternative relegation approach by Lara et al. expressed the short-period generating function as a power series in the eccentricity, with convergence depending on the value of the eccentricity [127]. Recently, Sansottera et al. derived the asymptotic estimates for the relegation algorithm given a generic perturbed Hamiltonian system [129]. Ely presented a numerical approach to compute mean to osculating transformations up tp first order using the Fast Fourier Transform that is applicable to various types of perturbations such as nonspherical gravitation, the atmospheric drag, solar radiation pressure, and third-bodies [130].

A survey of the progress in AST was presented in 1999 by Wnuk [131]. His survey paper noted that there is not a single theory that includes the zonal and tesseral harmonics up to an arbitrary degree and order, at least second-order perturbations for the tesseral harmonics, coupled effects due to the zonal and tesseral terms, resonance effects, and is also free of all the eccentricity and inclination related singularities including the critical inclination.

1.2.2 Resonance in Satellite Theories and Other Perturbations

1.2.2.1 Critical Inclination

The singularity in artificial satellite theories at the critical inclination has given rise to some controversies over the years, the famous one between Brouwer and Vinti*. In Vinti's theory, which provides an exact solution for a special case of the zonal gravitational potential, the critical inclination singularity does not appear. This is due to the consequence of the special case: $b \equiv 1 + J_4/J_2^2 = 0$ in Vinti's potential, which is of course not true in case of Earth considering

*http://derastrodynamics.com/docs/brouwer_vs_vinti_v1.pdf

the values of these coefficients from the present day more accurate gravity models. The singularity disappears when the same assumption is made in Brouwer and Garfinkel theories also as noted by these authors. Garfinkel generalized the Vinti index (b) to higher zonal harmonics and also showed that when the disturbing function for Vinti's theory is considered, it also yields the same singularity as Brouwer's theory based on the Keplerian ellipse [38]. To remove the critical inclination singularity, Hori and Garfinkel proposed approximate methods that are valid in the neighborhood of the critical inclination value $\cos^{-1} 1/\sqrt{5}$ for J_2. Hori derived the long-period variations, valid in the neighborhood of the critical inclination, by expanding the generating function in the powers of $\sqrt{J_2}$ and making use of the energy integral [132]. Similarly, Garfinkel expanded the energy integral using Taylor series, and showed that in the neighborhood of the critical inclination, the equations of motion (including terms up to first order only) of the one degree of freedom short-period averaged system resembles that of a simple pendulum and thus the solution is reduced to the elliptic functions [133]. Different than previous theories, a second-order analytical theory only for secular and long-periodic variations of the orbital plane and non-elliptical orbit motion in that plane is proposed by Struble. Like Garfinkel, he also showed that near the critical inclination, the apsidal motion reduces to that of a simple pendulum [134, 135]. Hagihara applied his general theory of libration to the critical inclination problem [136] and a similar analysis using the elliptic integrals was provided by Kozai [137] to gain further insight into the conditions that lead to the libation of the pericenter near the critical inclination. It is known that the resonance between the mean motion with respect to the node and the mean motion with respect to the periapsis causes an increase in the magnitude, 25 times greater than otherwise, of the perturbation when the mean inclination is near the critical value [53, 138]. Message et al. showed that with the help of elliptic integrals or functions, the theories valid for any inclination value can be constructed [139]. Izsak showed that the first order solutions in powers of $\sqrt{J_2}$ in the vicinity of the critical inclination breakdown when higher order terms due to J_2 and J_4 are included, additionally the similarity with the simple pendulum of this problem is lost too [140]. Izsak's solution removed the critical inclination singularity for terms up to second order due to J_2^2 and J_4. It is noted that for Earth, the width of the critical

inclination resonance region is only 1° when the second and fourth zonal harmonic are considered [54].

A formal solution for the resonance problem up to fourth order using a hybrid Bohlin-von Zeipel technique was given by Garfinkel, which he applied to the problem of the critical inclination and the 24-hour artificial satellites [141]. After a considerable work on his so-called the ideal resonance problem (see [142, 143, 144, 145]) and using Hori's techniques, Garfinkel proposed a first-order in $\sqrt{J_2}$ global theory for the artificial satellites that is valid for any value of the inclination [146, 147]. An exposition on the critical inclination problem in the satellite theories including analysis in the phase space is given by Coffey et al. [148] and a survey of this problem by Jupp [149]. A comprehensive treatment of the frozen orbits by analyzing the equilibria of the short-period averaged Hamiltonian with zonal harmonics included up to degree nine is given by Coffey et al. [150]. A more recent analysis of the critical inclination singularity using the polar variables is given by Lara [151, 152].

A clever device to avoid the numerical singularity at the critical inclination is due to R. H. Smith as given in Reference [153]. The term $(4 - 5\sin^2 i)$ appears in the denominator of the long-periodic generating function and is a factor in the argument of perigee rate due to the second zonal harmonic. At the critical inclination, this term vanishes and to avoid the resulting singularity, the following modified form of this term can be used:

$$\frac{1}{X} = \begin{cases} \frac{1-\exp(-100X^2)}{X}, & \text{if } X \neq 0 \\ 0, & \text{if } X = 0 \end{cases} \tag{1.19}$$

where

$$X = 4 - 5\sin^2 i$$

For the inclinations far away from the critical inclination value, $1/X$ evaluates to its proper value. Whereas in the close vicinity of the critical inclination, the exponential term approaches 1 faster

than X approaches 0 and as a result, provides a smooth spline across the discontinuity [153].

1.2.2.2 Resonant Orbits

Musen and Bailie computed a theory for the 24-hour satellites (in geosynchronous orbits) that included secular effects due to the second and fourth zonal harmonics, and periodic effects due to the ellipticity of the equator. They used Bohlin's resonance theory and solved the Hamilton-Jacobi equation to compute a series solution in powers of the eccentricity and a certain parameter that depends on the main critical argument in a nonresonance case [154]. Allan provided a theory for the resonant orbits including the effects of all the tesseral harmonics by retaining only the resonant terms in a disturbing function expressed in the classical orbital elements (similar to the one derived by Kaula [30]) and using Lagrange's planetary equations [155]. Vagners used the von Zeipel method to compute analytic theories for non-equatorial near-circular orbits at or near resonance due to the tesseral harmonics, along with the long-period effects due to the zonal harmonics. An averaging based perturbation method suited for computing the solutions for a nonlinear resonance problem is presented by Morrison [156]. Another method to treat orbital resonances using two-variable expansion procedure is proposed by Eckstein and Shi, which also remains valid for the equatorial and circular orbits [157]. Resonance effects on the sub-synchronous orbits and elliptic synchronous orbits are computed analytically by Gedeon [158]. A closed-form solution for the deviations in the semimajor axis and the longitude of a synchronous satellite due to the zonal and tesseral harmonics as well as the luni-solar perturbations is computed by Kamel et al. [159]. Romanowicz used Hori's method to compute a general solution for the resonant orbits of an arbitrary eccentricity in the presence of tesseral harmonics [160]. Another theory for the analytical treatment of resonance effects on the satellite orbits is given by Lane [161].

1.2.2.3 Atmospheric Drag Perturbations

Since the oblateness of Earth does not cause any secular change in the inclination of the artificial satellites, Vinti derived an analytical theory for the variation of the orbital inclination due to atmospheric drag [162]. Sterne derived the secular variations of all the orbital elements due to a

rotating planetary atmosphere [163]. Izsak computed the first-order secular and periodic variations of the orbital elements due to the atmospheric drag with a modified form of the exponential density model [164]. Cook, King-Hele and Walker presented the first of a series of papers on the satellite theory for the drag effects [165, 166]. A rigorous theory for the atmospheric drag was computed by Brouwer and Kozai, which used the von Zeipel method to compute a unified satellite theory for the atmospheric drag and zonal spherical harmonics [167]. They expanded the spherical exponential density model terms in powers of the eccentricity and the mean anomaly to derive secular and mixed secular (due to the coupling between the short-period terms of the drag-free solution and the atmospheric drag effects) terms up to second order and the periodic terms up to first order, however their series solution converges slowly. It should be noted that the earlier (and some of the later) works of King-Hele separated the drag perturbations from the oblateness effects and treated them separately [53]. Otterman and Lichtenfeld computed analytic expressions for drag effects on the radial and in-track motion of a satellite in a near circular orbit [168]. An extension of Vinti's theory to account for the atmospheric drag perturbations is given by Watson et al. [169]. Hoots and France used the method of averaging to compute a satellite theory for the first four zonal harmonics and the atmospheric drag with any empirical atmospheric density model [153]. They expressed the secular effects due to the atmospheric drag on the orbital elements as definite integrals, which can be computed using numerical quadrature without resorting to series expansions in the eccentricity. The quadrature and the atmospheric density values are computed only during initialization and the prediction at later times are accomplished using completely analytic expressions. The coupling between the drag and zonal spherical harmonics is also included by using the osculating altitude at each step in the numerical quadrature.

1.2.2.4 Third Body Perturbations

The perturbation effects due to the third-bodies, such as Sun and the Moon in case of satellites in orbits around Earth, become significant for the satellites in medium to high altitude orbits. Additionally, they must be included in the theories when the satellite observations are used to numerically estimate the spherical harmonic coefficients. While there were earlier studies of

including luni-solar perturbations in AST going back to 1950 by Spitzer, Cook was the first to compute first-order solution for the secular and long-period effects due to a third body, without assuming small orbital eccentricity [170, 171]. He used Lagrange's planetary equations to compute the changes in the orbital elements during one revolution of the satellite in addition to the rates of the orbital elements averaged over a complete revolution. He also provided corresponding expressions for the changes in the orbital elements due to the solar radiation pressure. In Russian literature, Lidov provided a similar analytical theory for the third-body perturbation effects on the orbits of the artificial satellites [172]. Kaula computed a very efficient form of luni-solar disturbing function for an artificial satellite that was similar in form to his gravitational disturbing function [173]. Musen presented a numerical integration method, referred to as Halphen-Goursat method, with step sizes significantly long to compute secular effects for an interval of many years [174]. Kaufman computed a first-order semianalytic satellite theory with short-period variations due to Sun and the moon computed using the Lie-series perturbation theory of Kamel [175]. Danielson et al. presented the implementation of the semianalytic satellite theory that incorporated third-body perturbations with secular and periodic variations up to first order using the generalized method of averaging [99]. Ely and Howell investigated the effects of luni-solar perturbations along with tesseral resonant effects on the orbits with nonzero eccentricity and inclination [176]. Broucke considered the long-term perturbations due to third-bodies on the orbits of artificial satellites using a double analytic averaging approach [177]. He discovered in case of third-body perturbations, a critical inclination of 39° plays an important role, for orbits with the inclinations less than the critical value have a circulating apse line and for the inclination values above that, the circular orbits are unstable and their eccentricities increase. Saedeleer derived an analytical theory of a lunar satellite with the lunar oblateness, the triaxiality of its equator, and third-body perturbation due to Earth without resorting to any series expansions in the eccentricity or inclination [178]. He formulated the complete Hamiltonian in the rotating frame fixed to the moon to avoid a time-dependent Hamiltonian, and considered the terms arising due to the rotating frame as a first-order perturbation with the rest as second-order.

1.2.3 Satellite Relative Motion

The relative motion between two or more satellites flying in orbits around a central body, is affected by differential perturbations. These effects can arise due to the small differences in the orbital elements of the satellites as well as their physical characteristics in case of the atmospheric drag and solar radiation pressure. The accurate models and solutions for the satellite relative motion have widespread application in the analysis and control of rendezvous and proximity operations, satellite swarms or constellations, and formations. In satellite constellations, e.g. GPS constellation, the orbits of individual satellites are comparatively widely separated, and the inter-satellite communication is not used for guidance and control purposes. In contrast, the inter-satellite communication is typically a requirement in order to maintain the desired geometry of the whole satellite formation about a reference orbit, which may or may not be occupied by a reference satellite.

The literature on modeling and control of the satellite relative motion likely starts from the pioneering work of Clohessy and Wiltshire published in 1960 [179]. They derived the equations of relative motion for satellite rendezvous along with their solution in Keplerian dynamics by assuming a circular reference orbit and linearizing the gravity terms by assuming the inter-satellite distances small compared to the radius of the satellite in the reference orbit. Interestingly, these equations can be obtained instantly from Hill's lunar equations (see Reference [180], Chapter 10), which can be considered as an approximation to the planar circular restricted three-body problem, if the third body is assumed to stay close to the smaller primary at all times and the mass of the smaller primary is neglected. The original reference frame (with x axis in a direction opposite to the along-track direction) used by Clohessey and Wilshire to derive their rendezvous equations, is not popular in the modern literature. Instead, the rendezvous equations are expressed in Hill's frame with modern definitions of radial (x), along-track (y), and cross-track (z) directions. Perhaps due to these reasons, these equations of satellite rendezvous are also referred to as Hill-Clohessy-Wiltshire (HCW) equations. Three difference researchers came up with the linear equations of

satellite relative motion for elliptic reference orbits independently, namely D. F. Lawden* in his famous book on optimal rocket trajectories [181], Tschauner and Hempel [182], and de Vries [183]. A detailed treatment of these equations along with their solutions in the form of state transition matrices (STM) are provided in Reference [184]. A number of researchers have also looked at augmenting the linear equations of satellite relative motion in Cartesian coordinates by including the second-order nonlinearity and eccentricity effects [185, 186, 187, 188] as well as effects due to the perturbations such as atmospheric drag [189], third-bodies [190] and Earth's nonspherical gravitational field [191, 192, 190, 193, 194]. Marchad and Howell considered the relative motion problem for the spacecraft formations in the restricted three-body problem as opposed to the Keplerian dynamics [195].

A different approach to describe the satellite relative motion is to use the difference between the orbital elements of the satellites participating in the formation. This approach has an advantage over the relative motion description in Cartesian coordinates (HCW equations and its variations) because it lends itself to a straightforward methodology for incorporating various perturbation effects using the results from the artificial satellite theories. Therefore, more recent efforts have focused on the utilization of the artificial satellite theories for the problem of perturbed satellite relative motion [196, 197, 198, 199, 200, 201]. In this approach, the difference between the orbital elements of the two satellites in a formation are propagated in time under the influence of various perturbation forces using the differential secular and periodic variations of the orbital elements. In order to convert the small differences in the orbital elements into the relative Cartesian or curvilinear states, Garrison et al. [202] and Alfriend et al. [197] proposed a linear transformation. An exact nonlinear transformation, called the unit-sphere method, is derived by Vadali [203].

Gim and Alfriend developed the relative motion state transition matrix, GA-STM, which includes the first-order secular, long-period, and short-period effects due to the dominant second zonal harmonic J_2 [204]. GA-STM uses a geometric method for converting the osculating relative orbital elements to the curvilinear orbit frame. Yan et al. presented a similar approach for

*a space futurist, a contentious talker on (New Zealand) radio and more. Interesting biosketch at `http://www.massey.ac.nz/~wwifs/mathnews/centrefolds/25/Dec1982.shtml`

constructing relative motion state transition matrix using the unit-sphere approach [205]. Schaub developed the analytical techniques to minimize the secular drifts between the relative orbits of the satellites due to the differential oblateness and atmospheric drag effects [206]. Alfriend and Yan proposed a modeling error index for comparing the accuracy of the different analytical theories for the perturbed relative motion of the satellites [207]. Wnuk and Golebiewska developed an analytical solution to propagate the relative orbital elements for the geopotential coefficients up to an arbitrary degree and order using the differential perturbations approach [208, 209, 210]. They used the Kaula-type satellite theory, which uses eccentricity expansions, to derive the expressions for the differential perturbation effects. Sengupta computed a second-order state transition tensor for propagating perturbed satellite relative motion [211]. Sengupta et al. derived a model for propagating the averaged relative motion between two satellites about an oblate planet. This model was further used to filter out short-period perturbations of the desired frequencies from the relative states [212]. Roscoe et al. derived the effects due to third-body perturbations on satellite formations [213]. Yan et al. used the first-order Kaula theory to compute the short-period effects recursively for tesseral harmonics 20×20, and incorporated these effects in the GA-STM [214]. Johnson extended Hoot's theory to second-order and used it to formulate the GA-STM in terms of Hoot's variables, which are nonsingular for the equatorial and circular reference orbits [215]. Koenig et al. derived a STM for propagating differential orbital elements of satellites in arbitrary elliptic orbits that incorporated first-order secular effects due to the second zonal harmonic as well as the differential drag [216]. Biria and Russell derived STM for perturbed satellite relative motion based on Vinti's intermediary that incorporated the second and third zonal harmonic along with a portion of the fourth zonal harmonic [217]. As the STM is derived for Vinti's potential without incorporating any additional perturbations, their STM remains valid at the critical inclination. A recent survey paper on satellite relative motion dynamical models is given in Reference [218].

1.3 Remaining Challenges

In the past 50 to 60 years, a significant amount of literature on various aspects of the artificial satellite theories: ranging from modeling the effects of conservative and non-conservative pertur-

bations to the elimination of singularities due to critical inclination and the resonant tesserals, have been published. Interestingly, a quote by Deprit [49] in 1981 on the main problem reads: "So much having been published about the main problem in the theory of an artificial satellite, it may be taken as axiomatic that a claim of originality may (and probably will) be met by a statement of the opposite. With all this wealth, empty spaces nevertheless exist where an author can contribute more than an inadvertent duplication or a personal derivation of results already in print. We believe the present communication falls into one of the cracks." The present author borrows these words of Deprit to communicate that a few "cracks" or "empty spaces" still exist in the problem of the artificial satellite theory, most noticeably in the case of the tesseral harmonics. Specifically, there are no existing methods for computing nonresonant perturbation effects due to an arbitrary tesseral harmonic, without resorting to the use of series expansions. Additionally, the majority of the analytic solutions for the perturbed satellite relative motion are limited to including only the first-order effects due to a first few zonal harmonics. These along with a few more limitations of the existing theories for the absolute and relative motion of the artificial satellites are discussed as follows:

- The satellite theories incorporating the short-period, long-period and secular effects up to order three due to the zonal harmonics are documented in the literature. However, a completely analytic artificial satellite theory with the generalized expressions for an arbitrary zonal harmonic incorporating at least the second-order secular, long-period, and short-period effects does not exist in the literature. Generalized expressions effect quick implementation of a satellite theory and eliminate the need for symbolic manipulation software such as poisson series processors to compute expressions for a specific zonal harmonic.

- There are no existing solutions for the exact Delaunay normalization of the perturbed Keplerian Hamiltonian with the tesseral and sectorial spherical harmonics. Available methods resort to series expansions in either the eccentricity or the ratio of the satellite's mean motion to the rotational velocity of the central body. Both of the approaches lose accuracy for an orbit with medium to high value of the eccentricity and additionally, produce a large number

of terms for each harmonic. The method of relegation for normalizing the tesseral Hamiltonian produces two separate theories for the sub-synchronous and super-synchronous orbit regimes.

- No single artificial satellite theory includes secular and periodic effects due to an arbitrary zonal or tesseral harmonic, perturbation due to the resonant spherical harmonics in closed-form in the eccentricity, and is also free of singularities for zero eccentricity, zero inclination and the critical inclination. It should be noted that the perturbation effects due to the "equatorial ellipticity" terms (C_{22} and S_{22} spherical harmonics) can be as significant as the third and fourth zonal harmonics in case of Earth.

- No existing theories for the perturbed satellite relative motion include the secular and periodic variations due to the zonal and tesseral harmonic perturbations.

- In case of the satellite formations, the existing along-track drift mitigation conditions have to be explicitly derived for each zonal harmonic. No generalized expressions exist that can be used to compute the initial conditions for the satellites in a formation to reduce the along-track drift caused by an arbitrary zonal harmonic. Additionally, the initial orbital elements to establish a general circular orbit (GCO) (see [184]) type relative orbit for an equatorial and circular reference orbit are not known.

1.4 Contributions

Addressing all of the challenges discussed in the previous section in a single solution is (no doubt) a daunting task. In this work, a few of these challenges have been addressed and these contributions are discussed as follows:

- Chapter 3. A complete closed-form (in the eccentricity) artificial satellite theory for the zonal and tesseral gravitational harmonics is developed. First, explicit expressions for the secular, long-period and short-period variations due to the zonals from J_2 to J_6 are derived up to second-order for the nonsingular orbital elements. A zonal theory using the generalized

expressions for the secular, long-period, and short-period variations of the equinoctial orbital elements due to an arbitrary zonal harmonic is derived next. The zonal theory is followed by a novel solution for the exact Delaunay normalization of the tesseral Hamiltonian. Using this solution, generalized expressions for the periodic variations of the equinoctial elements are derived without resorting to any series expansions.

- Chapter 4. Using the satellite theories for absolute motion developed in Chapter 3, first a STM for perturbed satellite relative motion including the effects of the zonals from J_2 to J_6 is derived by using the explicit expressions for each of these zonals. To include the contributions of an arbitrary zonal harmonic, next a new STM using the equinoctial orbital elements is derived with the generalized expressions for the secular and periodic variations. The generalized STM with contributions from the zonal harmonics, is finally augmented with the periodic variations due to an arbitrary tesseral harmonic.

- Chapter 5. To facilitate the computations of the orbital elements for establishing a general satellite formation geometry, the expressions for the differential equinoctial elements of a satellite are derived. These differential elements are expressed in terms of the formation design parameters and are completely nonsingular for a circular and equatorial reference orbit. Next, the generalized expressions for the secular effects due to any zonal harmonic are used to derive a constraint on the differential semimajor axis of a satellite to mitigate the along-track formation drift. Further, two applications of the artificial satellite theories developed in Chapter 3 are provided: an analytical perturbed Lambert solver for elliptic orbit transfers and nonlinear uncertainty propagation for satellite orbits using point clouds.

2. PRELIMINARIES

An introduction to the various methods and techniques that are useful in the sequel is given in this Chapter. An overview of the canonical perturbation methods and their utilization for constructing the artificial satellite theories is provided. A brief outline of their derivation along with their pros and cons are discussed, starting from the von Zeipel method to the more modern Lie-series/Lie-transform based perturbation methods. Additionally, two different methods: the unit-sphere method and the geometric transformation, for modeling the satellite relative motion using differential orbital elements are presented. The theory behind the GA-STM is given in this Chapter, which is augmented in Chapter 4 to build a relative motion STM for the zonal and tesseral spherical harmonics.

2.1 Canonical Perturbation Methods

The analytic integration of a perturbed Hamiltonian system can be performed using canonical transformations in conjunction with the method of averaging. The perturbed Hamiltonian systems are defined by a Hamiltonian that consists of a dominant part and a relatively small perturbation part, often expressed as a power series in a small parameter. Therefore, the dominant part of the Hamiltonian is also referred to as the unperturbed or zeroth-order Hamiltonian. If an exact solution to the Hamilton-Jacobi equation corresponding to the zeroth-order Hamiltonian is known then a asymptotic series solution for the perturbed Hamiltonian system can be constructed using the Hamilton-Jacobi method. Essentially, it involves the computation of a generating function for a canonical transformation that expresses the perturbed system in terms of a new set of the canonical variables in which the systems becomes integrable up to a certain order. The form of the Hamiltonian in the new variables is typically chosen using the method of averaging. The methodology for a first-order solution is described as follows:

Consider a canonical system defined by a Hamiltonian $\mathcal{H}(\bar{q}, \bar{p}, t)$, where $\bar{q}$ and $\bar{p}$ are the generalized coordinate and conjugate momenta vectors, respectively. The Hamiltonian may be expressed

as a power series in a small parameter ϵ as shown below:

$$\mathcal{H}(\bar{p},\bar{q},t) = \mathcal{H}_0(\bar{q},\bar{p},t) + \sum_{k=1}^{N} \epsilon^k \mathcal{H}_k(\bar{q},\bar{p},t). \tag{2.1}$$

If the canonical system defined by $\mathcal{H}_0(\bar{q},\bar{p},t)$ is completely integrable, then a canonical transformation can always be found using the Hamilton-Jacobi method that transforms the unperturbed system expressed in the old variables $(\bar{q},\bar{p})$ to the new variables $(\bar{x},\bar{X})$ such that in the new variables, the Hamiltonian is a function of the new momenta $\bar{X}$ (typically action variables) only. The Hamiltonian in the new variables for the unperturbed system, represented as $\mathcal{K}_0(\bar{X},t)$ is related to $\mathcal{H}_0(\bar{q},\bar{p},t)$ through a generating function $S_0(\bar{q},\bar{X},t)$ using the following relation (see Reference [219], Chapter 9):

$$\mathcal{H}_0(\bar{q},\bar{p},t) + \frac{\partial}{\partial t} S_0(\bar{q},\bar{X},t) = \mathcal{K}_0(\bar{X},t), \tag{2.2}$$

where $\mathcal{K}_0$ is not a function of the new coordinates $\bar{x}$ (typically angle variables). As a result, the new momenta $\bar{X}$ are constants and additionally, $\bar{x}$ is a linear function of time. The transformation between the new and old variables is *generated* by S_0 using the following equations:

$$\bar{x} = \frac{\partial}{\partial \bar{X}} S_0(\bar{q},\bar{X},t), \quad \bar{p} = \frac{\partial}{\partial \bar{q}} S_0(\bar{q},\bar{X},t). \tag{2.3}$$

Using the above relations and noting that $\bar{X}$ is a constant vector, Eq. 2.2 can be written as a partial differential equation known as the Hamilton-Jacobi equation:

$$\mathcal{H}_0\left(\bar{q}, \frac{\partial}{\partial \bar{q}} S_0(\bar{q},t), t\right) + \frac{\partial}{\partial t} S_0(\bar{q},t) = \mathcal{K}_0(t). \tag{2.4}$$

When the parameter ϵ is not exactly zero but small, a canonical transformation of the form $S_0(\bar{q},\bar{X},t)$ with time-varying new variables $(\bar{x},\bar{X})$ may still be used. Therefore the following relation for the perturbed system similar to Eq. 2.2 is assumed to exist:

$$\mathcal{H}_0(\bar{q},\bar{p},t)+\sum_{k=1}^{N}\epsilon^k\mathcal{H}_k(\bar{q},\bar{p},t)+\frac{\partial}{\partial t}S_0(\bar{q},\bar{X},t)=\mathcal{K}(\bar{x},\bar{X},t) \tag{2.5}$$

.

Using Eq. 2.2, the above equation may be simplified to obtain the expression for the new Hamiltonian as

$$\mathcal{K}_0(\bar{X},t)+\sum_{k=1}^{N}\epsilon^k\mathcal{H}_k(\bar{q},\bar{p},t)=\mathcal{K}(\bar{x},\bar{X},t). \tag{2.6}$$

To simplify the notation, henceforth $\mathcal{K}_0(\bar{X},t)$ is represented as $\mathcal{H}_0(\bar{X},t)$ denoting the unperturbed Hamiltonian expressed using the new variables. The equations of motion of the perturbed system in the new variables is generated by Hamilton's canonical equations of motion as follows:

$$\begin{aligned}\dot{\bar{x}}&=\frac{\partial}{\partial\bar{X}}\mathcal{H}_0(\bar{X},t)+\sum_{k=1}^{N}\epsilon^k\frac{\partial}{\partial\bar{X}}\mathcal{H}_k(\bar{q}(\bar{x},\bar{X},t),\bar{p}(\bar{x},\bar{X},t),t),\\ \dot{\bar{X}}&=-\sum_{k=1}^{N}\epsilon^k\frac{\partial}{\partial\bar{x}}\mathcal{H}_k(\bar{q}(\bar{x},\bar{X},t),\bar{p}(\bar{x},\bar{X},t),t).\end{aligned} \tag{2.7}$$

The transformation equations between the old and new variables is still given by Eq. 2.3, using which, the above equations can be written completely in terms of the new variables as

$$\begin{aligned}\dot{\bar{x}}&=\frac{\partial}{\partial\bar{X}}\mathcal{H}_0(\bar{X},t)+\sum_{k=1}^{N}\epsilon^k\frac{\partial}{\partial\bar{X}}\mathcal{H}_k(\bar{x},\bar{X},t),\\ \dot{\bar{X}}&=-\sum_{k=1}^{N}\epsilon^k\frac{\partial}{\partial\bar{x}}\mathcal{H}_k(\bar{x},\bar{X},t).\end{aligned} \tag{2.8}$$

The above equations for the variations of the new variables $(\bar{x},\bar{X})$ in the presence of the perturbations are similar to the variation of parameters equations in the Hamiltonian framework, except that $\bar{x}$ is a linear function of time and not constant in the unperturbed motion. If $\mathcal{K}_0(t)$ in Eq. 2.2 is

chosen to be nil, then $\mathcal{H}_0(\bar{X}, t)$ vanishes. As a result, $\bar{x}$ becomes constant for $\epsilon = 0$ and the above equations indeed become variation of parameters equations.

If the unperturbed solution in terms of the old variables $(\bar{q}, \bar{p})$ is periodic with period T, then a first approximation to the perturbed Hamiltonian system can be obtained by replacing the perturbation $\mathcal{H}_k$ in Eq. 2.8 by its time-average $\langle \mathcal{H}_k \rangle$. For each momentum X_i that appears in H_0, the corresponding coordinate x_i is a linear functions of t, therefore as a result, the time-average can also be computed by collecting all the term in $\mathcal{H}_k$ to obtain $\langle \mathcal{H}_k \rangle$ that are not a function of x_i. Note that x_i are also termed as fast variables due to their linear dependence on time in the unperturbed case. The final first-order averaged canonical equations of motion are obtained as follows:

$$\begin{aligned} \dot{\bar{x}} &= \frac{\partial}{\partial \bar{X}} \mathcal{H}_0(\bar{X}, t) + \sum_{k=1}^{N} \epsilon^k \frac{\partial}{\partial \bar{X}} \langle \mathcal{H}_k(\bar{x}, \bar{X}, t) \rangle, \\ \dot{\bar{X}} &= -\sum_{k=1}^{N} \epsilon^k \frac{\partial}{\partial \bar{x}} \langle \mathcal{H}_k(\bar{x}, \bar{X}, t) \rangle, \end{aligned} \tag{2.9}$$

where

$$\langle \mathcal{H}_k(\bar{x}, \bar{X}, t) \rangle \; = \; \frac{1}{T} \int_0^T \mathcal{H}_k(\bar{x}, \bar{X}, t) \, \mathrm{d}t.$$

For solving the above integral, the slow variables $\bar{X}$ are held constant. The above formalism can be extended to obtain the higher approximation for the perturbed Hamiltonian system in a fashion that is similar to the generalized method of averaging. The von Zeipel method [28, 220, 221] given in the following subsection accomplishes this task by representing the generating function in a series form with ϵ as the small parameter and computing the higher-order terms in the series recursively by using a chain of partial differential equations.

2.1.1 The von Zeipel Method

The von Zeipel method is an improvement over the method of Poincaré, which itself is an improvement over Delaunay's method of perturbations. In the von Zeipel method, all the fast-

periodic terms are removed from the perturbed Hamiltonian using a single canonical transformation. In Delaunay's method, on the other hand, the disturbing function is treated term by term and a transformation is applied to each term separately to obtain the averaged terms without the use of the canonical transformation approach [220]. The important difference between the von Zeipel and Poincaré methods lies in the fact that in the former, the new Hamiltonian is allowed to be a function of the degenerate angle variables. This scheme allows the von Zeipel method to be applicable in case of degenerate unperturbed Hamiltonians (e.g., Keplerian Hamiltonian) unlike the latter method [14].

To determine an approximate higher-order solution to Eq. 2.8, von Zeipel introduced a transformation from the canonical system $(\bar{x}, \bar{X})$ to a new canonical system $(\bar{y}, \bar{Y})$ using a series form of the generating function as

$$S = x_i Y_i + \sum_{k=1}^{\infty} \epsilon^k S_k(\bar{x}, \bar{Y}, t), \tag{2.10}$$

and the associated equations

$$X_i = \frac{\partial}{\partial x_i} S(\bar{x}, \bar{Y}, t), \quad y_i = \frac{\partial}{\partial Y_i} S(\bar{x}, \bar{Y}, t), \tag{2.11}$$

which leads to the following equations:

$$\begin{aligned} \bar{X} &= \bar{Y} + \sum_{k=1}^{\infty} \epsilon^k \frac{\partial}{\partial \bar{x}} S_k(\bar{x}, \bar{Y}, t) \\ \bar{y} &= \bar{x} + \sum_{k=1}^{\infty} \epsilon^k \frac{\partial}{\partial \bar{Y}} S_k(\bar{x}, \bar{Y}, t). \end{aligned} \tag{2.12}$$

For convenience of notation, the Einstein summation convention is used whenever there is no scope for ambiguity. The new Hamiltonian $\mathcal{K}(\bar{y}, \bar{Y}, t)$ may also be represented as a power series in ϵ, then the following relation is obtained between the old Hamiltonian $\mathcal{H}(\bar{x}, \bar{X}, t)$ from Eq. 2.6, generating function S in Eq. 2.10, and $\mathcal{K}(\bar{y}, \bar{Y}, t)$ as

$$\sum_{k=0}^{N} \epsilon^k \mathcal{H}_k(\bar{x}, \bar{X}, t) + \sum_{k=1}^{\infty} \epsilon^k \frac{\partial}{\partial t} S_k(\bar{x}, \bar{Y}, t) = \sum_{k=0}^{\infty} \epsilon^k \mathcal{K}_k(\bar{y}, \bar{Y}, t), \tag{2.13}$$

where

$$\mathcal{H}_0(\bar{x}, \bar{X}, t) = \mathcal{H}_0(\bar{X}, t),$$

$$\sum_{k=0}^{\infty} \epsilon^k \mathcal{K}_k(\bar{y}, \bar{Y}, t) = \mathcal{K}(\bar{y}, \bar{Y}, t).$$

Substituting Eq. 2.12 in the above equations, it is transformed into

$$\sum_{k=0}^{N} \epsilon^k \mathcal{H}_k \left(\bar{x}, \bar{Y} + \sum_{k=1}^{\infty} \epsilon^k \frac{\partial}{\partial \bar{x}} S_k(\bar{x}, \bar{Y}, t), t \right) + \sum_{k=1}^{\infty} \epsilon^k \frac{\partial}{\partial t} S_k(\bar{x}, \bar{Y}, t) = \sum_{k=0}^{\infty} \epsilon^k K_k \left(\bar{x} + \sum_{k=1}^{\infty} \epsilon^k \frac{\partial}{\partial \bar{Y}} S_k(\bar{x}, \bar{Y}, t), \bar{Y}, t \right). \tag{2.14}$$

Expanding the left hand side of the above equation using Taylor's theorem and equating the coefficients of the same powers of ϵ, the following equations, referred to as homological equations, are obtained up to $\mathcal{O}(\epsilon^k)$ as follows:

$$\begin{aligned} \mathcal{H}_0(\bar{y}, \bar{Y}, t) &= \mathcal{K}_0(\bar{x}, \bar{Y}, t), \\ \frac{\partial}{\partial Y_i} \mathcal{H}_0(\bar{x}, \bar{Y}, t) \frac{\partial}{\partial x_i} S_1(\bar{x}, \bar{Y}, t) + \mathcal{H}_1(\bar{x}, \bar{Y}, t) + \frac{\partial}{\partial t} S_1(\bar{x}, \bar{Y}, t) &= \mathcal{K}_1(\bar{x}, \bar{Y}, t), \\ F_k(\bar{x}, \bar{Y}, t) + \mathcal{H}_k(\bar{x}, \bar{Y}, t) + \frac{\partial}{\partial t} S_k(\bar{x}, \bar{Y}, t) &= \mathcal{K}_k(\bar{x}, \bar{Y}, t), \end{aligned} \tag{2.15}$$

where F_k is a known function of H_s and S_s for $s = 0, 1, \ldots, (k-1)$. The complete expressions of F_k in recursive form are given in Reference [220]. The terms $\mathcal{K}_k$ and S_k can be chosen in any manner. Generally, the method of averaging is used to collect all the secular terms at each order in $\mathcal{K}_k$, and the remaining periodic terms become part of the partial differential equation, which then is solved to obtain S_k. Using the solution for S_k, the new variables $(\bar{y}, \bar{Y})$ can be completely expressed in terms of the old variables and vice-versa using substitution and inversion operations.

An important limitation of the von Zeipel method is apparent from the homological equations given in Eq. 2.15 by noting that the new Hamiltonian and the generating function is specified in terms of the mixed variables: old coordinates and the new momenta. As a consequence, the near-identity transformation between the old and new variables is not explicitly given. Additionally, the near-identity transformation is not canonically invariant, i.e., the expressions for K and S depend on the chosen canonical elements. A discussion of these and other limitations of the von Zeipel method is given in Reference [61].

2.1.2 Deprit's Perturbation Method Using Lie-Transforms

The limitations of the von Zeipel method were first removed by Hori by making use of the Lie-series based canonical transformations. These are truly near-identity transformations, and are a special case of the more general canonical transformations. A similar method by Deprit uses Lie-transform based nonconservative near-identity canonical transformations to convert a time-dependent Hamiltonian expressed in the old variables into a time-independent Hamiltonian in the new variables. The gravitational potential expanded in spherical harmonics depends on time for the case of the tesseral harmonics, therefore Deprit's original method is used in this work to build perturbation solutions (Hori's method also has been extended to time-dependent Hamiltonian, see [60] and Section 1.2.1.3). It is noted that the time-dependence of the Hamiltonian can also be removed by expressing it in the rotating frame fixed to the central body, however it requires an inconvenience of redefining the node angle in a rotating frame. A brief summary and important equations of Deprit's perturbation method are given in this section.

If a Hamiltonian $\mathcal{H}$, a function of canonical variables (x, X) and time t, can be written as a power series using a small parameter ϵ as shown below:

$$\mathcal{H}(x, X; t; \epsilon) = \mathcal{H}_0 + \epsilon\mathcal{H}_1 + \frac{\epsilon^2}{2!}\mathcal{H}_2 + O(\epsilon^3), \tag{2.16}$$

with the associated canonical equations as:

$$\dot{x} = \frac{\partial \mathcal{H}(x, X; t; \epsilon)}{\partial X}, \quad \dot{X} = -\frac{\partial \mathcal{H}(x, X; t; \epsilon)}{\partial x}, \tag{2.17}$$

then a canonical transformation can be constructed to transform the original variables into a new set of the canonical variables (y, Y) such that

$$\dot{y} = \frac{\partial \mathcal{K}(y, Y; t; \epsilon)}{\partial Y}, \quad \dot{Y} = -\frac{\partial \mathcal{K}(y, Y; t; \epsilon)}{\partial y}, \tag{2.18}$$

where

$$\mathcal{K}(y, Y; t; \epsilon) = \mathcal{K}_0 + \epsilon \mathcal{K}_1 + \frac{\epsilon^2}{2!}\mathcal{K}_2 + O(\epsilon^3).$$

In the above equations, $\mathcal{K}$ represents the transformed Hamiltonian (sometimes referred to as Kamiltonian), which is a function of the new variables (y, Y) and time t. The old variables can be expressed in terms of the new variables and vice versa using the following set of nonconservative or time-dependent transformations computed by evaluating the Poisson brackets $(\_, \_)$ of the new and old variables with a time-dependent generating function $\mathcal{W}$ as shown below:

$$\begin{aligned} x &= y + \epsilon(y, \mathcal{W}_1) + \tfrac{\epsilon^2}{2!}\left[(y, \mathcal{W}_2) + ((y, \mathcal{W}_1), \mathcal{W}_1)\right] + O(\epsilon^3), \\ X &= Y + \epsilon(Y, \mathcal{W}_1) + \tfrac{\epsilon^2}{2!}\left[(Y, \mathcal{W}_2) + ((Y, \mathcal{W}_1), \mathcal{W}_1)\right] + O(\epsilon^3), \end{aligned} \tag{2.19}$$

and

$$\begin{aligned} y &= x - \epsilon(x, \mathcal{W}_1) + \tfrac{\epsilon^2}{2!}\left[-(x, \mathcal{W}_2) + ((x, \mathcal{W}_1), \mathcal{W}_1)\right] + O(\epsilon^3), \\ Y &= X - \epsilon(X, \mathcal{W}_1) + \tfrac{\epsilon^2}{2!}\left[-(X, \mathcal{W}_2) + ((X, \mathcal{W}_1), \mathcal{W}_1)\right] + O(\epsilon^3), \end{aligned} \tag{2.20}$$

where

$$(\mathcal{E}, W) = \frac{\partial \mathcal{E}}{\partial l}\frac{\partial W}{\partial L} - \frac{\partial \mathcal{E}}{\partial L}\frac{\partial W}{\partial l} + \frac{\partial \mathcal{E}}{\partial g}\frac{\partial W}{\partial G} - \frac{\partial \mathcal{E}}{\partial G}\frac{\partial W}{\partial g} + \frac{\partial \mathcal{E}}{\partial h}\frac{\partial W}{\partial H} - \frac{\partial \mathcal{E}}{\partial H}\frac{\partial W}{\partial h},$$

$$\mathcal{W}(\_, \_; t; \epsilon) = \mathcal{W}_1 + \epsilon \mathcal{W}_2 + \frac{\epsilon^2}{2!}\mathcal{W}_3 + O(\epsilon^3).$$

In the above equations, the generating function $\mathcal{W}$ depends on time t, the small parameter ϵ, the new variables in Eq. 2.19, and the old variables in Eq. 2.20. The original Hamiltonian $\mathcal{H}$, the new Hamiltonian $\mathcal{K}$, and the generating function $\mathcal{W}$ for the near-identity Lie-transform based canonical transformations are related by the following equation:

$$\mathcal{H}(x, X, t; \epsilon) = \mathcal{K}(y, Y, t; \epsilon) + \epsilon \frac{\partial \mathcal{W}}{\partial t}. \tag{2.21}$$

The old Hamiltonian $\mathcal{H}$ can be expanded in terms of the new variables (y, Y) by using the transformation equations given in Eq. 2.19. Subsequently, by equating the coefficients of ϵ, the homological equations are found, which are given below up to order three [61]:

$$\begin{aligned}
\mathcal{H}_0 &= \mathcal{K}_0, \\
(\mathcal{H}_0, \mathcal{W}_1) - \frac{\partial \mathcal{W}_1}{\partial t} + \mathcal{H}_1 &= \mathcal{K}_1, \\
(\mathcal{H}_0, \mathcal{W}_2) - \frac{\partial \mathcal{W}_2}{\partial t} + (\mathcal{H}_1 + \mathcal{K}_1, \mathcal{W}_1) - \left(\frac{\partial \mathcal{W}_1}{\partial t}, \mathcal{W}_1\right) + \mathcal{H}_2 &= \mathcal{K}_2, \\
(\mathcal{H}_0, \mathcal{W}_3) - \frac{\partial \mathcal{W}_3}{\partial t} + (2\mathcal{H}_1 + \mathcal{K}_1, \mathcal{W}_2) + (\mathcal{H}_2 + 2\mathcal{K}_2, \mathcal{W}_1) - ((\mathcal{K}_1, \mathcal{W}_1), \mathcal{W}_1), & \\
- \left(\frac{\partial \mathcal{W}_2}{\partial t}, \mathcal{W}_1\right) + \mathcal{H}_3 &= \mathcal{K}_3.
\end{aligned} \tag{2.22}$$

In each of the above equations, there is a freedom in choosing $\mathcal{K}$ in any manner as desired. Typically, the method of averaging is used to set $\mathcal{K}$ equal to the average of the known terms. The remaining periodic terms become part of the partial differential equation, which then must be solved to find the generating function $\mathcal{W}$.

2.2 Delaunay Normalization of Perturbed Keplerian Hamiltonian

Delaunay normalization refers to a canonical transformation that converts a given Hamiltonian into Delaunay normal form [222]. For the perturbed Keplerian Hamiltonian, Delaunay normalization is performed by building a canonical transformation that makes one angle variable cyclic in the transformed Hamiltonian $\mathcal{K}$. Using the homological equations of Deprit's method given in Eq.

2.22, the terms in the series expansion of $\mathcal{K}$ may be chosen such that one of the angle variables is absent from $\mathcal{K}$, thus making the corresponding action variable an integral of the transformed system. For constructing satellite theories, averaging is used to eliminate the short-period terms (that are a function of the mean anomaly) from $\mathcal{H}$ in order to compute $\mathcal{K}$, in what is called a first Delaunay normalization. Specifically, at each order in Eq. 2.22, the corresponding terms in the series expansion of $\mathcal{K}$ is set equal to the average of each of the known terms with respect to the mean anomaly on the left hand side of the same equation. The remaining short-period terms then become part of the partial differential equation (PDE) of the unknown series term of $\mathcal{W}$ at each order, which is then solved to compute the short-period variations of the mean elements ($\mathcal{K}$ defines the mean elements). In case of the zonal spherical harmonics, the first Delaunay normalization results in a first-order linear PDE for each term in the series expansion of $\mathcal{W}$ with one independent variable, which can be solved in a straightforward manner without any special techniques at least up to order two [88].

2.3 Relative Motion Description Using Differential Orbital Elements

A more accurate approach to modeling satellite relative motion is based on the differences between the orbital elements of the participating satellites compared to modeling using the Cartesian coordinates. If the orbit of one of the satellites is chosen as the reference, referred to as the chief, then the states of a second satellite, referred to as the deputy, can be represented by simply the difference between its orbital elements and the chief's elements. In case of a small separation between the chief and the deputy compared to the radius of the chief's orbit, the orbital element differences can be assumed to be small. However, this statement may be violated in some cases if a singular description of the reference orbit is used, e.g., the argument of periapsis (AOP) and the right ascension of the ascending node (RAAN) elements, are undefined for the circular and equatorial orbits, respectively. In this work, the prograde version of the equinoctial elements are almost exclusively used, which are completely nonsingular, and their differences are guaranteed to remain small for small separations between the two satellites. As a result, the differential orbital elements of the deputy can be modeled as a first-order variations of the equinoctial elements

of the chief. This enables the construction of a linear transformation to convert differential orbital elements of the deputy to its Cartesian relative states in the Hill reference frame (also called LVLH frame). An exact nonlinear approach to model the relative Cartesian states using the orbital element differences is the unit-sphere method, which is described in the next subsection.

2.3.1 The Unit-Sphere Method

The unit-sphere method projects the motion of the satellites in a formation onto a unit-sphere, which results in decoupling of the periodic variations of the radius from the along-track and cross-track motions [184]. The motion of a satellite on the unit-sphere is projected by normalizing its Cartesian states by its radius and the projection is termed as the sub-satellite point. This approach is useful for analyzing satellite formations in which the prime interest is in the relative orbit geometries as seen along the radial direction. A brief summary of the important equations and results are given next (for more details, see [184], Chapter 7.)

Let C_0 and C_1 denote the direction cosine matrices of the Hill frame with respect to an inertial frame with the frames' origins attached to the chief and deputy, respectively. The relative position vector of the deputy's sub-satellite point with respect to the chief's sub-satellite point in the Hill frame of the chief can be written as:

$$\begin{bmatrix} \bar{x} \\ \bar{y} \\ \bar{z} \end{bmatrix}_C = C_0\, C_1^T \begin{bmatrix} 1 \\ 0 \\ 0 \end{bmatrix}_D - \begin{bmatrix} 1 \\ 0 \\ 0 \end{bmatrix}_C , \tag{2.23}$$

where $(\bar{x}, \bar{y}, \bar{z})$ denote the relative position coordinates of the deputy's projection on the unit-sphere with respect to the chief's projection. The superscript T denotes the transpose operator and the subscripts C and D indicate the frames of the chief and the deputy in which the vectors are coodinatized, respectively. The direction cosine matrices C_0 and C_1 can be parameterized by the orbital elements as shown below:

$$C_0 = C_3(\vartheta_0)\, C_1(i_0)\, C_3(\Omega_0), \tag{2.24}$$

$$C_1 = C_3(\vartheta_0 + \delta\vartheta)\, C_1(i_0 + \delta i)\, C_3(\Omega_0 + \delta\Omega), \tag{2.25}$$

where ϑ is the argument of the latitude of the chief and other orbital elements have their conventional meanings. The zero subscript indicates the orbital elements of the chief, and the elements preceded by δ indicate differential orbital elements of the deputy. The quantities C_1 and C_3 represent elementary rotation matrices of the type indicated by their subscript. By substituting Eqs. 2.24 and 2.25 into Eq. 2.23, the relative state vector of the deputy's projection on the unit-sphere can be expressed in terms of its differential orbital elements along with the chief's orbital elements without any approximations. The actual relative motion states (x, y, z) of the deputy can be obtained from its projection on the unit sphere using the following relations:

$$x = (r_1 - r_0) + r_1\bar{x}, \tag{2.26}$$

$$\begin{bmatrix} y \\ z \end{bmatrix} = r_1 \begin{bmatrix} \bar{y} \\ \bar{z} \end{bmatrix}. \tag{2.27}$$

The relative velocity states of the deputy can be obtained by differentiating Eqs. 2.23, 2.26-2.27. For small differential orbital elements, Eq. 2.25 can be simplified and substituted in Eq. 2.23 along with Eq. 2.24 to obtain the following approximations for the relative states of the deputy in the Hill frame of the chief:

$$\begin{aligned} x &= r_1 - r_0, \\ y &= r_1(\delta\vartheta + \partial\Omega\, \cos(i_0)), \\ z &= r_1(-\sin(i_0)\, \delta\Omega \cos(\vartheta_0 + \delta\vartheta) + \delta i \sin(\vartheta_0 + \delta\vartheta)). \end{aligned} \tag{2.28}$$

Further simplifications of the second and third equations, corresponding to the along-track and cross-track directions, can be performed by only retaining the zeroth-order terms in r_1 and $(\vartheta_0 + \delta\vartheta)$ as they are the coefficients of the first-order terms. Therefore, the final equations for the relative

motion are obtained as follows:

$$\begin{aligned} x &= r_1 - r_0, \\ y &= r_0(\delta\vartheta + \partial\Omega\, \cos(i_0)), \\ z &= r_0(-\sin(i_0)\, \delta\Omega \cos(\vartheta_0) + \delta i \sin(\vartheta_0)). \end{aligned} \tag{2.29}$$

2.3.2 The Geometric Transformation

Gim and Alfriend proposed the geometric transformation as part of their STM solution for the satellite relative motion that includes first-order secular and periodic effects due to J_2 [204]. Their approach involves the transformation of the differential orbital elements of the deputy to its relative states in a curvilinear frame attached to the chief by using the geometric transformation matrix. The curvilinear frame is defined with respect to an imaginary sphere with its origin at the chief and radius equal to chief's radius. The relative position with respect to the chief can be defined in terms of three coordinates: x represents the difference in the radii of the two satellites, and y and z represent the curvilinear distances along and perpendicular to the along-track direction of the chief, respectively. If $\bar{x}$ is the relative position and velocity vector in the curvilinear frame and $\delta\bar{e}$ is the differential orbital elements vector, then the geometric transformation matrix, Σ, is defined as

$$\bar{x} = \Sigma\, \delta\bar{e}. \tag{2.30}$$

To derive an expression for Σ, the first variation of the following equations:

$$\begin{aligned} [\bar{r}_1]_C &= C_0\, C_1^T\, [\bar{r}_1]_D\,, \\ [\bar{v}_1]_C &= C_0\, C_1^T\, [\bar{v}_1]_D\,, \end{aligned} \tag{2.31}$$

is taken with respect to the chief's orbital elements, where r_1 and v_1 represent position and velocity vectors of the deputy, respectively. The direction cosine matrices, C_0 and C_1, represents orientations of the Hill frames of the chief and deputy, respectively. If ϖ is the angular velocity vector of

the chief's frame, then the resulting variational equations can be written as:

$$\begin{aligned}
[\bar{r}_0 + \bar{x}]_C &= C_0 \left(C_0^T + \delta C_0^T\right) \left([\bar{r}_0]_C + \delta\,[\bar{r}_0]_C\right), \\
[\bar{v}_0 + \dot{\bar{x}} + \varpi \times \bar{x}]_C &= C_0 \left(C_0^T + \delta C_0^T\right) \left([\bar{v}_0]_C + \delta\,[\bar{v}_0]_C\right),
\end{aligned} \tag{2.32}$$

where

$$\begin{aligned}
[\bar{r}_0]_C &= [r_0 \;\; 0 \;\; 0]^T, \\
[\bar{v}_0]_C &= [v_{r0} \;\; v_{t0} \;\; 0]^T,
\end{aligned}$$

and $(v_{r0}, v_{t0}, 0)$ denote the components of the chief's velocity along radial, tangential and normal directions, respectively. By ignoring the second-order terms, the following linearized equations for the relative states of the deputy in the curvilinear frame are obtained:

$$\begin{aligned}
[\bar{x}]_C &= \delta\,[\bar{r}_0]_C + C_0\,\delta C_0^T \;\; [\bar{r}_0]_C, \\
[\dot{\bar{x}}]_C &= \delta\,[\bar{v}_0]_C + C_0\,\delta C_0^T \;\; [\bar{v}_0]_C - \varpi \times [\bar{x}]_C.
\end{aligned} \tag{2.33}$$

The variational quantities in the above equations are computed with respect to the orbital elements of the chief. The equinoctial elements can be used to formulate the geometric transformation matrix, which avoids singularities in case of circular or equatorial reference orbits (for details on the equinoctial elements, see [223].) The parameterizations of the position and velocity vectors of the chief in the Hill frame using the equinoctial elements $(a, \Psi, p_1, p_2, q_1, q_2)$ can be derived using the well-known two-body relations (see [224], Chapter 3) and are given below:

$$\begin{aligned}
r_0 &= \frac{a(1 - q_1^2 - q_2^2)}{(1 + q_1\cos(\Psi) + q_2\sin(\Psi))}, \\
v_{r0} &= \sqrt{\frac{\mu}{a(1 - q_1^2 - q_2^2)}}\,(q_1\sin(\Psi) - q_2\cos(\Psi)), \\
v_{t0} &= \sqrt{\frac{\mu}{a(1 - q_1^2 - q_2^2)}}\,(1 + q_1\cos(\Psi) + q_2\sin(\Psi)),
\end{aligned} \tag{2.34}$$

where

$$\Psi = f + g + h,$$
$$p_1 = \tan\left(\frac{i}{2}\right)\cos(h),$$
$$p_2 = \tan\left(\frac{i}{2}\right)\sin(h),$$
$$q_1 = e\cos(g+h),$$
$$q_2 = e\sin(g+h).$$

By treating classical elements as functions of the equinoctial elements, C_0 can also be parameterized in terms of the equinoctial elements using Eq. 2.24. It is noted that after all the variational quantities are determined and substituted, the coefficients of the differential equinoctial elements can be collected in a matrix, which becomes the geometric transformation matrix Σ as defined by Eq. 2.30. The expression for the along-track relative state y in terms of differential equinoctial elements, which becomes the second row of Σ, is given below as one example:

$$y = \frac{\sqrt{\mu p}}{v_{t0}}\left(\delta\Psi + \frac{2\,p_2}{1+p_1^2+p_2^2}\delta p_1 - \frac{2\,p_1}{1+p_1^2+p_2^2}\delta p_2\right). \tag{2.35}$$

Using the relations between the classical and equinoctial elements, it can be verified that the above expression for along-track position of the deputy in terms of differential equinoctial elements is equivalent to the expression computed using the unit-sphere method in Eq. 2.29.

The angular velocity vector, ϖ, is yet to be determined, which is required to compute the expressions for the relative velocities in Eq. 2.33. Knowing the angular rates, the components of ϖ can be computed in the chief's frame using $3-1-3$ rotations of the coordinate axes as shown below:

$$\varpi = C_3(\vartheta)C_1(i)\begin{bmatrix}0\\0\\\dot{\Omega}\end{bmatrix} + C_3(\vartheta)\begin{bmatrix}\dot{i}\\0\\0\end{bmatrix} + \begin{bmatrix}0\\0\\\dot{\vartheta}\end{bmatrix}. \tag{2.36}$$

Solving the above equation results in the following equation for the angular velocity vector:

$$\varpi = \begin{bmatrix}\dot{\Omega}\sin\vartheta\sin i + \dot{i}\cos\vartheta\\ \dot{\Omega}\cos\vartheta\sin i - \dot{i}\sin\vartheta\\ \dot{\vartheta} + \dot{\Omega}\cos i\end{bmatrix}. \tag{2.37}$$

Using the osculation constraint that the normal component of the inertial velocity in the Hill frame is nil, further simplifications of the above expression for ϖ is possible. Note that the inertial velocity of the chief expressed in the Hill frame can be written as:

$$[\bar{v}_0]_C = \dot{r}_0\hat{x} + r_0\,\varpi_n\hat{y} - r_0\,\varpi_t\hat{z}, \tag{2.38}$$

where $(\hat{x}, \hat{y}, \hat{z})$ are the three unit-vectors along the coordinate axes of the Hill frame. Therefore, the expression for the second component in Eq. 2.36, i.e., ϖ_t must be set to zero, which results in the following expression for the inclination rate:

$$\dot{i} = \frac{\dot{\Omega}\sin(i)\,\cos(\vartheta)}{\sin(\vartheta)}. \tag{2.39}$$

As a final step, the above relation is used to simplify the expression for ϖ_r and the resulting expression for the angular velocity vector is

$$\varpi = \begin{bmatrix}\frac{\dot{\Omega}\sin(i)}{\sin(\vartheta)} & 0 & \frac{h}{r_0^2}\end{bmatrix}^T, \tag{2.40}$$

where h is the magnitude of the specific angular momentum. It is noted that all the expressions involved in computing the geometric transformation matrix Σ are functions of the osculating orbital elements of the chief, and the node rate. The complete expressions for all the elements of Σ are

provided in Appendix C. If a transformation from the mean differential orbital elements to mean relative states in the curvilinear frame is sought, then the osculation constraint discussed above is no longer valid and the expression given in Eq. 2.37 must be used to compute the mean geometric transformation matrix. As a result, the mean angular rates of all three angles Ω, i, and ϑ would be required, which can be computed using the methods detailed in Chapter 3.

2.3.3 Gim-Alfriend State Transition Matrix

Using the geometric transformation, Gim and Alfriend [204] developed an analytic state transition matrix, known as the GA-STM, for the perturbed satellite relative motion in the presence of the J_2 harmonic perturbation. Specifically, GA-STM models the first-order secular, long-periodic and short-periodic variations due to J_2 by taking the first-order variations of the secular rates as well as the mean to osculating transformation of the chief with respect to the orbital elements. Using the geometric transformation matrix, it directly propagates the initial relative states of the deputy in the curvilinear frame from the initial to the final time.

GA-STM is formulated using three separate component matrices: the geometric transformation matrix Σ, the differential mean-to-osculating transformation matrix D, and the differential mean STM ϕ as shown below:

$$\Phi(t, t_0) = \Sigma(t)D(t)\phi(t, t_0)D^{-1}(t_0)\Sigma^{-1}(t_0). \tag{2.41}$$

The differential mean STM, ϕ, propagates the differential mean elements in time by taking a first-order variation of the mean rates of the chief's orbital elements. The differential mean elements are then converted into differential osculating elements, when multiplied by D. Finally, the geometric transformation matrix converts the differential osculating elements into the relative states in the curvilinear frame. Similarly, the initial relative states at t_0 can be converted to the initial differential mean elements by multiplication with the inverse of D and Σ in a sequence shown in the above equation, to form the complete GA-STM. All the three component matrices of GA-STM can be derived in terms of the equinoctial elements, thereby avoiding the zero eccentricity and zero

inclination singularities [225].

3. SATELLITE THEORY WITH ZONAL AND TESSERAL HARMONICS*

Using Deprit's perturbation method described in the previous chapter (see Section 2.1.2), the Delaunay normalization of a perturbed Keplerian Hamiltonian with the zonal, sectorial, and tesseral harmonics is carried out in this chapter to construct an artificial satellite theory devoid of any series expansion in powers of the eccentricity or in the ratio of the mean motion and Earth's angular velocity. For the zonal harmonics up to degree six, the explicit expressions for the secular and periodic effects are computed first, followed by the generalized expressions for the same that are valid for an arbitrary zonal harmonic. In case of the sectorial and tesseral harmonics, an exact approach to perform the Delaunay normalization is presented and it is showed that the conventional method of relegation can be considered as a special case of the proposed approach. Using these results, a complete artificial satellite theory for the all the gravitational spherical harmonics is constructed in terms of the equinoctial elements. The accuracy of this theory is validated against

*Reprinted in part with permission from

B. Mahajan, S.R. Vadali, and K.T. Alfriend, "Exact Delaunay normalization of the perturbed Keplerian Hamiltonian with tesseral harmonics," *Celestial Mechanics and Dynamical Astronomy*, vol. 130, no. 25, 2018. Copyright by Springer Science+Business Media B.V., part of Springer Nature 2018.

B. Mahajan, S. R. Vadali, and K. T. Alfriend, "Analytic solution of perturbed relative motion with zonal and tesseral harmonics," In *Spaceflight Mechanics 2017: Proceedings of the 27th AAS/AIAA Space Flight Mechanics Meeting* held February 5-9, 2017 San Antonio, Texas, U.S.A., pp. 1117-1134. [AAS 17-475] (Advances in the Astronautical Sciences; Vol. 160). San Diego, California: Published for the American Astronautical Society by Univelt, Inc. (2017).

B. Mahajan, S. R. Vadali, and K. T. Alfriend, "Exact normalization of the tesseral harmonics," In *Spaceflight Mechanics 2017: Proceedings of the 27th AAS/AIAA Space Flight Mechanics Meeting* held February 5-9, 2017 San Antonio, Texas, U.S.A. (pp. 2569-2588). [AAS 17-473] (Advances in the Astronautical Sciences; Vol. 160). San Diego, California: Published for the American Astronautical Society by Univelt, Inc. (2017).

B. Mahajan, S. R. Vadali, and K. T. Alfriend, "Analytic solution for satellite relative motion: The complete zonal gravitational problem," In *Spaceflight Mechanics 2016: Proceedings of the 26th AAS/AIAA Space Flight Mechanics Meeting* held February 14-18, 2016, Napa, California, U.S.A. (pp. 3325-3348). [AAS 16-262] (Advances in the Astronautical Sciences; Vol. 158). San Diego, California: Published for the American Astronautical Society by Univelt, Inc. (2016).

B. Mahajan, S. R. Vadali, and K. T. Alfriend, "Analytic solution for satellite relative motion with zonal gravity perturbations," In *Astrodynamics 2015: Proceedings of the AAS/AIAA Astrodynamics Specialist Conference* held August 9-13, 2015, Vail, Colorado, U.S.A. (pp. 3583-3598). [AAS 15-705] (Advances in Astronautical Sciences; Vol. 156). San Diego, California: Published for the American Astronautical Society by Univelt, Inc. (2016).

numerical orbit propagation in MATLAB as well as in GMAT tool*. The theories formulated in this chapter are used for deriving an analytic STM solution for the perturbed satellite relative motion in the following chapter.

3.1 Satellite Theory for Zonal Harmonics J_2-J_6

In this section, the secular variations up to order three and the periodic variations up to order two for the nonsingular element set are derived [1]. The expressions are computed explicitly for each of the zonals from J_2 to J_6 using symbolic computations in Maple software package†. Unlike the classical elements or the Delaunay elements, the nonsingular elements exhibit no singularity for the circular orbits. They are singular for the equatorial orbits, however. The definitions of the nonsingular elements along with the Delaunay elements in terms of the classical elements are:

$$\text{Delaunay: } \begin{bmatrix} l & g & h & L & G & H \end{bmatrix}^T,$$

$$\text{Nonsingular: } \begin{bmatrix} a & M+\omega & i & e\cos(\omega) & e\sin(\omega) & \Omega \end{bmatrix}^T,$$

where

$$l = M,\ \ g = \omega,\ \ h = \Omega,\ \ L = \sqrt{\mu a},\ \ G = L\sqrt{1-e^2},\ \ H = G\cos(i).$$

For the zonal problem, the gravitational potential expanded using the spherical harmonics is

$$U = \frac{\mu}{r}\left[1 - \sum_{n=2}^{\infty} J_n \left(\frac{R_e}{r}\right)^n P_n(sin(\phi))\right], \tag{3.1}$$

where $\sin(\phi) = \sin(i)\sin(f+g)$ (see Reference [42], Chapter 3). The symbols r, ϕ, R_e, μ, J_n and P_n represent the radial distance of the satellite, its geocentric latitude, radius of Earth (or the appropriate central body in case of non-Earth orbiters), gravitational parameter, zonal harmonic coefficients, and the Legendre polynomials of degree n, respectively. The corresponding Hamiltonian for the above system can be expressed as a power series in J_2 using a combination of the

*http://www.gmatcentral.org
†https://www.maplesoft.com/products/maple/

Delaunay and classical orbital elements. The magnitude of J_2 is at least three orders of magnitude greater than any other spherical harmonic. For many other planets also, J_2 is the dominant perturbation for orbiters with sufficiently small altitude. Therefore, for developing satellite theories up to order two, J_2 can be considered as a first-order perturbation with the higher degree and order spherical harmonics considered to be of order two. Using the definition of the Legendre polynomials and trigonometric identities, the Hamiltonian for the zonals J_2 to J_6 is derived as

$$\mathcal{H} = \mathcal{H}_0 + J_2\mathcal{H}_1 + \frac{J_2^2}{2!}\mathcal{H}_2, \tag{3.2}$$

where

$$\mathcal{H}_0 = -\frac{1}{2}\frac{\mu^2}{L^2}, \tag{3.3}$$

$$\mathcal{H}_1 = \frac{1}{4}\frac{\mu^4 {R_e}^2}{L^6}\left(\frac{a}{r}\right)^3\left(1 - 3\cos^2(i) - 3\sin^2(i)\cos\left(2g + 2f\right)\right), \tag{3.4}$$

$$\mathcal{H}_2 = H_{23} + H_{24} + H_{25} + H_{26},$$

$$H_{23} = \frac{2}{{J_2}^2}\frac{J_3\mu^5 {R_e}^3}{8L^8}\left(\frac{a}{r}\right)^4 \sin(i)\left(3\left(1 - 5\cos^2(i)\right)\sin\left(f + g\right) - 5\sin^2(i)\sin\left(3f + 3g\right)\right), \tag{3.5}$$

$$H_{24} = \frac{2}{{J_2}^2}\frac{J_4\mu^6 {R_e}^4}{8L^{10}}\left(\frac{a}{r}\right)^5\left[\left(\frac{9}{8} - \frac{45}{4}\cos^2(i) + \frac{105}{8}\cos^4(i)\right) + \left(\frac{-5}{2} + 20\cos^2(i) - \frac{35}{2}\cos^4(i)\right)\right.$$
$$\left.\cos\left(2f + 2g\right) + \left(\frac{35}{8} - \frac{35}{4}\cos^2(i) + \frac{35}{8}\cos^4(i)\right)\cos\left(4f + 4g\right)\right], \tag{3.6}$$

$$H_{25} = \frac{2}{{J_2}^2}\frac{J_5\,\mu^7 {R_e}^5\sin\left(i\right)}{32L^{12}}\left(\frac{a}{r}\right)^6\left[\frac{15}{2}\left(1 - 14\cos^2(i) + 21\cos^4(i)\right)\sin\left(f + g\right)\right.$$
$$\left. - \frac{35}{4}\left(1 - 10\cos^2(i) + 9\cos^4(i)\right)\sin\left(3\,f + 3\,g\right) + \frac{63}{4}\left(1 - 2\cos^2(i) + \cos^4(i)\right)\sin\left(5\,f + 5\,g\right)\right], \tag{3.7}$$

$$H_{26} = \frac{2}{{J_2}^2}\frac{J6\,\mu^8 {R_e}^6}{256\,L^{14}}\left(\frac{a}{r}\right)^7\left[25\left(1-21\cos^2(i)+63\cos^4(i)-\frac{231}{5}\cos^6(i)\right)\right.$$
$$-\frac{105}{2}\left(1-19\cos^2(i)+51\cos^4(i)-33\cos^6(i)\right)\cos\left(2\,g+2\,f\right)$$
$$+63\left(1-13\cos^2(i)+23\cos^4(i)-11\cos^6(i)\right)\cos\left(4\,f+4\,g\right)$$
$$\left.-\frac{231}{2}\left(1-3\cos^2(i)+3\cos^4(i)-\cos^6(i)\right)\cos\left(6\,f+6\,g\right)\right]. \tag{3.8}$$

The periodic terms present in the above zonal Hamiltonian are averaged out using Deprit's method in the following subsections.

3.1.1 Short-Period Effects

For the Delaunay normalization of the zonal Hamiltonian, the short-period terms that are functions of l are first separated from $\mathcal{H}$ using the homological equations of Deprit's method given in Eq. 2.22. The resulting short-period averaged Hamiltonian or Kamiltonian $\mathcal{K}$ includes only the secular and long-period effects. The zonal Hamiltonian is not a function of time, as a result, the short-period generating function does not depend on time. Deprit's homological equations after these simplifications are

$$\begin{aligned}
\mathcal{H}_0 &= \mathcal{K}_0,\\
(\mathcal{H}_0,\mathcal{W}_1)+\mathcal{H}_1 &= \mathcal{K}_1,\\
(\mathcal{H}_0,\mathcal{W}_2)+(\mathcal{H}_1+\mathcal{K}_1,\mathcal{W}_1)+\mathcal{H}_2 &= \mathcal{K}_2,\\
(\mathcal{H}_0,\mathcal{W}_3)+(2\mathcal{H}_1+\mathcal{K}_1,\mathcal{W}_2)+(\mathcal{H}_2+2\mathcal{K}_2,\mathcal{W}_1)-((\mathcal{K}_1,\mathcal{W}_1),\mathcal{W}_1)+\mathcal{H}_3 &= \mathcal{K}_3,
\end{aligned} \tag{3.9}$$

where

$$\mathcal{K} = \mathcal{K}_0 + J_2\mathcal{K}_1 + \frac{J_2^2}{2!}\mathcal{K}_2 + \frac{J_2^3}{3!}\mathcal{K}_3 + O(J_2^4), \tag{3.10}$$

$$\mathcal{W} = \mathcal{W}_1 + J_2\mathcal{W}_2 + \frac{J_2^2}{2!}\mathcal{W}_3 + O(J_2^3). \tag{3.11}$$

In the above equations, $\mathcal{W}$ represents the short-period generating function and $(\_,\_)$ denotes Poisson brackets. To compute $\mathcal{K}$ and $\mathcal{W}$ at each order successively, first a closed-form expression for the average value of all the known terms on the left hand side of Eq. 3.9, i.e., all terms except the first, is evaluated with respect to l. At each order, this average value is collected in the respective term from the series expansion of $\mathcal{K}$. The remaining periodic terms are integrated with respect to l for computing the series expansion terms of $\mathcal{W}$. The following formulae are used to derive the first-order terms of $\mathcal{K}$ and $\mathcal{W}$:

$$\mathcal{K}_1 = \frac{1}{2\pi}\int_0^{2\pi} \mathcal{H}_1 \mathrm{d}l, \tag{3.12}$$

$$\mathcal{W}_1 = -\frac{1}{\frac{\partial \mathcal{H}_0}{\partial L}} \int (\mathcal{K}_1 - \mathcal{H}_1)\, \mathrm{d}l. \tag{3.13}$$

The average of $\mathcal{W}_1$ with respect to l may not be zero and as a result, biases may exist in the short-period effects. Since, any expression that is not a function of l can be added to $\mathcal{W}_1$ as a constant of integration, the long-period term

$$-\frac{1}{8}\frac{\mu^2 R_e^2}{G^3}\left(1-\frac{H^2}{G^2}\right)\frac{e^2(1+2\eta)}{(1+\eta)^2}\sin 2g$$

can be added to $\mathcal{W}_1$ in order to remove its biases. It should be noted that a generating function with a zero average at every order does not necessarily produce periodic variations with zero average at second and higher orders due to the presence of the nonlinear terms in the transformations Eqs. 2.19-2.20. Ferraz-Mello has shown that a completely zero-average Hamiltonian system cannot be obtained using the canonical perturbation methods at orders higher than one [226]. Nonetheless, the accuracy of the theories are not affected by the presence of these biases, and the actual dynamics still oscillates about the "averaged" dynamics but with non-zero bias. In order to compute the short-period averaged Hamiltonian $\mathcal{K}$, the following definite integrals are useful [227]:

$$\tfrac{1}{2\pi}\textstyle\int_0^{2\pi} \cos(kf)\mathrm{d}l = -\left(\sqrt{\frac{1-\eta}{1+\eta}}\right)^k (k\eta+1),$$

$$\textstyle\int_0^{2\pi} \sin(kf)\mathrm{d}l = 0,$$

$$\int_0^{2\pi} (f-l)\,\mathrm{d}l = 0,$$

$$\int_0^{2\pi} (f-l)\cos(kf)\mathrm{d}l = 0, \quad \text{and} \quad \int_0^{2\pi} (f-l)\sin(kf)\mathrm{d}l = 0,$$

where

$$\eta = \sqrt{1-e^2}, \text{ and } k \in \mathbb{Z}.$$

The computation of J_2 contributions to $\mathcal{K}_2$ and $\mathcal{W}_2$ follows a similar approach. However, the process requires additional algebraic computations due to the presence of the Poisson bracket involving $(\mathcal{H}_1 + \mathcal{K}_1)$ and $\mathcal{W}_1$. One of the terms originating from $(\mathcal{K}_1, \mathcal{W}_1)$ includes the following non-reducible indefinite integral:

$$\int \left(\cos(2f+2g) + e\cos(f+2g) + \frac{e}{3}\cos(3f+2g)\right)\mathrm{d}l. \tag{3.14}$$

Aksnes showed that the above indefinite integral gets completely canceled by a term originating from $(\mathcal{H}_1, \mathcal{W}_1)$ [88]. Specifically, the following term, when integrated by parts, produces the same integral as above, with an opposite sign:

$$\frac{\partial \mathcal{H}_1}{\partial g}\frac{\partial \mathcal{W}_1}{\partial G} : (f-l)\sin(2g+2f)\left(1+e\cos(f)\right)^3.$$

After getting rid of the term in Eq. (3.14) with the help of the integral of the above term, the computation of J_2 contributions to $\mathcal{K}_2$ and $\mathcal{W}_2$ is straightforward. Since all the zonal harmonics of degree higher than J_2 are considered to be of the second-order and included in $\mathcal{H}_2$, their contributions $\Delta\mathcal{K}_2$ and $\Delta\mathcal{W}_2$ to $\mathcal{K}_2$ and $\mathcal{W}_2$, respectively, can be computed separately from those due to J_2. The following equations are used to compute the secular and short-periodic generating function contributions of all the higher zonal harmonics:

$$\Delta\mathcal{K}_2 = \frac{1}{2\pi}\int_0^{2\pi} \mathcal{H}_2\,\mathrm{d}l, \tag{3.15}$$

$$\Delta\mathcal{W}_2 = -\frac{1}{\frac{\partial \mathcal{H}_0}{\partial L}}\int (\Delta\mathcal{K}_2 - \mathcal{H}_2)\,\mathrm{d}l. \tag{3.16}$$

Given the complete short-period generating function, $\mathcal{W}$, for the zonal harmonics J_2 to J_6, the short-period variations due to these harmonics can be removed from the osculating elements, denoted by $\mathcal{E}$, using the near-identity transformation equations given in Eq. 2.19-2.20. The resulting short-period averaged elements $\mathcal{E}_{LP}$ retain the long-period and secular variations, and are related to $\mathcal{E}$ by the following transformations:

$$\begin{aligned} \mathcal{E} &= \mathcal{E}_{LP} + \epsilon(\mathcal{E}_{LP}, \mathcal{W}_1) + \tfrac{\epsilon^2}{2!}\left[(\mathcal{E}_{LP}, \mathcal{W}_2) + ((\mathcal{E}_{LP}, \mathcal{W}_1), \mathcal{W}_1)\right] + O(\epsilon^3), \\ \mathcal{E}_{LP} &= \mathcal{E} - \epsilon(\mathcal{E}, \mathcal{W}_1) + \tfrac{\epsilon^2}{2!}\left[-(\mathcal{E}, \mathcal{W}_2) + ((\mathcal{E}, \mathcal{W}_1), \mathcal{W}_1)\right] + O(\epsilon^3). \end{aligned} \tag{3.17}$$

It is noted that while the above near-identity transformation equations are derived in Section 2.1.2 to compute the periodic variations of the canonical elements, they can also be used to compute variations for any other set of elements. Specifically, $\mathcal{E}$, with or without subscript, represents non-singular element set in this section. However, in case of the canonical elements, the near-identity transformation equations provide better accuracy as there is no need to approximate the nonlinear relationship between the canonical and the chosen non-canonical element set. The Poisson brackets are, of course, always computed using the canonical elements (Delaunay elements in this work).

3.1.2 Long-Period Effects

Elimination of the short-period terms results in the short-period averaged Hamiltonian $\mathcal{K}$, which is a function of the action variables (L,G,H) and one angle variable g. A second Delaunay normalization removes the long-period terms that depend on g from $\mathcal{K}$, and produces a new double-averaged Hamiltonian $\bar{\mathcal{K}}$, and the long-period generating function $\bar{\mathcal{W}}$. Because $\bar{\mathcal{W}}$ is not a function of l, the homological equations simplify to the following:

$$
\begin{aligned}
\mathcal{K}_0 &= \bar{\mathcal{K}}_0, \\
\mathcal{K}_1 &= \bar{\mathcal{K}}_1, \\
\left(\bar{\mathcal{K}}_1 + \mathcal{K}_1, \bar{\mathcal{W}}_1\right) + \mathcal{K}_2 &= \bar{\mathcal{K}}_2, \\
\left(2\mathcal{K}_1 + \bar{\mathcal{K}}_1, \bar{\mathcal{W}}_2\right) + \left(\mathcal{K}_2 + 2\bar{\mathcal{K}}_2, \bar{\mathcal{W}}_1\right) - \left(\left(\bar{\mathcal{K}}_1, \bar{\mathcal{W}}_1\right), \bar{\mathcal{W}}_1\right) + \mathcal{K}_3 &= \bar{\mathcal{K}}_3,
\end{aligned}
\tag{3.18}
$$

where

$$
\bar{\mathcal{K}} = \bar{\mathcal{K}}_0 + J_2\bar{\mathcal{K}}_1 + \frac{J_2^2}{2!}\bar{\mathcal{K}}_2 + \frac{J_2^3}{3!}\bar{\mathcal{K}}_3 + O(J_2^4), \tag{3.19}
$$

$$
\bar{\mathcal{W}} = \bar{\mathcal{W}}_1 + J_2\bar{\mathcal{W}}_2 + \frac{J_2^2}{2!}\bar{\mathcal{W}}_3 + O(J_2^3). \tag{3.20}
$$

At each order in Eq. 3.18, all the terms independent of g are collected in $\bar{\mathcal{K}}$, and the remaining long-periodic terms are integrated with respect to g for computing $\bar{\mathcal{W}}$. It should be noted that the second-order long-period generating function $\bar{\mathcal{W}}_2$ is computed from the third-order homological equation. The mean action variables do not change with time and the constant mean rates of the angle variables are computed using Hamilton's equations. Using the complete long-period generating function $\bar{\mathcal{W}}$ for the zonal harmonics J_2 to J_6, the near-identity transformation between the mean elements $\mathcal{E}_m$, which retain only secular effects, and $\mathcal{E}_{LP}$ can be computed using the following equations:

$$
\begin{aligned}
\mathcal{E}_{LP} &= \mathcal{E}_m + \epsilon(\mathcal{E}_m, \bar{\mathcal{W}}_1) + \tfrac{\epsilon^2}{2!}\left[(\mathcal{E}_m, \bar{\mathcal{W}}_2) + ((\mathcal{E}_m, \bar{\mathcal{W}}_1), \bar{\mathcal{W}}_1)\right] + O(\epsilon^3), \\
\mathcal{E}_m &= \mathcal{E}_{LP} - \epsilon(\mathcal{E}_{LP}, \bar{\mathcal{W}}_1) + \tfrac{\epsilon^2}{2!}\left[-(\mathcal{E}_{LP}, \bar{\mathcal{W}}_2) + ((\mathcal{E}_{LP}, \bar{\mathcal{W}}_1), \bar{\mathcal{W}}_1)\right] + O(\epsilon^3).
\end{aligned}
\tag{3.21}
$$

3.1.3 Results

Using the results from the previous subsections, a second-order artificial satellite theory with contributions from J_2 to J_6 harmonics is implemented in MATLAB. Appendix A provides the explicit expressions for $\bar{\mathcal{K}}$ up to third order, $\mathcal{W}$, and $\bar{\mathcal{W}}$ up to second order for the zonal harmonics J_2 to J_6 computed using Maple. The accuracy of the satellite theory is validated using numerical

propagation in GMAT and the simulation results are given in this subsection. In GMAT, the JGM-3 gravity model, with degree six and order zero, was used for numerical propagation of an artificial satellite. The mean elements are chosen, and the initial osculating elements of the satellite are computed from the analytical mean-to-osculating transformation. In many applications of artificial satellite theories, the initial semimajor axis is corrected by data fitting. Even though the model error can be significantly reduced by this approach, this numerical procedure has not been adopted in this work. The theory developed has been utilized to determine the initial osculating elements required to numerically propagate the satellite orbit. It is noted that the numerical propagation can also be initialized by selecting arbitrary osculating initial conditions, and then computing the mean initial conditions for the analytical propagation by using the inverse mean-to-osculating transformation, as given in Eq. 2.20. Kinoshita's second-order theory [101], which is based on eccentricity expansions, is also implemented to compare the accuracy for moderate to high values of the orbital eccentricity. Kinoshita computed the generating functions up to order three for the short-period and long-period effects for J_2 by expanding the terms in powers of eccentricity up to $O(e^6)$. Using the generating functions up to order two from his work, the transformations were generated for the nonsingular elements using Hori's method [58]. The example orbits were propagated by using these two analytical theories as well as by GMAT, first for the main problem (i.e., including J_2 perturbation only). The mean initial elements of the orbit were chosen as: semimajor axis $13300\ km$, inclination 50°, argument of perigee 30°, and all the remaining angles 0°. The simulations were run for a period of ten days for a range of the orbital eccentricities. The osculating initial conditions for GMAT propagation were computed using the second-order transformation, including the short-period and long-period perturbations due to J_2, up to order two.

Figures 3.1 and 3.2 show the position and velocity propagation errors obtained from the two theories for the J_2 problem, computed using GMAT results as the true values. Both the theories included secular J_2 effects up to order three and long-period and short-period J_2 effects up to order two. However, the periodic effects computed using Kinoshita's theory are accurate up to $O(e^5)$ only. For this particular simulation case, the GMAT gravity model was also chosen to include

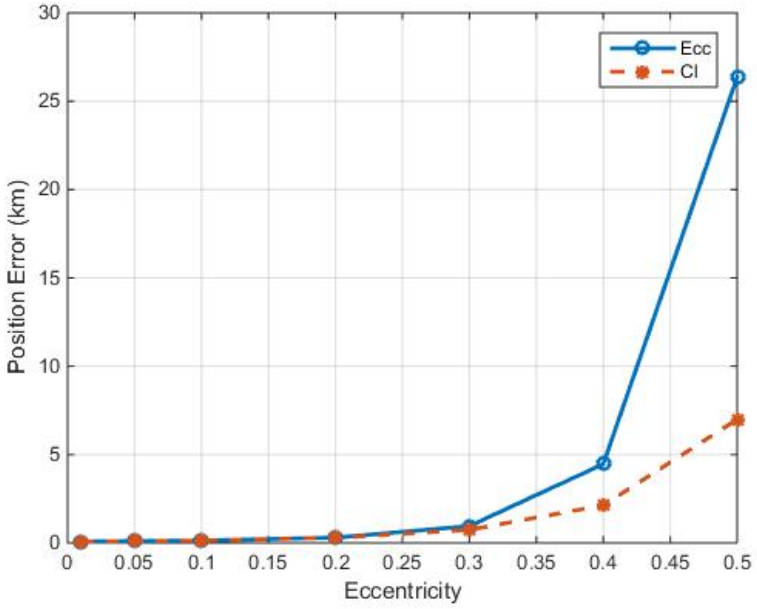

Figure 3.1: Absolute position errors versus the eccentricity in case of Kinoshita's theory (Ecc) and the closed-form theory (Cl) for the main problem of AST after 10 days of propagation [1].

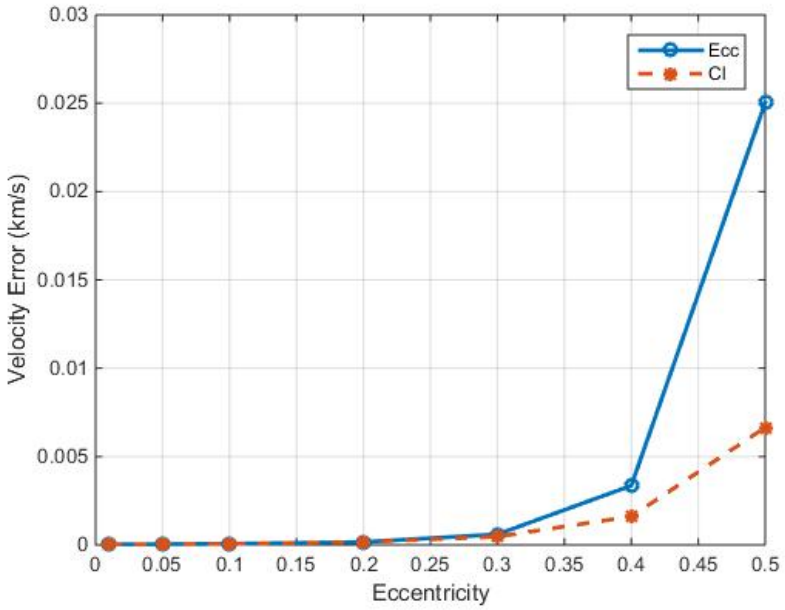

Figure 3.2: Absolute velocity errors versus the eccentricity in case of Kinoshita's theory (Ecc) and the closed-form theory (Cl) for the main problem of AST after 10 days of propagation [1].

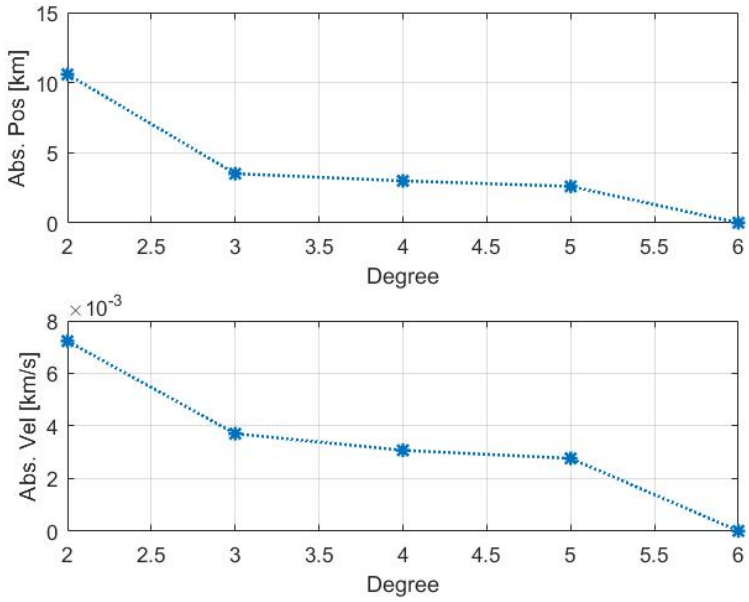

Figure 3.3: Absolute position and velocity errors after 10 days of propagation versus the degree up to which the zonal harmonics are included in the AST with explicit expressions. The initial mean classical elements are $[7100, 0.01, 50^{\circ}, 0, 0, 0]$.

only J_2 zonal harmonic. It is noted from these results that propagation errors from the closed-form and Kinoshita's theories are small and match very well up to eccentricity values of 0.2. For higher eccentricities, the closed-form theory shows significant improvement over Kinoshita's theory for position as well as velocity errors. This example was chosen to enable the testing of the theories for high eccentricity orbits. Next, three different orbits were propagated using GMAT with 6×0 gravity model, and the proposed satellite theory with the zonal harmonics included up to J_6 in an incremental manner. The resulting position and velocity errors of the theory are shown in Figures 3.3-3.5. The trends for the position and velocity errors for the three kinds of orbits including the circular one are similar, and a significant improvement in the accuracy is noted when the contributions of the zonal harmonics up to J_6 are included in the theory.

3.2 Satellite Theory for an Arbitrary Zonal Harmonic

This section presents the analytic theory of an artificial satellite, which is closed-form in eccentricity, for the complete zonal problem [228]. For any zonal harmonic J_n ($n \geq 3$), the generalized

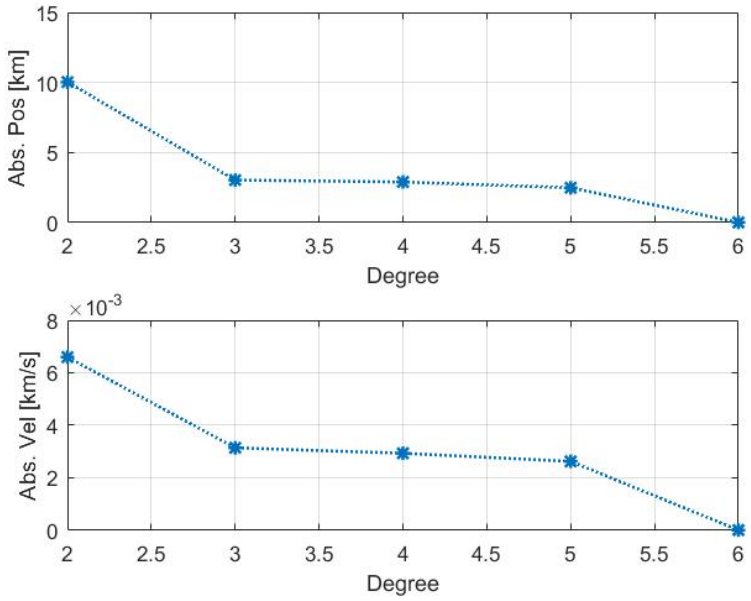

Figure 3.4: Absolute position and velocity errors after 10 days of propagation versus the degree up to which the zonal harmonics are included in the AST with explicit expressions. The initial mean classical elements are $[7100, 0, 50^\circ, 0, 0, 0]$.

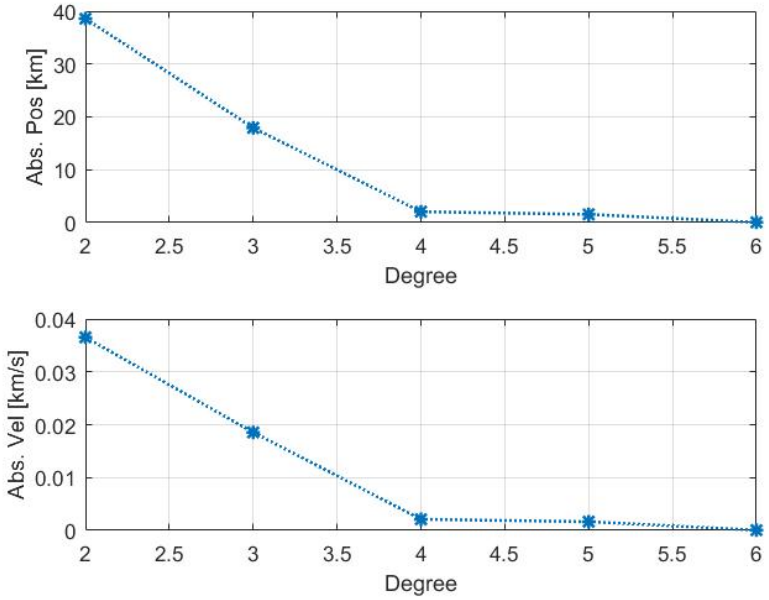

Figure 3.5: Absolute position and velocity errors after 10 days of propagation versus the degree up to which the zonal harmonics are included in the AST with explicit expressions. The initial mean classical elements are $[7100, 0, 50^\circ, 10^\circ, 20^\circ, 30^\circ]$.

analytic expressions for the second-order mean rates, first-order long-period, and second-order short-period effects are provided that give a readily accessible solution for the complete zonal problem. These analytic expressions are computed using the averaged Hamiltonian and the short-period generating function derived first by Saedeleer [117]. He considered all the zonal harmonics as the first-order perturbations, and computed the expressions for the first-order averaged Hamiltonian and short-period generating function valid for any zonal harmonic J_n ($n \geq 2$) using Deprit's method. In this work, J_2 is considered as the first-order perturbation as it is at least three orders of magnitude larger than other harmonic coefficients. The higher degree zonal harmonics J_n ($n \geq 3$) are considered as the second-order perturbations. The proposed approach simplifies the computation of the secular and short-period effects and also enables the computation of analytic expressions for the long-period effects up to first-order due to higher degree zonal harmonics. For J_2, the explicit expressions for the secular rates up to third-order and periodic variations up to second-order as discussed in the previous section are used. By using the generalized expressions derived in this section, the contributions to the secular and periodic effects due to any zonal harmonics J_n ($n \geq 3$) can be conveniently added to the J_2 solution without having to go through the process of Delaunay normalizations. It is noted that the generalized expressions derived in this section are not expressed in a recursive form, however it is certainly possible to express them in a recursive form for efficient computations. In case of the secular and long-period variations, Garfinkel and McAllister have provided expressions for an arbitrary zonal harmonic in terms of the associated Legendre polynomials in the eccentricity and inclination [38, 39].

The Hamiltonian for the complete zonal problem is obtained using the disturbing function given in Eq. 3.1, as shown below:

$$\mathcal{H} = \mathcal{H}_0 + J_2\mathcal{H}_1 + \frac{J_2^2}{2!}\mathcal{H}_2, \tag{3.22}$$

where

$$\mathcal{H}_0 = -\frac{1}{2}\frac{\mu^2}{L^2},$$

$$\mathcal{H}_1 = \frac{\mu R_e^2}{a^3}\left(\frac{a}{r}\right)^3 P_2(\sin\phi),$$
$$\mathcal{H}_2 = \sum_{n=3}^{\infty}\mathcal{H}_{2,n} = \sum_{n=3}^{\infty}\frac{2!}{J_2^2}J_n\frac{\mu R_e^n}{a^{n+1}}\left(\frac{a}{r}\right)^{n+1} P_n(\sin\phi).$$

The Hamiltonian $\mathcal{H}$ for the complete zonal problem can be normalized using Deprit's method by separating the secular and periodic effects. The first normalization for averaging out the short-period terms containing mean anomaly, l, produces a short-period generating function $\mathcal{W}$ and the singly-averaged Hamiltonian $\mathcal{K}$ that includes long-period as well as secular terms. A second normalization is necessary to separate the long-period terms containing the argument of perigee angle, g, to produce the doubly-averaged Hamiltonian $\bar{\mathcal{K}}$ consisting of only the secular effects as also discussed in the previous section. Because J_2 is considered as the only first-order perturbation, $\mathcal{K}_1$ and $\mathcal{W}_1$ obtained during the first normalization, have no contributions from the other zonals. The second-order perturbation term H_2 appear for the first time at the second order in Eq. 3.9, and involves computation of Poisson brackets only at the third order. As a result, the second-order contributions $\mathcal{K}_{2,n}$ to $\mathcal{K}_2$, and $\mathcal{W}_{2,n}$ to $\mathcal{W}_2$ due to any zonal harmonic J_n ($n \geq 3$) can be computed using the following equations:

$$\mathcal{K}_{2,n} = \frac{1}{2\pi}\int_0^{2\pi}\mathcal{H}_{2,n}\frac{r^2}{a^2\sqrt{1-e^2}}\,\mathrm{d}f, \tag{3.23}$$

$$\mathcal{W}_{2,n} = -\frac{1}{\frac{\partial\mathcal{H}_0}{\partial L}}\left(\mathcal{K}_{2,n}(l-f) - \int_p\mathcal{H}_{2,n}\frac{r^2}{a^2\sqrt{1-e^2}}\,\mathrm{d}f\right), \tag{3.24}$$

where the following relation is used to change the integration variable from the mean anomaly l to the true anomaly f:

$$\mathrm{d}l = \frac{r^2}{a^2\sqrt{1-e^2}}\mathrm{d}f.$$

The notation $\int_p$ indicates that the integration is performed for the periodic part of the integrand only, i.e., terms involving cosine and sine functions of the true or mean anomaly. By making use of the definition of $\mathcal{H}$ in Eq. 3.22, the above integrals can be written as

$$\mathcal{K}_{2,n} = \frac{1}{2\pi}\frac{2!}{J_2^2}J_n\frac{\mu R_e^n}{a^{n+1}\sqrt{1-e^2}}\int_0^{2\pi}\left(\frac{a}{r}\right)^{n-1}P_n(\sin(\phi))\,\mathrm{d}f, \tag{3.25}$$

$$\mathcal{W}_{2,n} = \sqrt{\frac{a^3}{\mu}}\left(K_{2,n}(f-l) + \frac{2!}{J_2^2}J_n\frac{\mu R_e^n}{a^{n+1}\sqrt{1-e^2}}\int_p\left(\frac{a}{r}\right)^{n-1}P_n(\sin(\phi))\,\mathrm{d}f\right), \tag{3.26}$$

where

$$\sin(\phi) = \sin(i)\sin(f+g),$$

and i represents the inclination. The following expansion formulae, including the definition for Legendre polynomials, can be used to transform the above integrals into a suitable form for integration [229]:

$$P_n(x) = \frac{1}{2^n}\sum_{j=0}^{\lfloor\frac{n}{2}\rfloor}\frac{(-1)^j(2n-2j)!}{j!\,(n-j)!\,(n-2j)!}x^{n-2j}, \tag{3.27}$$

$$\left(\frac{a}{r}\right)^{n-1} = \sum_{k=0}^{n-1}\binom{n-1}{k}\frac{e^k\cos^k(f)}{\eta^{2(n-1)}}, \tag{3.28}$$

$$\sin^{2n}(x) = \frac{1}{2^{2n}}\sum_{j=0}^{n-1}(-1)^{n-j}2\binom{2n}{j}\cos(2(n-j)x) + \binom{2n}{n}, \tag{3.29}$$

$$\sin^{2n-1}(x) = \frac{1}{2^{2n-2}}\sum_{j=0}^{n-1}(-1)^{n+j-1}\binom{2n-1}{j}\sin((2n-2j-1)x), \tag{3.30}$$

$$\cos^{2n}(x) = \frac{1}{2^{2n}}\sum_{k=0}^{n-1}2\binom{2n}{k}\cos(2(n-k)x) + \binom{2n}{n}, \tag{3.31}$$

$$\cos^{2n-1}(x) = \frac{1}{2^{2n-2}}\sum_{k=0}^{n-1}\binom{2n-1}{k}\cos((2n-2k-1)x), \tag{3.32}$$

where $\eta = \sqrt{1-e^2}$. The notations $\binom{}{}$, $\lfloor\ \rfloor$, $\lceil\ \rceil$ represent binomial coefficients, floor and ceil-

ing functions, respectively. Substituting the above formulae in Eqs. 3.25 and 3.26 results in the following integrals and their solutions [117]:

$$\int \cos^k(f)\mathrm{d}f = \frac{1}{2^k}\left(\sum_{s=0}^{\lfloor\frac{k-1}{2}\rfloor} 2\binom{k}{s}\frac{\sin(k-2s)f}{k-2s} + \lambda_k\binom{k}{\frac{k}{2}}f\right) \equiv \frac{1}{2^k}\left(C(f) + \lambda_k\binom{k}{\frac{k}{2}}f\right), \tag{3.33}$$

$$\int_0^{2\pi} \cos^k(f)\mathrm{d}f = \lambda_k\frac{1}{2^k}\binom{k}{\frac{k}{2}}2\pi, \tag{3.34}$$

$$\int_p \cos^k(f)\cos(cf)\mathrm{d}f = \frac{1}{2^k}\left\{\sum_{s=0}^{\lfloor\frac{k-1}{2}\rfloor}\binom{k}{s}\left(\frac{\sin(k-2s+c)f}{k-2s+c}\right)\right.$$
$$\left. + \sum_{\substack{s=0\\ s\neq s^*}}^{\lfloor\frac{k-1}{2}\rfloor}\binom{k}{s}\left(\frac{\sin(k-2s-c)f}{k-2s-c}\right) + \lambda_k\binom{k}{\frac{k}{2}}\frac{\sin(cf)}{c}\right\} \equiv \frac{1}{2^k}\left\{D_c(f)\right\}, \tag{3.35}$$

$$\int_0^{2\pi} \cos^k(f)\cos(cf)\mathrm{d}f = \begin{cases} \frac{\pi}{2^{k-1}}\binom{k}{\frac{k-c}{2}}, & \text{if } (k,c) \text{ have the same parity, and } (c \leq k) \\ 0, & \text{otherwise} \end{cases} \tag{3.36}$$

$$\int_p \cos^k(f)\sin(cf)\mathrm{d}f = \frac{1}{2^k}\left\{\sum_{s=0}^{\lfloor\frac{k-1}{2}\rfloor}\binom{k}{s}\left(\frac{-\cos(k-2s+c)f}{k-2s+c}\right)\right.$$
$$\left. + \sum_{\substack{s=0\\ s\neq s^*}}^{\lfloor\frac{k-1}{2}\rfloor}\binom{k}{s}\left(\frac{\cos(k-2s-c)f}{k-2s-c}\right) - \lambda_k\binom{k}{\frac{k}{2}}\frac{\cos(cf)}{c}\right\} \equiv \frac{1}{2^k}\left\{E_c(f)\right\}, \tag{3.37}$$

$$\int_0^{2\pi} \cos^k(f)\sin(cf)\mathrm{d}f = 0, \quad \text{for } (k,c) \in N \tag{3.38}$$

where

$$\lambda_k = 1 + \lfloor\frac{k}{2}\rfloor - \lceil\frac{k}{2}\rceil = \begin{cases} 1 & \text{for } k \text{ even} \\ 0 & \text{for } k \text{ odd,} \end{cases}$$

$$s^* = \frac{k-c}{2}.$$

Using the above results, Saedeleer computed the expressions for the integrals in Eqs. 3.25 and 3.26 for a general zonal harmonic, which are reproduced here after slight modifications [117]. For the even zonal harmonics J_n ($n \geq 3$), the results are

$$\mathcal{K}_{2,n} = \delta_n(a,e) \sum_{j=0}^{\lfloor \frac{n}{2} \rfloor} \beta_{j,n}(i) \sum_{\text{even } k=0}^{n-1} \frac{\alpha_{k,n}(e)}{2^k} \left\{ \binom{n-2j}{\frac{n}{2}-j} \binom{k}{\frac{k}{2}} + \sum_{p=0}^{\frac{n}{2}-j-1} \gamma_{p,j,n} \binom{k}{\frac{k-(n-2j-2p)}{2}} \cos(n-2j-2p)g \right\}, \quad (3.39)$$

$$\mathcal{W}_{2,n} = \sqrt{\frac{a^3}{\mu}} K_{2,n}(f-l) + \delta'_n(a,e) \sum_{j=0}^{\lfloor \frac{n}{2} \rfloor} \beta_{j,n}(i) \sum_{k=0}^{n-1} \frac{\alpha_{k,n}(e)}{2^k} \left\{ \binom{n-2j}{\frac{n}{2}-j} C(f) + \sum_{p=0}^{\frac{n}{2}-j-1} \gamma_{p,j,n} \left(\cos(n-2j-2p)g \; D_{n-2j-2p}(f) - \sin(n-2j-2p)g \; E_{n-2j-2p}(f) \right) \right\}, \quad (3.40)$$

while for the odd zonal harmonics ($n \geq 3$)

$$\mathcal{K}_{2,n} = \delta_n(a,e) \sum_{j=0}^{\lfloor \frac{n}{2} \rfloor} \beta_{j,n}(i) \sum_{\text{odd } k=0}^{n-1} \frac{\alpha_{k,n}(e)}{2^k} \sum_{p=0}^{\frac{n-1}{2}-j} \gamma_{p,j,n} \binom{k}{\frac{k-(n-2j-2p)}{2}} \sin(n-2j-2p)g, \quad (3.41)$$

$$\mathcal{W}_{2,n} = \sqrt{\frac{a^3}{\mu}} K_{2,n}(f-l) + \delta'_n(a,e) \sum_{j=0}^{\lfloor \frac{n}{2} \rfloor} \beta_{j,n}(i) \sum_{k=0}^{n-1} \frac{\alpha_{k,n}(e)}{2^k} \times \left\{ \sum_{p=0}^{\frac{n-1}{2}-j} \gamma_{p,j,n} \left(\cos(n-2j-2p)g \; E_{n-2j-2p}(f) + \sin(n-2j-2p)g \; D_{n-2j-2p}(f) \right) \right\}, \quad (3.42)$$

where

$$\delta_n(a,e) = 2\frac{J_n}{J_2^2}\frac{\mu R_e^n}{2^n \eta^{2n-1} a^{n+1}},$$

$$\delta'_n(a,e) = 2\frac{J_n}{J_2^2}\frac{\sqrt{\mu} R_e^n}{2^n \eta^{2n-1} a^{n-\frac{1}{2}}},$$

$$\beta_{j,n}(i) = \frac{(-1)^j (2n-2j)! \sin^{n-2j}(i)}{j!\,(n-j)!\,(n-2j)!\,2^{n-2j}},$$

$$\alpha_{k,n}(e) = e^k \binom{n-1}{k},$$

$$\gamma_{p,j,n} = (-1)^{\lfloor \frac{n}{2} \rfloor - j \mp p}\, 2\binom{n-2j}{p}.$$

The upper sign in the above formulae for γ applies for the case of n even and the lower sign for the case of n odd.

3.2.1 Secular Effects

The analytic expressions for the secular or mean rates of any set of orbital elements due to any zonal harmonic J_n ($n \geq 3$) can be derived using the results from Eqs. 3.39 and 3.41 by ignoring the long-period terms. In this subsection, expressions for the secular rates of the equinoctial elements for an arbitrary zonal harmonic are derived. The equinoctial elements are nonsingular for circular and equatorial orbits, however they are not canonical. As a result, the secular rates of the Delaunay elements are computed first, which can then be used to compute the rates of the equinoctial elements. After ignoring the terms dependent on g, the second-order Kamiltonian is only a function of the three action variables a, e, and i (or to be exact L, G, and H) for the even harmonics, and it is zero for the odd harmonics. The expressions for the mean rates of the Delaunay elements, $\mathcal{D}$, due to even harmonics are computed using Hamilton's equations as follows:

$$\dot{\mathcal{D}}_k = \frac{\partial \mathcal{K}_{2,n}}{\partial \mathcal{D}_{k+3}}, \quad \dot{\mathcal{D}}_{k+3} = -\frac{\partial \mathcal{K}_{2,n}}{\partial \mathcal{D}_k}, \quad \text{where } k = 1, 2, 3. \tag{3.43}$$

The following partial derivatives are required to compute the secular rates for the Delaunay elements:

$$\frac{\partial}{\partial L} = \frac{\partial a}{\partial L}\frac{\partial}{\partial a} + \frac{\partial e}{\partial L}\frac{\partial}{\partial e}, \tag{3.44}$$

$$\frac{\partial}{\partial G} = \frac{\partial e}{\partial G}\frac{\partial}{\partial e} + \frac{\partial i}{\partial G}\frac{\partial}{\partial i}, \tag{3.45}$$

$$\frac{\partial}{\partial H} = \frac{\partial i}{\partial H}\frac{\partial}{\partial i}. \tag{3.46}$$

Using the above partial derivatives and Eq. 3.43, the following expressions for the second-order contributions to the secular rates of the Delaunay elements due to any even zonal J_n ($n \geq 3$) can be computed:

$$\dot{l}_n = \delta_n(a,e)\sum_{j=0}^{\lfloor \frac{n}{2} \rfloor}\beta_{j,n}(i)\sum_{\text{even } k=0}^{n-1}\frac{\alpha_{k,n}(e)}{2^k}\binom{n-2j}{\frac{n}{2}-j}\binom{k}{\frac{k}{2}}\frac{1}{L}\left\{-3+k\frac{\eta^2}{e^2}\right\}, \tag{3.47}$$

$$\dot{g}_n = \delta_n(a,e)\sum_{j=0}^{\lfloor \frac{n}{2} \rfloor}\beta_{j,n}(i)\sum_{\text{even } k=0}^{n-1}\frac{\alpha_{k,n}(e)}{2^k}\binom{n-2j}{\frac{n}{2}-j}\binom{k}{\frac{k}{2}}\frac{1}{G}\left\{-(2n-1)-k\frac{\eta^2}{e^2}+\frac{(n-2j)}{\tan^2(i)}\right\}, \tag{3.48}$$

$$\dot{h}_n = \delta_n(a,e)\sum_{j=0}^{\lfloor \frac{n}{2} \rfloor}\beta_{j,n}(i)\sum_{\text{even } k=0}^{n-1}\frac{\alpha_{k,n}(e)}{2^k}\binom{n-2j}{\frac{n}{2}-j}\binom{k}{\frac{k}{2}}\frac{1}{H}\left\{-\frac{(n-2j)}{\tan^2(i)}\right\}, \tag{3.49}$$

$$\dot{L}_n = \dot{G}_n = \dot{H}_n = 0. \tag{3.50}$$

It is noted that the odd harmonics have no contributions to the second-order secular rates. The total secular rates of the Delaunay elements $\dot{\mathcal{D}}$ are found by adding the secular rates due to J_2 to the above contributions from the higher degree zonal harmonics. To avoid singularity issues, the equinoctial elements $\mathcal{E} = [a, \Lambda, p_1, p_2, q_1, q_2]^T$ are used in this work, which can be propagated from

the initial time t_0 to the final time t using the Delaunay element rates as follows:

$$
\begin{aligned}
a(t) &= a(t_0), \\
\Lambda(t) &= \Lambda(t_0) + (\dot{l} + \dot{g} + \dot{h})(t - t_0), \\
p_1(t) &= p_1(t_0)\cos(\dot{h}(t - t_0)) - p_2(t_0)\sin(\dot{h}(t - t_0)), \\
p_2(t) &= p_2(t_0)\cos(\dot{h}(t - t_0)) + p_1(t_0)\sin(\dot{h}(t - t_0)), \\
q_1(t) &= q_1(t_0)\cos((\dot{g} + \dot{h})(t - t_0)) - q_2(t_0)\sin((\dot{g} + \dot{h})(t - t_0)), \\
q_2(t) &= q_2(t_0)\cos((\dot{g} + \dot{h})(t - t_0)) + q_1(t_0)\sin((\dot{g} + \dot{h})(t - t_0)),
\end{aligned}
\tag{3.51}
$$

where

$$
\begin{aligned}
a &= a, \\
\Lambda &= l + g + h, \\
p_1 &= \tan\left(\frac{i}{2}\right)\cos(h), \\
p_2 &= \tan\left(\frac{i}{2}\right)\sin(h), \\
q_1 &= e\,\cos(g + h), \\
q_2 &= e\,\sin(g + h).
\end{aligned}
$$

3.2.2 Long-Period Effects

A second Delaunay normalization is needed to compute the long-period generating function. The first-order long-period generating function $\bar{\mathcal{W}}_1$ is computed using the following second-order equation from Eq. 3.18:

$$(\bar{\mathcal{K}}_1 + \mathcal{K}_1, \bar{\mathcal{W}}_1) + \mathcal{K}_2 = \bar{\mathcal{K}}_2, \tag{3.52}$$

where $\mathcal{K}_2$ represents the second-order singly-averaged Hamiltonian that includes the long-period terms dependent on g due to the zonals J_n ($n \geq 3$), $\bar{\mathcal{K}}_2$ is the second-order Kamiltonian with only the secular terms, and $\bar{\mathcal{W}}_1$ is the first-order generating function for long-period effects. Because J_2 harmonic has no long-period terms dependent on g, $\bar{\mathcal{K}}_1 = \mathcal{K}_1$. The Poisson bracket in the above equation can be evaluated to obtain $\bar{\mathcal{W}}_{1,n}$ for an arbitrary zonal harmonic J_n ($n \geq 3$) as shown below:

$$\bar{\mathcal{W}}_{1,n} = \frac{1}{2\frac{\partial \bar{\mathcal{K}}_1}{\partial G}} \int_{lp} \mathcal{K}_{2,n} \, \mathrm{d}g. \tag{3.53}$$

The notation $\int_{lp}$ denotes the integration of the long-periodic terms of the integrand only. The first-order Kamiltonian $\mathcal{K}_1$ has contributions from J_2 only, and its value is computed using the methods discussed in Subsection 3.1 and is given below:

$$\mathcal{K}_1 = -\frac{1}{4} \frac{{R_e}^2 \mu \, (3 \, \cos^2(i) - 1)}{a^3 \eta^3}. \tag{3.54}$$

Substituting the above value for $\mathcal{K}_1$, and $\mathcal{K}_{2,n}$ from Eqs. 3.39 and 3.41 into Eq. 3.53, the final expression for $\bar{\mathcal{W}}_1$ for the even zonal harmonics J_n ($n \geq 3$) is

$$\bar{\mathcal{W}}_{1,n} = -\frac{2}{3} \frac{a^{7/2}\eta^4}{\sqrt{\mu}{R_e}^2 \left(1 - 5\cos^2(i)\right)} \delta_n(a,e) \sum_{j=0}^{\lfloor \frac{n}{2} \rfloor} \beta_{j,n}(i) \sum_{\text{even } k=0}^{n-1} \frac{\alpha_{k,n}(e)}{2^k} \times \left\{ \sum_{p=0}^{\frac{n}{2}-j-1} \gamma_{p,j,n} \binom{k}{\frac{k-(n-2j-2p)}{2}} \frac{\sin(n-2j-2p)g}{(n-2j-2p)} \right\}, \tag{3.55}$$

while the same for the odd harmonics is

$$\bar{\mathcal{W}}_{1,n} = \frac{2}{3}\frac{a^{7/2}\eta^4}{\sqrt{\mu}{R_e}^2\left(1-5\cos^2\left(i\right)\right)}\delta_n(a,e)\sum_{j=0}^{\lfloor\frac{n}{2}\rfloor}\beta_{j,n}(i)\sum_{\text{odd } k=0}^{n-1}\frac{\alpha_{k,n}(e)}{2^k}\times$$
$$\left\{\sum_{p=0}^{\frac{n-1}{2}-j}\gamma_{p,j,n}\binom{k}{\frac{k-(n-2j-2p)}{2}}\frac{\cos(n-2j-2p)g}{(n-2j-2p)}\right\}. \quad (3.56)$$

The two expressions for $\bar{\mathcal{W}}_{2,n}$ for the even and odd zonal harmonics can be combined and succinctly written as follows:

$$\bar{\mathcal{W}}_{1,n} = \sin(i)W_1(a,e,i)W_2(g), \quad (3.57)$$

where

$$W_1(a,e,i) = \delta_n^{LP}(a,e)\sum_{j=0}^{\lfloor\frac{n}{2}\rfloor}\beta_{j,n}^{LP}(i)\sum_{\text{even[odd] } k=0}^{n-1}\frac{\alpha_{k,n}(e)}{2^k},$$

$$W_2(g) = \sum_{p=0}^{\lfloor\frac{n-1}{2}\rfloor-j}\gamma_{p,j,n}\binom{k}{\frac{k-(n-2j-2p)}{2}}\frac{(-\sin[\cos](n-2j-2p)g)}{(n-2j-2p)},$$

$$W_3(a,e,i) = \delta_n^{LP}(a,e)\sum_{j=0}^{\lfloor\frac{n}{2}\rfloor}\beta_{j,n}^{LP}(i)\sum_{\text{even[odd] } k=1}^{n-1}\frac{n-k}{k}\frac{\alpha_{k-1,n}(e)}{2^k},$$

$$W_4(g) = \sum_{p=0}^{\lfloor\frac{n-1}{2}\rfloor-j}\gamma_{p,j,n}\binom{k}{\frac{k-(n-2j-2p)}{2}}(-\cos[-\sin](n-2j-2p)g),$$

$$\delta_n^{LP}(a,e) = \frac{2}{3}\frac{a^{7/2}\eta^4}{\sqrt{\mu}{R_e}^2}\delta_n(a,e),$$

$$\beta_{j,n}^{LP}(i) = \frac{(-1)^j(2n-2j)!\sin^{n-2j-1}(i)}{(1-5\cos^2(i))j!\,(n-j)!\,(n-2j)!\,2^{n-2j}},$$

In the above equations, the square bracketed terms are used for the odd zonal harmonics only, and they replace the preceding terms that are used for the even zonal harmonics. It is noted that in the

above definition for $\beta_{j,n}^{LP}$, the power of $\sin(i)$, i.e., $n-2j-1$ can never be less than zero because in that case the corresponding W_2 and W_4 terms will be zero. Using the above results, the analytic expressions for the long-period effects due to any zonal harmonic J_n ($n \geq 3$) can be computed by evaluating the Poisson brackets for the equinoctial elements. These expressions for the first-order long-period variations are

$$\left(a, \bar{\mathcal{W}}_{1,n}\right) = 0, \tag{3.58}$$

$$\left(\Lambda, \bar{\mathcal{W}}_{1,n}\right) = \sin(i)\frac{W_1(a,e,i)}{\sqrt{\mu a}}\left[-\frac{2n-5}{\eta} - \frac{\eta k}{1+\eta} + \frac{10\cos(i)(1-\cos(i))}{\eta(1-5\cos^2(i))} + \frac{n-2j}{\eta}\left(\frac{-\cos(i)}{2\cos^2\left(\frac{i}{2}\right)}\right)\right] W_2(g), \tag{3.59}$$

$$\left(p_1, \bar{\mathcal{W}}_{1,n}\right) = \frac{\cos(i)}{2\eta\sqrt{\mu a}\cos^2\left(\frac{i}{2}\right)}\left[\sin(h)W_1\left\{(n-2j) - \frac{10\sin^2(i)}{1-5\cos^2(i)}\right\}W_2 - \cos(h)W_1W_4\right], \tag{3.60}$$

$$\left(p_2, \bar{\mathcal{W}}_{1,n}\right) = \frac{\cos(i)}{2\eta\sqrt{\mu a}\cos^2\left(\frac{i}{2}\right)}\left[-\cos(h)W_1\left\{(n-2j) - \frac{10\sin^2(i)}{1-5\cos^2(i)}\right\}W_2 - \sin(h)W_1W_4\right], \tag{3.61}$$

$$\left(q_1, \bar{\mathcal{W}}_{1,n}\right) = \sin(i)\frac{\sin(g+h)}{\eta\sqrt{\mu a}}\left[W_1\left\{e(2n-5) - \frac{5e\sin(2i)\tan\left(\frac{i}{2}\right)}{1-5\cos^2(i)} + \frac{e\cos(i)(n-2j)}{2\cos^2\left(\frac{i}{2}\right)}\right\}W_2 + \eta^2 W_3 k W_2\right] + \sin(i)\frac{\eta}{\sqrt{\mu a}}\cos(g+h)W_3W_4, \tag{3.62}$$

$$\left(q_2, \bar{\mathcal{W}}_{1,n}\right) = -\sin(i)\frac{\cos(g+h)}{\eta\sqrt{\mu a}}\left[W_1\left\{e(2n-5) - \frac{5e\sin(2i)\tan\left(\frac{i}{2}\right)}{1-5\cos^2(i)} + \frac{e\cos(i)(n-2j)}{2\cos^2\left(\frac{i}{2}\right)}\right\}W_2 + \eta^2 W_3 k W_2\right] + \sin(i)\frac{\eta}{\sqrt{\mu a}}\sin(g+h)W_3W_4. \quad (3.63)$$

In the above equation, the order of the terms in a product must be preserved because of the presence of the summation indices. With the above results, the first-order long-period variations due to an arbitrary zonal harmonic J_n ($n \geq 3$) can be added to $\mathcal{E}_m$ as well as subtracted from $\mathcal{E}_{LP}$ using the near-identity transformations given in Eq. 3.21.

3.2.3 Short-Period Effects

The second-order short-period generating function for any zonal harmonic J_n ($n \geq 3$), given in Eqs. 3.40 and 3.42, can be written succinctly in a unified form for the even and odd zonal harmonics as:

$$\mathcal{W}_{2,n} = W_1(a,e,i,f,l,g) + W_2(a,e,i)W_3(f,g), \quad (3.64)$$

where

$$W_1(a,e,i,f,l,g) = \sqrt{\frac{a^3}{\mu}}\mathcal{K}_{2,n}(f-l),$$

$$\mathcal{K}_{2,n} = \delta_n(a,e)\sum_{j=0}^{\lfloor\frac{n}{2}\rfloor}\beta_{j,n}(i)\sum_{\text{even[odd]}\ k=0}^{n-1}\frac{\alpha_{k,n}(e)}{2^k}\left\{\lambda_n\binom{n-2j}{\frac{n}{2}-j}\binom{k}{\frac{k}{2}} + \sum_{p=0}^{\lfloor\frac{n-1}{2}\rfloor-j}\gamma_{p,j,n}\binom{k}{\frac{k-(n-2j-2p)}{2}}(\cos[\sin](n-2j-2p)g)\right\},$$

$$\beta_{j,n}(i) = \frac{(-1)^j (2n-2j)! \sin^{n-2j}(i)}{j!\,(n-j)!\,(n-2j)!\,2^{n-2j}},$$

$$W_2(a,e,i) = \delta'_n(a,e) \sum_{j=0}^{\lfloor \frac{n}{2} \rfloor} \beta_{j,n}(i) \sum_{k=0}^{n-1} \frac{\alpha_{k,n}(e)}{2^k},$$

$$\begin{aligned} W_3(f,g) = \lambda_n \binom{n-2j}{\frac{n}{2}-j} C(f) \\ + \sum_{p=0}^{\lfloor \frac{n-1}{2} \rfloor - j} \gamma_{p,j,n} \left\{ \sum_{s=0}^{\lfloor \frac{k-1}{2} \rfloor} \binom{k}{s} \left(\frac{\sin[-\cos]((k-2s+c)f+cg)}{k-2s+c} \right) \right. \\ \left. + \sum_{\substack{s=0 \\ s \neq s^*}}^{\lfloor \frac{k-1}{2} \rfloor} \binom{k}{s} \left(\frac{\sin[\cos]((k-2s-c)f-cg)}{k-2s-c} \right) + \lambda_k \binom{k}{\frac{k}{2}} \frac{\sin[-\cos](cf+cg)}{c} \right\}, \end{aligned}$$

$$c = n - 2j - 2p.$$

In the above equations, the square-bracketed terms applies for odd harmonics, which replaces the proceeding terms valid for the even harmonics. The analytic expressions for the second-order short-period effects due to any zonal harmonic greater than J_2 for the equinoctial elements can be computed by evaluating the corresponding Poisson brackets. These formulae are computed by hand, and are given below:

$$(a, \mathcal{W}_{2,n}) = -2\sqrt{\frac{a}{\mu}} \left[\sqrt{\frac{a^3}{\mu}} \mathcal{K}_{2,n} \left(\frac{\partial f}{\partial l} - 1 \right) + W_2 \left(\frac{\partial W_3}{\partial f} \right) \frac{\partial f}{\partial l} \right], \tag{3.65}$$

$$\begin{aligned} (\Lambda, \mathcal{W}_{2,n}) = \frac{3}{\sqrt{\mu a}} W_1 + \sqrt{\frac{a^3}{\mu}} \left\{ (f-l)\mathcal{K}_{2,n}^{LGH} + K_{2,n} f_{LG} \right\} \\ - \frac{W_2}{\eta\sqrt{\mu a}} \left\{ \frac{\cos(i)}{1+\cos(i)}(n-2j) + (2n-1) + \frac{k\eta^2}{1+\eta} \right\} W_3 + W_2 \left(\frac{\partial W_3}{\partial f} \right) f_{LG}, \end{aligned} \tag{3.66}$$

$$(p_1, \mathcal{W}_{2,n}) = \frac{1}{\eta\sqrt{\mu a}} \frac{\cos(i)}{1+\cos(i)} \left[-\sin(h) \left\{ \sqrt{\frac{a^3}{\mu}} (f-l) \left(-\mathcal{K}_{2,n}(n-2j)\right) - W_2(n-2j)W_3 \right\} \right.$$
$$\left. - \cos(h) \left\{ \sqrt{\frac{a^3}{\mu}} (f-l) \frac{\partial \mathcal{K}_{2,n}}{\partial g} + W_2 \frac{\partial W_3}{\partial g} \right\} \right], \quad (3.67)$$

$$(p_2, \mathcal{W}_{2,n}) = \frac{1}{\eta\sqrt{\mu a}} \frac{\cos(i)}{1+\cos(i)} \left[\cos(h) \left\{ \sqrt{\frac{a^3}{\mu}} (f-l) \left(-\mathcal{K}_{2,n}(n-2j)\right) - W_2(n-2j)W_3 \right\} \right.$$
$$\left. - \sin(h) \left\{ \sqrt{\frac{a^3}{\mu}} (f-l) \frac{\partial \mathcal{K}_{2,n}}{\partial g} + W_2 \frac{\partial W_3}{\partial g} \right\} \right], \quad (3.68)$$

$$(q_1, \mathcal{W}_{2,n}) = -\sin(g+h) \left\{ \sqrt{\frac{a^3}{\mu}} (f-l) \mathcal{K}_{2,n}^{eGH} - \sqrt{\frac{a^3}{\mu}} \frac{\partial f}{\partial e} \frac{\eta}{\sqrt{\mu a}} \mathcal{K}_{2,n} \right.$$
$$\left. - \left(\frac{\partial W_2}{\partial e} \frac{\eta}{\sqrt{\mu a}} + \frac{e}{\eta\sqrt{\mu a}} \frac{1}{1+\cos(i)} W_2^i \right) W_3 - \frac{\partial f}{\partial e} \frac{\eta}{\sqrt{\mu a}} W_2 \frac{\partial W_3}{\partial f} \right\}$$
$$- \cos(g+h) \left\{ W_1^{lge} + W_{23}^{lge} \right\}, \quad (3.69)$$

$$(q_2, \mathcal{W}_{2,n}) = \cos(g+h) \left\{ \sqrt{\frac{a^3}{\mu}} (f-l) \mathcal{K}_{2,n}^{eGH} - \sqrt{\frac{a^3}{\mu}} \frac{\partial f}{\partial e} \frac{\eta}{\sqrt{\mu a}} \mathcal{K}_{2,n} \right.$$
$$\left. - \left(\frac{\partial W_2}{\partial e} \frac{\eta}{\sqrt{\mu a}} + \frac{e}{\eta\sqrt{\mu a}} \frac{1}{1+\cos(i)} W_2^i \right) W_3 - \frac{\partial f}{\partial e} \frac{\eta}{\sqrt{\mu a}} W_2 \frac{\partial W_3}{\partial f} \right\}$$
$$- \sin(g+h) \left\{ W_1^{lge} + W_{23}^{lge} \right\}, \quad (3.70)$$

where

$$f_{LG} = \frac{\partial f}{\partial L} + \frac{\partial f}{\partial G} = -\sqrt{\frac{1-\eta}{1+\eta}}\frac{\sin(f)}{\eta}\left(\frac{2+e\cos(f)}{\sqrt{\mu a}}\right),$$

$$\frac{\partial f}{\partial l} = \frac{(1+e\cos(f))^2}{\eta^3},$$

$$\frac{\partial f}{\partial e} = \frac{(2+e\cos(f))\sin(f)}{\eta^2},$$

$$\frac{\partial W_2}{\partial e} = (2n-1)\frac{e}{\eta^2}W_2 + \delta_n'(a,e)\sum_{j=0}^{\lfloor \frac{n}{2} \rfloor}\beta_{j,n}(i)\sum_{k=1}^{n-1}\frac{(n-k)\alpha_{k-1,n}(e)}{2^k},$$

$$W_2^i = \sin(i)\frac{\partial W_2}{\partial i} = \cos(i)\left(W_2(n-2j)\right),$$

$$\begin{aligned}\frac{\partial W_3}{\partial f} = \lambda_n\binom{n-2j}{\frac{n}{2}-j}\sum_{s=0}^{\lfloor \frac{k-1}{2} \rfloor} 2\binom{k}{s}\cos(k-2s)f \\ + \sum_{p=0}^{\lfloor \frac{n-1}{2} \rfloor - j}\gamma_{p,j,n}\left\{\sum_{s=0}^{\lfloor \frac{k-1}{2} \rfloor}\binom{k}{s}\left(\cos[\sin]((k-2s+c)f+cg)\right)\right. \\ \left. + \sum_{\substack{s=0 \\ s\neq s^*}}^{\lfloor \frac{k-1}{2} \rfloor}\binom{k}{s}\left(\cos[-\sin]((k-2s-c)f-cg)\right) + \lambda_k\binom{k}{\frac{k}{2}}\cos[\sin](cf+cg)\right\},\end{aligned}$$

$$\begin{aligned}\frac{\partial W_3}{\partial g} = \sum_{p=0}^{\lfloor \frac{n-1}{2} \rfloor - j}\gamma_{p,j,n}\left\{\sum_{s=0}^{\lfloor \frac{k-1}{2} \rfloor}\binom{k}{s}\left(\frac{\cos[\sin]((k-2s+c)f+cg)}{k-2s+c}\right)c\right. \\ \left. - \sum_{\substack{s=0 \\ s\neq s^*}}^{\lfloor \frac{k-1}{2} \rfloor}\binom{k}{s}\left(\frac{\cos[-\sin]((k-2s-c)f-cg)}{k-2s-c}\right)c + \lambda_k\binom{k}{\frac{k}{2}}\cos[\sin](cf+cg)\right\},\end{aligned}$$

$$\mathcal{K}_{2,n}^{LGH} = \frac{\partial \mathcal{K}_{2,n}}{\partial L} + \frac{\partial \mathcal{K}_{2,n}}{\partial G} + \frac{\partial \mathcal{K}_{2,n}}{\partial H}$$
$$= \delta_n(a,e) \sum_{j=0}^{\lfloor \frac{n}{2} \rfloor} \beta_{j,n}(i) \sum_{\text{even[odd]}\ k=0}^{n-1} \frac{\alpha_{k,n}(e)}{2^k} \frac{1}{G} \left\{ -2(n+1) - (n-2j) \frac{\cos(i)}{2\cos^2\left(\frac{i}{2}\right)} \right\}$$
$$\times \left\{ \lambda_n \binom{n-2j}{\frac{n}{2}-j} \binom{k}{\frac{k}{2}} + \sum_{p=0}^{\lfloor \frac{n-1}{2} \rfloor - j} \gamma_{p,j,n} \binom{k}{\frac{k-(n-2j-2p)}{2}} (\cos[\sin](n-2j-2p)g) \right\},$$

$$\mathcal{K}_{2,n}^{eGH} = e\frac{\partial \mathcal{K}_{2,n}}{\partial G} + e\frac{\partial \mathcal{K}_{2,n}}{\partial H}$$
$$= \delta_n(a,e) \sum_{j=0}^{\lfloor \frac{n}{2} \rfloor} \beta_{j,n}(i) \sum_{\text{even[odd]}\ k=0}^{n-1} \frac{\alpha_{k,n}(e)}{2^k} \frac{1}{G} \left\{ -e(2n-1) - \frac{k\eta^2}{e} - e(n-2j) \frac{\cos(i)}{2\cos^2\left(\frac{i}{2}\right)} \right\}$$
$$\times \left\{ \lambda_n \binom{n-2j}{\frac{n}{2}-j} \binom{k}{\frac{k}{2}} + \sum_{p=0}^{\lfloor \frac{n-1}{2} \rfloor - j} \gamma_{p,j,n} \binom{k}{\frac{k-(n-2j-2p)}{2}} (\cos[\sin](n-2j-2p)g) \right\},$$

$$\frac{\partial \mathcal{K}_{2,n}}{\partial g} = \delta_n(a,e) \sum_{j=0}^{\lfloor \frac{n}{2} \rfloor} \beta_{j,n}(i) \sum_{\text{even[odd]}\ k=0}^{n-1} \frac{\alpha_{k,n}(e)}{2^k}$$
$$\times \left\{ \sum_{p=0}^{\lfloor \frac{n-1}{2} \rfloor - j} \gamma_{p,j,n} \binom{k}{\frac{k-(n-2j-2p)}{2}} (n-2j-2p)(-\sin[\cos](n-2j-2p)g) \right\},$$

$$W_1^{lge} = \frac{\partial W_1}{\partial l}\frac{\partial e}{\partial L} + \frac{\partial W_1}{\partial g}\frac{\partial e}{\partial G}$$
$$= \frac{a}{2\mu\eta} \left(4\cos(f) + e\cos(2f) + e\frac{2\eta^2 + 3\eta + 3}{1+\eta} \right) \mathcal{K}_{2,n}$$
$$- \frac{a\eta}{\mu}(f-l) \left\{ \delta_n(a,e) \sum_{j=0}^{\lfloor \frac{n}{2} \rfloor} \beta_{j,n}(i) \sum_{\text{even[odd]}\ k=1}^{n-1} \frac{\alpha_{k-1,n}(e)}{2^k} \frac{n-k}{k} \right.$$

$$\left. \sum_{p=0}^{\lfloor \frac{n-1}{2} \rfloor - j} \gamma_{p,j,n} \binom{k}{\frac{k-(n-2j-2p)}{2}} (n-2j-2p)(-\sin[\cos](n-2j-2p)g) \right\},$$

$$\begin{aligned} W_{23}^{lge} &= W_2 \frac{\partial W_3}{\partial f}\frac{\partial f}{\partial l}\frac{\partial e}{\partial L} + W_2 \frac{\partial W_3}{\partial g}\frac{\partial e}{\partial G} \\ &= \delta_n'(a,e) \sum_{j=0}^{\lfloor \frac{n}{2} \rfloor} \beta_{j,n}(i) \left\{ \frac{1}{2\eta\sqrt{\mu a}} \left(4\cos(f) + e\cos(2f) + 3e\right) \sum_{p=0}^{\lfloor \frac{n-1}{2} \rfloor - j} \gamma_{p,j,n} \cos[\sin](cf+cg) \right. \\ &\qquad \left. + \sum_{k=1}^{n-1} \frac{\alpha_{k-1,n}(e)}{2^k} \frac{n-k}{k} \frac{\eta^2}{\sqrt{\mu a}} \left(\frac{\partial \mathcal{W}_3}{\partial f}\frac{\partial f}{\partial l} - \frac{1}{\eta}\frac{\partial \mathcal{W}_3}{\partial g} \right) \right\}. \end{aligned}$$

With the above results, the second-order short-period variations due to an arbitrary zonal harmonic J_n ($n \geq 3$) can be added to $\mathcal{E}_{LP}$ as well as subtracted from $\mathcal{E}$ using the near-identity transformations given in Eq. 3.17.

3.2.4 Results

The analytic expressions derived in the previous subsections for the second-order short-period effects, the first-order long-period effects, and the second-order secular effects have been verified for the zonals J_3 and J_4 using Maple. The explicit expressions for the secular rates up to third-order, the long-period and short-period effects up to second-order due to J_2, computed in Section 3.1, are incorporated with the generalized expressions for an arbitrary zonal harmonic to construct a satellite theory for all the zonal harmonics without using any series expansions in the eccentricity.

To validate this satellite theory, GMAT numerical propagator with 70×0 JGM-3 gravity model is used as the truth model. Three different orbits are propagated analytically and numerically for ten days to compute position and velocity errors. The osculating initial semimajor axis for all the simulated orbits is equal to 7100 km. The first orbit has the osculating eccentricity equal to 0.01 and the inclination equal to 50°, and the other two orbits are circular and have zero inclination. Figures 3.6-3.8 show the absolute position and velocity root-sum-square (RSS) errors after ten days of propagation versus the harmonic degree up to which the zonal harmonics are included in

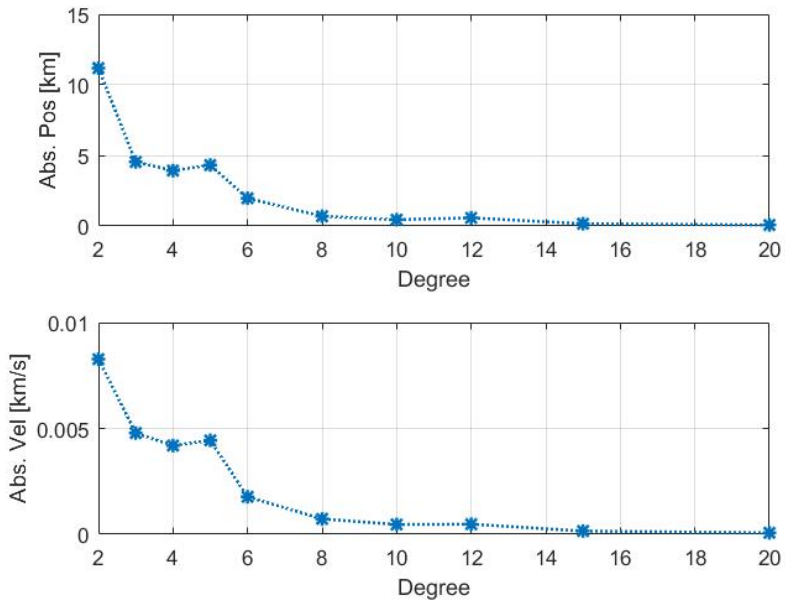

Figure 3.6: Absolute position and velocity errors after 10 days of propagation versus the degree up to which the zonal harmonics are included in the AST with generalized expressions. The initial osculating classical elements are $[7100, 0.01, 50^\circ, 0^\circ, 0^\circ, 0^\circ]$.

the theory for the three simulated orbits. The improvements in the position and velocity errors are clearly seen for all the three orbits with the increase in the number of zonal harmonics included.

3.3 The Hamiltonian with Tesseral Harmonics

The previous two sections detailed a satellite theory for the complete zonal gravitational problem. The effects of the tesseral harmonics on the motion of an artificial satellite of Earth is significant, especially due to C_{22} and S_{22} (the equatorial ellipticity). Moreover, the resonant effects of the tesseral harmonics with smaller magnitudes can also produce large propagation errors in the position and velocity if these effects are not taken into account. The existing methods to include the short-period effects of the tesseral harmonics in satellite theories, rely on the series expansions of the disturbing function in powers of either the eccentricity or the ratio of mean motion to Earth's angular velocity. These series expansions not only produce prohibitive large expressions, but also compromise the accuracy for orbits with medium to high values of the eccentricity. In this section, a perturbed Keplerian Hamiltonian with the tesseral harmonics is formulated. The following

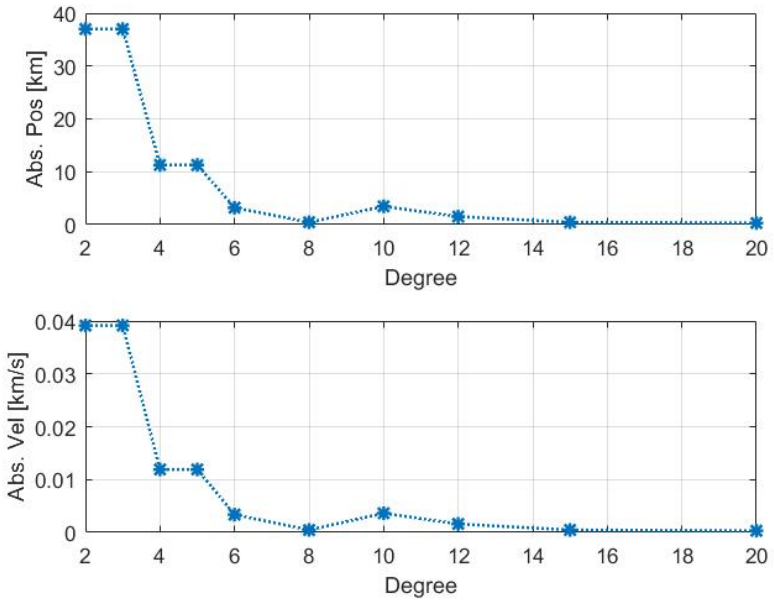

Figure 3.7: Absolute position and velocity errors after 10 days of propagation versus the degree up to which the zonal harmonics are included in the AST with generalized expressions. The initial osculating classical elements are $[7100, 0, 0°, 0°, 0°, 0°]$.

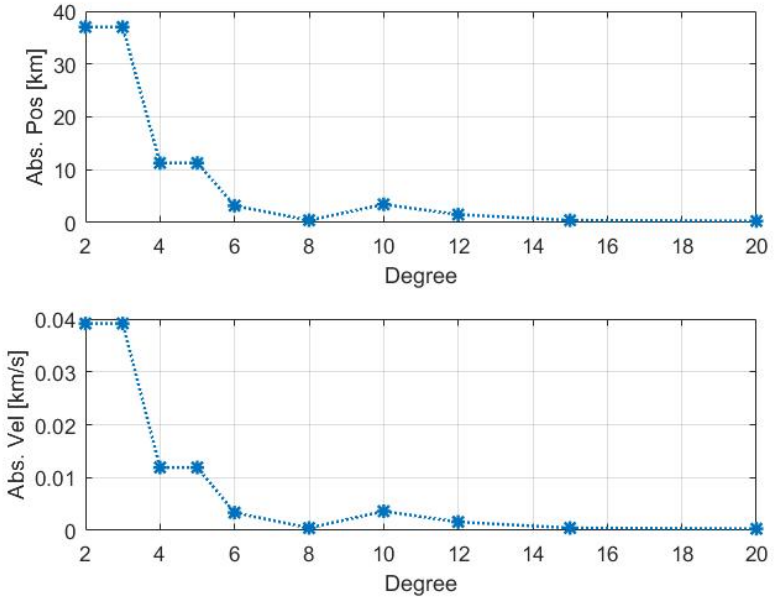

Figure 3.8: Absolute position and velocity errors after 10 days of propagation versus the degree up to which the zonal harmonics are included in the AST with generalized expressions. The initial osculating classical elements are $[7100, 0, 0°, 10°, 20°, 30°]$.

two sections discuss the two different approaches to perform Delaunay normalization of such a Hamiltonian without using series expansions in the eccentricity.

The tesseral disturbing function depends on the longitude of the satellite, when expressed in an inertial frame. In this work, Kaula's form of the geopotential, which is expressed in the inertial frame using the classical orbital elements and the Greenwich Sidereal Time, is used as the disturbing function for the tesserals [42]. The Hamiltonian formulated in the classical orbital elements, instead of the polar-nodal or Whittaker elements, results in simpler perturbation equations. Kaula's gravitational potential, expressed in terms of the true anomaly, is [42]

$$V_{nm} = \frac{\mu R_e^n}{r^{n+1}} \sum_{p=0}^{p=n} F_{nmp}(i) \left[CS_1 \cos(\Psi) + CS_2 \sin(\Psi) \right], \tag{3.71}$$

where

$$\Psi \equiv (n-2p)(f+g) + m(h-\theta),$$

$$CS_1 = \begin{cases} C_{nm} & \text{if } n-m \text{ is even} \\ -S_{nm} & \text{if } n-m \text{ is odd,} \end{cases}$$

$$CS_2 = \begin{cases} S_{nm} & \text{if } n-m \text{ is even} \\ C_{nm} & \text{if } n-m \text{ is odd.} \end{cases}$$

This representation of the disturbing potential contains a mix of the classical and Delaunay elements. The letters n and m represent the degree and order of the potential V_{nm}, respectively; θ represent the Greenwich Sidereal Time; and C_{nm} and S_{nm} are the spherical harmonic coefficients. Instead of using the original definition of the inclination function $F_{nmp}(i)$ given by Kaula, the following more computationally efficient definition is used in the present work [230, 231]:

$$F_{nmp}(i) = (-1)^{E\left(\frac{n-m+1}{2}\right)} \frac{(n+m)!}{2^n p!\,(n-p)!} \sum_{j=\max(n-2p-m,\,0)}^{j=\min(n-m,\,2n-2p)} (-1)^j \times \binom{2n-2p}{j} \binom{2p}{n-m-j} \cos^{2n-s}\left(\frac{i}{2}\right) \sin^s\left(\frac{i}{2}\right), \quad (3.72)$$

where $s = m - n + 2p + 2j$ and $E()$ represents the Entier (also called integer part) function. The above definition of the inclination function has only one summation compared to three present in Kaula's inclination function. This representation of the disturbing potential is also more computationally efficient than the one using the polar-nodal variables given by Segerman and Coffey [126].

Subsequent developments in this paper involve the integration of the disturbing potential with respect to f, a task made easier if the explicit occurrences of r in V_{nm} are eliminated by substituting the orbit equation. The powers of the cosine function introduced by the orbit equation are converted into the multiples of its argument using the following formulae [229]:

$$(1 + e\cos f)^{n+1} = \sum_{s=0}^{n+1} \binom{n+1}{s} e^s \cos^s f, \quad (3.73)$$

$$\cos^s f = \frac{1}{2^{s-1}} \left\{ \sum_{k=0}^{\lfloor \frac{s-1}{2} \rfloor} \binom{s}{k} \cos((s-2k)f) + \frac{\lambda_s}{2} \binom{s}{\frac{s}{2}} \right\}, \quad (3.74)$$

where λ_s is defined as

$$\lambda_s = \begin{cases} 1 & \text{s is even} \\ 0 & \text{s is odd.} \end{cases} \quad (3.75)$$

By using the trigonometric identities for converting the product of terms to sum of terms, the following expression for V_{nm} can be computed:

$$V_{nm} = \frac{\mu R_e^n}{a^{n+1}\eta^{2n+2}} \sum_{p=0}^{n} \sum_{s=0}^{n+1} F_{nmp}(i) e^s \binom{n+1}{s} \frac{1}{2^s} \left[\sum_{k=0}^{\lfloor \frac{s-1}{2} \rfloor} \binom{s}{k} \right.$$
$$\times \left[CS_1 \left(\cos(\Psi_1) + \cos(\Psi_2) \right) + CS_2 \left(\sin(\Psi_1) + \sin(\Psi_2) \right) \right]$$
$$\left. + \lambda_s \binom{s}{\frac{s}{2}} \left[CS_1 \cos(\Psi) + CS_2 \sin(\Psi) \right] \right], \quad (3.76)$$

where

$$\Psi_1 \equiv (n - 2p + s - 2k)f + (n - 2p)g + m(h - \theta),$$

$$\Psi_2 \equiv (n - 2p - s + 2k)f + (n - 2p)g + m(h - \theta),$$

and η is the eccentricity function equal to $\sqrt{1 - e^2}$ and $\lfloor \rfloor$ represents the floor function. In case of Earth, the oblateness coefficient C_{20}(=-J_2) is at least three orders of magnitude greater than any other zonal or tesseral coefficient. Therefore, the complete Hamiltonian $\mathcal{H}$ is expressed as a power series in C_{20} with $\mathcal{H}_0$ being the unperturbed Keplerian Hamiltonian as shown below:

$$\mathcal{H} = \mathcal{H}_0 + \epsilon \mathcal{H}_1 + \frac{\epsilon^2}{2!} \mathcal{H}_2, \quad (3.77)$$

where

$$\epsilon = C_{20} = -J_2,$$
$$\mathcal{H}_0 = -\frac{\mu^2}{2L^2},$$
$$\mathcal{H}_1 = -\frac{V_{20}}{C_{20}},$$
$$\mathcal{H}_2 = -\frac{2!}{C_{20}^2} V_{nm},\ m \neq 0 \text{ if } n = 2.$$

In the above equation, $\mathcal{H}_1$ is the oblateness disturbing potential, and $\mathcal{H}_2$ is the disturbing potential for the remaining spherical harmonics. It is noted that the negative signs in the above definitions of

$\mathcal{H}_0$, $\mathcal{H}_1$, and $\mathcal{H}_2$ are the result of considering the angle variables (l, g, h) as the first three canonical variables and the action variables (L, G, H) as the last three.

To perform the Delaunay normalization of the above Hamiltonian with the tesseral harmonics, the homological equations with the nonconservative canonical transformations of Deprit's method given in Eq. 2.22 can be used. As before, the zonal harmonics with degree higher than two enter these homological equations at second order through $\mathcal{H}_2$. As a result, there is no coupling between these zonal and tesseral harmonics, and the tesseral part of the second-order homological equation can be separated from all the zonal contributions as shown below:

$$(\mathcal{H}_0, \mathcal{W}_2^T) - \frac{\partial \mathcal{W}_2^T}{\partial t} + \mathcal{H}_2^T = \mathcal{K}_2^T, \tag{3.78}$$

where

$$\mathcal{H}_2^T = -\frac{2!}{C_{20}^2} V_{nm}\bigg|_{m\neq 0}.$$

The superscript T in the above equation indicates that these terms include only tesseral contributions. Through the disturbing function V_{nm}, there are short-period terms present in $\mathcal{H}_2^T$ that depend simultaneously on f and θ. The remaining terms that are only dependent on θ are called m-daily terms as they repeat m-times a day [42]. If the resonance effects due to tesserals are ignored then there is no secular or long-period contributions to $\mathcal{K}_2^T$ from any of the terms in $\mathcal{H}_2^T$, i.e. $\mathcal{K}_2^T$ can be taken as zero. The resulting PDE for the second-order short-period tesseral generating function $\mathcal{W}_2^T$ is obtained as follows:

$$-\tilde{n}\frac{\partial \mathcal{W}_2^T}{\partial l} - w_E \frac{\partial \mathcal{W}_2^T}{\partial \theta} + \mathcal{H}_2^T = 0, \tag{3.79}$$

where

$$\tilde{n} = \frac{\partial \mathcal{H}_0}{\partial L} = \frac{\mu^2}{L^3},$$

$$\frac{\partial}{\partial \theta} = \frac{1}{w_E}\frac{\partial}{\partial t}.$$

In the above equation, $\tilde{n}$ and w_E represent the mean motion and the Earth's angular velocity, respectively.

The advantage of formulating the Hamiltonian in the Delaunay elements is evident from the above equation, which is a linear first-order PDE in two independent variables l and θ as opposed to three in case of the similar PDE in the polar-nodal variables; the third independent variable being the radial distance r [126]. A closed-form solution of the above PDE, if feasible, completes the Delaunay normalization of the Hamiltonian up to order two. However, a closed-form analytic solution is not known to exist for this PDE without first expanding the true-anomaly dependent terms in $\mathcal{H}_2$ in powers of the eccentricity [121]. Nevertheless, two different approaches for solving this PDE in closed-form in the eccentricity are discussed in the following two sections.

3.4 Relegation of the Tesseral Harmonics

The method of relegation uses an iterative approach to normalize the tesseral Hamiltonian and compute the short-period generating function that is closed-form in the eccentricity. In this section, a reformulation of the method of relegation to normalize the Hamiltonian expressed in the Delaunay elements is presented [232]. Unlike the original formulation [126] of this method in the polar-nodal variables, its convergence criteria are better illustrated using the Delaunay elements. An alternative formulation of this method in the Delaunay elements is also proposed by Lara et al. that produces a series representation of the tesseral short-period generating function in powers of the eccentricity [127].

In the relegation method, an approximate solution of Eq. 3.79 is chosen that only partially satisfies the homological equation. The residual produced by this approximate solution gets multiplied by a term having a value less than unity. This residual becomes the new perturbation Hamiltonian term for the next iteration and after a sufficient number of iterations, it becomes small enough to be safely relegated to the next higher order. To illustrate this method, a residual term $\mathcal{R}^T$ is added

to Eq. 3.79, with the subscript j representing an iteration as shown below:

$$\tilde{n}\frac{\partial \mathcal{W}_{2,j}^{T}}{\partial l} + w_E \frac{\partial \mathcal{W}_{2,j}^{T}}{\partial \theta} - \mathcal{H}_{2,j}^{T} = \mathcal{R}_{j}^{T}. \tag{3.80}$$

Two separate flavors of the relegation method, one applicable for the sub-synchronous and other for the super-synchronous orbit regimes, are needed and are given below for solving the above equation.

Sub-Synchronous Relegation. If $\mathcal{W}_{2,j}^{T}$ is chosen to satisfy the constraint

$$\tilde{n}\frac{\partial \mathcal{W}_{2,j}^{T}}{\partial l} - \mathcal{H}_{2,j}^{T} = 0 \tag{3.81}$$

then the approximate solution of Eq. 3.80 is given as

$$\mathcal{W}_{2,j}^{T} = \frac{1}{\tilde{n}} \int \gamma \, \mathcal{H}_{2,j}^{T} \, \mathrm{d}f, \tag{3.82}$$

where

$$\gamma = \frac{\eta^3}{(1 + e\,\cos(f))^2},$$

$$\mathrm{d}f = \frac{1}{\gamma}\mathrm{d}l.$$

This approximate solution is substituted back into Eq. 3.80 to obtain the residual

$$\mathcal{R}_{j}^{T} = \int \delta \, \gamma \, \frac{\partial \mathcal{H}_{2,j}^{T}}{\partial \theta} \, \mathrm{d}f, \tag{3.83}$$

where

$$\delta = \frac{w_E}{\tilde{n}}.$$

It is noted that for the sub-synchronous orbits, $\delta < 1$. To continue the iterations further, the above

residual is collected in $\mathcal{H}^T_{2,j+1}$, i.e. $\mathcal{H}^T_{2,j+1} = \mathcal{R}^T_j$, and a new $\mathcal{W}^T_{2,j+1}$ is computed by repeating the same process. The iterations are started by choosing $\mathcal{H}^T_{2,0} = \mathcal{H}^T_2$. If the residual $\mathcal{R}^T_j$ is smaller in magnitude than the original perturbation $\mathcal{H}^T_{2,j}$, then the method of relegation is guaranteed to converge. In order to estimate an upper bound of the residual for any value of f, the following bounds on the function γ are noted for an elliptic orbit:

$$\frac{\eta^3}{(1+e)^2} = \gamma_{\text{min}} \leq \gamma \leq \gamma_{\text{max}} = \frac{\eta^3}{(1-e)^2}. \tag{3.84}$$

In the limit that the eccentricity approaches 1, the values of γ_{min} and γ_{max} approach 0 and ∞, respectively. The differentiation and integration operation in Eq. 3.83 produce the coefficients of θ and f in the numerator and denominator, respectively. The minimum and maximum coefficient of f can be determined using the expression for the Hamiltonian given in Eq. 3.76, which are 1 and $2n+1$, respectively. As a result, the maximum magnitude that the residual corresponding to a single term in $\mathcal{H}^T_{2,j}$, can attain during one orbit is found using Eq. 3.83 as follows:

$$\mathcal{R}^T_{j,\text{max}} = m\,\delta\,\gamma_{\text{max}}\,|\mathcal{H}^T_{2,j}|. \tag{3.85}$$

It is noted that the minimum coefficient value of f that appears in the denominator of right hand side of the above equation is used in calculating the upper bound on the residual. Thus, a sufficient condition for the relegation method to converge is

$$m\,\delta\,\gamma_{\text{max}} < 1. \tag{3.86}$$

Hence, for the sub-synchronous orbits of medium to high eccentricities, the method of relegation will converge slowly, especially for the tesserals with $m > 1$. If the above condition holds, then after a sufficient number of iterations d, the residual can be deemed small enough to be safely ignored at the current perturbation order and the tesseral short-period contributions are captured in the multiple $\mathcal{W}^T_{2,j}$ terms, where j runs from 0 to d. All these terms are summed together to get the complete short-period generating function for the tesserals.

Super-Synchronous Relegation. The relegation approach for super-synchronous orbits begins with the following choice of the constraint for $\mathcal{W}_{2,j}^T$ derived using Eq. 3.80:

$$w_E \frac{\partial \mathcal{W}_{2,j}^T}{\partial \theta} - \mathcal{H}_{2,j}^T = 0. \tag{3.87}$$

Solving the above equation, an approximate solution of Eq. 3.79 and the corresponding residual are obtained as:

$$\mathcal{W}_{2,j}^T = \frac{1}{w_E} \int \mathcal{H}_{2,j}^T \, \mathrm{d}\theta, \tag{3.88}$$

$$\mathcal{R}_j^T = \int \frac{1}{\delta \, \gamma} \frac{\partial \mathcal{H}_{2,j}^T}{\partial f} \, \mathrm{d}\theta. \tag{3.89}$$

The iterations are continued by using the residual $\mathcal{R}_j^T$ from the previous iteration as the new perturbation term $\mathcal{H}_{2,j+1}^T$. Using the same approach as for the sub-synchronous case, the maximum value the residual corresponding to a single term in $\mathcal{H}_{2,j}^T$, can attain over one complete orbit for the super-synchronous case is

$$\mathcal{R}_{j,\text{max}}^T = \frac{2n+1}{m\delta \, \gamma_{\text{min}}} |\mathcal{H}_{2,j}^T|, \tag{3.90}$$

where $2n+1$ is the maximum coefficient of f in $\mathcal{H}_{2,j}^T$ and m is the coefficient of θ. The convergence condition for the super-synchronous obits is

$$\frac{2n+1}{m\delta \, \gamma_{\text{min}}} < 1. \tag{3.91}$$

For the super-synchronous orbits, $\delta > 1$. For orbits with periods approaching resonant values, the convergence degrades for both super-synchronous as well as sub-synchronous orbits due to the fact that δ approaches unity. Similar to sub-synchronous case, the convergence of the method of relegation depends on e, n, and m. However, it is emphasized that the two sufficient conditions Eqs. 3.86 and 3.91 for the convergence of the relegation method in case of sub-synchronous and

super-synchronous orbits, respectively, are derived using the upper bounds on the residuals in the two cases. It is possible that the method of relegation will converge , albeit slower, even if these conditions are not satisfied in certain cases. It should also be noted that there are no singularities present in the expressions for the generating functions $\mathcal{W}_{2,j}^{T}$ for resonant orbits.

m-daily Terms

All the terms in $\mathcal{H}_{2,j}^{T}$ from Eq. 3.78 that do not depend on f are characterized as m-daily terms (see [233], Chapter 9). It is noted that these m-daily terms also depend on h and g, which are generally associated with the long-period terms. In case of the nonresonant tesseral harmonics, there are no pure long-period terms in $\mathcal{H}_{2,j}^{T}$. For Earth, the secular rates (from which the short-period terms are averaged out) of h and g due to the dominant J_2 zonal harmonic are given as (see [224], Chapter 10):

$$\frac{\mathrm{d}\bar{h}}{\mathrm{d}t} = -9.96 \left(\frac{R_e}{a}\right)^{3.5} (1-e^2)^{-2} \cos i \quad \text{degrees/day}, \tag{3.92}$$

$$\frac{\mathrm{d}\bar{g}}{\mathrm{d}t} = 5.0 \left(\frac{R_e}{a}\right)^{3.5} (1-e^2)^{-2} (5\cos^2 i - 1) \quad \text{degrees/day}. \tag{3.93}$$

An upper bound on the above angular rates can be obtained by considering equatorial orbits with semimajor axis equal to the radius of Earth, and as a consequence, the eccentricity must be assumed zero. Therefore, these upper bounds for the rates of $\bar{h}$ and $\bar{g}$ are approximately -10° and 20° per day, respectively. It can be easily verified that these upper bounds hold well for the typical orbits, for which the perigee does not fall below Earth's radius. In case of the tesseral harmonics, these upper bounds are expected to be a periodic function of $\bar{h}$ and $\bar{g}$, and also much smaller in amplitude than that due to J_2. Considering the longest period of a pure m-daily term (which do not depend on g and f) as 1 day, the periodic rates of all the terms in $\mathcal{H}_{2,j}^{T}$ that do not depend on f (the m-daily terms of the tesseral potential) can be approximated well by m times the angular velocity of Earth. Therefore, the m-daily terms repeat m times a day approximately.

To avoid secular terms in $\mathcal{W}_{2,j}^{T}$, the contributions from the m-daily terms are captured in a sep-

arate generating function $\mathcal{W}_2^{\text{md}}$. This generating function can be computed in closed form without any iterations by directly integrating the m-daily part of $\mathcal{H}_2^T$ as shown below:

$$\mathcal{W}_2^{md} = \frac{1}{w_E} \int \mathcal{H}_2^{\text{md}} \, \mathrm{d}\theta, \tag{3.94}$$

where the superscript *md* is used to indicate that only the m-daily terms are included in the above integrand.

Considering the above results, it is noted that the method of relegation is an iterative approach, with different expressions for the tesseral short-period generating functions for the sub-synchronous and super-synchronous orbit regimes. The generating function corresponding to each iteration captures only a part of the complete short-period contribution. The number of terms in the generating function increases significantly with each iteration. For instance, in one implementation of the relegation algorithm using the polar-nodal variables, the number of terms in the generating function easily exceeded one thousand after four iterations for C_{22} and S_{22} tesseral harmonics [126]. Another limitation of the relegation method is evident from the residual expressions given in Eq. 3.85 and 3.90. For both sub-synchronous and super-synchronous cases, since γ is an unbounded monotonic increasing function of the eccentricity, the convergence criterion typically dictates small orbital eccentricities.

3.5 Exact Delaunay Normalization of the Tesseral Perturbation Hamiltonian

An exact solution for the PDE given in Eq. 3.79 is presented in this section, which accomplishes the Delaunay normalization of the tesseral Hamiltonian without using the eccentricity expansions and also avoids the convergence limitations of the relegation method discussed in the previous section [234, 232]. It is a linear first-order PDE with two independent variables and its exact solution can be reduced to quadrature using the method of characteristics to obtain the generating function for the short-periodic effects due to the tesseral harmonics.

The method of characteristics is a powerful technique for solving a linear or quasi-linear PDE such as the one-dimensional wave equation [235]. In this method, a characteristic curve is found

along which the PDE reduces to an ordinary differential equation (ODE). If the characteristic curves for the PDE given in Eq. 3.79 are chosen as the general solution of the equation

$$\frac{d\theta}{dl} = \frac{w_E}{\tilde{n}} = \delta \tag{3.95}$$

then this PDE is transformed into the following ODE for $\mathcal{W}_2^T$:

$$\frac{d\mathcal{W}_2^T}{dl} - \frac{1}{\tilde{n}}\mathcal{H}_2^T = 0. \tag{3.96}$$

Before the above ODE can be integrated, all the appearances of θ in $\mathcal{H}_2^T$ have to be removed using the solutions for the characteristic curves. These characteristic curves are found by integrating Eq. 3.95 and are given as follows:

$$\theta = \delta\, l + \theta_0, \tag{3.97}$$

where θ_0 is a constant. The above relation for θ, when substituted in the expression for $\mathcal{H}_2^T$ given in Eq. 3.77 results in the following equation:

$$\mathcal{H}_2^T = -\frac{2!}{C_{20}^2}\frac{\mu R_e^n}{r^{n+1}}\sum_{p=0}^{p=n} F_{nmp}(i)\,[CS_1\,\{\cos(\alpha)\cos(\beta) - \sin(\alpha)\sin(\beta)\} + CS_2\,\{\sin(\alpha)\cos(\beta) + \cos(\alpha)\sin(\beta)\}], \tag{3.98}$$

where

$$\alpha \equiv (n-2p)f - m\delta\, l, \tag{3.99}$$

$$\bar{\beta} \equiv (n-2p)g + m(h-\theta_0). \tag{3.100}$$

The ODE in Eq. 3.96 with $\mathcal{H}_2^T$ given above can now be integrated along the characteristic curves and the solution is given as follows:

$$\mathcal{W}_2^T = -\frac{2!}{C_{20}^2}\frac{\mu R_e^n}{\tilde{n}}\sum_{p=0}^{p=n} F_{nmp}(i)\left[CS_1\left\{\cos(\bar{\beta})\int\frac{\cos(\alpha)}{r^{n+1}}\,\mathrm{d}l - \sin(\bar{\beta})\int\frac{\sin(\alpha)}{r^{n+1}}\,\mathrm{d}l\right\}\right.$$
$$\left. +CS_2\left\{\cos(\bar{\beta})\int\frac{\sin(\alpha)}{r^{n+1}}\,\mathrm{d}l + \sin(\bar{\beta})\int\frac{\cos(\alpha)}{r^{n+1}}\,\mathrm{d}l\right\}\right] + F(\theta_0, a, e, i, h, g), \quad (3.101)$$

where F is an arbitrary function. The final step to obtain the solution of the original PDE is to substitute back the value of the constant θ_0 from Eq. 3.97 in the above solution. After this substitution and the change of integration variable from l to f, the solution in the final form is given as follows:

$$\mathcal{W}_2^T = -\frac{2!}{C_{20}^2}\frac{\mu R_e^n}{\tilde{n}\, a^{n+1}\eta^{2n-1}}\sum_{p=0}^{p=n} F_{nmp}(i)\left[CS_1\left\{\cos(\beta)I_1^{nmp} - \sin(\beta)I_2^{nmp}\right\}\right.$$
$$\left. +CS_2\left\{\cos(\beta)I_2^{nmp} + \sin(\beta)I_1^{nmp}\right\}\right]$$
$$+ F(\theta - \delta\, l, a, e, i, h, g), \quad (3.102)$$

where

$$\beta \equiv (n-2p)g + m(h - \theta + \delta\, l), \quad (3.103)$$

$$I_1^{nmp} \equiv \int \cos((n-2p)f - m\delta\, l)(1 + e\cos f)^{n-1}\,\mathrm{d}f, \quad (3.104)$$

$$I_2^{nmp} \equiv \int \sin((n-2p)f - m\delta\, l)(1 + e\cos f)^{n-1}\,\mathrm{d}f. \quad (3.105)$$

The above result provides an exact and very succinct solution for the generating function $\mathcal{W}_2^T$ for an arbitrary tesseral spherical harmonic. It satisfies the PDE given in Eq. 3.79 exactly, which can be easily verified by substituting this solution back into the PDE. In addition, F is an arbitrary function of the first five classical orbital elements and $\theta - \delta\, l$ and can be chosen to make the

time-average of $\mathcal{W}_2^T$ zero, if required. Otherwise, it can safely be assumed to be equal to zero. A major advantage of this solution is that it remains valid for an arbitrary elliptic orbit in both: the sub-synchronous as well as super-synchronous orbit regimes simultaneously, and avoids any singularities for the resonant orbits as well. A similar solution for the generating function that accomplishes the normalization of a perturbed Keplerian system using the method of characteristics was also proposed by Palacián [236]. His solution applies to a generic form of the perturbed Keplerian Hamiltonian (see Eq. (14) in [236]) that represents only a part of the complete tesseral Hamiltonian used in this work. Palacián acknowledged that the integrals present in his solution cannot be evaluated analytically except in some special cases, and a numerical quadrature must be performed for computing a solution. However, he arbitrarily chose the lower limit of integration for these integrals as zero, and ignored the computation of the integration constant (see Proposition 4.1). It is seen through simulations in this work that ignoring the integration constant while evaluating the integrals using the numerical quadrature affects the accuracy of the proposed theory significantly.

The general solution for $\mathcal{W}_2^T$ contains integrals I_1^{nmp} and I_2^{nmp}, and they need to be evaluated for computing $\mathcal{W}_2^T$ and its partial derivatives. It is noted that these integrals are functions of the true and mean anomaly simultaneously and as a consequence, a closed-form solution for I_1^{nmp} or I_2^{nmp} is not known to exist. Additionally, their integrands are generally not periodic functions because of the presence of δ, which is generally an irrational number, except for some special cases. Nevertheless, these integrals represent only a part of the complete generating function and a series representation of them can be obtained by expanding their integrands either by using the typical eccentricity expansions of the true anomaly or by using the integration by parts method. Additionally, they can be computed numerically to arbitrary precision (in theory). These three different ways to compute a solution for I_1^{nmp} and I_2^{nmp} and their partial derivatives are discussed in the following subsections.

3.5.1 Evaluation of Quadratures Using Eccentricity Expansion

The well-known elliptic expansion of f in terms of e and l up to $\mathcal{O}(e^7)$ is [224]

$$f = l + \left(2\,e - \frac{1}{4}\,e^3 + \frac{5\,e^5}{96}\right)\sin(l) + \left(\frac{5}{4}\,e^2 - \frac{11\,e^4}{24} + \frac{17\,e^6}{192}\right)\sin(2\,l) + \left(\frac{13\,e^3}{12} - \frac{43\,e^5}{64}\right)\sin(3\,l) + \left(\frac{103\,e^4}{96} - \frac{451\,e^6}{480}\right)\sin(4\,l) + \frac{1097\,e^5\sin(5\,l)}{960} + \frac{1223\,e^6\sin(6\,l)}{960} + \mathcal{O}(e^7). \quad (3.106)$$

The series solutions of I_1^{nmp} and I_2^{nmp} can be obtained for an arbitrary tesseral harmonic by substituting the above relation in Eqs. 3.104 and 3.105, and expanding the integrands using Taylor series about $e = 0$. These series solutions are known to be convergent for low to moderate values of the eccentricity (approx. $e < 0.7$), therefore a term-by-term differentiation can be performed to compute the partial derivatives of I_1^{nmp} and I_2^{nmp}. The results can be substituted in Eq. 3.102 to compute $\mathcal{W}_2^T$ and its partial derivatives. All of these operations can easily be mechanized using any off-the-shelf symbolic algebra package. The series solutions of I_1^{nmp} and I_2^{nmp} up to $\mathcal{O}(e^2)$ are given below for ready reference:

$$I_1^{nmp} = -\frac{\sin(\overline{\alpha})}{\delta\,m - n + 2\,p} + \left(-1/2\,\frac{(3\,n - 4\,p + 1)\sin(l + \overline{\alpha})}{\delta\,m - n + 2\,p - 1} - 1/2\,\frac{(n - 4\,p - 1)\sin(l - \overline{\alpha})}{\delta\,m - n + 2\,p + 1}\right) e + \left(1/4\,\frac{(3\,n^2 - 16\,np + 16\,p^2 + 3\,n - 2)\sin(\overline{\alpha})}{\delta\,m - n + 2\,p} - 1/8\,\frac{(9\,n^2 - 24\,np + 16\,p^2 + 14\,n - 18\,p + 4)\sin(2\,l + \overline{\alpha})}{\delta\,m - n + 2\,p - 2} + 1/8\,\frac{(n^2 - 8\,np + 16\,p^2 - 4\,n + 18\,p + 4)\sin(2\,l - \overline{\alpha})}{\delta\,m - n + 2\,p + 2}\right) e^2 + \mathcal{O}(e^3), \quad (3.107)$$

$$I_2^{nmp} = \frac{\cos(\overline{\alpha})}{\delta\,m - n + 2\,p} + \left(-1/2\,\frac{(n - 4\,p - 1)\cos(l - \overline{\alpha})}{\delta\,m - n + 2\,p + 1} + 1/2\,\frac{(3\,n - 4\,p + 1)\cos(l + \overline{\alpha})}{\delta\,m - n + 2\,p - 1}\right) e + \left(1/8\,\frac{(n^2 - 8\,np + 16\,p^2 - 4\,n + 18\,p + 4)\cos(2\,l - \overline{\alpha})}{\delta\,m - n + 2\,p + 2}\right.$$

$$+1/8\,\frac{(9\,n^2-24\,np+16\,p^2+14\,n-18\,p+4)\cos(2\,l+\overline{\alpha})}{\delta\,m-n+2\,p-2}$$
$$-1/4\,\frac{(3\,n^2-16\,np+16\,p^2+3\,n-2)\cos(\overline{\alpha})}{\delta\,m-n+2\,p}\Bigg)\,e^2+\mathcal{O}(e^3), \quad (3.108)$$

where

$$\bar{\alpha}=(n-2p)l-m\delta l.$$

Evaluation of I_1^{nmp} and I_2^{nmp} by using the eccentricity expansions as shown above introduces singularities for the orbits with periods close to the resonant values because of the appearance of the denominators of the form $(n-2p-m\delta)$ in the series solutions. This drawback can be avoided by finding series representations of these integrals using the integration by parts method as discussed in the following subsection.

3.5.2 Evaluation of Quadratures Using Integration by Parts

Since δ appears as a coefficient of the mean anomaly in I_1^{nmp} and I_2^{nmp}, the repeated differentiation or integration of their integrands can produce powers of δ multiplying the numerator or denominator of the same integrands. This observation motivates the application of the integration by parts method to produce a series representation of I_1^{nmp} and I_2^{nmp}. The repeated application of the integration by parts method is equivalent to the iterations performed in the method of relegation in Section 3.4, for the two methods produce the same solution for the generating function. As for the method of relegation, the series solutions of ${I_1}^{nm}$ and ${I_2}^{nm}$ using integration by parts are also different for the sub-synchronous and super-synchronous orbit regimes.

Sub-Synchronous case

Before applying integration by parts to ${I_1}^{nm}$ and I_2^{nmp}, the integration variable is changed to l and the terms containing f and l are separated from each other. Using trigonometric identities, Eqs. 3.104 and 3.105 can be written as shown below:

$$I_1^{nmp} = \frac{1}{\eta^3} \int \left(\cos(m\delta l) A_0(f) + \sin(m\delta l) B_0(f)\right) \, \mathrm{d}l, \tag{3.109}$$

$$I_2^{nmp} = \frac{1}{\eta^3} \int \left(\cos(m\delta l) B_0(f) - \sin(m\delta l) A_0(f)\right) \, \mathrm{d}l, \tag{3.110}$$

where

$$A_0(f) = \cos\left((n-2p)f\right) \, (1 + e\cos(f))^{n+1},$$

$$B_0(f) = \sin\left((n-2p)f\right) \, (1 + e\cos(f))^{n+1}.$$

Repeated application of the integration by parts, with each term containing l considered as the first function, produces a series expansion of these integrals in the powers of δ. These series solutions of I_1^{nmp} and I_2^{nmp} up to $\mathcal{O}(\delta^4)$ are as given below:

$$\begin{aligned} I_1^{nm} = \frac{1}{\eta^3} \big[& \cos(m\delta l) \left(A_1 - (m\delta)B_2 - (m\delta)^2 A_3 + (m\delta)^3 B_4 + (m\delta)^4 A_5 - \dots\right) \\ & + \sin(m\delta l) \left(B_1 + (m\delta)A_2 - (m\delta)^2 B_3 - (m\delta)^3 A_4 + (m\delta)^4 B_5 + \dots\right) \big], \end{aligned} \tag{3.111}$$

$$\begin{aligned} I_2^{nm} = \frac{1}{\eta^3} \big[& -\sin(m\delta l) \left(A_1 + (m\delta)B_2 - (m\delta)^2 A_3 - (m\delta)^3 B_4 + (m\delta)^4 A_5 + \dots\right) \\ & + \cos(m\delta l) \left(B_1 - (m\delta)A_2 + (m\delta)^2 B_3 + (m\delta)^3 A_4 - (m\delta)^4 B_5 - \dots\right) \big], \end{aligned} \tag{3.112}$$

where for $k \geq 1$

$$A_k(f) = \int \gamma \, A_{k-1}(f) \mathrm{d}f,$$

$$B_k(f) = \int \gamma \, B_{k-1}(f) \mathrm{d}f.$$

Th expressions of A_k and B_k appearing in the above equations are only functions of the true anomaly and as a result, they are integrable. As k increases, the magnitudes of A_k and B_k are guaranteed to decrease if $\gamma_{\text{max}} < 1$, where γ_{max} is the maximum value of γ for any f (see Eq. 3.84). Therefore, the sufficient condition for the series solutions of I_1^{nmp} and I_2^{nmp} to converge is

$$m \, \delta \, \gamma_{\text{max}} < 1. \tag{3.113}$$

It is noted that the coefficients of f that are produced while evaluating A_k and B_k appear in the denominator of the left hand side of the above inequality condition. Using formulae given in Eqs. 3.73 and 3.74, it can be verified that these coefficients are lower bounded by unity. Therefore, the above convergence criterion is valid for any tesseral harmonic.

Super-Synchronous case

For super-synchronous orbits, $\delta > 1$. Therefore, each term containing f is treated as the first function in the application of integration by parts to Eqs. 3.109 and 3.110, resulting in the following series solutions of I_1^{nmp} and I_2^{nmp} up to $\mathcal{O}(\delta^{-4})$:

$$I_1^{nm} = \frac{1}{\eta^3}\left[\frac{\cos(m\delta l)}{m\delta}\left(-B_0 + \frac{A^1}{(m\delta)} + \frac{B^2}{(m\delta)^2} - \frac{A^3}{(m\delta)^3} - \frac{B^4}{(m\delta)^4} + \dots\right) + \frac{\sin(m\delta l)}{m\delta}\left(A_0 + \frac{B^1}{(m\delta)} - \frac{A^2}{(m\delta)^2} - \frac{B^3}{(m\delta)^3} + \frac{A^4}{(m\delta)^4} + \dots\right)\right], \tag{3.114}$$

$$I_2^{nm} = \frac{1}{\eta^3}\left[\frac{\cos(m\delta l)}{m\delta}\left(-A_0 + \frac{B^1}{(m\delta)} + \frac{A^2}{(m\delta)^2} - \frac{B^3}{(m\delta)^3} - \frac{A^4}{(m\delta)^4} + \dots\right) + \frac{\sin(m\delta l)}{m\delta}\left(B_0 + \frac{A^1}{(m\delta)} - \frac{B^2}{(m\delta)^2} - \frac{A^3}{(m\delta)^3} + \frac{B^4}{(m\delta)^4} + \dots\right)\right], \tag{3.115}$$

where for $k \geq 1$

$$A^k = \frac{1}{\gamma}\frac{\partial A^{k-1}}{\partial f},$$

$$B^k = \frac{1}{\gamma}\frac{\partial B^{k-1}}{\partial f}.$$

Since the absolute values of the coefficients of f in A_0 and B_0 are bounded by $2n+1$, the sufficient condition for the convergence of the above series solutions of I_1^{nmp} and I_2^{nmp} is

$$\frac{2n+1}{m\delta\gamma_{\text{min}}} < 1. \tag{3.116}$$

It is not a coincidence that the convergence criteria for sub-synchronous and super-synchronous orbits given in this section are identical to the criteria obtained earlier for the method of relegation (see Eqs. 3.86 and 3.91 in Section 3.4). In fact, the above series solutions of I_1^{nmp} and I_2^{nmp} if substituted in Eq. 3.102, gives the same solution for the tesseral generating function $\mathcal{W}_{2,j}^T$ as produced by the method of relegation. Each expansion order in the series solutions of I_1^{nmp} and I_2^{nmp} corresponds to that from an iteration in the method of relegation. The exact solution presented in this section is, therefore, can be considered as a more general method, of which the method of relegation is a special case.

3.5.3 Evaluation of Quadratures Numerically

The two approximate approaches for evaluating the indefinite integrals I_1^{nmp} and I_2^{nmp}, which are needed to compute the tesseral generating function, have different limitations. The approach using the eccentricity expansion has inherent singularities for resonant elliptic orbits and a large number of terms must be retained in the eccentricity expansions for medium to high values of the orbital eccentricity. In contrast, the series solutions found in the previous subsection using integration by parts produce large expressions for each term in the series. Also, the domain of convergence are limited by the convergence criteria. Another approach to evaluate these integrals

to arbitrary precision (in theory) is by numerical quadrature. The numerical approach not only produces very compact expressions for the short-period variations of the orbital elements due to tesserals, it also avoids the singularities and convergence limitations of the previous two methods.

The integrands of I_1^{nmp} and I_2^{nmp} are not periodic functions due to the presence of the irrational number δ. As a consequence, the current value of the true anomaly, which is used as the upper limit for the numerical quadrature, must take into account the number of orbital periods passed since the initial time, i.e., it must not be wrapped between 0 and 2π. The lower limit for the quadrature is arbitrary and can be taken as 0. However, the values of these indefinite integrals at the lower limit, i.e., $f = 0$ are required, which can be computed by using either of the previous two approaches discussed. This hybrid approach uses the eccentricity expansions or the integration by parts method only to evaluate I_1^{nmp} and I_2^{nmp} at a single point, $f = 0$, and produces more accurate results as will be seen in the following section. With this discussion, the solutions of these integrals are now represented as follows:

$$I_1^{nmp} = \int_0^f \cos((n-2p)f - m\delta\, l)(1 + e\cos f)^{n-1}\,\mathrm{d}f, \tag{3.117}$$

$$I_2^{nmp} = I_2^{nmp}|_{f=0} + \int_0^f \sin((n-2p)f - m\delta\, l)(1 + e\cos f)^{n-1}\,\mathrm{d}f. \tag{3.118}$$

It can be easily verified that $I_1^{nmp} = 0$ at $f = 0$. It is noted that by using the true anomaly as the integration variable in the quadratures, the need to solve Kepler's equation at each step is avoided. The minimum step size needed for the numerical quadrature should take into account the highest frequency component present in the integrands of I_1^{nmp} and I_2^{nmp}. Using formulae in Eqs. 3.73 and 3.74, the largest numerical coefficient of f in the integrands is obtained as $2n - 1$. Therefore, the highest frequency component in the integrands has the time-period as $2\pi/(2n-1)$.

From an operational point of view, the numerical quadrature approach has many advantages. The exact solution for $\mathcal{W}_2^T$, which is closed-form in the eccentricity is very compact in size compared to the approximate solutions generated by the method of relegation. This stems from the fact that the term $(1 + e\cos(f))^{n-1}$ need not be expanded for evaluating these quadratures I_1^{nmp} and

I_2^{nmp}. The numerical quadrature approach is also well-suited for parallel computations for faster execution. Moreover, unlike the method of relegation, no separate treatment for m-daily terms is required and their contributions are included in the proposed solution without any approximations.

3.6 Satellite Theory with Tesseral Harmonics

The solution for the tesseral generating function obtained in the previous section have been implemented into an artificial satellite theory, which includes tesseral short-period and m-daily effects. The expressions for the second-order variations of the equinoctial orbital elements valid for an arbitrary tesseral are provided below. The tesseral contributions are required in addition to the secular and periodic contributions of the zonal harmonics developed in Sections 3.1 and 3.2 to formulate a complete satellite theory valid for an Earth-like nonspherical central body.

Provided a generating function for the periodic variations computed using the Deprit's method, the expressions for the periodic variations of any set of orbital elements can be computed by evaluating the Poisson brackets in the near-identity transformations given in Eqs. 2.19 and 2.20. The second-order tesseral contributions in the mean to osculating transformation depend on the Poisson bracket $(\mathcal{E}, \mathcal{W}_2^T)$, where $\mathcal{E}$ represents the equinoctial elements. Using the definitions of the equinoctial elements (see Eq. 3.51), the following expressions for their variations valid for any tesseral harmonic are obtained:

$$(a, \mathcal{W}_2^T) = -2\sqrt{\frac{a}{\mu}}\frac{\partial f}{\partial l}\frac{\partial \mathcal{W}_2^T}{\partial f}, \tag{3.119}$$

$$(\Lambda, \mathcal{W}_2^T) = 2\sqrt{\frac{a}{\mu}}\frac{\partial \mathcal{W}_2^T}{\partial a} - \frac{\eta}{L}\sqrt{\frac{1-\eta}{1+\eta}}\frac{\partial \mathcal{W}_2^T}{\partial e} - \frac{\partial \mathcal{W}_2^T}{\partial i}\left(\frac{\tan(\frac{i}{2})}{G}\right), \tag{3.120}$$

$$(p_1, \mathcal{W}_2^T) = \frac{\sin(h)}{G(1+\cos i)}\frac{\partial \mathcal{W}_2^T}{\partial i} - \frac{\cos h}{(1+\cos i)}\frac{1}{G}\mathcal{W}_{2,gh}^T, \tag{3.121}$$

$$(p_2, \mathcal{W}_2^T) = \frac{-\cos(h)}{G(1+\cos i)}\frac{\partial \mathcal{W}_2^T}{\partial i} - \frac{\sin h}{(1+\cos i)}\frac{1}{G}\mathcal{W}_{2,gh}^T, \tag{3.122}$$

$$(q_1, \mathcal{W}_2^T) \;=\; -\sin(g \;+\; h)\left(\frac{-\eta}{L}\frac{\partial \mathcal{W}_2^T}{\partial e} - e\frac{\partial \mathcal{W}_2^T}{\partial i}\frac{\tan(\frac{i}{2})}{G}\right) \;-\; \frac{\eta^2}{L}\cos(g \;+\; h)\mathcal{W}_{2,lg}^T, \quad (3.123)$$

$$(q_2, \mathcal{W}_2^T) \;=\; \cos(g \;+\; h)\left(\frac{-\eta}{L}\frac{\partial \mathcal{W}_2^T}{\partial e} - e\frac{\partial \mathcal{W}_2^T}{\partial i}\frac{\tan(\frac{i}{2})}{G}\right) \;-\; \frac{\eta^2}{L}\sin(g \;+\; h)\mathcal{W}_{2,lg}^T, \quad (3.124)$$

where

$$\mathcal{W}_{2,gh}^T \equiv \frac{1}{\sin i}\left(\cos i\frac{\partial \mathcal{W}_2^T}{\partial g} - \frac{\partial \mathcal{W}_2^T}{\partial h}\right), \quad (3.125)$$

$$\mathcal{W}_{2,lg}^T \equiv \frac{1}{e}\left(\frac{\partial \mathcal{W}_2^T}{\partial l} - \frac{1}{\eta}\frac{\partial \mathcal{W}_2^T}{\partial g}\right). \quad (3.126)$$

The apparent singularities in the above expressions for $\mathcal{W}_{2,gh}^T$ and $\mathcal{W}_{2,lg}^T$ are only artificial, and they are eliminated when the expression for $\mathcal{W}_2^T$ is substituted into these equations. The final expressions for these terms after canceling out the singular terms along with the partial derivatives of I_1^{nmp} and I_2^{nmp} needed to compute the above expressions are provided in Appendix B. As for I_1^{nmp} and I_2^{nmp}, their partial derivatives can also be computed using any of the three methods discussed in the previous section: the eccentricity expansion, integration by parts, or numerical quadrature. Specifically, for computing the partial derivatives of I_1^{nmp} and I_2^{nmp} with respect to e using numerical quadrature, they can be evaluated by first changing the variable of integration from f to l, and then taking the partial derivative of the integrands. The rest of the partial derivatives of the two integrals can be easily evaluated using Leibniz's rule.

3.6.1 Results

By incorporating the expressions for the orbital element variations due to the tesseral harmonics into the satellite theory with zonal harmonics developed in the previous sections, a complete satel-

Table 3.1: Initial classical elements for the two test orbits.

IC	a	e	i	Ω	ω	M
Orbit-1	12159.596 km	0.01	5°	0°	270°	0°
Orbit-2	18520 km	0.35	100°	0°	270°	0°

lite theory for a nonspherical Earth-like gravitational body is implemented in MATLAB. It is emphasized that the resulting satellite theory is valid for any tesseral of arbitrary degree and order. The tesseral short-period and m-daily variations are computed by evaluating I_1^{nmp}, I_2^{nmp}, and their partial derivatives. The eccentricity expansion approach as well as the adaptive quadrature algorithm available in MATLAB (the *integral* command) with tolerance set to 10^{-9} are used to generate the results. The accuracy of this theory is ascertained by comparison with the results obtained from a variable-step, variable-order Adams-Bashforth-Moulton integrator (MATLAB *ode113* command) with JGM-3 Earth's gravity model and tolerances set to 10^{-11}.

The two different initial condition sets are chosen, one with a small and the other with a moderate value of the eccentricity to showcase the accuracy improvements obtained by using the proposed approach. These initial osculating classical orbital elements, given in Table 3.1, are taken from Reference [127] and the results are compared with the results of the Lara's formulation of the method of relegation in the same reference. The zonal satellite theory used in this section is semi-analytic, i.e., the secular and long-period rates are numerically integrated for propagating the mean elements, in order to compare the results with Lara's theory. It is noted that the secular and long periodic effects due to J_2 are included up to $\mathcal{O}(J_2^3)$ in the averaged Hamiltonian, and the short-period effects up to $\mathcal{O}(J_2^2)$ in the generating function. A step-by-step algorithm for the semi-analytic integration of the geopotential using the proposed approach is as follows:

1. Choose the osculating initial elements;

2. Compute the integrals I_1^{nmp} and I_2^{nmp}, and their partials by numerical quadrature with the lower limit $f = 0$. Compute integrals values at $f = 0$ using either the eccentricity expansion or by integration by parts method;

3. An alternative to the previous step is to use the eccentricity expansion or the integration by parts method to directly evaluate the indefinite integrals and their partials for a given value of f;

4. Using the results from Step 2 or 3, compute the periodic variations due to the tesseral harmonics using Eqs. 3.119-3.124;

5. Compute the zonal short-periodic variations and using the inverse transformation given in Eq. 2.20, compute the mean initial conditions;

6. Numerically integrate the mean initial conditions using equations capturing secular and long-period effects of the zonal harmonics;

7. Convert the mean variables at the desired time back to the osculating variables by evaluating the transformation equations given in Eq. 2.19. Use the same approach as in Steps 2 or 3 to compute the tesseral short-period contributions.

The initial conditions from Table 3.1 are propagated numerically as well as semi-analytically with gravity model 2×2 using the above algorithm, and the differences in the classical orbital elements over a period of 30 days are plotted in Figures 3.9-3.16. The numerical quadrature based approach (as described in Step 2 of the above algorithm) was used for Orbit-1 in Figures 3.9-3.10 and for Orbit-2 in Figures 3.13-3.14. The eccentricity expansion approach was used to generate the corresponding results shown in Figures 3.11-3.12 and 3.15-3.16 for the same two orbits. Comparing the plots for Orbit-1 in Figures 3.9-3.10 and 3.11-3.12, it is seen that the exact solution for the variations due to tesserals using numerical quadrature has the same accuracy as the eccentricity expansion approach as expected for this near-circular orbit. However, significant difference in the accuracy of the two approaches became apparent for Orbit-2, which has a higher eccentricity of 0.35, as seen in Figures 3.13-3.14 and 3.15-3.16. Here, the numerical quadrature based exact solution for the tesseral periodic variations outperforms the eccentricity expansion based approach significantly for all the elements. The peak semimajor axis error for the numerical quadrature approach is smaller than that for the eccentricity expansion approach by a factor of 20.

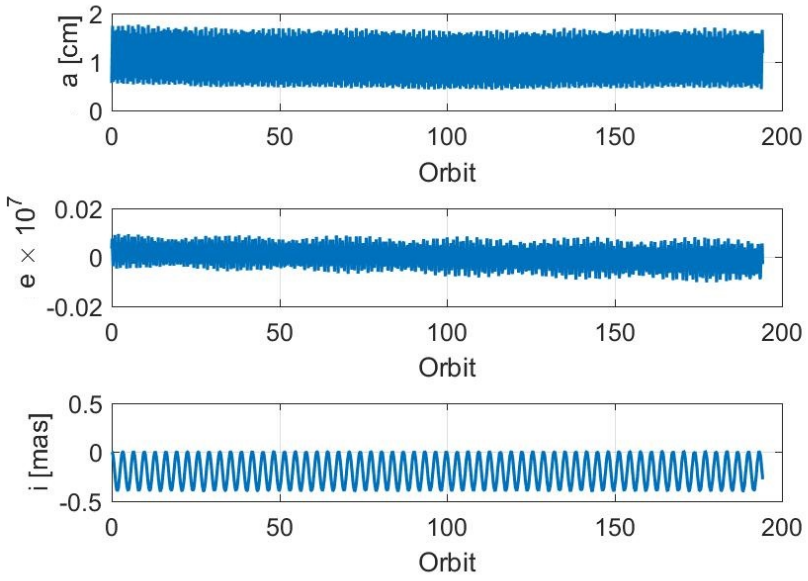

Figure 3.9: Propagation errors for Orbit-1 in the first three classical elements for 2×2 semi-analytic satellite theory with the tesseral periodic variations computed by numerical quadrature. The propagation time corresponds to 30 days with data points plotted at 30 minute intervals.

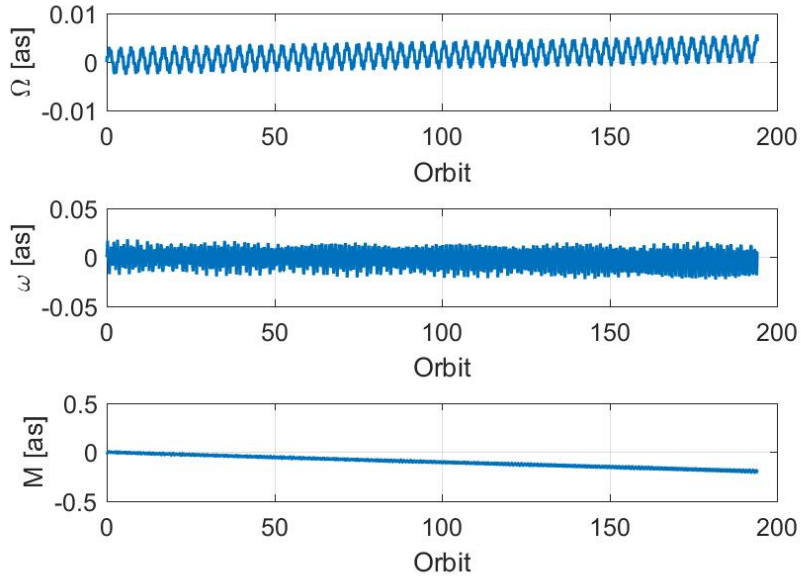

Figure 3.10: Propagation errors for Orbit-1 in the last three classical elements for 2×2 semi-analytic satellite theory with the tesseral periodic variations computed by numerical quadrature. The propagation time corresponds to 30 days with data points plotted at 30 minute intervals.

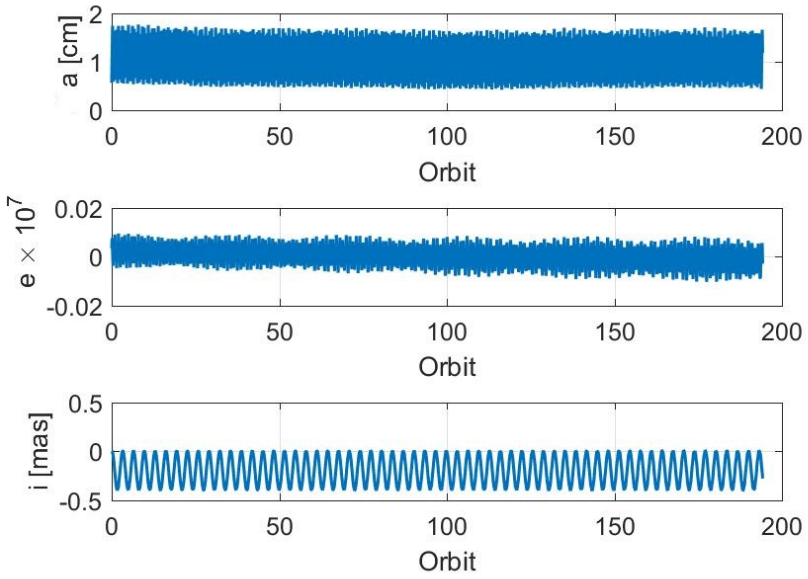

Figure 3.11: Propagation errors for Orbit-1 in the first three classical elements for 2×2 semi-analytic satellite theory with the tesseral periodic variations computed using the series solution in powers of the eccentricity. The propagation time corresponds to 30 days with data points plotted at 30 minute intervals.

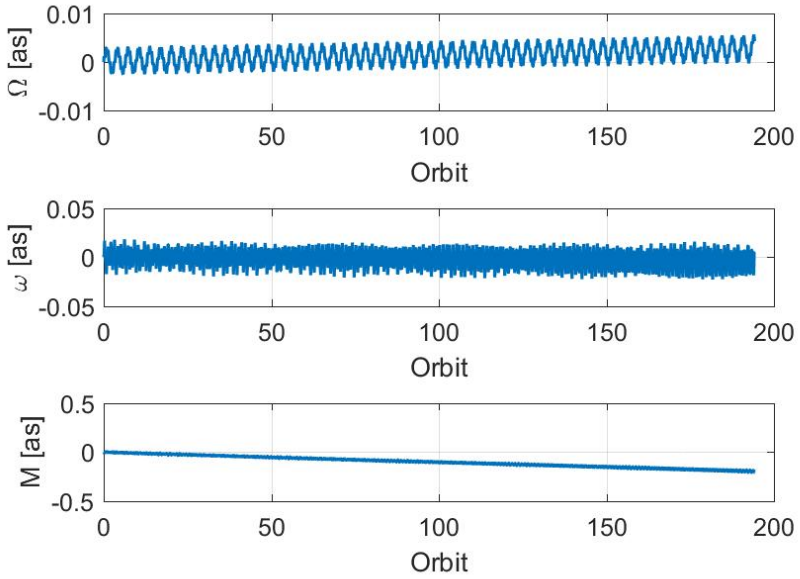

Figure 3.12: Propagation errors for Orbit-1 in the last three classical orbital elements for 2×2 semi-analytic satellite theory with the tesseral periodic variations computed using the series solution in powers of the eccentricity. The propagation time corresponds to 30 days with data points plotted at 30 minute intervals.

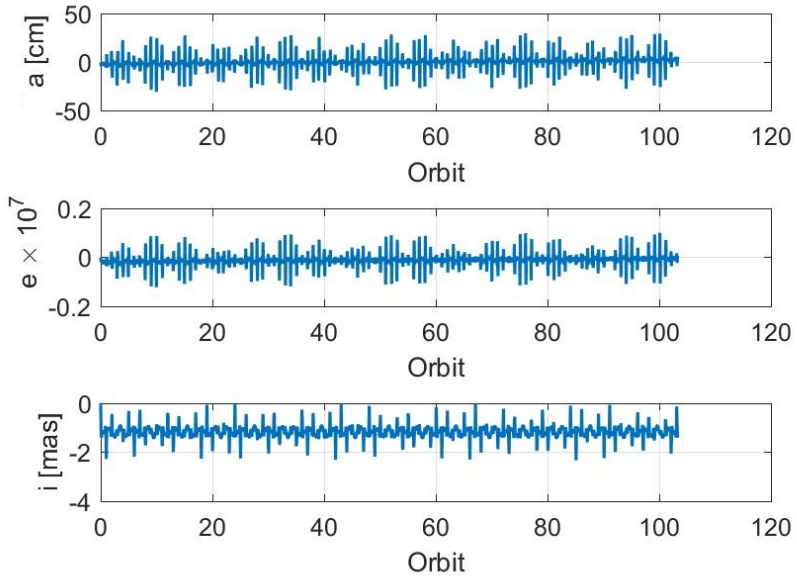

Figure 3.13: Propagation errors for Orbit-2 in the first three classical elements for 2×2 semi-analytic satellite theory with the tesseral periodic effects computed by numerical quadrature. The propagation time corresponds to 30 days with data points plotted at 30 minute intervals.

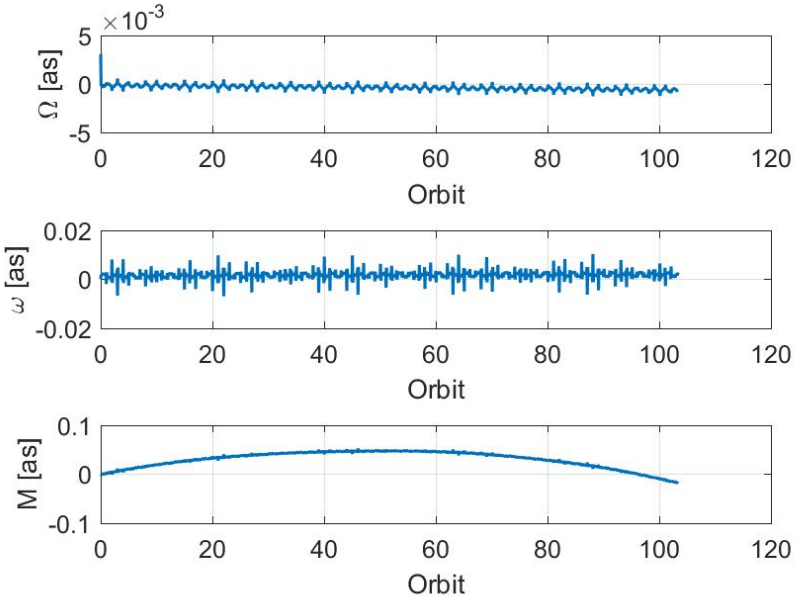

Figure 3.14: Propagation errors for Orbit-2 in the last three classical elements for 2×2 semi-analytic satellite theory with the tesseral periodic effects computed by numerical quadrature. The propagation time corresponds to 30 days with data points plotted at 30 minute intervals.

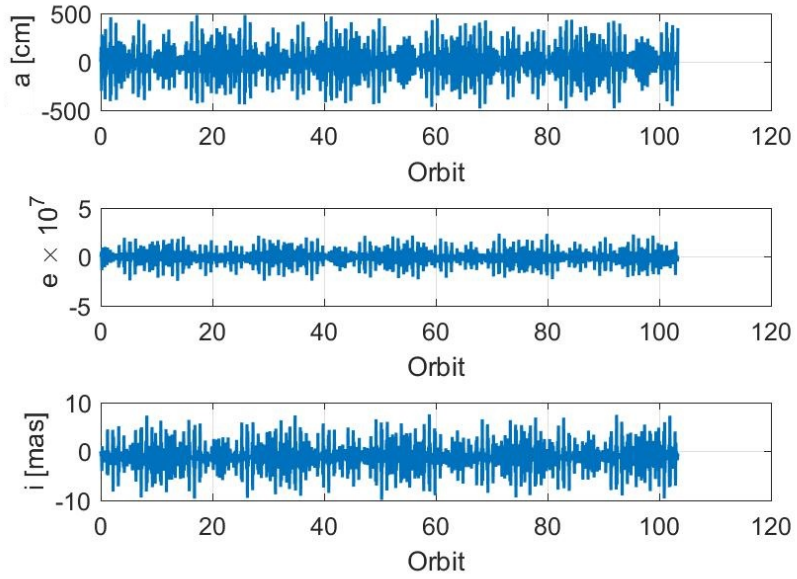

Figure 3.15: Propagation errors for Orbit-2 in the first three classical elements for 2×2 semi-analytic satellite theory with the tesseral periodic effects computed using the series solution in powers of the eccentricity. The propagation time corresponds to 30 days with data points plotted at 30 minute intervals.

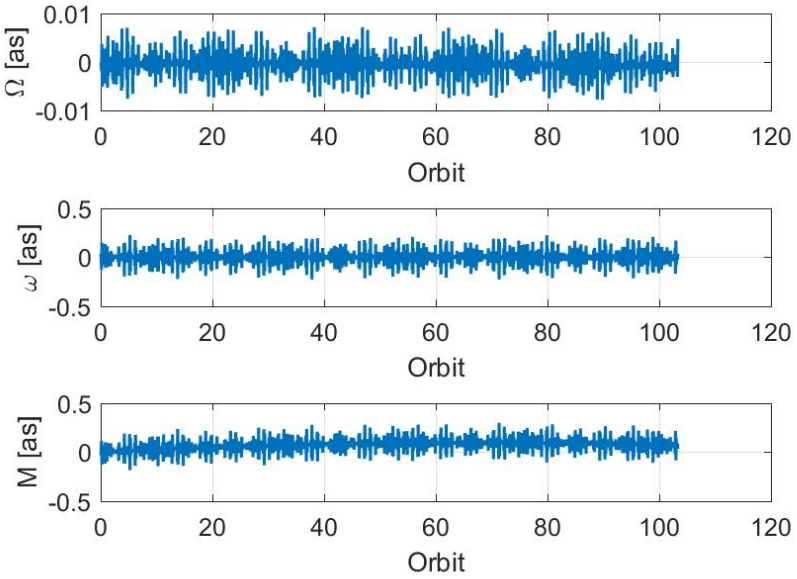

Figure 3.16: Propagation errors for Orbit-2 in the last three classical elements for 2×2 semi-analytic satellite theory with the tesseral periodic effects computed using the series solution in powers of the eccentricity. The propagation time corresponds to 30 days with data points plotted at 30 minute intervals.

The position and velocity errors for these two approaches for Orbit-1 and Orbit-2 are shown in Figures 3.17-3.20. It is noted that the smaller propagation errors for Orbit-2 compared to Orbit-1 are attributed to higher inclination of the former orbit. The proposed theory for tesseral periodic variations outperforms Lara's version of the method of relegation for both Orbit-1 and Orbit-2, when I_1^{nmp} and I_2^{nmp}, and their partial derivatives are computed numerically. The results in Figures 3.9-3.16 should be compared with Figures 2 and 4 of Reference [127]. For the near-circular Orbit-1, the proposed solution with I_1^{nmp} and I_2^{nmp} computed by eccentricity expansions, produce more accurate results than those from Lara's method of relegation after one iteration. In case of Orbit-2, Lara's method with five iterations produces better results than the proposed solution with eccentricity expansion based approach for all the elements except for the mean anomaly, for which Lara's method produces a secular growth in the error. It is noted that the mean anomaly has more significant contributions to position and velocity errors than other elements.

Figure 3.21 presents a comparison of the position and velocity errors for a 2×0 and a 6×6 completely analytic artificial satellite theory. The errors were computed by differencing the states propagated for a day using a 70×70 JGM-3 GMAT numerical propagator. It is noted that the 6×6 fully analytic theory provides more than $50\,\%$ improvement in the position and velocity predictions over 1 day and the errors between the two theories has a more than a linear growth with time.

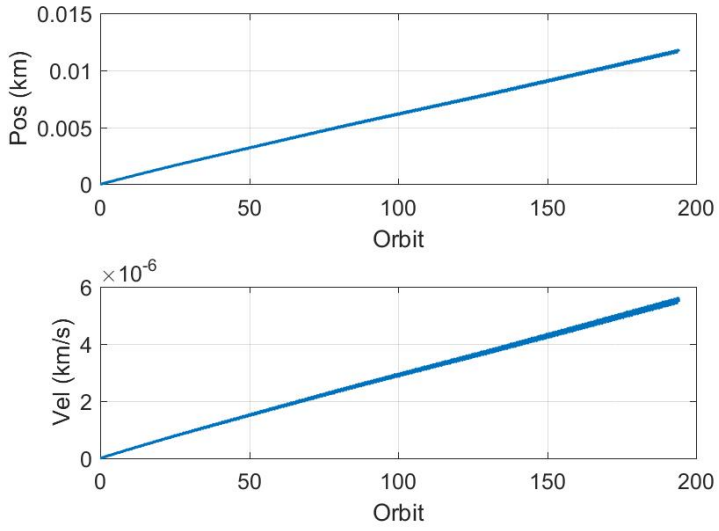

Figure 3.17: Position and velocity errors for Orbit-1 using 2×2 semi-analytic satellite theory including tesseral periodic effects computed using numerical quadrature. The propagation time corresponds to 30 days with data points plotted at 30 minute intervals. Neglecting the tesseral corrections in the semi-analytic theory for this orbit results in position and velocity errors of respectively, 80 km and 0.038 km/s in 30 days.

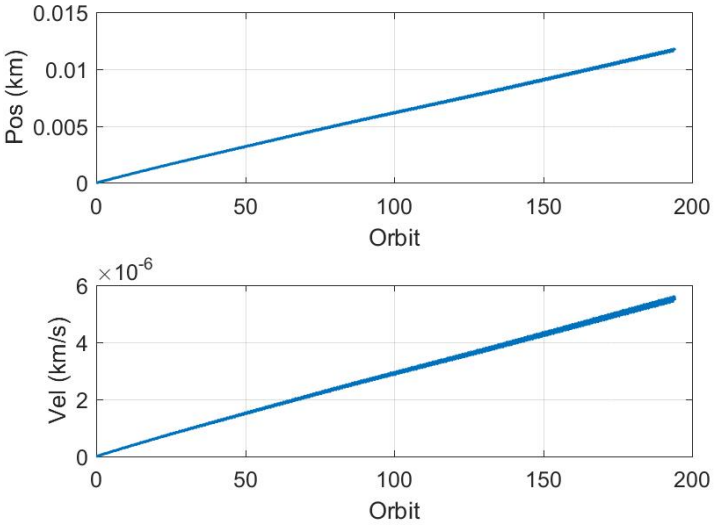

Figure 3.18: Position and velocity errors for Orbit-1 using 2×2 semi-analytic satellite theory including tesseral short-period effects computed using the eccentricity expansion. The propagation time corresponds to 30 days with data points plotted at 30 minute intervals. Neglecting the tesseral corrections in the semi-analytic theory for this orbit results in position and velocity errors of respectively, 80 km and 0.038 km/s in 30 days.

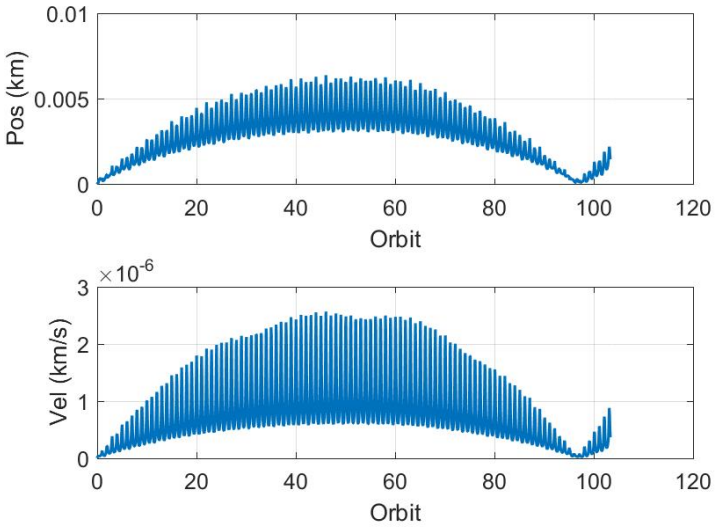

Figure 3.19: Position and velocity errors for Orbit-2 using 2×2 semi-analytic satellite theory including the tesseral short-period effects computed using numerical quadrature. The propagation time corresponds to 30 days with data points plotted at 30 minute intervals. Neglecting the tesseral contributions in the semi-analytic theory for this orbit results in position and velocity errors of respectively, 9.6 km and 0.004 km/s in 30 days.

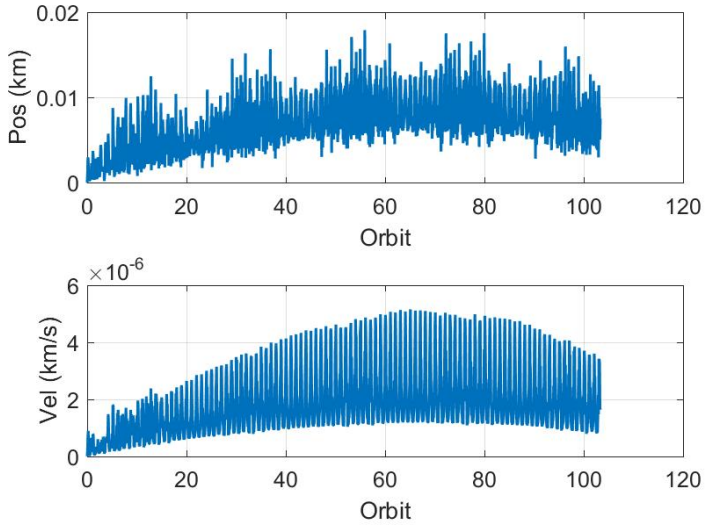

Figure 3.20: Position and velocity errors for Orbit-2 using 2×2 semi-analytic satellite theory including the tesseral short-period effects computed using the eccentricity expansion. The propagation time corresponds to 30 days with data points plotted at 30 minute intervals. Neglecting the tesseral contributions in the semi-analytic theory for this orbit results in position and velocity errors of respectively, 9.6 km and 0.004 km/s in 30 days.

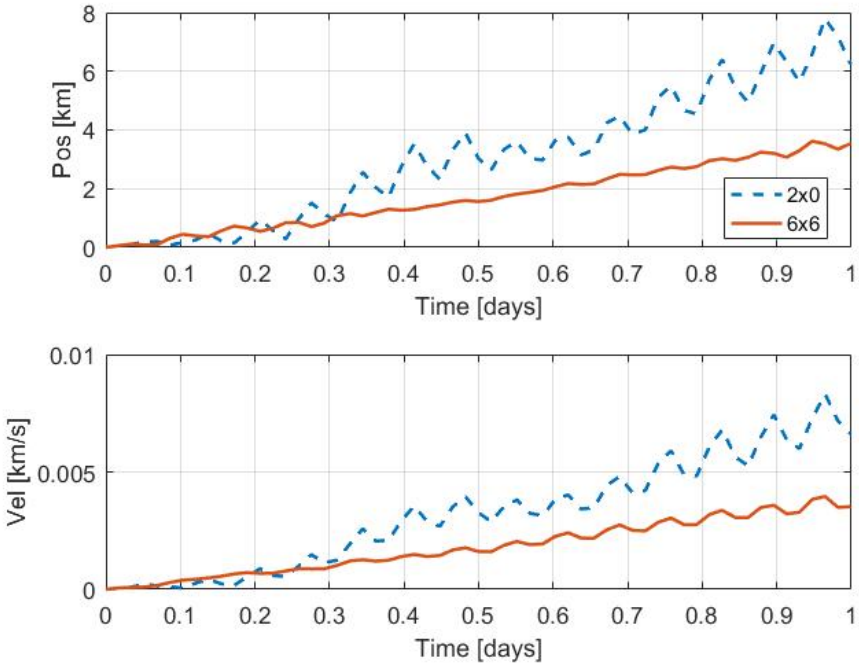

Figure 3.21: Absolute position and velocity errors with respect to 70×70 GMAT for 2×0 and 6×6 Exact Theory using quadrature. The initial osculating classical elements are $[7100, 0.05, 50^\circ, 10^\circ, 20^\circ, 30^\circ]$.

4. RELATIVE MOTION STATE TRANSITION MATRIX*

The advantages of modeling the satellite relative motion in terms of the differential orbital elements become apparent when the perturbation effects need to be incorporated into the analytic solutions. If the analytical expressions for the variations of the orbital elements in the presence of perturbations are available, then the task of incorporating the same perturbation effects in the solutions for the relative motion essentially reduces to computing Jacobian matrices of the element variations. It is noted that the order up to which the perturbation effects are included in the relative motion solution, depends on the order of the expressions for the orbital element variations and not on the linearized relationship between the orbital elements of the reference satellite and the relative states.

The artificial satellite theories developed in the previous chapter for the zonal and tesseral harmonics are used to derive a state transition matrix for the perturbed relative motion, referred to as RM-STM, in this chapter. The GA-STM framework, described in Section 2.3.3, is used for deriving the two versions of RM-STM: the first includes zonal harmonics J_2 to J_6 using the expressions for secular and periodic variations explicitly derived for each zonal (see Section 3.1), and the second uses the generalized expressions for the secular and periodic variations due to any

*Reprinted in part with permission from

B. Mahajan, S. R. Vadali, and K. T. Alfriend, "Analytic solution of perturbed relative motion with zonal and tesseral harmonics," In *Spaceflight Mechanics 2017: Proceedings of the 27th AAS/AIAA Space Flight Mechanics Meeting* held February 5-9, 2017 San Antonio, Texas, U.S.A., pp. 1117-1134. [AAS 17-475] (Advances in the Astronautical Sciences; Vol. 160). San Diego, California: Published for the American Astronautical Society by Univelt, Inc. (2017).

B. Mahajan, S. R. Vadali, and K. T. Alfriend, "Analytic solution for satellite relative motion: The complete zonal gravitational problem," In *Spaceflight Mechanics 2016: Proceedings of the 26th AAS/AIAA Space Flight Mechanics Meeting* held February 14-18, 2016, Napa, California, U.S.A. (pp. 3325-3348). [AAS 16-262] (Advances in the Astronautical Sciences; Vol. 158). San Diego, California: Published for the American Astronautical Society by Univelt, Inc. (2016).

B. Mahajan, S. R. Vadali, and K. T. Alfriend, "Analytic solution for satellite relative motion with zonal gravity perturbations," In *Astrodynamics 2015: Proceedings of the AAS/AIAA Astrodynamics Specialist Conference* held August 9-13, 2015, Vail, Colorado, U.S.A. (pp. 3583-3598). [AAS 15-705] (Advances in Astronautical Sciences; Vol. 156). San Diego, California: Published for the American Astronautical Society by Univelt, Inc. (2016).

zonal or tesseral harmonic (see Section 3.2 and 3.6). For the dominant harmonic J_2, the secular effects are included up to order $\mathcal{O}(J_2^3)$, and short-period and long-period effects up to $\mathcal{O}(J_2^2)$ using the explicitly derived expressions in Section 3.1 in both versions of the RM-STM. The derivation of these two versions of the RM-STM and the results showing improvements in the prediction of relative motion in the presence of zonal and tesseral harmonic perturbations are presented in the following subsections.

4.1 STM for Zonal Harmonics J_2-J_6

Following the GA-STM framework, the three component matrices (see Section 2.3.3) to propagate the relative states in the presence of perturbations are computed using the explicit expressions for the variations of the orbital elements due to the zonal harmonics J_2-J_6 [1]. This is accomplished by computing Jacobian of the secular rates, and the mean to osculating transformation. The nonsingular element set $[a, l+g, i, e\cos(g), e\sin(g), h]$ is used to compute the Jacobian, and as a result singularities for the circular reference orbits are avoided. The geometric transformation matrix, Σ, from Section 2.3.2 is derived using the nonsingular elements for computing the relative states in the curvilinear frame given the differential osculating nonsingular elements. The angular velocity of the Hill frame attached to the reference satellite needed for Σ, is computed in exact form for zonal harmonics J_2-J_6 using the Lagrange planetary equations. The RM-STM Φ for the zonal harmonics J_2-J_6 can be represented in a similar form as that of the original GA-STM (see Eq. 2.41) as shown below:

$$\Phi(t,t_0) = \Sigma(t)\, D(t)\, \phi_m(t,t_0)\, \left(\Sigma(t_0)\, D(t_0)\right)^{-1}, \tag{4.1}$$

where D is the differential mean to osculating transformation matrix for the nonsingular elements, ϕ_m is the differential STM for the mean nonsingular elements, and t_0 and t are the initial and final time, respectively. The component matrices of Φ are derived in the following subsections.

4.1.1 The Geometric Transformation Matrix

The derivation in Section 2.3.2 shows that adding the effects of any perturbation in Σ amounts to incorporating its effects in the angular velocity ϖ of the Hill frame attached to the reference satellite or the chief. This is because of the fact that Σ only depends on the osculating elements of the chief and ϖ. For deriving Σ in terms of the nonsingular elements, the following expressions for the chief's position and velocity components are used in Eq. 2.33:

$$\begin{aligned} r_0 &= \frac{a(1-q_1^2-q_2^2)}{(1+q_1\cos(\vartheta)+q_2\sin(\vartheta))}, \\ v_{r0} &= \sqrt{\frac{\mu}{a(1-q_1^2-q_2^2)}}\left(q_1\sin(\vartheta)-q_2\cos(\vartheta)\right), \\ v_{t0} &= \sqrt{\frac{\mu}{a(1-q_1^2-q_2^2)}}\left(1+q_1\cos(\vartheta)+q_2\sin(\vartheta)\right), \end{aligned} \tag{4.2}$$

where

$$\vartheta = f + g,$$

$$q_1 = e\,\cos g,$$

$$q_2 = e\,\sin g,$$

and the subscript 0 represents that these quantities are for the chief. The symbolic computations required for computing the expressions for each element of Σ matrix are done in Maple. To compute ϖ given in Eq. 2.40, Lagrange planetary equation (see Reference [224]) for node angle rate is used to compute the radial component of ϖ as follows:

$$\varpi_r = \frac{1}{\tilde{n}\,a\,b\,\sin\vartheta}\frac{\partial R}{\partial i}, \tag{4.3}$$

where b is semiminor axis, and R represents the disturbing function. A straightforward way to evaluate the expression for the radial component of ϖ is to use the Hamiltonian (without the two-body part H_0) for the zonal harmonics given in Eq. 3.22 as the disturbing function R. As a result, the equation for ϖ_r is obtained as

$$\varpi_r = \frac{1}{\tilde{n}\, a\, b\, \sin\vartheta} \frac{\partial}{\partial i} \left(\sum_{n=2}^{\infty} J_n \frac{\mu R_e^n}{a^{n+1}} \left(\frac{a}{r}\right)^{n+1} P_n(\sin i\, \sin\vartheta) \right). \tag{4.4}$$

A general expression for Legendre polynomials P_n is given in Eq. 3.27, which after substitution in the above equation, and carrying out the differentiation yields

$$\varpi_r = \frac{\cos i}{\tilde{n}\, a\, b} \sum_{n=2}^{\infty} J_n \frac{\mu R_e^n}{a^{n+1}} \left(\frac{a}{r}\right)^{n+1} \frac{1}{2^n} \times \sum_{j=0}^{\lfloor \frac{n}{2} \rfloor} \frac{(-1)^j (2n-2j)!\,(n-2j)}{j!\,(n-j)!\,(n-2j)!} \sin^{n-2j-1} i\, \sin^{n-2j-1}\vartheta. \tag{4.5}$$

The above expression has no singularities and is valid for any zonal harmonic. To compute the ϖ_r for zonal harmonics from J_2 to J_6, the first summation is performed only from $n = 2$ to $n = 6$ in the above expression. It is noted that for the polar orbits, the angular velocity of the Hill frame has no component in the radial direction, which results in no regression of the node.

With the expression for ϖ valid for any zonal harmonics derived, all the quantities for computing Σ are known. The inverse of Σ is also required for the relative motion STM as seen in Eq. 4.1, which can be computed symbolically or numerically. Since the inverse of Σ is only required once at the initial time, there is no particular advantage in computing the expressions for the inverse matrix symbolically.

4.1.2 Differential Mean to Osculating Transformation Matrix

The differential mean to osculating transformation matrix, D, captures the periodic effects due to perturbations on the differential mean elements. For the orbital elements, the periodic variations are computed using the two separate transformations: short-period and long-period for a fully analytic satellite theory as seen in Chapter 3. Therefore, D is computed using the two separate matrices: D_{LP} for the long-period and D_{SP} for the short-period variations as shown below:

$$D(t) = D_{SP}(t)\, D_{LP}(t), \tag{4.6}$$

where D_{LP} and D_{SP} are the Jacobian matrices of the corresponding near-identity transformations, and t represents the time. The near-identity transformations for the zonal harmonics J_2 to J_6 are give in Eqs. 3.17 for the short-period, and in 3.21 for the long-period variations. Using these equations, any element of D_{SP} and D_{LP} matrices with i and j indicating its row and column, respectively, is computed using the following equations:

$$\begin{aligned}
[D_{SP}]_{i,j} =& \frac{\partial [\mathcal{E}]_i}{\partial [\mathcal{E}_{LP}]_j}, \\
=& \delta_{i,j} + \epsilon \frac{\partial ([\mathcal{E}_{LP}]_i, \mathcal{W}_1)}{\partial [\mathcal{E}_{LP}]_j} + \frac{\epsilon^2}{2!} \left[\frac{\partial ([\mathcal{E}_{LP}]_i, \mathcal{W}_2)}{\partial [\mathcal{E}_{LP}]_j} + \frac{\partial (([\mathcal{E}_{LP}]_i, \mathcal{W}_1), \mathcal{W}_1)}{\partial [\mathcal{E}_{LP}]_j} \right] + O(\epsilon^3),
\end{aligned} \tag{4.7}$$

$$\begin{aligned}
[D_{LP}]_{i,j} =& \frac{\partial [\mathcal{E}_{LP}]_i}{\partial [\mathcal{E}_m]_j}, \\
=& \delta_{i,j} + \epsilon \frac{\partial ([\mathcal{E}_m]_i, \bar{\mathcal{W}}_1)}{\partial [\mathcal{E}_m]_j} + \frac{\epsilon^2}{2!} \left[\frac{\partial ([\mathcal{E}_m]_i, \bar{\mathcal{W}}_2)}{\partial [\mathcal{E}_m]_j} + \frac{\partial (([\mathcal{E}_m]_i, \bar{\mathcal{W}}_1), \bar{\mathcal{W}}_1)}{\partial [\mathcal{E}_m]_j} \right] + O(\epsilon^3),
\end{aligned} \tag{4.8}$$

where δ is the Kronecker delta; $\mathcal{E}_m$, $\mathcal{E}_{LP}$ and $\mathcal{E}$ represent the mean, short-period averaged, and osculating nonsingular elements, respectively; and a square bracket with subscripts indicates an element of the matrix or vector. The computations in the above equations are lengthy but straightforward and, were performed using Maple in this work. While the above results are derived for the nonsingular elements, they are still expressed in terms of the classical orbital elements, specifically the eccentricity and the inclination. The author's experience is that the artificial singularities in the expressions with respect to the circular or equatorial orbits are easier to remove especially using symbolic algebra software like Maple. This is due to the fact that all the singular terms with e or $(\sin i)$ in the denominator can be easily separated out from the rest.

4.1.3 Differential Mean STM

The differential mean STM, ϕ_m, propagates the differential mean elements from the initial time t_0 to the final time t. In case of the Delaunay elements, the mean rates are zero for the action variables (L, G, H) and constants for the angle variables (l, g, h). However, this is not true for the nonsingular elements as they are nonlinear functions of the Delaunay elements. Therefore, ϕ_m for the nonsingular elements is computed by taking a first-order variation of the mean nonsingular elements $\mathcal{E}_m$ at the final time expressed as functions of the mean Delaunay elements $\mathcal{D}_m$, with respect to the mean nonsingular elements at the initial time. To illustrate the process, consider $\mathcal{E}_m$ as a nonlinear vector function $\bar{F}$ of $\mathcal{D}_m$ as shown below:

$$\mathcal{E}_m(t) = \bar{F}\left(\mathcal{D}_m(t)\right), \tag{4.9}$$

where

$$\mathcal{D}_m(t) = \mathcal{D}_m(t_0) + \dot{\mathcal{D}}(t - t_0),$$

and $\dot{\mathcal{D}}$ represents the rates of the mean Delaunay elements, which are functions of the action variables only. A single element of ϕ_m, i.e., $[\phi_m]_{i,j}$ is computed by using the chain rule as given below:

$$\begin{aligned}
[\phi_m(t, t_0)]_{i,j} =& \frac{\partial[\bar{F}]_i}{\partial[\mathcal{E}_m(t_0)]_j}, \\
=& \frac{\partial[\bar{F}]_i}{\partial[\mathcal{D}_m(t)]_k} \left(\delta_{k,p} + \frac{\partial[\dot{\mathcal{D}}]_k}{\partial[\mathcal{D}_m(t_0)]_p}(t - t_0)\right) \frac{\partial[\mathcal{D}_m(t_0)]_p}{\partial[\mathcal{E}_m(t_0)]_j}.
\end{aligned} \tag{4.10}$$

In the above equation, the Einstein convention is used. The partial derivatives of the mean rates of the Delaunay elements $\dot{\mathcal{D}_m}$ can be computed by first deriving the Hessian matrix of the Kamiltonian $\bar{\mathcal{K}}$ defined in Eq. 3.18. Similar to the cases earlier, all of the symbolic computations in this section were performed in Maple.

4.1.4 Results

The MATLAB simulation results of the nonsingular element version of the RM-STM with the perturbations effects of J_2-J_6 harmonics included are given here. The accuracy is validated by comparing the propagation results with numerical propagation in GMAT with 6×0 JGM-3 gravity model. A projected circular orbit (PCO) formation (see Section 5.1) consisting of the two satellites, the chief and deputy, is simulated with the formation size of 1 km. The initial conditions are the mean elements of the chief, and the osculating elements were computed using the analytic mean to osculating transformation to start the numerical propagation. In addition to the relative states generated by the STM, the two satellite's analytically propagated states are also directly differenced, and the results (relative states) are plotted in the curvilinear frame for comparison. In all the results, the errors are computed by subtracting the relative states generated using the STM and direct differencing method from the numerically propagated relative states, and picking the maximum error value from a single orbit after the specified propagation time. Figure 4.1 shows the root-sum-square (RSS) relative position error after ten days of propagation for the STM and the direct differencing method, including the secular effects of J_2-J_6 up to order three, short-period and long-period effects of J_2 only up to order two. The initial chief's mean elements are chosen as: the semimajor axis 7100 km, inclination 50°, and the rest of the angles equal to 0°. The errors are plotted for a range of the orbital eccentricities of the chief. It is observed that the STM results match those of the direct differencing for the range of the eccentricity values considered. In the results shown in Figure 4.2, the long-period as well as short-period effects due to J_3-J_6 harmonics up to order two are also added in the theory. It is noticed that the relative position errors were brought down from $850\ m$ to less than $16\ m$ after ten days of propagation for $e = 0.5$ by adding long-period and short-period effects of the zonal harmonics J_3 to J_6.

Figures 4.3-4.5 show the RSS relative position errors for three different reference orbits (chief's orbits). The errors are plotted against the harmonic degree up to which the zonal harmonics are included in the analytic theory. It is noticed that the position errors in the first two figures increase after adding J_3 effects in the theory, however they gradually decrease after adding contributions of

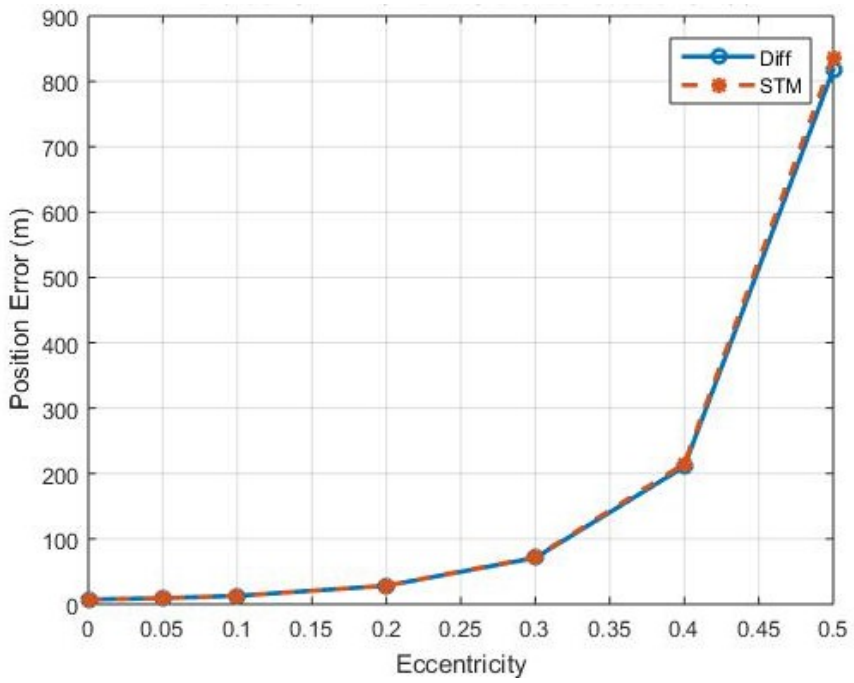

Figure 4.1: Relative position errors of the RM-STM and direct differencing (Diff) method after 10 days of propagation with J_2-J_6 secular effects up to $O(J_2^3)$ and J_2 short-period and long-period effects up to $O(J_2^2)$ included [1].

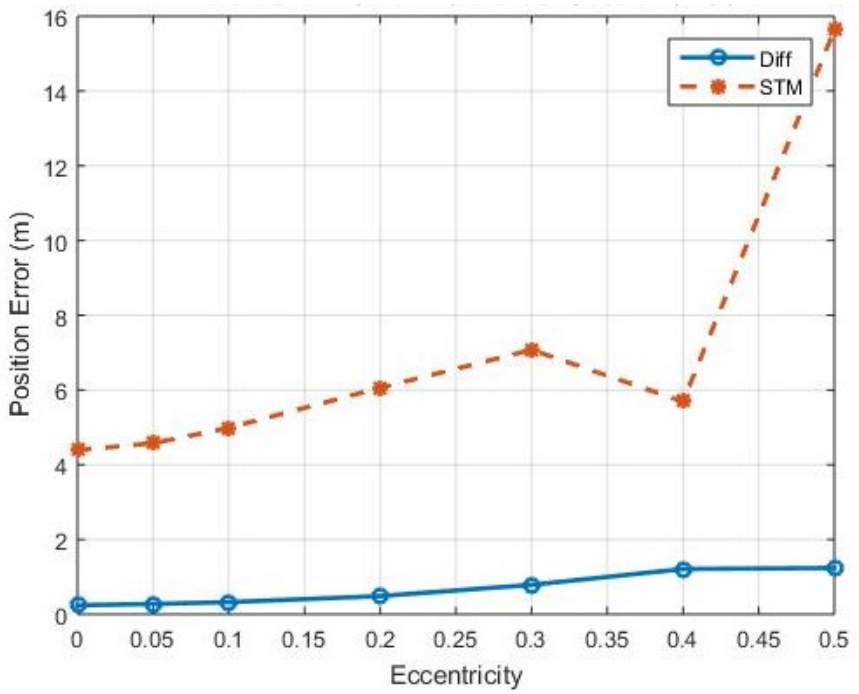

Figure 4.2: Relative position errors of the RM-STM and direct differencing (Diff) method after 10 days of propagation with J_2-J_6 secular effects up to $O(J_2^3)$ and J_2-J_6 short-period and long-period effects up to $O(J_2^2)$ included [1].

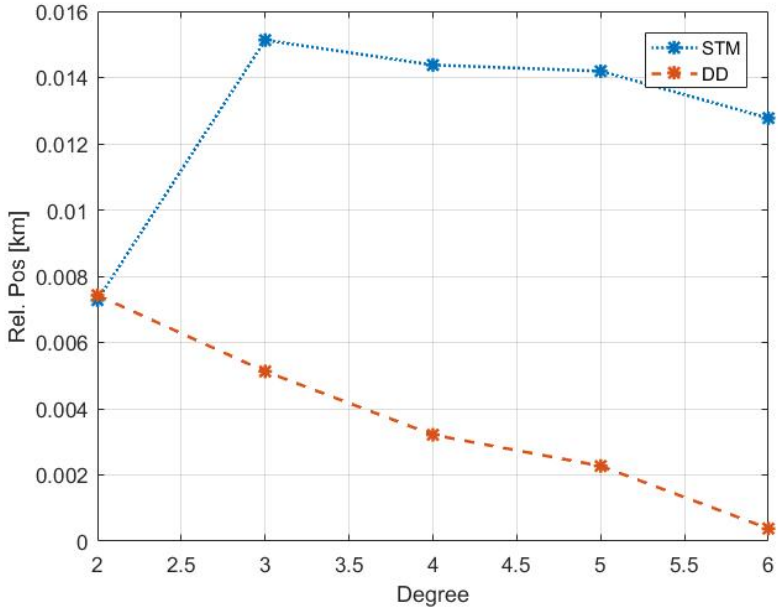

Figure 4.3: Relative position errors of the RM-STM and direct differencing (Diff) method after 10 days of propagation. The initial mean classical elements of the chief are $[7100, 0.01, 50^\circ, 0^\circ, 0^\circ, 0^\circ]$.

the higher zonal harmonics. This may be explained by the fact that the data points in all the plots correspond to the maximum errors obtained during a single orbit just after ten days of propagation, and not necessarily correspond to the same time epochs. Figure 4.6 shows the RSS relative position errors of the RM-STM and direct differencing method for different formation sizes after ten days of propagation. The geometric transformation in RM-STM is a linear representation of a nonlinear transformation. This linearization error is clearly shown in this figure for large formation sizes. The position errors in case of the direct differencing method were smaller as expected, since the latter method does not involve any approximation for converting relative orbital elements into the curvilinear frame.

4.2 STM for the Complete Zonal Problem

The satellite theory developed in Section 3.2 provides generalized expressions for the secular, short-period, and long-period variations of the equinoctial orbital elements due to an arbitrary zonal harmonic J_n ($n \geq 3$). These generalized expressions are very compact in size compared

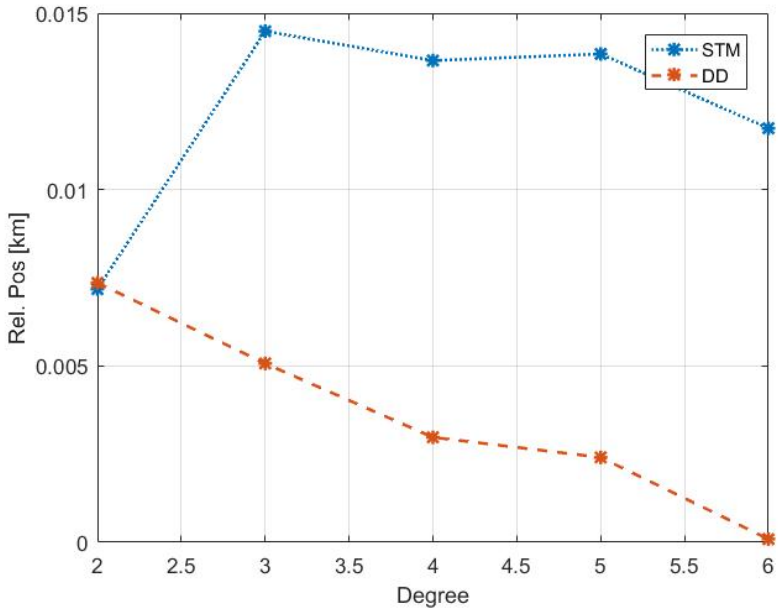

Figure 4.4: Relative position errors of the RM-STM and direct differencing (Diff) method after 10 days of propagation. The initial mean classical elements of the chief are $[7100, 0, 50^\circ, 0^\circ, 0^\circ, 0^\circ]$.

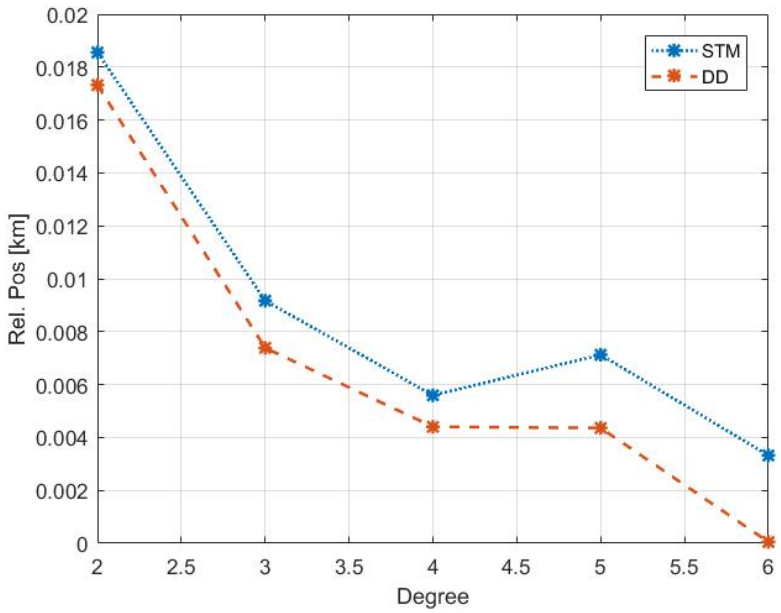

Figure 4.5: Relative position errors of the RM-STM and direct differencing (Diff) method after 10 days of propagation. The initial mean classical elements of the chief are $[7100, 0, 50^\circ, 10^\circ, 20^\circ, 30^\circ]$.

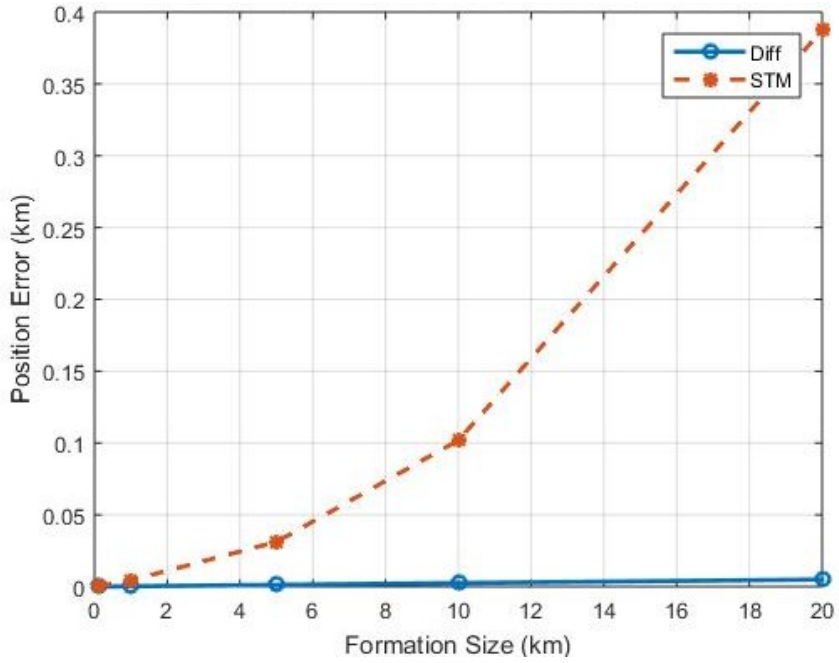

Figure 4.6: Relative position errors of the RM-STM and direct differencing (Diff) method versus formation size after 10 days of propagation with J_2-J_6 secular effects up to $O(J_2^3)$ and J_2-J_6 short-period and long-period effects up to $O(J_2^2)$ included. The initial mean classical elements of the chief are $[7100, 0.01, 50^\circ, 0^\circ, 0^\circ, 0^\circ]$ [1].

to the explicit expressions derived for each of the zonal harmonics up to J_6 for the absolute and relative motion theories in Section 3.1 and 4.1, respectively. The size of the explicit expressions for the higher zonal harmonics becomes prohibitively large. Therefore, a new relative motion STM using the satellite theory of Section 3.2 is derived in this section that includes the perturbation effects due to an arbitrary number of zonal harmonics [228]. This RM-STM is derived using the equinoctial elements and as a result, it contains no singularities for circular or equatorial reference orbits. It is noted that for J_2, the explicit expressions for the long-period, and short-period effects up to $\mathcal{O}(J_2^2)$, and secular rates up to $\mathcal{O}(J_2^3)$ are used that are derived in Section 3.1. The following subsections discuss how the contributions of an arbitrary zonal harmonic (with degree higher than two) are included in the component matrices in order to obtain the RM-STM for the complete zonal gravitational problem.

4.2.1 The Geometric Transformation Matrix

The derivation of the geometric transformation matrix in terms of the equinoctial elements is given in Section 2.3.2. The expression for the angular velocity of the Hill frame of the reference satellite, valid for an arbitrary number of zonal harmonics, has already been derived in Section 4.1.1 and the expression for the radial component is given in Eq. 4.5. There is no other modifications required in Σ to accommodate an arbitrary number of zonal harmonics for converting differential equinoctial elements to the relative states in the curvilinear frame.

4.2.2 Differential Mean to Osculating Transformation Matrix

Given the short-period, and long-period generating functions ($\mathcal{W}$, and $\bar{\mathcal{W}}$, respectively), the differential mean to osculating transformation matrix, D, can be computed using Eqs. 4.7 and 4.8, with $\mathcal{E}$ representing the equinoctial elements. The expressions for the long-period, and short-period variations of the equinoctial elements due to an arbitrary zonal harmonic J_n ($n \geq 3$) are given in Eqs. 3.58-3.63, and 3.65-3.70, respectively. Contrary to the derivations in the previous section, the Jacobian of these variations with respect to the equinoctial elements for computing D_{LP} and D_{SP} matrices, are derived by hand. The artificial singularities corresponding to the zero value of the eccentricity and inclination are completely removed from the expressions by combining the singular terms and canceling the singularities. The resulting D matrix includes the short-period effects up to $\mathcal{O}(J_2^2)$, and long-period effects up to $\mathcal{O}(J_2)$ due to an arbitrary zonal harmonic J_n ($n \geq 3$). Due to their large size, the generalized expressions for the elements of D matrix are not provided in this work, however they are implemented in the MATLAB code provided in the supplementary files (see Appendix D).

4.2.3 Differential Mean STM

The procedure to derive the differential mean STM, ϕ_m, follows the same approach as described in Section 4.1.3 with the exception that in this section, the equinoctial elements are exclusively used. The Delaunay element rates, $\dot{\mathcal{D}}$, due to an arbitrary zonal harmonic J_n ($n \geq 3$) are given in Section 3.2.1, which are used in Eq. 4.10 to compute the elements of ϕ_m matrix. The mean

equinoctial element set, represented as $\mathcal{E}_m$, are now considered as a vector function $\bar{F}$ of $\mathcal{D}$ in Eq. 4.10. Using these equations, the generalized expressions for each of the elements of ϕ_m with no singularities for the circular or equatorial orbits, are derived by hand in this work .

4.2.4 Results

The equinoctial element version of the RM-STM for the complete zonal gravitational problem is implemented in MATLAB, and the code is provided in the supplementary files (see Appendix D). For validating its accuracy, a formation of two satellites, the chief and deputy, with formation size 1 km is simulated in GMAT using a 70×0 JGM-3 gravity model. The mean initial conditions of the deputy are computed according to a projected circular orbit (PCO) type formation (see Section 5.1). The orbits of the chief and deputy are propagated for ten days in GMAT, and the relative position and velocity states in the curvilinear frame are computed. Using the RM-STM developed in this section, the same relative states are also propagated for ten days analytically. The errors are computed by subtracting the relative states generated using the RM-STM from the GMAT propagated states, and picking the maximum error value from a single orbit after the specified propagation time. Figures 4.7-4.9 show the RSS relative position errors in the curvilinear frame for the PCO formation after ten days of propagation for three different reference orbits, including a circular and equatorial reference orbit also. The errors are plotted against the harmonic degree up to which the zonal harmonics are included in the RM-STM. It is noted that in all the cases, the maximum relative position error is less than 20 m after ten days of propagation for the RM-STM with zonal harmonics included up to J_{20}. It should be noted that the data points in all the plots correspond to the maximum errors obtained during a single orbit just after ten days of propagation, and not necessarily correspond to the same time epochs.

4.3 Inclusion of Tesseral Harmonics in the STM

The short-period and m-daily variations of the equinoctial elements up to $\mathcal{O}(J_2^2)$ due to an arbitrary tesseral harmonic are derived in Section 3.6. The secular or long-period variations due to the resonant tesserals are ignored in this work. As a result, the tesseral harmonics only contribute

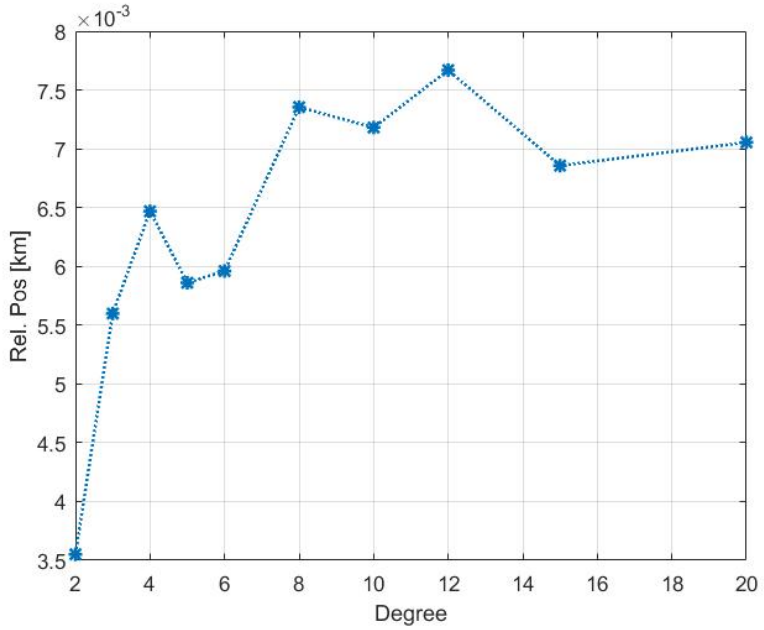

Figure 4.7: Relative position errors after 10 days of propagation versus the degree up to which the zonal harmonics are included in the RM-STM. The initial osculating classical elements of the chief are $[7100, 0.01, 50°, 0°, 0°, 0°]$.

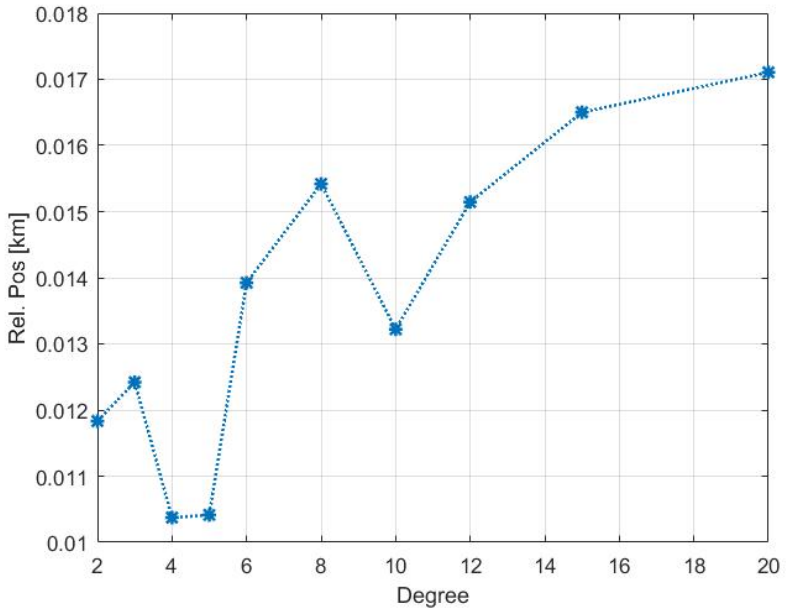

Figure 4.8: Relative position errors after 10 days of propagation versus the degree up to which the zonal harmonics are included in the RM-STM. The initial osculating classical elements of the chief are $[7100, 0, 0°, 0°, 0°, 0°]$.

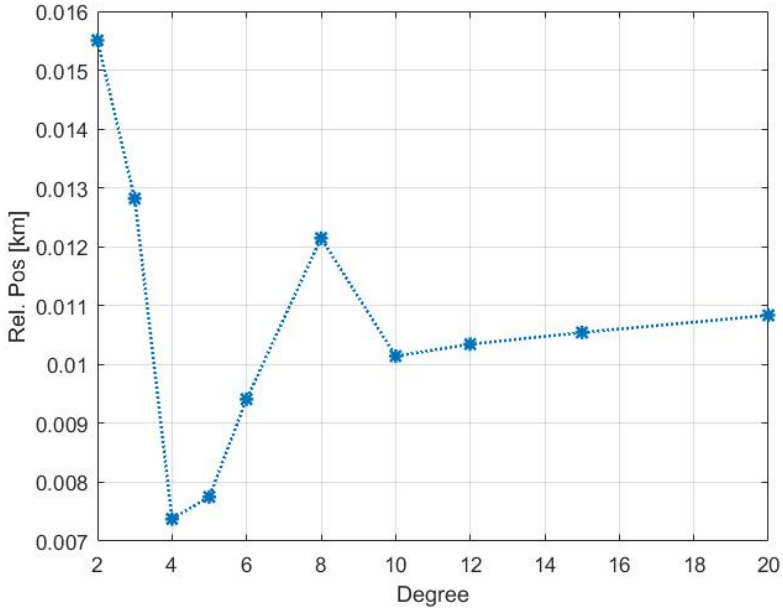

Figure 4.9: Relative position errors after 10 days of propagation versus the harmonic degree up to which the zonal harmonics are included in the RM-STM. The initial osculating classical elements of the chief are $[7100, 0, 0^\circ, 10^\circ, 20^\circ, 30^\circ]$.

to the differential long-period to short-period transformation matrix (D_{SP}) and to the geometric transformation matrix (Σ) in the form of the angular velocity expression for the Hill frame centered at the chief [237]. The Jacobain matrix D_{SP} for tesseral harmonics is computed by taking partials of the generalized expressions for the short-period variations of the equinoctial elements given in Eqs. 3.119-3.124. The Tesseral D_{SP} matrix is then added to D_{SP} matrix for the zonal contributions given in Section 4.2.2.

The Tesseral harmonic contributions to the angular velocity vector of the Hill frame attached to the reference satellite (or the chief) are derived here. As seen in the previous section, the expression for the radial component of the angular velocity ϖ needs to include the perturbation effects. Since the radial component is a function of the node angle rate, Lagrange planetary equation for $\dot{\Omega}$ with the following expression for the disturbing function given in Reference [42] (Chapter 3) is used:

$$R = -\frac{\mu R_e^n}{r^{n+1}} \sum_{t=0}^{k} T_{nmt} \sin^{n-m-2t}(i)\, \mathcal{R}_e \left[(C_{nm} - jS_{nm}) \cos m(\Omega - \theta) + \right.$$
$$\left. (S_{nm} + jC_{nm}) \sin m(\Omega - \theta) \right] \sum_{s=0}^{m} \binom{m}{s} j^s \sin^{n-m-2t+s} \vartheta \cos^{m-s} \vartheta \cos^s i, \tag{4.11}$$

where

$$T_{nmt} = \frac{(-1)^t\,(2n-2t)!}{2^n\, t!\,(n-t)!\,(n-m-2t)!}.$$

In the above equation, k is equal to the integer part of $(n-m)/2$, j is the imaginary unit, and $\mathcal{R}_e$ denote the real part. Differentiating R with respect to i and dividing by $\sin\vartheta$ results in the following equation:

$$\frac{1}{\sin\vartheta}\frac{\partial R}{\partial i} = -\frac{\mu R_e^n}{r^{n+1}} \sum_{t=0}^{k} T_{nmt} \sum_{s=0}^{m} \binom{m}{s} \mathcal{R}_e \left[j^s (C_{nm} - jS_{nm}) \cos m(\Omega - \theta) + \right.$$
$$\left. j^s (S_{nm} + jC_{nm}) \sin m(\Omega - \theta) \right] \sin^{n-m-2t+s-1} \vartheta \cos^{m-s} \vartheta$$
$$\times \left((n-m-2t) \sin^{n-m-2t-1} i \cos^{s+1} i - s \sin^{n-m-2t+1} i \cos^{s-1} i \right). \tag{4.12}$$

The above equation has no singularities. If the power of $\sin\vartheta$ is -1, then the only non-negative value s can have is 0. Similarly for the inclination related singularities, the coefficients of the singular terms vanish. By substituting the above result in Eq. 4.3, the complete expression for the radial component of the angular velocity of the chief's frame is computed for any arbitrary zonal or tesseral harmonic.

4.3.1 Results

The accuracy improvements for the satellite relative motion by including the tesseral short-period effects in the RM-STM is ascertained by comparing the results with numerically propagated orbits of the two satellites. A variable-step, variable-order Adams-Bashforth-Moulton integrator

(MATLAB *ode113* command) with JGM-3 Earth's gravity model and tolerances set to 10^{-11} was used as the numerical propagator. The initial conditions for the reference satellite or the chief for numerical propagation are taken from Table 3.1. Using a PCO formation (see Section 5.1), the mean initial equinoctial elements for the deputy are chosen based on a formation baseline of $1\,\mathrm{km}$ and phase angle 0°. The errors are computed by differencing the RM-STM propagated relative states from the numerically propagated orbits of the chief and deputy.

For the analytical propagation of the deputy's relative orbit using the RM-STM, the initial relative states are generated from the differential equinoctial elements using the inverse geometric transformation matrix. To use the correct initial conditions consistent with the analytical model is a crucial step. Initial conditions for the relative orbit computed using the linearized models such as the solutions of Hill-Clohessy-Wiltshire equations (see Reference [184], chapter 5) are not consistent with the relative motion STM, and produces relatively larger errors. For RM-STM, if the initial relative states in the curvilinear frame are not available, it is recommended to compute the differential orbital elements first by differencing the orbital elements of the chief and the deputy, and then use the inverse geometric transformation matrix to compute the relative states. The mean and osculating elements of the chief are computed and propagated using the methods described in Chapter 3. It is noted that in all the simulation results given in this section, the tesseral short-period effects are computed by evaluating the I_1^{nmp}, and I_2^{nmp} integrals as well as their partial derivatives using the adaptive quadrature algorithm available in MATLAB (the *integral* command) with tolerance set to 10^{-9}.

Figures 4.10 and 4.11 show the relative position errors in the curvilinear frame for the deputy with the analytical propagation using a 2×0, and 2×2 RM-STM, respectively. It should be noted that the 2×0 RM-STM includes the secular effects up to order three and periodic effects up to order two, in comparison the GA-STM includes only the first-order secular and periodic effects for J_2. The force model for the numerical propagation was 2×2 in both cases, and Orbit-1 from Table 3.1 was chosen as the reference orbit. The relative position errors after thirty days of propagation improved from $15\,\mathrm{m}$ to less than $1\,\mathrm{m}$. For a different reference orbit chosen for the chief, Orbit-2

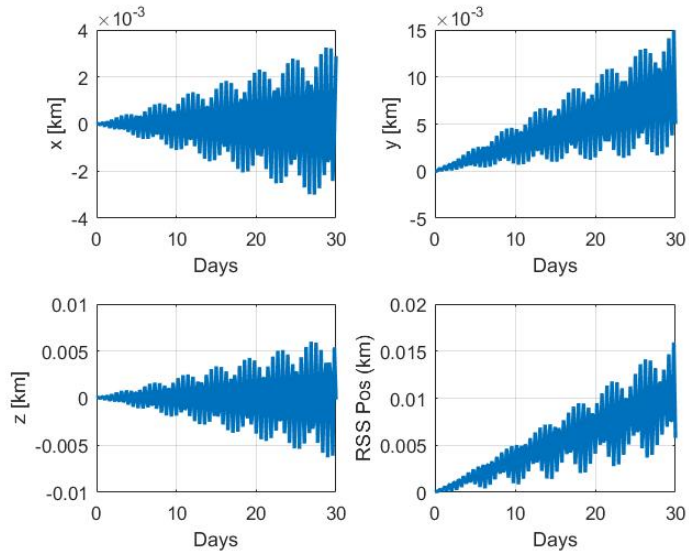

Figure 4.10: Relative position errors corresponding to reference orbit-1 of the 2×0 RM-STM with 2×2 numerical propagation as the truth model.

from Table 3.1, the similar results are shown in Figures 4.12 and 4.13. The relative position errors did not improve by adding tesseral harmonics in this case. It is noted that the less improvement in the absolute motion errors was also observed in Section 3.6.1 for this particular orbit. The high inclination of Orbit-2 is the reason as the tesserals do not affect the orbits with high inclination significantly.

Figure 4.14 presents a comparison of the relative position errors after 1 day of propagation incurred by a 2×0, and a 6×6 RM-STM. For this simulation, the numerical propagation was performed in GMAT with 70×70 JGM-3 gravity model. It is noticed that for the chosen reference orbit, the inclusion of tesseral harmonics improved the prediction of the along-track motion of the deputy by a significant amount when compared with the zonal RM-STM.

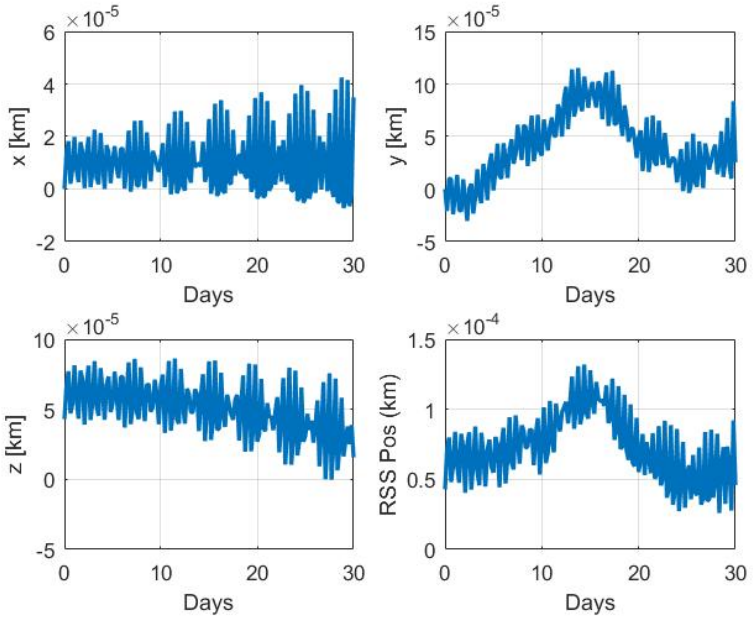

Figure 4.11: Relative position errors corresponding to reference orbit-1 of the 2×2 RM-STM with 2×2 numerical propagation as the truth model.

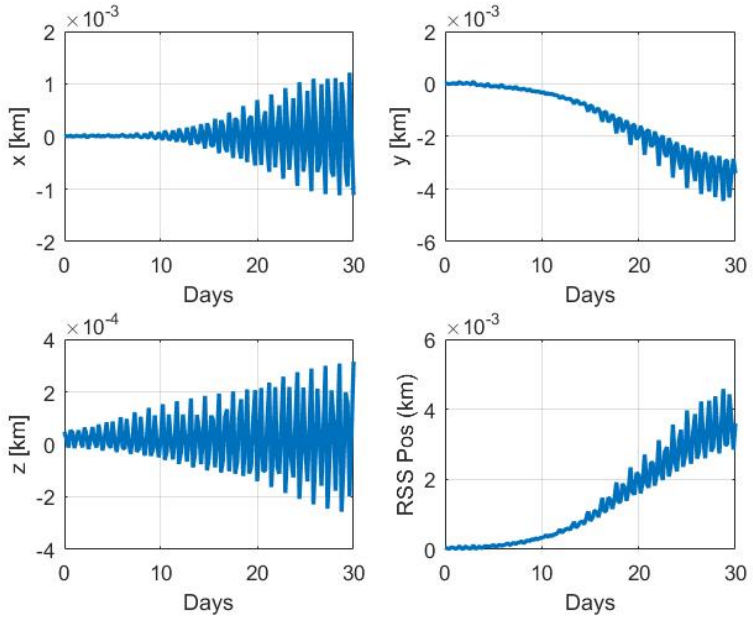

Figure 4.12: Relative position errors corresponding to reference orbit-2 of the 2×0 RM-STM with 2×2 numerical propagation as the truth model.

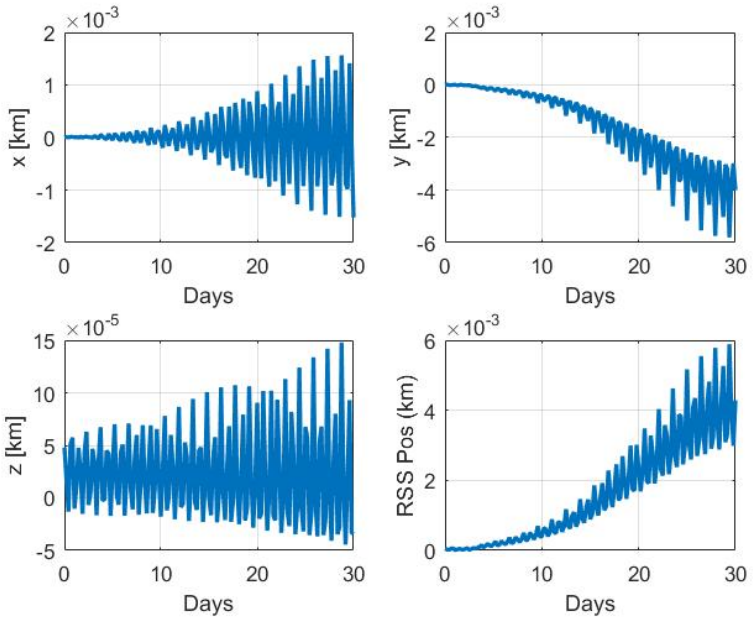

Figure 4.13: Relative position errors corresponding to reference orbit-2 of the 2×2 RM-STM with 2×2 numerical propagation as the truth model.

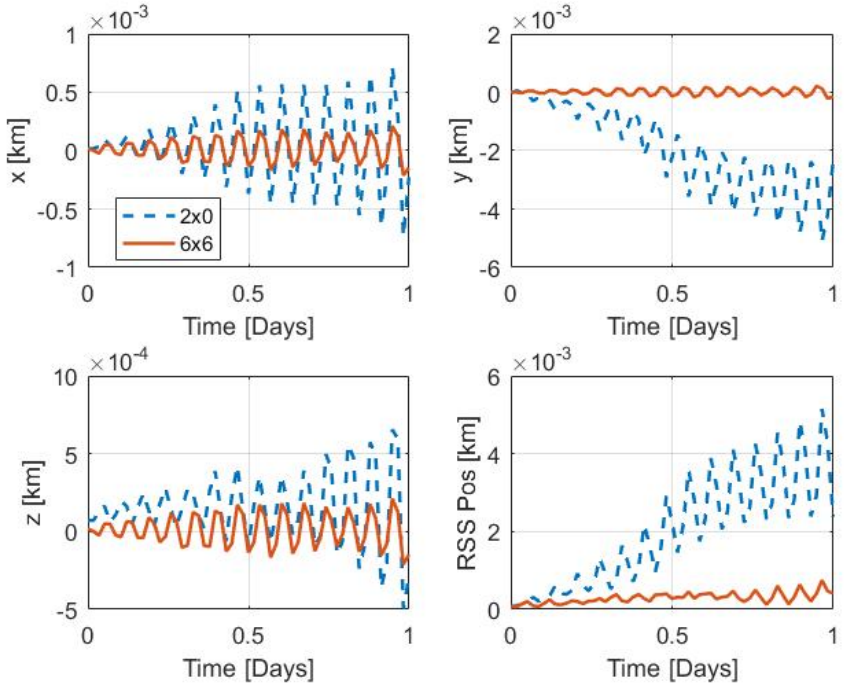

Figure 4.14: Relative position errors of the 2×0 and 6×6 RM-STM with 70×70 numerical propagation in GMAT as the truth model. The initial osculating classical elements of the chief are $[7100, 0.05, 50^\circ, 10^\circ, 20^\circ, 30^\circ]$.

5. FORMATION FLYING AND MISCELLANEOUS APPLICATIONS

A few applications of the theories developed in the previous chapters for the absolute and relative motion of satellites are presented here. First, initial conditions are derived in the form of the differential equinoctial elements required for establishing a general relative orbit of a deputy satellite around a chief satellite. The differential equinoctial elements are chosen to avoid singularities in case of the equatorial or circular reference orbits of the chief. Previous research has shown that the dominant second zonal harmonic causes significant along-track drift between the chief and deputy satellites if the initial conditions are not chosen by taking these effects into account. To extend these results to higher zonal harmonics, a drift mitigation condition for preventing the along-track drift including the secular effects due to an arbitrary zonal harmonic, is derived in this chapter. Also, two more applications using the results of Chapter 3 on the artificial satellite theories with the zonal and tesseral harmonics are presented. The first one demonstrates an analytic algorithm for solving the perturbed Lambert's problem for elliptic orbital transfers in the presence of the nonspherical gravitational perturbations. The second application demonstrates the efficient nonlinear propagation of the orbit uncertainties in time using point clouds.

5.1 Initial Conditions for Formation Establishment

The conventional way of specifying the geometry of the satellite formations is to use the constants of the particular bounded solutions of Hill-Clohessy-Wiltshire (HCW) equations. In contrast to the modeling of relative motion using the differential orbital elements, the HCW equations use Cartesian coordinates to model relative states in the Hill frame, and are derived by linearizing the nonlinear gravitational terms along with assuming circular reference orbit (see Reference [184]). The HCW equations are

$$\ddot{x} - 2\tilde{n}\dot{y} - 3\tilde{n}^2 x = 0, \tag{5.1}$$

$$\ddot{y} + 2\tilde{n}\dot{x} = 0, \tag{5.2}$$

$$\ddot{z} + \tilde{n}^2 z = 0, \tag{5.3}$$

where x, y, and z are the relative states in the radial, along-track and cross-track directions, respectively; and $\tilde{n}$ is the reference satellite's (or chief's) mean motion. A particular solution of the HCW equations, which is bounded, is as follows:

$$x = \rho_x \sin(\tilde{n}t + \alpha_x), \tag{5.4}$$

$$y = \rho_y + 2\rho_x \cos(\tilde{n}t + \alpha_x), \tag{5.5}$$

$$z = \rho_z \sin(\tilde{n}t + \alpha_z), \tag{5.6}$$

where the five constants, ρ_x, ρ_y, ρ_z, α_x, and α_z, are determined from the five initial conditions. The remaining initial condition is used to satisfy the constraint

$$\dot{y}(t_0) = -2\tilde{n}x(t_0) \tag{5.7}$$

on the initial along-track velocity to remove the secular terms from the general solution of the HCW equations.

Many different kinds of the relative orbit geometries can be obtained for different values of the five constants. For example, the projected circular orbit (PCO) formations, which are characterized by having a circular projection of the relative orbit in the yz-plane, can be designed by choosing

$$\rho_z = 2\rho_x \tag{5.8}$$

$$\alpha_x = \alpha_z \tag{5.9}$$

For more types of feasible orbit geometries, see Reference [184] (Chapter 5). Once the desired

relative orbit geometry is established, the initial differential orbital elements of the deputy satellite are needed for numerical or analytical propagation of its absolute states. The relationship between the five constants and the differential nonsingular elements is given in Reference [184]. To avoid singularity issues for circular and equatorial reference orbits, a similar relationship between the differential equinoctial elements and the five constants of the HCW bounded solution is derived here. In Reference [215], similar results are given for the PCO formations, which is a special case of the results presented in this section.

To derive the expressions for the differential equinoctial elements using the HCW solution constants, we substitute the following relations between the classical and equinoctial elements:

$$\delta h = -\frac{\sin(h)\delta p_1 - \cos(h)\delta p_2}{\sqrt{p_1^2 + p_2^2}}, \tag{5.10}$$

$$\delta h(1 - \cos(i)) = -2\frac{p_2\delta p_1 - p_1\delta p_2}{1 + p_1^2 + p_2^2}, \tag{5.11}$$

$$\delta i = \frac{2}{(1 + p_1^2 + p_2^2)}(\cos(h)\delta p_1 + \sin(h)\delta p_2), \tag{5.12}$$

$$\cos(\vartheta) = \cos(\Psi)\cos(h) + \sin(\Psi)\sin(h), \tag{5.13}$$

$$\sin(\vartheta) = \sin(\Psi)\cos(h) - \cos(\Psi)\sin(h), \tag{5.14}$$

$$\sin i = 2\frac{\sqrt{p_1^2 + p_2^2}}{1 + p_1^2 + p_2^2}, \tag{5.15}$$

into Eq. 2.29 for the along-track and cross-track motions to obtain the following results:

$$y = r\left(\delta\Psi + \frac{2}{1 + p_1^2 + p_2^2}\left(p_2\delta p_1 - p_1\delta p_2\right)\right), \tag{5.16}$$

$$z = \frac{2\,r}{1 + p_1^2 + p_2^2}\left(\sin\Psi\,\delta p_1 - \cos\Psi\,\delta p_2\right). \tag{5.17}$$

The quantity $\delta\Psi$ in the above equation can be expressed in terms of mean longitude by expanding in powers of the eccentricity and retaining only the first order term as shown below:

$$
\begin{aligned}
\delta\Psi &= \delta(f+g+h), \\
&= \delta(l+g+h+2e\sin l), \\
&= \delta\Lambda + 2\delta\left(e\sin\left(\Lambda - \tan^{-1}\frac{q_2}{q_1}\right)\right), \\
&= \delta\Lambda + 2\delta\left(\sin\Lambda\, q_1 - \cos\Lambda\, q_2\right), \\
&= \delta\Lambda + 2\left(\sin\Lambda\, q_2 + \cos\Lambda\, q_1\right)\delta\Lambda + 2\left(\sin\Lambda\,\delta q_1 - \cos\Lambda\,\delta q_2\right).
\end{aligned}
\tag{5.18}
$$

With the help of the last result, the along-track and cross-track motions can now be completely specified in terms of differential equinoctial elements. Before equating the above results to the solution of the HCW equations, the assumption of a circular reference orbit is made by approximating Ψ by Λ, and r by a. If it is assumed that the chief crosses the ascending node at the $t = 0$, then the quantity $\tilde{n}t$ in Eq. 5.4 can be replaced by $\Lambda - \Omega$, and the resulting equations in $y - z$ plane are:

$$
\begin{aligned}
y &= \rho_y + 2\rho_x\cos(\Lambda)\cos(\alpha'_x) - 2\rho_x\sin(\Lambda)\sin(\alpha'_x), \\
z &= \rho_z\sin(\Lambda)\cos(\alpha'_z) + \rho_z\cos(\Lambda)\sin(\alpha'_z),
\end{aligned}
\tag{5.19}
$$

where $\alpha'_x = \alpha_x - \Omega$ and $\alpha'_z = \alpha_z - \Omega$. The final step requires equating the coefficients of the $\sin\Lambda$ and $\cos\Lambda$ terms in Eqs. 5.16 and 5.19 and using Eq. 5.18 as well as $\Psi = \Lambda$ to get the following relations:

$$\delta p_1 = \frac{1+p_1^2+p_2^2}{2a}\rho_z\,\cos\alpha'_z \tag{5.20}$$

$$\delta p_2 = -\frac{1+p_1^2+p_2^2}{2a}\rho_z\,\sin\alpha'_z \tag{5.21}$$

$$\delta q_1 = -\frac{\rho_x}{a}\sin\alpha'_x \tag{5.22}$$

$$\delta q_2 = -\frac{\rho_x}{a}\cos\alpha'_x \tag{5.23}$$

$$\delta\Lambda = -\frac{\rho_y}{a(1+2q_1\cos\Lambda + 2q_2\sin\Lambda)} \tag{5.24}$$

Using the above result, the differential equinoctial elements for any given formation geometry specified using the constants of the HCW bounded solution can be computed. It is noted that α'_x and α'_z are different from the phase angles that appear in the HCW solution. However, they retain the property that their value specify the phase angles of the deputy with respect to the along-track and cross-track direction when the chief crosses the ascending node.

5.2 Along-Track Formation Drift Mitigation

If the assumptions of a spherical central body, circular reference orbit, and small separation between the two satellites in Keplerian orbits are made, then a global condition for periodic relative motion is

$$\delta a = 0, \tag{5.25}$$

where δa is the difference between the semimajor axes of the two satellites. The above condition ensures that the two satellites have matching angular rates. A more general condition to prevent drifts between the two satellites using energy arguments, which does not assume small separation and circular reference orbit, is given in Reference [184] (Chapter 4). On the other hand, if the assumption of the spherical central body is relaxed, and then a modification of the above drift mitigation condition is required that captures the effects due to nonspherical gravitational perturbations.

In the presence of zonal harmonic perturbations, the node angle h, the argument of periapsis g, and the mean motion $\tilde{n}$ have secular as well as periodic variations. The variations in these quantities, in turn, cause variations in the radial, along-track and cross-track motions of the deputy satellite. In this section, an along-track drift mitigation condition for δa that negates the secular drifts caused by any arbitrary zonal harmonic is derived. To negate the drifts in the cross-track and radial directions, additional constraints on the differential elements are needed. However, more than one constraint on the differential elements causes a loss in degrees of freedom in choosing a formation geometry.

The along-track motion of a deputy satellite can be written in terms of differential orbital elements assuming small formation size as (see Section 2.3.1):

$$y = r\left(\delta\vartheta + \delta h\cos(i)\right), \tag{5.26}$$

where $\delta\vartheta$ can be expressed in terms of the mean argument of the latitude λ after taking the first-order variations as follows:

$$\delta\vartheta = \delta\lambda + 2\left(\sin l\,\delta e - e\cos\lambda\,\delta l\right). \tag{5.27}$$

Ignoring the periodic terms and the eccentricity of the chief's orbit, the following equation for the along-track secular drift is obtained:

$$y = a\left(\delta\lambda + \delta h\cos(i)\right). \tag{5.28}$$

Using the mean elements of the chief in the above equation and differentiating with respect to time, the secular drift rate of the deputy in the along-track direction is obtained as follows:

$$\dot{y} = a\left(\delta\dot{\lambda} + \delta\dot{h}\cos(i)\right). \tag{5.29}$$

Thus, the following constraint on the differential element rates must be satisfied to negate the along-track drift assuming small formations about a circular reference orbit:

$$\delta\dot{\lambda} + \delta\dot{h}\cos(i) = 0. \tag{5.30}$$

For J_2, the secular rates of l, g, and h are derived in Section 3.1 up to $\mathcal{O}(J_2^3)$. The secular rates due to an arbitrary zonal harmonic J_n with $n \geq 3$ up to $\mathcal{O}(J_2)$ are given in Eqs. 3.47-3.49. Taking first order variations of these secular rates with respect to a, e and i, and substituting in the above constraint equation yields the constraint for δa in terms of δe and δi that must be satisfied to negate the along-track drift. In this section, the drift mitigation condition for an arbitrary zonal harmonic

is derived to first order. To simplify the derivation, Eq. 5.30 can be written as

$$\delta(\dot{\mathcal{L}}) + \dot{h}\sin i\,\delta i = 0, \tag{5.31}$$

where the term $\dot{\mathcal{L}} = \dot{\lambda} + \dot{h}\cos i$ can be written using Eqs. 3.47-3.49 as

$$\dot{\mathcal{L}} = \frac{\delta_n(a,e)}{L}\sum_{j=0}^{\lfloor \frac{n}{2} \rfloor}\beta_{j,n}(i)\sum_{\text{even } k=0}^{n-1}\frac{\alpha_{k,n}(e)}{2^k}\binom{n-2j}{\frac{n}{2}-j}\binom{k}{\frac{k}{2}}\left\{-3-\frac{2n-1}{\eta}-k\frac{\eta}{1+\eta}\right\}. \tag{5.32}$$

By taking variations of the above equation, we obtain:

$$\frac{\partial\dot{\mathcal{L}}}{\partial a}\delta a + \frac{\partial\dot{\mathcal{L}}}{\partial e}\delta e + \left(\frac{\partial\dot{\mathcal{L}}}{\partial i} + \dot{h}\sin i\right)\delta i = 0, \tag{5.33}$$

which can be solved to obtain the final result for the along-track drift mitigation constraint for δa in the presence of an arbitrary zonal harmonic:

$$\delta a = -\left(\frac{\partial\dot{\mathcal{L}}}{\partial a}\right)^{-1}\left(\frac{\partial\dot{\mathcal{L}}}{\partial e}\delta e + \left(\frac{\partial\dot{\mathcal{L}}}{\partial i} + \dot{h}\sin i\right)\delta i\right). \tag{5.34}$$

It is emphasized that the assumptions such as the circular reference orbit and small formation size, are assumed in deriving the above result.

5.2.1 Results

The absolute motion of the two satellites in a PCO-type formation are propagated numerically to ascertain the improvements in preventing the along-track drift between the satellites in formation. The mean initial conditions for the chief were chosen as: $[a = 6700\,\text{km}, e = 0.03, i = 50^\circ, \Omega = 10^\circ, \omega = 20^\circ, M = 30^\circ]$. The mean initial equinoctial elements of the deputy are computed using the formulae given in Eq. 5.20 with the data: $[\rho_z = 2\rho_x = 1\,\text{km}, \rho_y = 0, \alpha'_x = \alpha'_z = -10^\circ]$. The drift constraint on the mean δa of the deputy was computed for the two separate cases: with only J_2 effects included up to $\mathcal{O}(J_2)$ referred as the J_2 drift condition, and for the second, the effects of the zonal harmonics from J_2 to J_{10} are included up to $\mathcal{O}(J_2^2)$ in the drift

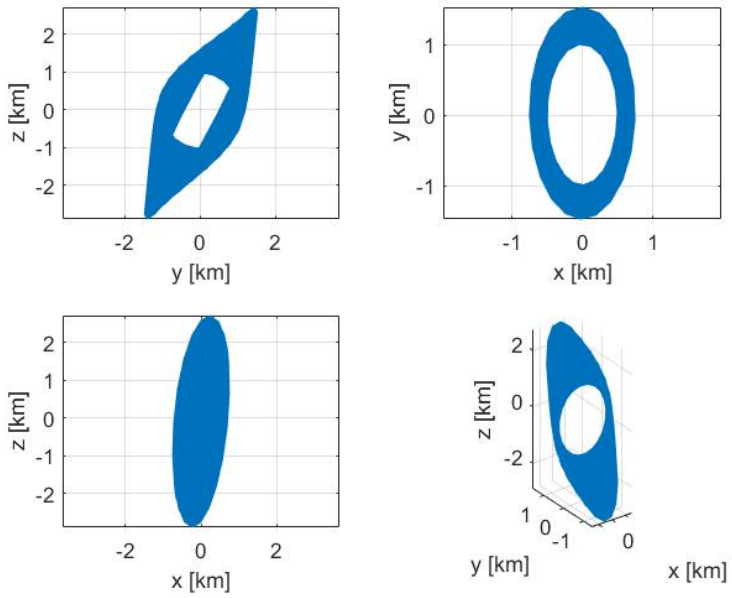

Figure 5.1: PCO-type relative orbit of the deputy with J_2 drift condition on δa for a time span of 30 days.

condition referred to as the J_n condition. The osculating conditions for the numerical propagation were computed using a mean to osculating transformation with effects due to 10×10 spherical harmonics included. The force model for the numerical propagation also includes 10×10 spherical harmonics. Figures 5.1 and 5.2 shows the deputy's relative orbit, and its along-track drift with J_2 drift condition for a time span of thirty days. It is noted that the higher degree zonal harmonics contribute less than $25\,\mathrm{m}$ to the along-track drift. The results for the J_n drift condition is given in Figures 5.3 and 5.4, which shows that the J_n drift condition has successfully negated the along-track drift due to the higher zonal harmonics. The along-track drifts shown in Figures 5.2 and 5.4 are computed using Eq. 5.28.

5.3 Perturbed Lambert Solver for Elliptic Orbit Transfers

In this section, the artificial satellite theory for the zonal and tesseral harmonics is used to solve the perturbed Lambert's problem for elliptic orbital transfers. The two-body Lambert's problem is a boundary-value problem for the Keplerian motion, and its solution provides a Keplerian transfer

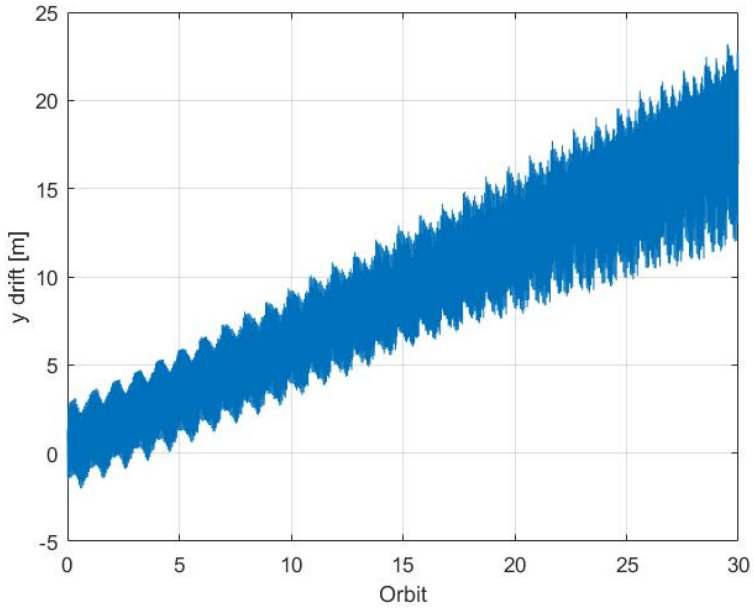

Figure 5.2: Along-track drift of the deputy with J_2 drift condition on δa for a time span of 30 days.

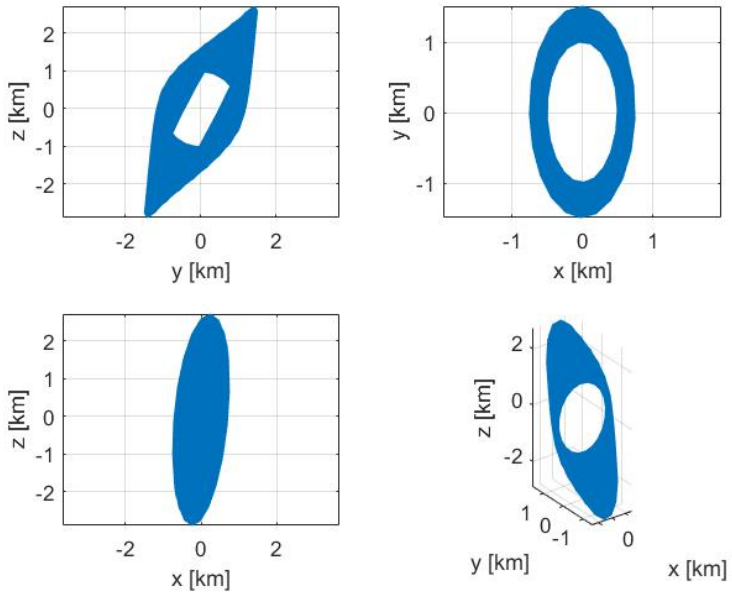

Figure 5.3: PCO-type relative orbit of the deputy with J_n drift condition ($n = 10$) on δa for a time span of 30 days.

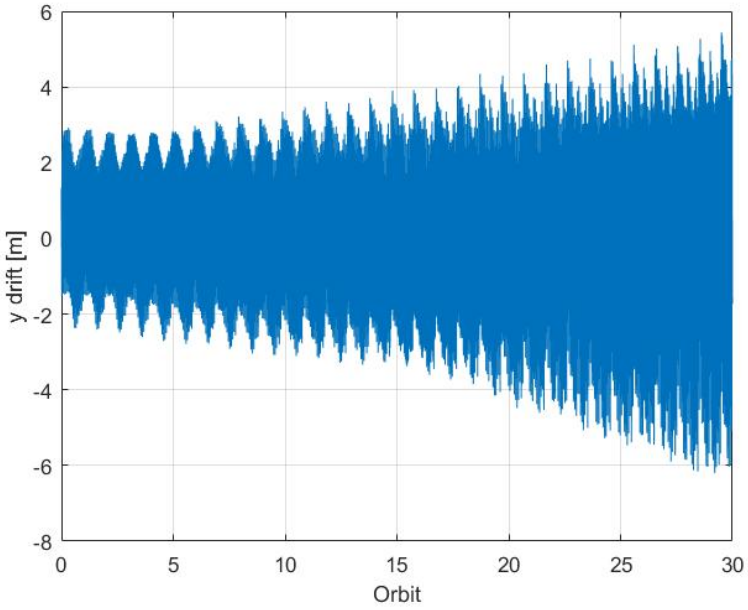

Figure 5.4: Along-track drift of the deputy with J_n drift condition ($n = 10$) on δa for a time span of 30 days.

orbit that connects the two given positions in a given transfer time. Solving the Lambert's problem amounts to finding the initial velocity that completes the initial state vector, which when propagated forward in time for the given transfer duration, achieves the final desired position. A detailed introduction to the two body Lambert's problem and the techniques for its solution are provided by Battin [224]. In the presence of nonspherical gravitational perturbations, the exact solution to the two-body Lambert's problem can exhibit significant error if the transfer time is sufficiently long, e.g., in case of multiple revolution transfer orbits.

If an analytic solution to a dynamical system, whose time evolution is described by ordinary differential equations, is available then solving a boundary value problem for that dynamical system is reduced to finding roots of a set of nonlinear equations. The artificial satellite theories developed in Chapter 3 provides an approximate analytic solution for propagating bounded orbits of a spacecraft in the vicinity of a nonspherical central body. A Lambert solver for computing perturbed elliptic transfer orbits can be formulated by utilizing these satellite theories for the analytic propagation, replacing the numerical propagation in the conventional shooting methods based

perturbed Lambert solvers. The advantage of the analytical propagation lies not just in the faster propagation, but also in the availability of the analytic sensitivity matrices that are needed for the numerical root solving algorithms that are required for the solution.

To formulate a perturbed Lambert solver, the position and velocity states at the final time are computed analytically using the initial position and a guess for the initial velocity. The difference between the analytically propagated states and the desired final position provides three nonlinear constraint equations with the three components of the initial velocity as their roots. The two-body Lambert solver can provide the guess for the initial velocities or the roots, which are further refined by the perturbed Lambert solver by applying Newton's method to drive the three nonlinear constraints to zero, i.e., nullify the error between the propagated final position and the desired final position. The steps to implement a perturbed elliptic Lambert solver using the artificial satellite theories for analytical propagation are given in Figure 5.5.

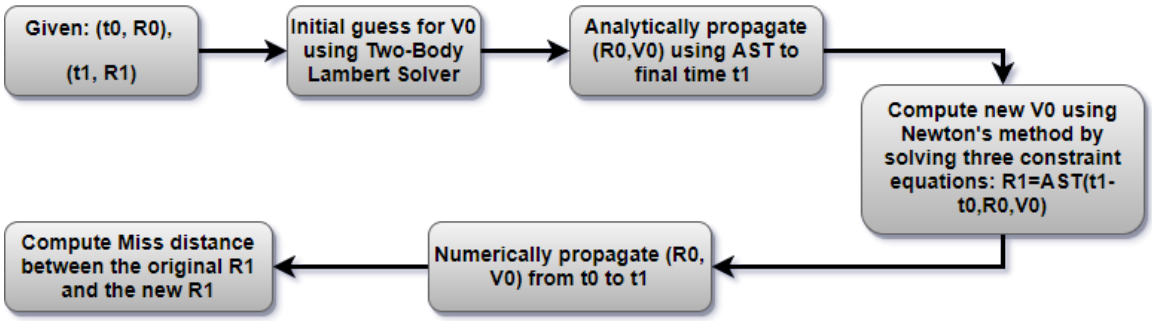

Figure 5.5: Algorithm for the perturbed Lambert solver for elliptic orbital transfers. The final step is only required to assess the performance of the Lambert solver.

To validate the performance and accuracy of the perturbed Lambert solver for a multiple revolution orbit transfer, a MATLAB simulation is built that generated a true elliptic transfer orbit in a 20×20 JGM-3 gravity field. The true transfer orbit has its perigee at $6500\,\mathrm{km}$, and apogee at $60\,000\,\mathrm{km}$. The inclination of the transfer orbit was chosen to be 5° and rest of all the initial elements are zero. The transfer time was chosen as 3.35 times the orbital period or 2.34 days. Using

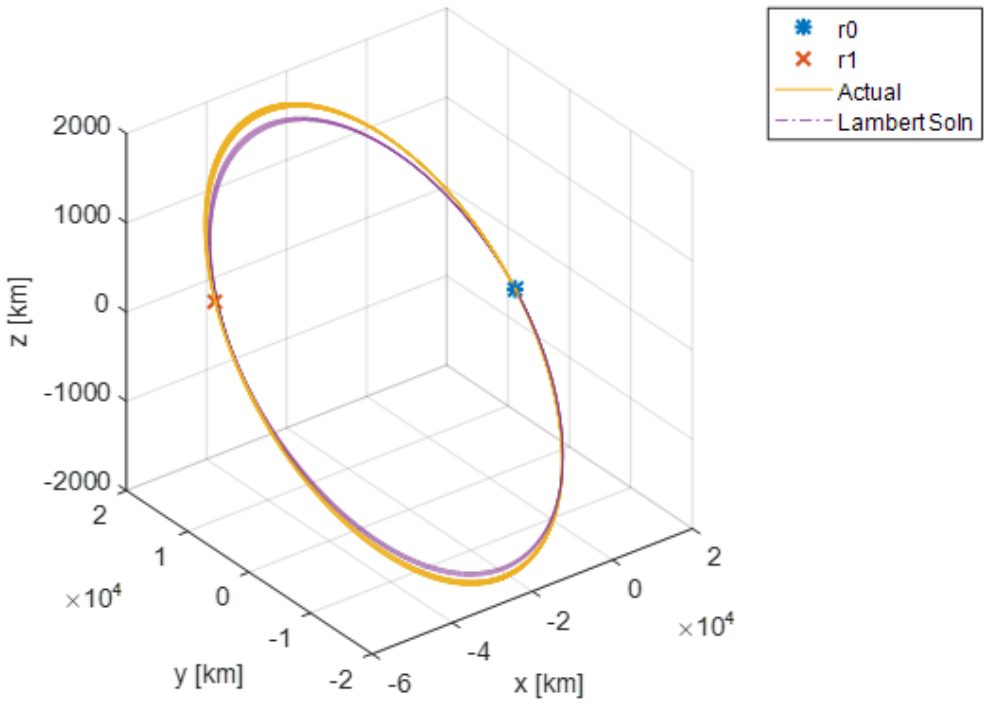

Figure 5.6: Actual multiple-revolution transfer orbit and the two-body Lambert solution transfer orbit propagated numerically in 20×20 gravity field.

a two-body Lambert solver*, a multiple revolution (with 3 complete revolutions) solution when propagated in the 20×20 JGM-3 gravity field for the given transfer time, the final position misses the desired one by more than $2500\,\mathrm{km}$. Figure 5.6 shows the true transfer orbit and the two-body Lambert transfer solution. The initial velocities and the final positions of the actual transfer orbit and the two-body Lambert solution are given in Table 5.1 and 5.2, respectively.

Next, the initial velocity from the two-body Lambert solver was improved using the perturbed Lambert solver that used a 6×6 JGM-3 gravity model to propagate the transfer orbit. The improved results for initial velocity and the final position are shown in Tables 5.1 and 5.2, respectively. Additionally, the results for a perturbed Lambert solver that used numerical propagation instead of the artificial satellite theories (AST) are also given. The accuracy of the perturbed Lambert solver

*https://www.mathworks.com/matlabcentral/fileexchange/39530-lambert-s-problem

Table 5.1: Initial velocities of the actual transfer orbit, the two-body Lambert solution, and the perturbed Lambert solution using AST. All quantities are expressed in the inertial frame. The unit is $\mathrm{km/sec}$.

Initial Velocities	v_x	v_y	v_z
True	0	10.4794	0.916828
TB Lambert	-0.0492813	10.4823	0.845299
Pert. Lambert (Num.)	0.000022525	10.4794	0.916559
Pert. Lambert (AST)	-0.000439634	10.4794	0.917053

Table 5.2: Final position of the actual transfer orbit, the two-body Lambert solution, and the perturbed Lambert solution using AST. All quantities are expressed in the inertial frame. The unit is km.

Final Positions	x	y	z
True	-56615.5996	7736.43904	623.869684
TB Lambert	-57510.0563	5406.3636	386.348638
Pert. Lambert (Num.)	-56610.8217	7744.97721	624.434857
Pert. Lambert (AST)	-56608.9156	7744.01436	624.691054

using AST is significantly more than the two body Lambert solver and very slightly worse than the perturbed Lambert solver with numerical propagation. The time taken for the Newton's method to converge for the perturbed Lambert solver with numerical and analytical propagation is $80\,\mathrm{sec}$ and $68\,\mathrm{sec}$, respectively. The finite differencing was used to compute sensitivity matrices in both the cases in this simulation. For longer transfer times and with analytic sensitivity matrices provided to the Newton's method solver, the perturbed Lambert solver with analytic propagation is expected to have even further speed improvements.

5.4 Nonlinear Uncertainty Propagation Using Point Clouds

It is well known that the orbit propagation is an example of a highly nonlinear dynamical process. If the initial uncertainty in the orbital states is Gaussian, then the mean and covariance propagation using the linearized models of the orbital dynamics, induces errors in the posteriori uncertainty estimation, which grow over time. The initial Gaussian uncertainty in the states of a satellite loses its Gaussian properties quickly over time within a few days. These phenomena

affect the performance of the estimation filters like the first-order Extended Kalman Filter (EKF). The Unscented Kalamn Filter (UKF) avoids the limitations (to a degree) of the linearized propagation of the Gaussian uncertainty by propagating a small number of sigma points carefully sampled about the mean, using the actual nonlinear dynamics. The mean and covariance can then be reconstructed from the propagated sigma points. Because the UKF also assumes that the uncertainty is Gaussian, its performance also suffers for highly nonlinear dynamics and non-Gaussian initial uncertainty. Particle Filter (PF) is a Monte Carlo based algorithm that propagates a large number of sample points generated from the initial distribution, through the nonlinear dynamics. The mean and covariance as well as the higher moments of the posterior distribution can then be computed from the propagated sample points. It is clear that PF, and to some extent the UKF also, are computationally intensive algorithms and significant improvement in their execution performance can be achieved by efficiently propagating the sample and sigma points through the nonlinear orbital dynamics.

The artificial satellite theories developed in this work provides a rapid and fairly accurate means of propagating point clouds (sample points) through the nonspherical gravitational field of a central body. The theories, being completely analytic, are capable of propagating all the sample points in the point cloud to the final time in a single step unlike numerical integration that must take small time steps to maintain accuracy. To demonstrate the usefulness of the satellite theories for the nonlinear uncertainty propagation using point clouds, a MATLAB simulation is implemented that propagates 50 sample points analytically as well as numerically. The time evolution of the point cloud is then shown for both type of propagations to compare the analytically propagated distribution of sample points to that of the numerical propagation.

An initial orbit was chosen with the classical orbital elements as [$7100\,\mathrm{km}$, 0.05, 50°, 10°, 20°, 30°]. A point cloud about this mean orbit was generated by adding normally distributed noise to the position and velocity states in the radial, along-track, and cross-track directions. The standard deviations for the noise distribution were chosen as $500\,\mathrm{m}$, $1\,\mathrm{m}$, and $1\,\mathrm{m}$ in the three directions, respectively. Similarly, the noise in the velocity states were generated using standard

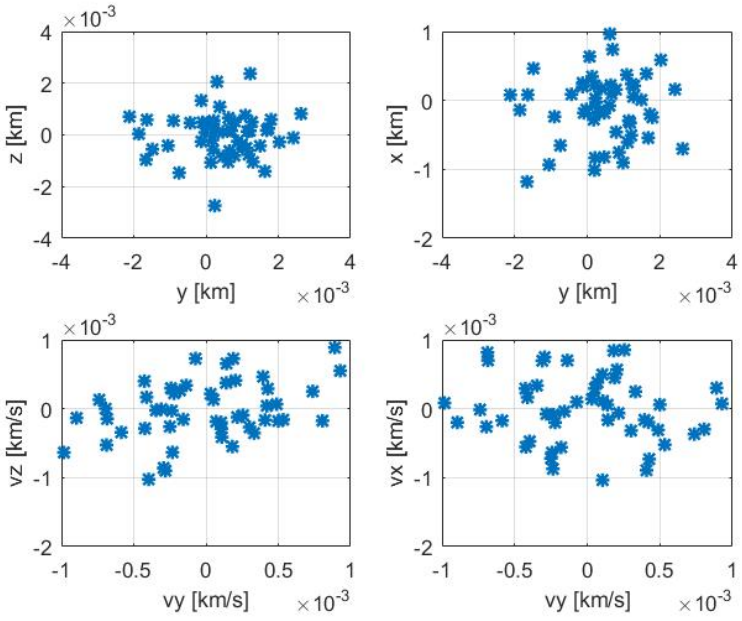

Figure 5.7: Position and velocity point cloud at the initial time.

deviations of $0.5\,\mathrm{m/sec}$ in all three directions. The projections of position and velocity point clouds in the Hill frame at the initial time are shown in Figure 5.7. All the 50 cloud points were first propagated numerically using a 6×6 JGM-3 gravity model, and then analytically using the second-order 6×6 satellite theory for the zonal and tesseral harmonics developed in Chapter 3. The time evolution of the point clouds using numerical and analytical propagation after 1 day is shown in Figure 5.8 and 5.9. Similar plots after 5 and 10 days of propagation are shown in Figures 5.10-5.13. The results show that the nonlinear uncertainty propagation using the artificial satellite theories is very accurate when compared to the numerically propagated distribution. Figures 5.10 and 5.10 clearly show that the point cloud is no longer resemble a Gaussian distribution in the Cartesian coordinates after five days of propagation through the nonspherical gravitational field. Nevertheless, the artificial satellite theory based point cloud propagation has reproduced the non-Gaussian uncertainty dynamics quite accurately.

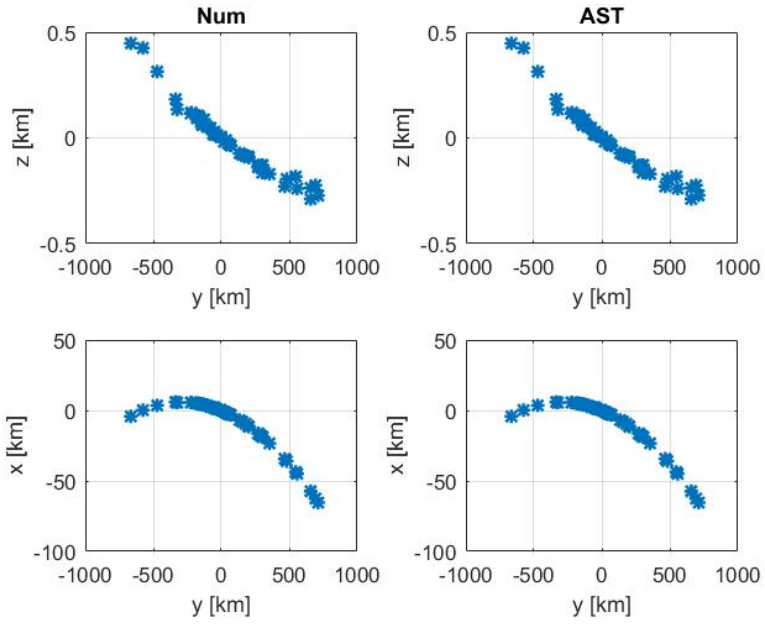

Figure 5.8: Point cloud for position states after 1 day for numerical (Num) and analytical (AST) propagation.

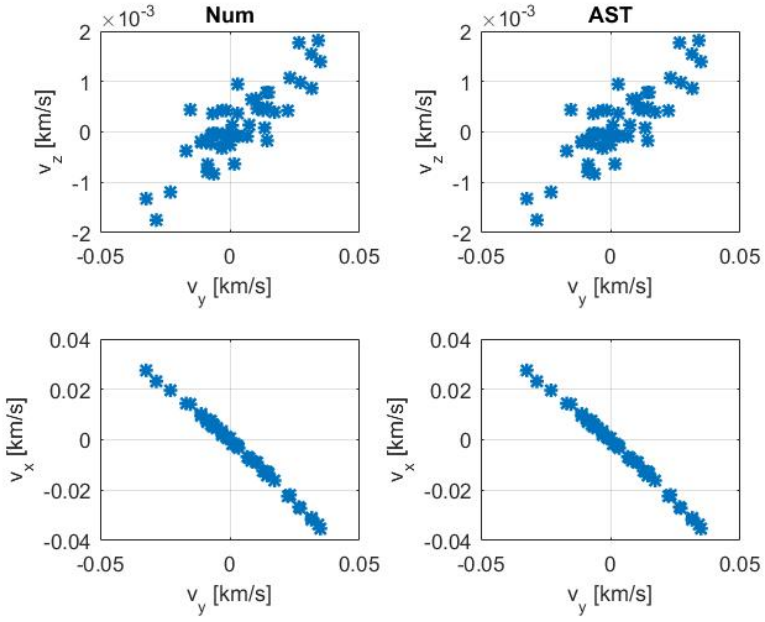

Figure 5.9: Point cloud for velocity states after 1 day for numerical (Num) and analytical (AST) propagation.

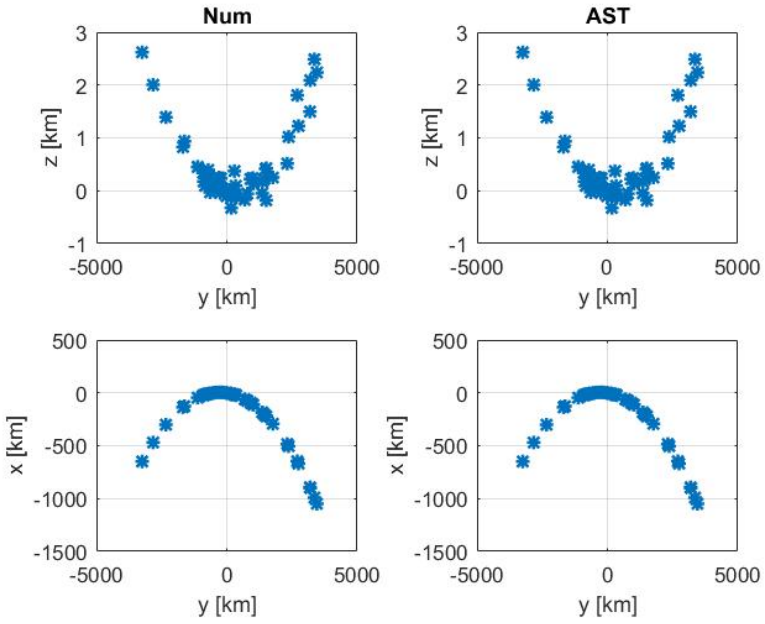

Figure 5.10: Point cloud for position states after 5 days for numerical (Num) and analytical (AST) propagation.

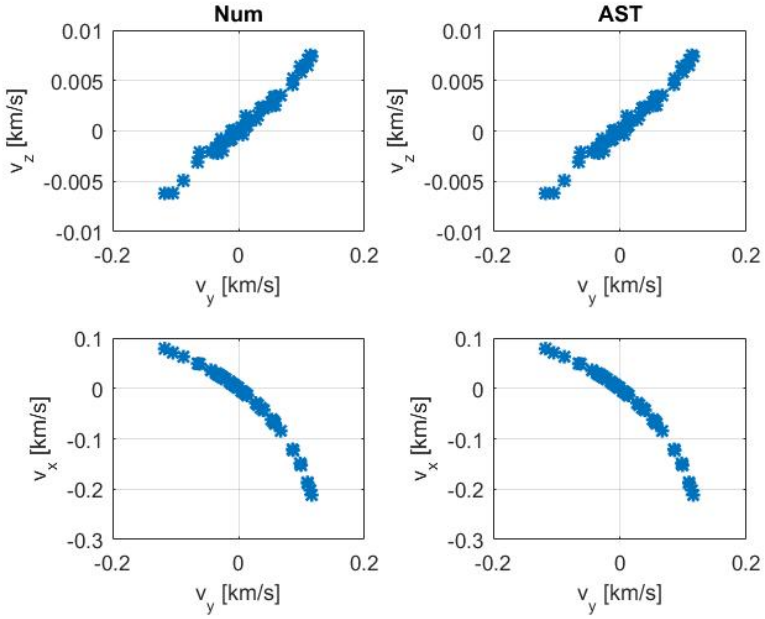

Figure 5.11: Point cloud for velocity states after 5 days for numerical (Num) and analytical (AST) propagation.

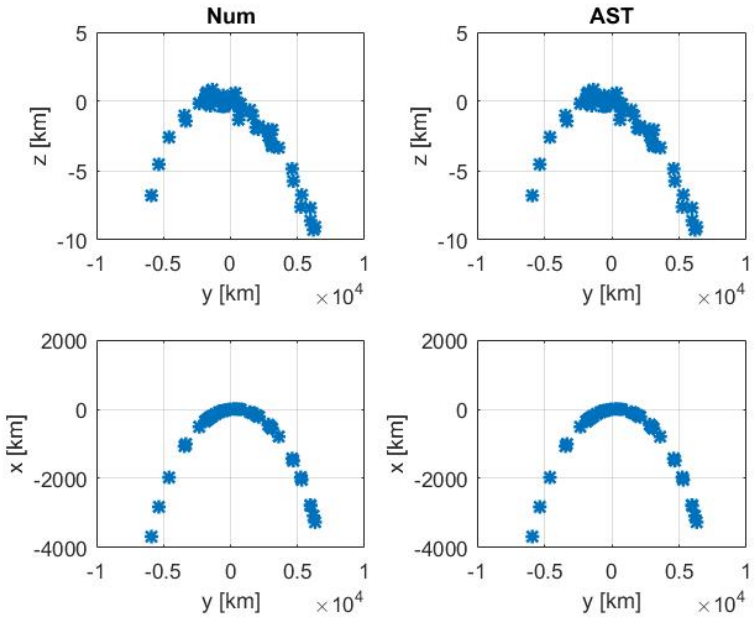

Figure 5.12: Point cloud for position states after 10 days for numerical (Num) and analytical (AST) propagation.

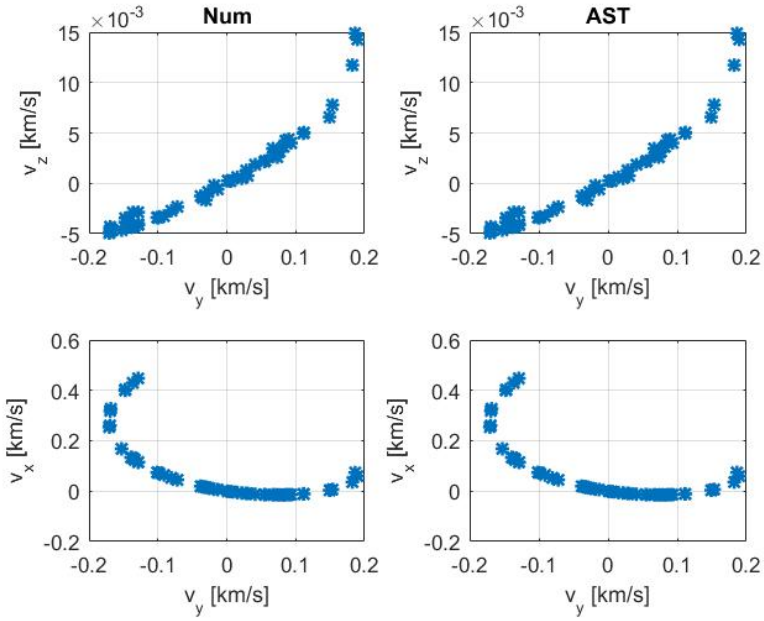

Figure 5.13: Point cloud for velocity states after 10 days for numerical (Num) and analytical (AST) propagation.

6. SUMMARY AND CONCLUSIONS

An artificial satellite theory (AST) for the complete nonspherical gravitational problem, i.e., including all the zonal, sectorial, and tesseral spherical harmonics is formulated. The analytic theory does not rely on any series expansion in powers of either the eccentricity or the small ratio of the satellite's mean motion and the angular velocity of the central body. As a result, it is closed-form in the eccentricity and does not loose accuracy for highly elliptic orbits. The generalized expressions that are computed for the secular, long-periodic, m-daily, and short-periodic variations of the equinoctial orbital elements are compact in form, and valid for an arbitrary spherical harmonic. Additionally, it provides a unified satellite theory for the sub-synchronous and super-synchronous orbit regimes, with no singularities for the resonant orbits. Many of these advantages, especially in case of the tesseral harmonics, are a direct consequence of the exact solution presented in this work for the Delaunay normalization of the tesseral Hamiltonian. Compared to the past methods for constructing this Delaunay normalization approximately, the exact solution is more compact and can be computed with almost arbitrary accuracy using the numerical quadrature algorithms. The numerical quadrature is ideally suited for parallel computations to reduce the computational time as all the function evaluations can be performed independently without any need for inter-process communication. Additionally, it is shown that the conventional approaches like the method of relegation can be derived from the exact solution. The results presented showed that the tesseral harmonics, especially the equatorial ellipticity terms, have a significant effect on the absolute motion and ignoring these severely affects the accuracy of the artificial satellite theories except for the high inclination near-polar orbits. A majority of the effects due to the tesseral harmonics manifest themselves in the anomalistic motion of the satellites. Perturbation effects due to the tesseral and sectorial harmonics diminish with increasing inclination, with highest effects on the near-equatorial orbits. The theories developed in this work are fully analytic, therefore, long-term propagation is inexpensive for the execution times even with the computation of the numerical quadratures.

The relative motion state transition matrix (RM-STM) is derived for the complete gravitational problem by including the secular and periodic effects due to the zonal, sectorial and tesseral harmonics. The RM-STM showed improvements in the long-term prediction accuracy of the perturbed satellite relative motion in the presence of the nonspherical gravitational perturbations, especially in the along-track direction for the relative position. For the reference orbits with high inclination, the improvements in the relative position prediction were not significant similar to the case of the absolute motion. For establishing a satellite formation, the initial conditions for the differential equinoctial elements are derived that are completely nonsingular for the equatorial and circular reference orbits. These five initial conditions (differential semimajor axis being zero for the two-body dynamics) are expressed in terms of the five formation design parameters for a generalized circular orbit type formation, using which many different formation geometries can be designed.

The theories developed in this work for the absolute and relative motion have many benefits for mission analysis and designing guidance and control laws for stationkeeping and formation maintenance. Using an accurate analytic model for the dynamical system increases the accuracy and fuel efficiency of the guidance and control algorithms. Similarly, estimation algorithms can benefit from the accurate propagation of the states and the associated uncertainties using the analytical methods. A few of these applications using the results from the artificial satellite theories developed in this work, are presented. First, a new drift mitigation condition is derived that nullifies the along-track drift of a deputy satellite with respect to a reference satellite in the presence of any zonal spherical harmonic. The results showed that any drift caused by the higher zonal harmonics in the along-track direction was removed by using the along-track drift condition. Next, a multiple revolution perturbed Lambert solver using AST is formulated. This analytic perturbed Lambert solver provides an accurate and fast algorithm for computing multiple revolution elliptic orbit transfers in the presence of the nonspherical gravitational perturbations. The simulation showed the accuracy of the analytic perturbed Lambert solver matches that of the numerical propagation based Lambert solver. Further improvements, especially in computation time, over the latter

are expected with the use of analytic sensitivity matrices and for longer time of flights for orbital transfers. Lastly, the accuracy and efficiency of the developed artificial satellite theory is demonstrated for the nonlinear propagation of the orbital uncertainties using point clouds. The accurate propagation of the point cloud distributions over long time intervals provides significant performance improvements for the estimation filters like the unscented Kalman filter and the particle filter, which uses sample points to propagate uncertainty distributions.

6.1 Further Study

Looking at the results presented in this work, it can be concluded that the goals stated in Chapter 1 have been achieved. The artificial satellite theories for the absolute and relative motion have been derived in a general form, which includes the perturbations effects due to any arbitrary spherical harmonic, without the need for series expansions in the eccentricity or the ratio of the satellite's mean motion to the rotational velocity of the central body. For the absolute and relative motion, the results showed that the tesseral and sectorial harmonics have a significant effect on the prediction accuracy of the analytical theories, except only for the orbits with high inclinations. There are a few areas in which the current work can be extended further. This includes the inclusion of the secular and long-period effects due to the resonant tesserals in the satellite theories and the relative motion STM. With secular and long-period variations due to tesseral harmonics included, the satellites in resonant orbits can also be propagated with better accuracy. Other areas for further extension of this work may include the addition of the analytical expressions for other dominant perturbations, namely the atmospheric drag, and the third-body perturbations. The generalized expressions derived in this work for the secular, long-period, m-daily, and short-period variations due to the zonal and tesseral harmonics can also be expressed in a recursive form. This will greatly increase the execution speed of the proposed satellite theories for the absolute and relative motion.

REFERENCES

[1] B. Mahajan, S. R. Vadali, and K. T. Alfriend, "Analytic solution for satellite relative motion with zonal gravity perturbations," in *Astrodynamics 2015: Proceedings of the AAS/AIAA Astrodynamics Specialist Conference*, vol. 156, (Vail, CO), pp. 3583–3598, Univelt Inc., aug 2015.

[2] D. Brouwer, "A new determination of the mass of Titan by Hill's Method," *Boulettin of the Astronomical Institutes of the Netherlands*, vol. II, no. 57, pp. 119–120, 1924.

[3] D. Brouwer, "Integration of the equations of general planetary theory in rectangular coordinates," *The Astronomical Journal*, vol. 51, pp. 1–14, 1944.

[4] P. Musen, "On the high order effects of the methods of Krylov-Bogoliubov and Poincare," Tech. Rep. TN- D03128, NASA, 1966.

[5] D. Brouwer, "The motion of a particle with negligible mass under the gravitational attraction of a spheroid," *The Astronomical Journal*, vol. 51, pp. 223–231, 1946.

[6] L. Spitzer, "Perturbations of a satellite orbit," *Journal of British Interplanetary Society*, vol. 9, p. 131, 1950.

[7] L. Blitzer, M. Weisfeld, and A. D. Wheelon, "Perturbations of a satellite's orbit due to the Earth's oblateness," *Journal of Applied Physics*, vol. 27, no. 10, pp. 1141–1149, 1956.

[8] D. G. King-Hele, "The descent of an earth-satellite through the upper atmosphere," *Journal of British Interplanetary Society*, no. 15, pp. 314–323, 1956.

[9] R. J. Davis, F. L. Whipple, and J. B. Zirker, "The orbit of a small satellite," in *Scientific Uses of Earth Satellites* (J. A. V. Allen, ed.), Chapman and Hall Limited, 1956.

[10] T. E. Sterne, "The gravitational orbit of a satellite of an oblate planet," *The Astronomical Journal*, vol. 63, no. 1255, pp. 28–40, 1958.

[11] B. Garfinkel, "On the motion of a satellite of an oblate planet," *The Astronomical Journal*, vol. 63, no. 1257, pp. 88–96, 1958.

[12] D. Brouwer, "Outline of general theories of the Hill-Brown and Delaunay types for orbits of artificial satellites," *The Astronomical Journal*, vol. 63, no. 1264, pp. 433–438, 1958.

[13] E. Deprit and A. Deprit, "Poincare's Method Nouvelle by skew composition," *Celestial Mechanics and Dynamical Astronomy*, vol. 74, pp. 175–197, 1999.

[14] S. Ferraz-Mello, *Canonical Perturbation Theories-Degenrate Systems and Resonance*. Springer, 2007.

[15] I. Izsák, "On the first order secular perturbations of an artificial satellite in the gravitational field of the oblate Earth," *Communications of the Konkoly Observatory*, vol. IV, 1, no. 43, pp. 1–13, 1958.

[16] D. G. King-Hele, "The effect of the earth's oblateness on the orbit of a near satellite," *Proceedings of the Royal Society of London. Series A, Mathematical and Physical Sciences*, vol. 247, no. 1248, pp. 49–72, 1958.

[17] J. P. Vinti, "New method of solution for unretarded satellite orbits," *Journal of Research of the National Bureau of Standards. Section B-Mathematics and Mathematical Physics*, vol. 62B, no. 2, pp. 105–116, 1959.

[18] J. P. Vinti, "Improvement of the spheroidal method of artificial satellites," *The Astronomical Journal*, vol. 74, no. 1, pp. 25–34, 1969.

[19] I. G. Izsak, "A theory of satellite motion about an oblate planet I. A second-order solution of Vinti's dynamical problem," tech. rep., SAO Special Report # 52, 1960.

[20] I. G. Izsak, "A second-order solution of Vinti's dynamical problem," *Smithsonian Contributions to Astrophysics*, vol. 6, pp. 81–107, 1963.

[21] J. P. Vinti, "Formulae of an accurate intermediary orbit of an artificial satellite," *The Astronomical Journal*, vol. 66, no. 9, pp. 514–516, 1961.

[22] J. P. Vinti, "Theory of an accurate intermediary orbit for satellite astronomy," *Journal of Research of the National Bureau of Standards. Section B-Mathematics and Mathematical Physics*, vol. 65B, no. 3, p. 169, 1961.

[23] I. G. Izsak, "On satellite orbits with very small eccentricities," *The Astronomical Journal*, vol. 66, no. 3, pp. 129–131, 1961.

[24] D. Brouwer and G. M. Clemence, *Methods of Celestial Mechanics*. Academic press Inc., 1961.

[25] V. V. Beletsky, *Essays on the Motion of Celestial Bodies*. Springer Basel AG, 2001.

[26] E. P. Aksenov, E. A. Grebenikov, and V. G. Demin, "The generalized problem of motion about two fixed centers and its application to the theory of artificial earth satellites," *Soviet Astronomy*, vol. 7, no. 2, p. 491, 1963.

[27] B. Garfinkel, "The orbit of a satellite of an oblate planet," *The Astronomical Journal*, vol. 64, no. 1959, pp. 353–366, 1959.

[28] D. Brouwer, "Solution of the problem of artificial satellite theory without drag," *The Astronomical Journal*, vol. 64, no. 1274, pp. 378–396, 1959.

[29] N. L. Bonavito, S. Watson, and H. Walden, "An accuracy and speed comparison of the Vinti and Brouwer orbit prediction methods," Tech. Rep. TN D-5203, Goddard Space Flight Center, 1969.

[30] W. M. Kaula, "Analysis of gravitational and geometric aspects of geodetic utilization of satellites," *Geophysical Journal of the Royal Astronomical Society*, vol. 5, no. 2, pp. 104–133, 1961.

[31] Y. Kozai, "Second-order solution of artificial satellite theory without air drag," *The Astronomical Journal*, vol. 67, no. 7, pp. 446–461, 1962.

[32] J. V. Breakwell and J. Vagners, "On error bounds and initialization in satellite orbit theories," *Celestial Mechanics*, vol. 2, no. 2, pp. 253–264, 1970.

[33] R. H. Lyddane, "Small eccentricities or inclinations in the Brouwer theory of the artificial satellite," *Astronomical Journal*, vol. 68, no. 8, pp. 555–558, 1963.

[34] G.-i. Hori, "The motion of a hyperbolic artificial satellite around the oblate earth," *The Astronomical Journal*, vol. 66, no. 6, pp. 258–263, 1961.

[35] T. J. Lang, *Spheroidal solution for unbounded orbits about an oblate planet*. PhD thesis, Massachusetts Institute of Technology, 1969.

[36] P. Musen, "A modified hansen's theory as applied to the motion of artificial satellites," Tech. Rep. D-492, National Aeronautics and Space Administration, 1960.

[37] I. G. Izsak, "A note on perturbation theory," *The Astronomical Journal*, vol. 68, no. 8, pp. 559–561, 1963.

[38] B. Garfinkel and G. T. Mcallister, "The zonal harmonic perturbations of an artificial satellite," *The Astronomical Journal*, vol. 69, no. 7, pp. 453–459, 1964.

[39] B. Garfinkel, "Addition theorem for a derivatve of a legendre polnomial," *The Astronomical Journal*, vol. 69, no. 8, pp. 567–569, 1964.

[40] B. Garfinkel, "Tesseral harmonic perturbations of an artificial satellite," *The Astronomical Journal*, vol. 70, no. 10, pp. 784–786, 1965.

[41] B. Garfinkel, "Zonal and tesseral harmonic perturbations of an artificial satellite," in *The Theory of Orbits in the Solar System and in Stellar Systems. Proceedings from Symposium no. 25.* (G. I. Kontopoulos, ed.), pp. 323–325, Academic Press, London, 1964.

[42] W. M. Kaula, *Theory of Satellite Geodesy*. Dover Publications, Inc., 1st ed., 1966.

[43] B. Garfinkel, "The disturbing function for an artificial satellite," *The Astronomical Journal*, vol. 70, no. 9, pp. 699–703, 1965.

[44] K. Aksnes, "On the dynamical theory of a near-earth satellite, I," *Astrophysica Norvegica*, vol. X, no. 4, pp. 69–77, 1965.

[45] R. Cid and J. F. Lahulla, "Perturbaciones de corto perlodo en el movimiento de un satOite artificial, en funci6n de las variables de Hill," *Publ. Rev. Acad. Ciencias Zaragoza*, vol. 24, pp. 159–165, 1969.

[46] R. Cid and J. F. Lahulla, "Perturbaciones de segundo orden y corto perlodo, para el movimiento de un sat˜lite artificial en las variables de Hill," *Publ. Rev. A cad. Ciencias Zaragoza*, vol. 26, pp. 333–343, 1971.

[47] A. Deprit and S. Ferrer, "Note on Cid's radial intermediary and the method of averaging," *Celestial Mechanics*, vol. 40, pp. 335–343, 1987.

[48] B. Garfinkel and K. Aksnes, "Spherical coordinate intermediaries for an artificial satellite," *The Astronomical Journal*, vol. 75, no. 1, pp. 85–91, 1970.

[49] A. Deprit, "The elimination of the parallax in satellite theory," *Celestial Mechanics*, vol. 24, no. 2, pp. 111–153, 1981.

[50] J. V. Breakwell and R. Pringle Jr., "Resonances affecting motion Near the Earth-Moon equilateral libration points," in *AIAA/ION Astrodynamics Specialist Conference*, no. 65-683, 1965.

[51] A. Deprit, "A third order canonical approximation of the general solution of the restricted problem of three bodies in the neighbourhood of L4," in *Proceedings of I.A.U.:The Theory of Orbits in the Solar System and in Stellar Systems* (G. I. Kontopoulos, ed.), no. Symposium no. 25, (Thessaloniki), Academic press, aug 1966.

[52] H. B. Schechter, "Three-dimensional nonlinear stability analysis of the sun-perturbed earth-moon equilateral points," *AIAA Journal*, vol. 6, no. 7, pp. 1223–1229, 1968.

[53] D. Brouwer, "Progress and problems in analytical celestial mechanics," in *Space Age Astronomy*, (Pasadena, CA), 1962.

[54] D. Brouwer, "Review of celestial mechanics," *Annual Review of Astronomy and Astrophysics*, vol. 1, no. 1, pp. 219–234, 1963.

[55] J. Kevorkian, "von Zeipel method and the two-variable expansion procedure," *The Astronomical Journal*, vol. 71, no. 9, pp. 878–885, 1966.

[56] W. T. Kyner, "Averaging methods in celestial mechanics," in *International Astronomical Union. Symposium no. 25*, vol. 25, (Thessaloniki), p. 26, Academic Press, London, aug 1966.

[57] J. Meffroy, "On Von Zeipel's method in general planetary theory," *SAO Special Report*, vol. 229, 1966.

[58] G. Hori, "Theory of General Perturbations with Unspecified Canonical Variables," *Publications of the Astronomical Society of Japan*, vol. 18, no. 4, pp. 287–296, 1966.

[59] G.-i. Hori, "Non-linear coupling of two harmonic oscillations," *Publications of the Astronomical Society of Japan*, vol. 19, no. 2, p. 229, 1967.

[60] W. A. Mersman, "A new algorithm for the Lie transformation," *Celestial Mechanics*, vol. 3, no. 1, pp. 81–89, 1970.

[61] A. Deprit, "Canonical transformations depending on a small parameter," *Celestial Mechanics*, vol. 1, no. 1, pp. 12–30, 1969.

[62] A. A. Kamel, "Expansion formulae in canonicall transformations depending upon a small parameter," *Celestial Mechanics*, vol. 1, no. 1, pp. 12–30, 1969.

[63] A. Aly Kamel, "Perturbation method in the theory of nonlinear oscillations," *Celestial Mechanics*, vol. 3, no. 1, pp. 90–106, 1970.

[64] J. Henrard, "On a perturbation theory using Lie transforms," *Celestial Mechanics*, vol. 3, no. 1, pp. 107–120, 1970.

[65] A. A. Kamel, "Perturbation theory based on Lie Transforms and its application to the stability of motion near Sun-perturbed Earth-Moon triangular Libration points," Tech. Rep. CR-1622, NASA, 1970.

[66] J. A. Campbell and W. H. Jefferys, "Equivalence of the perturbation theories of Hori and Deprit," *Celestial Mechanics*, vol. 2, no. 4, pp. 467–473, 1970.

[67] H. Shniad, "The equivalence of von Zeipel mappings and Lie transforms," *Celestial Mechanics*, vol. 2, no. 1, pp. 114–120, 1970.

[68] G.-i. Hori, "Comparison of two perturbation theories based on canonical transformations," *Publications of the Astronomical Society of Japan*, vol. 22, pp. 191–198, 1970.

[69] G.-i. Hori, "Theory of general perturbations," in *Recent Advances in Dynamical Astronomy: Proceedings of the NATO Advanced Study Institute in Dynamical Astronomy* (B. D. Tapley and V. Szebehely, eds.), pp. 231–249, Cortina D'Ampezzo, Italy: Springer Netherlands, 1973.

[70] W. A. Mersman, "Explicit recursive algorithms for the construction of equivalent canonical transformations," *Celestial Mechanics*, vol. 3, no. 3, pp. 384–389, 1971.

[71] W. A. Mersman, "Explicit recursive algorithms for the construction of equivalent canonical transformations," *Celestial Mechanics*, vol. 3, no. 3, pp. 384–389, 1971.

[72] U. Kirchgraber, "Uniform treatment of canonical perturbation theories," *Journal fur die Reine und Angewandte Mathematik*, vol. 1973, no. 259, pp. 86–100, 1973.

[73] A. A. Kamel, "Lie transforms and the Hamiltonization of non-Hamiltonian systems," *Celestial Mechanics*, vol. 4, no. 3-4, pp. 397–405, 1971.

[74] G.-i. Hori, "Theory for general perturbations for non-canonical systems," *Publications of the Astronomical Society of Japan*, vol. 23, pp. 567–587, 1971.

[75] J. S. Choi and B. D. Tapley, "An extended canonical perturbation method," *Celestial Mechanics*, vol. 7, no. 1, pp. 77–90, 1973.

[76] T. Baenas, A. Escapa, J. M. Ferrándiz, and J. Getino, "Application of first-order canonical perturbation method with dissipative Hori-like kernel," *International Journal of Non-Linear Mechanics*, vol. 90, no. January, pp. 11–20, 2017.

[77] D. P. Stern, "A new formulation of canonical perturbation theory," *Celestial Mechanics*, vol. 3, no. 2, pp. 241–246, 1971.

[78] D. P. Stern, "Classical adiabatic perturbation theory," *Journal of Mathematical Physics*, vol. 12, no. 10, pp. 2231–2242, 1971.

[79] M. Eckstein, Y. Shi, and J. Kevorkian, "Use of the energy integral to evauate higher-order terms in the time history of satellite motion," *The Astronomical Journal*, vol. 71, no. 5, pp. 301–305, 1966.

[80] K. Aksnes, "On the dynamical theory of a near-Earth satellite II," *Astrophisica Norvegica*, vol. X, no. 8, pp. 149–169, 1967.

[81] K. Aksnes, "A second-order artificial satellite theory based on an intermediate orbit," *The Astronomical Journal*, vol. 75, no. 9, pp. 1066–1076, 1970.

[82] K. Aksnes, "On the use of the Hill variables in artificial satellite theory: Brouwer's theory," *Astronomy & Astrophysics*, vol. 17, pp. 70–75, 1972.

[83] A. Deprit and D. L. Richardson, "Comments on Aksnes ' intermediary," *Celestial Mechanics*, vol. 28, pp. 253–273, 1982.

[84] P. J. Cefola, "Equinoctial orbit elements - Application to artificial satellite orbits," in *AIAA/AAS Astrodynamics Conference*, no. 72-937, 1972.

[85] B. Garfinkel, G.-i. Hori, and K. Aksnes, "On the mixed-secular terms in perturbed intermediaries," *The Astronomical Journal*, vol. 75, no. 5, pp. 651–656, 1970.

[86] A. Deprit and A. Rom, "The main problem of artificial satellite theory for small and moderate eccentricities," *Celestial Mechanics*, vol. 2, no. 2, pp. 166–206, 1970.

[87] Y. Kozai, "Second-order solution of artificial satellite theory without air drag," *The Astronomical Journal*, vol. 67, no. 7, pp. 446–461, 1962.

[88] K. Aksnes, "A note on 'The main problem of satellite theory for small eccentricities, by A. Deprit and A. Rom, 1970'," *Celestial Mechanics*, vol. 4, no. 1, pp. 119–121, 1971.

[89] B. C. Getchell, "Orbit computation with the Vinti potential and universal variables," *Journal of Spacecraft*, vol. 7, no. 4, pp. 405–409, 1970.

[90] K. T. Alfriend, R. Dasenbrock, H. Pickard, and A. Deprit, "The extended phase space formulation of the Vinti problem," *Celestial Mechanics*, vol. 16, no. 4, pp. 441–458, 1977.

[91] R. A. Gordon, "An analytical iterative algorithm for the prediction of special satellite orbit points with the Brouwer orbit theory," *Celestial Mechanics*, vol. 7, no. 2, pp. 280–290, 1973.

[92] A. A. Kamel and R. Tibbitts, "Some useful results on initial node locations for near-equatorial circular satellite orbits," *Celestial Mechanics*, vol. 8, no. 1, pp. 45–73, 1973.

[93] K. T. Alfriend and C. E. Velez, "The application of general perturbation theories to the artificial satellite problem," *Acta Astronautica*, vol. 2, pp. 577–591, jul 1975.

[94] G. E. O. Giacaglia, "The equations of motion of an artificial satellite in nonsingular variables," *Celestial Mechanics*, vol. 15, no. 2, pp. 191–215, 1977.

[95] P. J. Cefola, "A recursive formulation for the tesseral disturbing function in equinoctial variables," in *AIAA/AAS Astrodynamics Specialist Conference*, no. 76-839, (San Diego, California), aug 1976.

[96] W. D. McClain, "A recursively formulated first-order semianalytic artificial satellite theory based on the generalized method of averaging-II," Tech. Rep. CSC/TR-78/6001, Computer Science Corporation, may 1978.

[97] P. J. Cefola and W. D. McClain, "A recursive formulation of the short-periodic perturbations in equinoctial variables," in *AIAA/AAS Astrodynamics Conference*, no. 78-1383, AIAA/AAS Astrodynamics Conference, aug 1978.

[98] R. J. Proulx, W. D. McClain, L. W. Early, and P. J. Cefola, "A theory for the short periodic motion due to the tesseral harmonic gravity field," in *AAAS/AIAA Astrodynamics Specialist Conference*, (Lake Tahoe, Nevada), 1981.

[99] D. A. Danielson, C. P. Sagovac, B. Neta, and L. W. Early, "Semianalytic satellite theory: mathematical algorithms," tech. rep., Naval Postgraduate School, 1994.

[100] J. F. San-Juan, M. Lara, R. López, L. M. . López, B. Weeden, and P. J. Cefola, "Allocation of DSST in the new implementation of Astrody (Web Tools)," *Advanced Maui Optical and Space Surveillance Technologies Conference 2012*, vol. 2007, no. 8617, pp. 339–355, 2012.

[101] H. Kinoshita, "Third-order solution of an artificial satellite theory," in *Dynamics of Planets and Satellites and Theories of Their Motion* (V. Szebehely, ed.), vol. 72 of *Astrophysics and Space Science Library*, pp. 241–257, Springer Netherlands, 1978.

[102] F. R. Hoots, "A nonsingular reformulation of the Brouwer geopotential theory," in *AIAA/AAS Astrodynamics Specialist Conference*, no. 79-137, (Provincetown, Massachusetts), 1979.

[103] G. Scheifele, "Généralisation des éléments de Delaunay en mécanique céleste. Application au mouvement d'un satellite artificiel," in *Comptes Rendus de l'Academie des Sciences Paris, Sér. A, Tome 271*, 1970.

[104] G. Scheifele, "On nonclassical canonical systems," *Celestial Mechanics*, vol. 2, no. 3, pp. 296–310, 1970.

[105] V. R. Bond, "The development of the Poincare-similar elements with eccentric anomaly as the independent variable," *Celestial Mechanics*, vol. 14, no. 3, pp. 287–311, 1976.

[106] G. Scheifele and O. Graf, "Analytical satellite theories based on a new set of canonical elements," in *AIAA Mechanics and Control Flight Conference*, no. 74-838, (Anaheim, CA), aug 1974.

[107] A. Deprit, "A note concerning the TR-transformation," *Celestial Mechanics*, vol. 23, no. 4, pp. 299–305, 1981.

[108] D. G. Saari, "Regularization and the artificial Earth satellite problem," *Celestial Mechanics*, vol. 9, pp. 55–72, 1974.

[109] A. Deprit, "Delaunay normalizations," *Celestial Mechanics*, vol. 26, pp. 9–21, 1982.

[110] A. Deprit, "The main problem in the theory of artificial satellites to order four," *Journal of Guidance, Control, and Dynamics*, vol. 4, no. 2, pp. 201–206, 1981.

[111] M. Lara, J. F. San-Juan, and L. M. López-Ochoa, "Proper averaging via parallax elimination," in *Advances in the Astronautical Sciences*, vol. 150, pp. 315–331, 2014.

[112] M. Lara, J. F. San-Juan, and L. M. López-Ochoa, "Delaunay variables approach to the elimination of the perigee in Artificial Satellite Theory," *Celestial Mechanics and Dynamical Astronomy*, pp. 39–56, 2014.

[113] S. L. Coffey and A. Deprit, "Third-order solution to the main problem in satellite theory," *Journal of Guidance, Control, and Dynamics*, vol. 5, no. 4, pp. 366–371, 1982.

[114] K. T. Alfriend and S. L. Coffey, "Elimination of the perigee in the satellite problem," *Celestial Mechanics*, vol. 32, pp. 163–172, 1984.

[115] R. Cid, S. Ferrer, and M. L. Sein-Echaluce, "On the radial intermediaries and the time transformation in satellite theory," *Celestial Mechanics*, vol. 38, pp. 191–205, 1986.

[116] S. Breiter, "Second-Order Solution For The Zonal Problem Of Satellite Theory," *Celestial Mechanics and Dynamical Astronomy*, vol. 67, no. 3, pp. 237–249, 1997.

[117] B. De Saedeleer, "Complete zonal problem of the Artificial Satellite: Generic Compact analytic first order in closed form," *Celestial Mechanics and Dynamical Astronomy*, vol. 91, no. 3-4, pp. 239–268, 2005.

[118] M. Lara, "Efficient formulation of the periodic corrections in Brouwer's gravity solution," *Mathematical Problems in Engineering*, vol. 2015, pp. 1–19, 2015.

[119] M. Lara, "LEO intermediary propagation as a feasible alternative to Brouwer's gravity solution," *Advances in Space Research*, vol. 56, no. 3, pp. 367–376, 2015.

[120] W. D. McClain, "A recursively formulated first-order semianalytic artificial satellite theory based on the generalized method of averaging-I," Tech. Rep. CSC/TR-77/6010, Computer Science Corporation, nov 1977.

[121] S. L. Coffey and K. T. Alfriend, "Short period elimination for the tesseral harmonics," in *Advances in the Astronautical Sciences*, vol. 46, pp. 87–101, AAS/AIAA Astrodynamics Specialist Conference, Lake Tahoe, aug 1981.

[122] E. Wnuk, "Tesseral harmonic perturbations for higher order and degree harmonics," *Celestial Mechanics*, vol. 44, no. 1-2, pp. 179–191, 1988.

[123] E. Wnuk, "Second order perturbations due to the gravity potential of a planet," in *From Newton to Chaos* (A. E. Roy and B. A. Steves, eds.), vol. 336 of *NATO ASI Series*, pp. 259–267, Springer US, 1995.

[124] J. F. Palacián, *Teoria del satelite artificial: armonicos teserales y su relegacion mediante simplificaciones algebraicas*. Ph.d. thesis, Universidad de Zaragoza, 1992.

[125] A. Deprit, J. Palacián, and E. Deprit, "The relegation algorithm," *Celestial Mechanics and Dynamical Astronomy*, vol. 79, no. 3, pp. 157–182, 2001.

[126] A. M. Segerman and S. L. Coffey, "An analytical theory for tesseral gravitational harmonics," *Celestial Mechanics and Dynamical Astronomy*, vol. 76, pp. 139–156, 2000.

[127] M. Lara, J. F. San-Juan, and L. M. Lòpez-Ochoa, "Averaging tesseral effects: closed form relegation versus expansions of elliptic motion," *Mathematical Problems in Engineering*, vol. 2013, no. 570127, 2013.

[128] M. Lara, J. F. San-Juan, and L. M. Lopez-Ochoa, "Efficient semi-analytic integration of GNSS orbits under tesseral effects," *Acta Astronautica*, vol. 102, pp. 355–366, 2014.

[129] M. Sansottera and M. Ceccaroni, "Rigorous estimates for the relegation algorithm," *Celestial Mechanics and Dynamical Astronomy*, vol. 127, no. 1, pp. 1–18, 2017.

[130] T. A. Ely, "Transforming mean and osculating elements using numerical methods," *Journal of the Astronautical Sciences*, vol. 62, no. 1, pp. 21–43, 2015.

[131] E. Wnuk, "Recent progress in analytical orbit theories," *Advances in Space Research*, vol. 23, no. 4, pp. 677–687, 1999.

[132] G.-i. Hori, "The motion of an artificial satellite in the vicinity of the critical Inclination," *The Astronomical Journal*, vol. 65, no. 5, pp. 291–299, 1960.

[133] B. Garfinkel, "On the motion of a satellite in the vicinity of the critical inclination," *The Astronomical Journal*, vol. 65, no. 10, pp. 624–627, 1960.

[134] R. A. Struble, "A geometrical derivation of the satellite equations," *Journal of Mathematical Analysis and Applications*, vol. 1, pp. 300–307, 1960.

[135] R. A. Struble, "The geometry of the orbits of artificial satellites," *Arch. Rational Mech. Anal.*, vol. 7, pp. 87–104, 1960.

[136] Y. Hagihara, "Libration of an earth satellite with critical inclination," *Smithsonian Contributions to Astrophysics*, vol. 5, no. 5, pp. 39–50, 1961.

[137] Y. Kozai, "Motion of a particle with critical inclination in the gravitational field of a spheroid," *Smithsonian Contributions to Astrophysics*, vol. 5, no. 5, pp. 53–58, 1961.

[138] B. Garfinkel, "Comment on Anthony G. Lubowe's paper 'How critical is the critical inclination?'," *Celestial Mechanics*, vol. 1, no. 11, 1969.

[139] P. J. Message, G.-I. Hori, and B. Garfinkel, "On the critical case in the motion of an artificial satellite," *The Observatory*, no. 929, pp. 168–170, 1962.

[140] I. G. Izsak, "On the critical inclination in satellite theory," *SAO Special Report*, vol. 1, pp. 1–24, 1962.

[141] B. Garfinkel, "Formal solution in the problem of small divisors," *The Astronomical Journal*, vol. 71, no. 8, pp. 657–669, 1966.

[142] B. Garfinkel, "On the ideal resonance problem," *Celestial Mechanics*, vol. 2, 1970.

[143] B. Garfinkel, "Regularization in the ideal resonance problem," *Celestial Mechanics*, vol. 5, pp. 189–203, 1972.

[144] B. Garfinkel, "Normality conditions in the ideal resonance problem," *Celestial Mechanics*, vol. 6, pp. 151–166, 1972.

[145] B. Garfinkel, "Ignorable coordinates in the ideal resonance problem," *Celestial Mechanics*, vol. 7, pp. 205–224, 1973.

[146] B. Garfinkel, "The global solution in the problem of the critical inclination," *Celestial Mechanics*, vol. 8, pp. 125–126, 1973.

[147] B. Garfinkel, "On Resonance in Celestial Mechanics," *Celestial Mechanics*, vol. 28, pp. 275–290, 1982.

[148] S. L. Coffey, A. Deprit, and B. R. Miller, "The critical inclination in artificial satellite theory," *Celestial Mechanics*, vol. 39, no. 4, pp. 365–406, 1986.

[149] A. H. Jupp, "The critical inclination problem - 30 years of progress," *Celestial Mechanics*, vol. 43, no. 1-4, pp. 127–138, 1987.

[150] S. L. Coffey, A. Deprit, and E. Deprit, "Frozen orbits for satellites close to an Earth-like planet," *Celestial Mechanics & Dynamical Astronomy*, vol. 59, no. 1, pp. 37–72, 1994.

[151] M. Lara, "A polar variables view on the critical inclination problem in artificial satellite theory," *Advances in the Astronautical Sciences*, vol. 153, pp. 561–572, 2015.

[152] M. Lara, "On inclination resonances in Artificial Satellite Theory," *Acta Astronautica*, vol. 110, pp. 239–246, 2015.

[153] F. R. Hoots and R. G. France, "An analytic satellite theory using gravity and a dynamic atmosphere," *Celestial Mechanics*, vol. 40, no. 1, pp. 1–18, 1987.

[154] P. Musen and A. E. Bailie, "On the motion of a 24-hour satellite," *Journal of Geophysical Research*, vol. 67, no. 3, pp. 1123–1132, 1962.

[155] R. R. Allan, "On the motion of nearly synchronous satellites," *Proceedings of the Royal Society of London. Series A, Mathematical and Physical Sciences*, vol. 288, no. 1412, pp. 60–68, 1965.

[156] J. A. Morrison, "An averaging scheme for some nonlinear resonance problems," *SIAM Journal on Applied Mathematics*, vol. 16, no. 5, pp. 1024–1047, 1968.

[157] M. C. Eckstein and Y.-Y. Shi, "Asymptotic solutions for orbital resonances due to the general geopotential," *The Astronomical Journal*, vol. 74, no. 4, pp. 551–562, 1969.

[158] G. S. Gedeon, "Tesseral resonance effects on satellite orbits," *Celestial Mechanics*, vol. 1, pp. 167–189, 1969.

[159] A. A. Kamel, D. Ekman, and R. Tibbits, "East-West staionkeeping requirements of nearly synchronous satellites due to Earth's triaxiality and Luni-Solar effects," *Celestial Mechanics*, vol. 8, pp. 129–148, 1973.

[160] B. A. Romanowicz, "On the Tesseral-Harmonics resonance problem in artificial satellite theory," tech. rep., Smithsonian Institution Astrophysical Observatory, 1975.

[161] M. T. Lane, "An analytical treatment of resonance effects on satellite orbits," *Celestial Mechanics*, vol. 42, no. 1-4, pp. 3–38, 1987.

[162] J. P. Vinti, "Theory of the effect of drag on the orbital inclination of an earth satellite," *Journal of Research of the National Bureau of Standards*, vol. 62, no. 2, pp. 79–88, 1959.

[163] T. E. Sterne, "The effect of the rotation of a planetary atmosphere upon the orbit of a close satellite," *The Astronomical Journal*, vol. 64, p. 54, 1959.

[164] I. G. Izsak, "Periodic drag perturbations of artificial satellites," *The Astronomical Journal*, vol. 65, no. 6, pp. 355–357, 1960.

[165] G. Cook, D. King-Hele, and D. Walker, "The Contraction of Satellite Orbits Under the Influence of Air Drag. I. With Spherically Symmetrical Atmosphere," *Royal Society of London Proceedings Series A*, vol. 257, pp. 224–249, 1960.

[166] D. G. King-Hele and D. M. C. Walker, "The contracion of satellite orbits under the influence of air drag Part VII: orbits of high eccentricity, with scale height dependent on altitude," tech. rep., Royal Aircraft Establishment, 1986.

[167] D. Brouwer and G.-I. Hori, "Theoretical evaluation of atmospheric drag effects in the motion of an artificial satellite," *The Astronomical Journal*, vol. 66, no. 5, pp. 193–225, 1961.

[168] J. Otterman and K. Lichtenfeld, "Effects of air drag on near-circular satellite orbits," *Journal of Spacecraft and Rockets*, vol. 1, no. 5, pp. 513–519, 1964.

[169] J. S. Watson, G. D. Mistretta, and N. L. Bonavito, "An analytic method to account for drag in the Vinti satellite theory," *Celestial Mechanics*, vol. 11, no. 2, pp. 145–177, 1973.

[170] G. Cook, "Luni-solar perturbations of the orbit of an earth satellite," *Geophysical Journal International*, vol. 5, no. 3, pp. 271–291, 1962.

[171] G. E. Cook, "Basic theory for PROD, a program for computing the development of satellite orbits," *Celestial Mechanics*, vol. 7, no. 3, pp. 301–314, 1973.

[172] M. Lidov, "The evolution of orbits of artificial satellites of planets under the action of gravitational perturbations of external bodies," *Planetary and Space Science*, vol. 9, no. 10, pp. 719–759, 1962.

[173] W. M. Kaula, "Development of the lunar and solar disturbing functions for a close satellite," *The Astronomical Journal*, vol. 67, no. 5, pp. 300–303, 1962.

[174] P. Musen, "A discussion of Halphen's method of secular perturbations and its application to the determination of long-range effects in the motion of celestial bodies," *Review of Geophysics*, vol. 1, no. 1, pp. 85–122, 1963.

[175] B. Kaufman, "First order semianalytic satellite theory with recovery of the short period terms due to third body and zonal perturbations," *Acta Astronautica*, vol. 8, no. 5-6, pp. 611–623, 1981.

[176] T. A. Ely and K. C. Howell, "Dynamics of artificial satellite orbits with tesseral resonances including the effects of luni- solar perturbations," *Dynamics and Stability of Systems*, vol. 12, no. 4, pp. 243–269, 1997.

[177] R. A. Broucke, "Long-term third-body effects via double averaging," *Journal of Guidance, Control, and Dynamics*, vol. 26, no. 1, pp. 27–32, 2003.

[178] B. De Saedeleer, "Analytical theory of a lunar artificial satellite with third body perturbations," *Celestial Mechanics and Dynamical Astronomy*, vol. 95, no. 1-4, pp. 407–423, 2006.

[179] W. H. Clohessy and R. S. Wiltshire, "Terminal Guidance System for Satellite Rendezvous," *Journal of the Aerospace Sciences*, vol. 27, no. 9, pp. 653–658, 1960.

[180] V. Szebehely, *Theory of Orbits: The Restricted Problem of Three Bodies*. Academic Press, 1967.

[181] D. F. Lawden, *Optimal Trajectories for Space Navigation*. London: Butterworths, 1963.

[182] J. Tschauner and P. Hempel, "Optimale Beschleunigeungsprograme fur das Rendezvous-Manover," *Astronautica Acta*, vol. 10, pp. 296–307, 1964.

[183] J. P. de Vries, "Elliptic elements in terms of small increments of position and velocity components," *AIAA Journal*, vol. 1, no. 11, pp. 2626–2629, 1963.

[184] K. T. Alfriend, S. R. Vadali, P. Gurfil, J. P. How, and L. S. Breger, *Spacecraft Formation Flying: Dynamics, Control and Navigation*. Elsevier Ltd., 1st ed., 2010.

[185] S. S. Vaddi, S. R. Vadali, and K. T. Alfriend, "Formation flying: Accommodating nonlinearity and eccentricity perturbations," *Advances in the Astronautical Sciences*, vol. 112 II, no. 2, pp. 985–1004, 2002.

[186] C. D. Karlgaard and F. H. Lutze, "Second-order relative motion equations," *Advances in the Astronautical Sciences*, vol. 109 III, no. 1, pp. 2429–2448, 2002.

[187] E. Kolemen and N. J. Kasdin, "Relative spacecraft motion: A hamiltonian approach to eccentricity perturbations," *Advances in the Astronautical Sciences*, vol. 119, no. SUPPL., pp. 3075–3085, 2005.

[188] R. E. Sherrill, A. J. Sinclair, S. C. Sinha, and T. A. Lovell, "Time-varying transformations for Hill-Clohessy-Wiltshire solutions in elliptic orbits," *Celestial Mechanics and Dynamical Astronomy*, vol. 119, no. 1, pp. 55–73, 2014.

[189] E. D. Silva, "A formulation of the Clohessy-Wiltshire equations to include dynamic atmospheric drag," in *AIAA/AAS Astrodynamics Spec*, no. 2008-644, (Honolulu), aug 2008.

[190] S. R. Ploen, D. P. Scharf, F. Y. Hadaegh, and a. B. Acikmese, "Dynamics of earth orbiting formations," *Collection of Technical Papers - AIAA Guidance, Navigation, and Control Conference, Aug 16-19 2004*, vol. 3, pp. 1957–1563476703, 2004.

[191] S. A. Schweighart and R. J. Sedwick, "High-fidelity linearized J2 model for satellite formation flight," *Journal of Guidance, Control, and Dynamics*, vol. 25, pp. 1073–1080, nov 2002.

[192] W. E. Wiesel, "Relative satellite motion about an oblate planet," *Journal of Guidance, Control, and Dynamics*, vol. 25, no. 4, pp. 776–785, 2002.

[193] N. J. Kasdin, P. Gurfil, and E. Kolemen, "Canonical modelling of relative spacecraft motion via epicyclic orbital elements," *Celestial Mechanics and Dynamical Astronomy*, vol. 92, no. 4, pp. 337–370, 2005.

[194] P. Gurfil, "Generalized solutions for relative spacecraft orbits under arbitrary perturbations," *Acta Astronautica*, vol. 60, no. 2, pp. 61–78, 2007.

[195] K. C. Howell and B. G. Marchand, "Natural and non-natural spacecraft formations near the L1 and L2 libration points in the sun-earth/moon ephemeris system," *Dynamical Systems: An International Journal*, vol. 20, no. 1, pp. 149–173, 2005.

[196] S. R. Vadali, H. Schaub, and K. T. Alfriend, "Initial conditions and fuel-optimal control for formation flying of satellites," *Proceedings of the AIAA Guidance, Navigation, and Control Confere and Exhibit*, no. 3, 1999.

[197] K. T. Alfriend, H. Schaub, and D.-W. Gim, "Gravitational perturbations, nonlinearity and circular orbit assumption effects on formation flying control strategies," in *AAS Guidance and Control Conference*, vol. 104, (Breckenridge, CO), feb 2000.

[198] H. Schaub, S. R. Vadali, J. L. Junkins, and K. T. Alfriend, "Spacecraft formation flying control using mean orbit elements," *Journal of the Astronautical Sciences*, vol. 48, no. 1, pp. 69–87, 2000.

[199] H. Schaub and K. T. Alfriend, "J2 invariant relative orbits for spacecraft formations," *Celestial Mechanics and Dynamical Astronomy*, vol. 79, no. 2, pp. 77–95, 2001.

[200] H. Schaub, "Relative Orbit Geometry Through Classical Orbit Element Differences," *Journal of Guidance, Control, and Dynamics*, vol. 27, no. 5, pp. 839–848, 2004.

[201] S. D'Amico, *Autonomous formation flying in low Earth orbit*. PhD thesis, TU Delft, 2010.

[202] J. Garrison, T. Gardner, and P. Axelrad, "Relative motion in highly elliptical orbits," in *Advances in the Astronautical Sciences*, vol. 89, 1995.

[203] S. Vadali, "An analytical solution for relative motion of satellites," in *5th Dynamics and Control of Systems and Structures in Space Conference*, (Cranfield, UK, Cranfield University), 2002.

[204] D.-W. Gim and K. T. Alfriend, "State transition matrix of relative motion for the perturbed noncircular reference orbit," *Journal of Guidance, Control, and Dynamics*, vol. 26, no. 6, pp. 956–971, 2003.

[205] H. Yan, P. Sengupta, S. R. Vadali, and K. T. Alfriend, "Development of a state transition matrix for relative motion using the unit sphere approach," in *14th AAS/AIAA Spaceflight Mechanics*, 2004.

[206] H. Schaub, "Incorporating secular drifts into the orbit element difference description of relative orbits," *Advances in the Astronautical Sciences*, vol. 114, no. SUPPL., pp. 227–246, 2003.

[207] K. T. Alfriend and H. Yan, "Evaluation and comparison of relative motion theories," *Journal of Guidance, Control, and Dynamics*, vol. 28, no. 2, pp. 254–261, 2005.

[208] E. Wnuk and J. Golebiewska, "The relative motion of Earth orbiting satellites," *Celestial Mechanics and Dynamical Astronomy*, vol. 91, no. 3-4, pp. 373–389, 2005.

[209] E. Wnuk and J. Golebiewska, "Dynamics of satellite formations on eccentric orbits," *Advances in the Astronautical Sciences*, vol. 119, no. 054-158, pp. 861–877, 2005.

[210] E. Wnuk and J. Golebiewska, "Propagation of the relative satellite motion in a formation in the presence of gravitational perturbations," in *AIAA/AAS Astrodynamics Specialist Conference*, no. 2008-6763, (Honolulu, Hawaii), aug 2008.

[211] P. Sengupta, S. R. Vadali, and K. T. Alfriend, "Second-order state transition for relative motion near perturbed, elliptic orbits," *Celestial Mechanics and Dynamical Astronomy*, vol. 97, no. 2, pp. 101–129, 2007.

[212] P. Sengupta, S. R. Vadali, and K. T. Alfriend, "Averaged relative motion and applications to formation flight near perturbed orbits," *Journal of Guidance, Control, and Dynamics*, vol. 31, no. 2, pp. 258–272, 2008.

[213] C. W. T. Roscoe, S. R. Vadali, and K. T. Alfriend, "Third-body perturbation effects on satellite formations," *Advances in the Astronautical Sciences*, vol. 147, pp. 483–502, 2013.

[214] H. Yan, S. P. Vadali, and K. T. Alfriend, "Relative motion state transition matrix including gravitational perturbations," in *25th AAS/AIAA Space Flight Mechanics Meeting*, no. 15-339, (Williamsburg), jan 2015.

[215] K. W. Johnson, *Approaches for modeling satellite relative motion*. PhD thesis, Texas A&M University, 2016.

[216] A. W. Koenig, T. Guffanti, and S. D'Amico, "New state transition matrices for spacecraft relative motion in perturbed orbits," *Journal of Guidance, Control, and Dynamics*, vol. 40, no. 7, pp. 1749–1768, 2017.

[217] A. D. Biria and R. P. Russell, *A satellite relative motion model including J2 and J3 via Vinti's intermediary*, vol. 130. Springer Netherlands, 2018.

[218] J. Sullivan, S. Grimberg, and S. D'Amico, "Comprehensive survey and assessment of spacecraft relative motion dynamics models," *Journal of Guidance, Control, and Dynamics*, vol. 40, no. 8, pp. 1837–1859, 2017.

[219] H. Goldstein, C. Poole, and J. Safko, *Classical Mechanics*. Addison Wesley, third ed., 2000.

[220] G. E. O. Giacaglia, "Notes on Von Zeipel's Method," tech. rep., Goddard Space Flight Center, Greenbelt, Maryland, 1964.

[221] A. H. Nayfeh, *Perturbation Methods*. John Wiley & Sons, New York, 1973.

[222] A. Deprit, "Delaunay normalisations," *Celestial Mechanics*, vol. 26, pp. 9–21, 1982.

[223] R. A. Broucke and P. J. Cefola, "On the equinoctial orbit elements," *Celestial Mechanics*, vol. 5, no. 3, pp. 303–310, 1972.

[224] R. H. Battin, *An Introduction to the Mathematics and Methods of Astrodynamics*. AIAA Education Series, 1987.

[225] D.-W. Gim and K. T. Alfriend, "Satellite Relative Motion Using Differential Equinoctial Elements," *Celestial Mechanics and Dynamical Astronomy*, vol. 92, no. 4, pp. 295–336, 2005.

[226] S. Ferraz-Mello, "Do average Hamiltonians exist?," *Celestial Mechanics and Dynamical Astronomy*, vol. 73, no. 1-4, pp. 243–248, 1999.

[227] P. Sengupta, *Dynamics and control of satellite relative motion in a central gravitational field*. Phd dissertation, Texas A&M University, 2006.

[228] B. Mahajan, S. R. Vadali, and K. T. Alfriend, "Analytic solution for satellite relative motion: the complete zonal gravitational problem," in *Spaceflight Mechanics 2016: Proceedings of the 26th AAS/AIAA Space Flight Mechanics Meeting*, vol. 158, (Napa, CA), pp. 3325–3348, Univelt Inc., feb 2016.

[229] I. S. Gradshteyn and I. M. Ryzhik, *Table of Integrals, Series and Products*. Elsevier Ltd., 8th ed., 2014.

[230] H. Yan, S. R. Vadali, and K. T. Alfriend, "A recursive formulation of the satellite perturbed relative motion problem," in *2014 AIAA/AAS Astrodynamics Specialist Conference*, (San Diego, California), aug 2014.

[231] N. Emeljanov and A. Kanter, "A method to compute inclination functions and their derivatives.," *Manuscripta Geodetica*, vol. 14, pp. 77–83, mar 1989.

[232] B. Mahajan, S. R. Vadali, and K. T. Alfriend, "Exact Delaunay normalization of the perturbed Keplerian Hamiltonian with tesseral harmonics," *Celestial Mechanics and Dynamical Astronomy*, vol. 130, no. 3, p. 25, 2018.

[233] D. A. Vallado, *Fundamentals of Astrodynamics and Applications*. Microcosm, Inc, fourth ed. ed., 2001.

[234] B. Mahajan, S. R. Vadali, and K. T. Alfriend, "Exact normalization of the tesseral harmonics," in *Spaceflight Mechanics 2017: Proceedings of the 27th AAS/AIAA Spaceflight Mechanics Meeting*, vol. 160, (San Antonio, Texas), pp. 2569–2588, Univelt Inc., feb 2017.

[235] R. Haberman, *Applied Partial Differential Equations: With Fourier Series and Boundary Value Problems*. Prentice Hall, 4th ed., 2003.

[236] J. Palacián, "Normal forms for perturbed Keplerian systems," *Journal of Differential Equations*, vol. 180, no. 2, pp. 471–519, 2002.

[237] B. Mahajan, S. R. Vadali, and K. T. Alfriend, "Analytic Solution of perturbed relative motion with zonal and tesseral harmonics," in *Spaceflight Mechanics 2017: Proceedings of the 27th*

AAS/AIAA Spaceflight Mechanics Meeting, vol. 160, (San Antonio, Texas), pp. 1117–1134, Univelt Inc., feb 2017.

APPENDIX A

SECULAR HAMILTONIAN AND PERIODIC GENERATING FUNCTIONS FOR J_2-J_6

A.1 Secular Hamiltonian up to Third Order

$\mathbf{J_2}$ Contribution

$$\begin{aligned}\bar{\mathcal{K}}_{J_2} = \Bigg(& -\frac{-261\,G^{10}+15456\,G^8H^2-165490\,G^6H^4+659500\,G^4H^6-1052425\,G^2H^8+640500\,H^{10}}{2048\,G^{17}\left(G^2-5\,H^2\right)^2L^3} \\ & -\frac{180\,G^{11}-2700\,G^9H^2+13320\,G^7H^4-16920\,G^5H^6-42300\,G^3H^8+94500\,GH^{10}}{2048\,G^{17}\left(G^2-5\,H^2\right)^2L^4} \\ & -\frac{-156\,G^{12}-2058\,G^{10}H^2+38112\,G^8H^4-168372\,G^6H^6+265020\,G^4H^8-154050\,G^2H^{10}}{2048\,G^{17}\left(G^2-5\,H^2\right)^2L^5} \\ & -\frac{468\,G^{13}-11052\,G^{11}H^2+88840\,G^9H^4-301720\,G^7H^6+417700\,G^5H^8-205500\,G^3H^{10}}{2048\,G^{17}\left(G^2-5\,H^2\right)^2L^6} \\ & -\frac{9\,G^{14}-414\,G^{12}H^2+5730\,G^{10}H^4-25800\,G^8H^6+40725\,G^6H^8-20250\,G^4H^{10}}{2048\,G^{17}\left(G^2-5\,H^2\right)^2L^7}\Bigg){R_e}^6\mu^8J^3 \\ & +\Bigg(\frac{15\,G^4-30\,G^2H^2-105\,H^4}{128\,G^{11}L^3}+\frac{15}{128\,G^{11}L^4}\left(-4/5\,G^5+\frac{24\,G^3H^2}{5}-\frac{36\,GH^4}{5}\right) \\ & +\frac{15}{128\,G^{11}L^5}\left(-G^6+\frac{18\,G^4H^2}{5}-G^2H^4\right)\Bigg){R_e}^4\mu^6J^2+1/4\,\frac{J\mu^4{R_e}^2\left(G^2-3\,H^2\right)}{L^3G^5}-1/2\,\frac{\mu^2}{L^2}. \end{aligned} \tag{A.1}$$

$\mathbf{J_3}$ Contribution

$$\bar{\mathcal{K}}_{J_3} = \frac{{J_3}^2{R_e}^4\mu^6}{J}\left(-\frac{9\,G^4-72\,G^2H^2+75\,H^4}{32\,G^{11}L^3}+3/16\,\frac{G^4-9\,G^2H^2+10\,H^4}{G^9L^5}\right). \tag{A.2}$$

$\mathbf{J_4}$ Contribution

$$\bar{\mathcal{K}}_{J_4} = \frac{1}{2048\,G^{17}\left(G^2-5\,H^2\right)^2L^7}\Bigg(\Big(45\,G^{14}-164\,G^{13}L-1005\,G^{12}H^2+174\,G^{12}L^2$$

$$+ 2972\,G^{11}H^2L - 540\,G^{11}L^3 + 4050\,G^{10}H^4 + 3738\,G^{10}H^2L^2 - 115\,G^{10}L^4 - 14120\,G^9H^4L$$
$$+ 12420\,G^9H^2L^3 + 2430\,G^8H^6 - 44580\,G^8H^4L^2 - 6725\,G^8H^2L^4 - 6280\,G^7H^6L$$
$$- 106200\,G^7H^4L^3 - 33375\,G^6H^8 + 90420\,G^6H^6L^2 + 68450\,G^6H^4L^4 + 148300\,G^5H^8L$$
$$+ 419400\,G^5H^6L^3 + 39375\,G^4H^{10} + 180150\,G^4H^8L^2 - 112610\,G^4H^6L^4 - 164500\,G^3H^{10}L$$
$$- 751500\,G^3H^8L^3 - 372750\,G^2H^{10}L^2 - 372175\,G^2H^8L^4 + 472500\,GH^{10}L^3$$
$$+ 634375\,H^{10}L^4\Big){R_e}^6\mu^8 J_4\ J\Big) - \frac{\left(9\,G^2 - 15\,L^2\right)\left(3\,G^4 - 30\,G^2H^2 + 35\,H^4\right)\ J_4\ {R_e}^4\mu^6}{128\,G^{11}L^5}$$
$$- \frac{75}{2048\,G^{17}\left(G^2 - 5\,H^2\right)^2 L^7 J}\Bigg((G-L)\,(G+L)\,(-H+G)\,(H+G)\left(G^2 - 7\,H^2\right)$$
$$\times\Big(3\,G^8 - 50\,H^2G^6 - 5\,G^6L^2 + 209\,H^4G^4 + 76\,G^4H^2L^2 - 210\,H^6G^2 - 303\,G^2H^4L^2$$
$$+ 280\,H^6L^2\Big){R_e}^6\mu^8 {J_4}^2\Big). \quad \text{(A.3)}$$

$\mathbf{J_5}$ Contribution

$$\bar{\mathcal{K}}_{J_5} = \frac{-1}{256\,G^{17}L^7J}\Bigg(\Big(135\,G^{10} - 2700\,H^2G^8 - 600\,G^8L^2 + 7875\,H^4G^6 + 11250\,G^6H^2L^2$$
$$+ 525\,G^6L^4 - 5670\,H^6G^4 - 31500\,G^4H^4L^2 - 9450\,G^4H^2L^4 + 22050\,G^2H^6L^2 + 25725\,G^2H^4L^4$$
$$- 17640\,H^6L^4\Big){R_e}^6\mu^8 J_5\ J_3\Big) + \frac{1}{98304\,G^{23}\left(G^2 - 5\,H^2\right)^2 L^9 J}\Big(37300\,G^{18} - 1443000\,G^{16}H^2$$
$$- 247875\,G^{16}L^2 + 19154400\,G^{14}H^4 + 9441150\,G^{14}H^2L^2 + 513450\,G^{14}L^4 - 107480800\,G^{12}H^6$$
$$- 124222725\,G^{12}H^4L^2 - 19305300\,G^{12}H^2L^4 - 317275\,G^{12}L^6 + 280906500\,G^{10}H^8$$
$$+ 693564900\,G^{10}H^6L^2 + 251908650\,G^{10}H^4L^4 + 11796750\,G^{10}H^2L^6 - 335953800\,G^8H^{10}$$
$$- 1799011725\,G^8H^8L^2 - 1398940200\,G^8H^6L^4 - 152758725\,G^8H^4L^6 + 146853000\,G^6H^{12}$$
$$+ 2133006750\,G^6H^{10}L^2 + 3602124750\,G^6H^8L^4 + 843902500\,G^6H^6L^6 - 924280875\,G^4H^{12}L^2$$
$$- 4236113700\,G^4H^{10}L^4 - 2158309125\,G^4H^8L^6 + 1820778750\,G^2H^{12}L^4 + 2519499150\,G^2H^{10}L^6$$
$$- 1075102875\,H^{12}L^6\Big){R_e}^8\mu^{10}{J_5}^2. \quad \text{(A.4)}$$

$\mathbf{J_6}$ Contribution

$$\bar{\mathcal{K}}_{J_6} = \frac{2625}{32768\,G^{23}\left(G^2-5\,H^2\right)^2 L^9 J}\Bigg(J_6\,\left(G^2-H^2\right)\left(G^2-L^2\right)\Bigg(4\,G^{14}-146\,G^{12}H^2-21\,G^{12}L^2$$
$$+1654\,G^{10}H^4+739\,G^{10}H^2L^2+21\,G^{10}L^4-7614\,G^8H^6-8186\,G^8H^4L^2-717\,G^8H^2L^4+14574\,G^6H^8$$
$$+37006\,G^6H^6L^2+7788\,G^6H^4L^4-9240\,G^4H^{10}-69201\,G^4H^8L^2-34632\,G^4H^6L^4+42735\,G^2H^{10}L^2$$
$$+63351\,G^2H^8L^4-38115\,H^{10}L^4\Bigg){R_e}^8\mu^{10}J_4\Bigg)+\frac{1}{196608\,G^{23}\left(G^2-5\,H^2\right)^2L^9}\Bigg(\Bigg(5775\,G^{18}$$
$$+36600\,G^{17}L-183750\,G^{16}H^2-60075\,G^{16}L^2-1278000\,H^2G^{15}L-123200\,G^{15}L^3+3908625\,G^{14}H^4$$
$$-357750\,G^{14}H^2L^2+383625\,G^{14}L^4+12765000\,H^4G^{13}L+4088000\,H^2G^{13}L^3-113400\,G^{13}L^5$$
$$-26781300\,G^{12}H^6+2145375\,G^{12}H^4L^2-4643250\,G^{12}H^2L^4-189805\,G^{12}L^6-51511200\,H^6G^{11}L$$
$$-38696000\,H^4G^{11}L^3+3855600\,H^2G^{11}L^5+76014225\,G^{10}H^8+19986300\,G^{10}H^6L^2$$
$$+37185375\,G^{10}H^4L^4+131950\,G^{10}H^2L^6+81669000\,H^8G^9L+141724800\,H^6G^9L^3$$
$$-44339400\,H^4G^9L^5-94767750\,G^8H^{10}-149755725\,G^8H^8L^2-222037500\,G^8H^6L^4$$
$$+9794225\,G^8H^4L^6-28350000\,H^{10}G^7L-168504000\,H^8G^7L^3+237595680\,H^6G^7L^5$$
$$+42879375\,G^6H^{12}+363872250\,G^6H^{10}L^2+822697575\,G^6H^8L^4-4627980\,G^6H^6L^6$$
$$-17325000\,H^{12}G^5L-61320000\,H^{10}G^5L^3-639644040\,H^8G^5L^5-261174375\,G^4H^{12}L^2$$
$$-1607807250\,G^4H^{10}L^4-299253675\,G^4H^8L^6+138600000\,H^{12}G^3L^3+823964400\,H^{10}G^3L^5$$
$$+1065920625\,G^2H^{12}L^4+1008414750\,G^2H^{10}L^6-392931000\,H^{12}GL^5-792185625\,H^{12}L^6\Bigg)$$
$$\times\,{R_e}^8\mu^{10}J_6\,J\Bigg)$$
$$+\frac{\left(75\,G^4-350\,G^2L^2+315\,L^4\right)\left(5\,G^6-105\,G^4H^2+315\,G^2H^4-231\,H^6\right)J_6\,{R_e}^6\mu^8}{2048\,L^7G^{17}}$$
$$-\frac{1}{8388608\,G^{29}\left(G^2-5\,H^2\right)^2L^{11}J}\Bigg(3675\,{J_6}^2\left(G^2-L^2\right)\left(G^2-H^2\right)\Bigg(545\,G^{18}-25839\,G^{16}H^2$$
$$-4471\,G^{16}L^2+412656\,G^{14}H^4+209397\,G^{14}H^2L^2+11307\,G^{14}L^4-2682234\,G^{12}H^6$$
$$-3317308\,G^{12}H^4L^2-522477\,G^{12}H^2L^4-8181\,G^{12}L^6+8062581\,G^{10}H^8+21452382\,G^{10}H^6L^2$$
$$+8197848\,G^{10}H^4L^4+372519\,G^{10}H^2L^6-11062359\,G^8H^{10}-63957003\,G^8H^8L^2$$
$$-52663662\,G^8H^6L^4-5781996\,G^8H^4L^6+5499450\,G^6H^{12}+86839533\,G^6H^{10}L^2$$
$$+155604663\,G^6H^8L^4+36859914\,G^6H^6L^6-42656130\,G^4H^{12}L^2-209039589\,G^4H^{10}L^4$$

$$- 107843841\,G^4H^8L^6 + 101483910\,G^2H^{12}L^4 + 143241615\,G^2H^{10}L^6 - 68683230\,H^{12}L^6\Big){R_e}^{10}\mu^{12}\Bigg). \quad \text{(A.5)}$$

A.2 First-Order Short-Period Generating Function

$$\mathcal{W}_1 = \Bigg(1/4\,\frac{\left(G^2-3\,H^2\right)e\sin\left(f\right)}{G^5} - 3/8\,\frac{e\left(-H+G\right)\left(H+G\right)\sin\left(f+2\,g\right)}{G^5}$$
$$-1/8\,\frac{e\left(-H+G\right)\left(H+G\right)\sin\left(3\,f+2\,g\right)}{G^5} - 3/8\,\frac{\left(-H+G\right)\left(H+G\right)\sin\left(2\,g+2\,f\right)}{G^5}$$
$$+1/4\,\frac{\left(G^2-3\,H^2\right)\left(f-l\right)}{G^5}\Bigg){R_e}^2\mu^2. \quad \text{(A.6)}$$

A.3 Second-Order Short-Period Generating Function

$\mathbf{J_2}$ Contribution

$$\mathcal{W}_2 = \Bigg(\frac{\left(3\,f-3\,l\right)\left(15\,si^2-14\right)si^2\left(\eta^2-1\right)\cos\left(2\,g\right)}{32\,\eta^7L^7}$$
$$+\frac{\left(9\,f-9\,l\right)\left(5\,si^2-4\right)si^2\sqrt{-\eta^2+1}\cos\left(f+2\,g\right)}{16\,\eta^7L^7}$$
$$+3/16\,\frac{\left(f-l\right)\left(5\,si^2-4\right)si^2\sqrt{-\eta^2+1}\cos\left(3\,f+2\,g\right)}{\eta^7L^7}$$
$$+\frac{\left(9\,f-9\,l\right)\left(5\,si^2-4\right)si^2\cos\left(2\,g+2\,f\right)}{16\,\eta^7L^7}$$
$$-\frac{\left(27\,\eta^2si^4+90\,\eta\,si^4-36\,\eta^2si^2+171\,si^4-264\,\eta\,si^2+12\,\eta^2-372\,si^2+144\,\eta+180\right)\sqrt{-\eta^2+1}\sin\left(f\right)}{\left(64+64\,\eta\right)\eta^7L^7}$$
$$-\frac{\left(15\,\eta\,si^4-93\,si^4+24\,\eta\,si^2+168\,si^2-24\,\eta-72\right)\left(\eta-1\right)\sin\left(2\,f\right)}{128\,\eta^7L^7}+\frac{\left(3\,si^2-2\right)^2\left(\eta-1\right)\sqrt{-\eta^2+1}\sin\left(3\,f\right)}{64\,\eta^7L^7}$$
$$+\frac{\left(45\,\eta^2si^2-612\,\eta\,si^2-30\,\eta^2-693\,si^2+576\,\eta+630\right)si^2\sqrt{-\eta^2+1}\sin\left(f+2\,g\right)}{\left(128+128\,\eta\right)\eta^7L^7}$$
$$+\frac{\left(15\,\eta^2-15\right)si^4\sin\left(2\,f+4\,g\right)}{256\,\eta^7L^7}$$
$$+\frac{\left(3\,\eta^2si^2+100\,\eta\,si^2-2\,\eta^2+181\,si^2-64\,\eta-118\right)si^2\sqrt{-\eta^2+1}\sin\left(3\,f+2\,g\right)}{\left(128+128\,\eta\right)\eta^7L^7}$$
$$-\frac{3\sqrt{-\eta^2+1}si^4\sin\left(3\,f+4\,g\right)}{64\,\eta^7L^7}-\frac{\left(39\,\eta\,si^2+93\,si^2-30\,\eta-66\right)si^2\left(\eta-1\right)\sin\left(4\,f+2\,g\right)}{128\,\eta^7L^7}$$

$$+\frac{\left(3\,\eta^2+9\right)si^4\sin\left(4\,f+4\,g\right)}{256\,\eta^7L^7}-\frac{\left(9\,si^2-6\right)si^2\left(\eta-1\right)\sqrt{-\eta^2+1}\sin\left(5\,f+2\,g\right)}{128\,\eta^7L^7}$$
$$+\frac{3\sqrt{-\eta^2+1}si^4\sin\left(5\,f+4\,g\right)}{64\,\eta^7L^7}-\frac{\left(3\,\eta^2-3\right)si^4\sin\left(6\,f+4\,g\right)}{256\,\eta^7L^7}$$
$$-\frac{\left(9\,si^2-6\right)si^2\left(\eta-1\right)\sqrt{-\eta^2+1}\sin\left(-2\,g+f\right)}{128\,\eta^7L^7}+\frac{\left(3\,\eta^2si^2-6\,\eta^2-21\,si^2+30\right)si^2\sin\left(2\,g+2\,f\right)}{32\,\eta^7L^7}$$
$$-\frac{\left(15\,\eta^2si^4+24\,\eta^2si^2+105\,si^4-24\,\eta^2-240\,si^2+120\right)\left(f-l\right)}{64\,\eta^7L^7}\Bigg)\,{R_e}^4\mu^4. \quad \text{(A.7)}$$

$\mathbf{J_3}$ Contribution

$$\mathcal{W}_2=\frac{J_3\,{R_e}^3\mu^3}{J^2}\Bigg(3/16\,\frac{si\,\left(5\,si^2-4\right)e^2\,\cos\left(f-g\right)}{L^5\eta^5}+3/8\,\frac{si\,\left(5\,si^2-4\right)\left(\eta^2-3\right)\cos\left(f+g\right)}{L^5\eta^5}$$
$$+\frac{5\,si^3e^2\,\cos\left(f+3\,g\right)}{16\,L^5\eta^5}-3/8\,\frac{e\,si\,\left(5\,si^2-4\right)\cos\left(2\,f+g\right)}{L^5\eta^5}+5/8\,\frac{e\,si^3\cos\left(2\,f+3\,g\right)}{L^5\eta^5}$$
$$-1/16\,\frac{si\,\left(5\,si^2-4\right)e^2\,\cos\left(3\,f+g\right)}{L^5\eta^5}-\frac{5\,si^3\left(\eta^2-3\right)\cos\left(3\,f+3\,g\right)}{24\,L^5\eta^5}+\frac{5\,e\,si^3\cos\left(4\,f+3\,g\right)}{16\,L^5\eta^5}$$
$$+1/16\,\frac{si^3e^2\,\cos\left(5\,f+3\,g\right)}{L^5\eta^5}+3/4\,\frac{e\,si\,\left(5\,si^2-4\right)\left(f-l\right)\sin\left(g\right)}{L^5\eta^5}\Bigg). \quad \text{(A.8)}$$

$\mathbf{J_4}$ Contribution

$$\mathcal{W}_2=\frac{{R_e}^4\mu^4J_4}{J^2}\Bigg(-\frac{15\,si^2\left(7\,si^2-6\right)e^2\left(f-l\right)\cos\left(2\,g\right)}{32\,L^7\eta^7}$$
$$-\frac{9\,e\left(35\,si^4-40\,si^2+8\right)\left(\eta^2-5\right)\sin\left(f\right)}{128\,L^7\eta^7}+\frac{\left(315\,si^4-360\,si^2+72\right)e^2\sin\left(2\,f\right)}{128\,L^7\eta^7}$$
$$+\frac{e^3\left(35\,si^4-40\,si^2+8\right)\sin\left(3\,f\right)}{128\,L^7\eta^7}+\frac{15\,esi^2\left(7\,si^2-6\right)\left(\eta^2-5\right)\sin\left(f+2\,g\right)}{64\,L^7\eta^7}$$
$$+\frac{35\,e^3si^4\sin\left(f+4\,g\right)}{256\,L^7\eta^7}+\frac{105\,si^4e^2\sin\left(2\,f+4\,g\right)}{256\,L^7\eta^7}+\frac{5\,esi^2\left(7\,si^2-6\right)\left(\eta^2-5\right)\sin\left(3\,f+2\,g\right)}{64\,L^7\eta^7}$$
$$-\frac{35\,esi^4\left(\eta^2-5\right)\sin\left(3\,f+4\,g\right)}{256\,L^7\eta^7}-\frac{35\,si^4\left(3\,\eta^2-5\right)\sin\left(4\,f+4\,g\right)}{256\,L^7\eta^7}$$
$$-\frac{e^3si^2\left(7\,si^2-6\right)\sin\left(5\,f+2\,g\right)}{64\,L^7\eta^7}-\frac{21\,esi^4\left(\eta^2-5\right)\sin\left(5\,f+4\,g\right)}{256\,L^7\eta^7}+\frac{35\,si^4e^2\sin\left(6\,f+4\,g\right)}{256\,L^7\eta^7}$$
$$+\frac{5\,e^3si^4\sin\left(7\,f+4\,g\right)}{256\,L^7\eta^7}-\frac{5\,e^3si^2\left(7\,si^2-6\right)\sin\left(-2\,g+f\right)}{64\,L^7\eta^7}$$

$$+\frac{5\,si^2\left(7\,si^2-6\right)\left(3\,\eta^2-5\right)\sin\left(2\,g+2\,f\right)}{32\,L^7\eta^7}-\frac{15\,si^2\left(7\,si^2-6\right)e^2\sin\left(2\,g+4\,f\right)}{128\,L^7\eta^7}$$
$$-\frac{\left(105\,si^4-120\,si^2+24\right)\left(3\,\eta^2-5\right)\left(f-l\right)}{64\,L^7\eta^7}\Bigg). \quad \text{(A.9)}$$

$\mathbf{J_5}$ Contribution

$$\mathcal{W}_2=\frac{J_5\,{R_e}^5\mu^5}{J^2}\Bigg(-\frac{15\,si\,\left(f-l\right)\left(21\,si^4-28\,si^2+8\right)\left(3\,\eta^2-7\right)e\sin\left(g\right)}{64\,\eta^9L^9}$$
$$-\frac{63\,si^5e^3\cos\left(2\,f+5\,g\right)}{256\,\eta^9L^9}-\frac{63\,si^5e^3\cos\left(8\,f+5\,g\right)}{1024\,\eta^9L^9}-\frac{7\,si^5e^4\cos\left(9\,f+5\,g\right)}{1024\,\eta^9L^9}$$
$$-\frac{63\,si^5e^4\cos\left(f+5\,g\right)}{1024\,\eta^9L^9}-\frac{63\,si^5\left(3\,\eta^4-30\,\eta^2+35\right)\cos\left(5\,f+5\,g\right)}{2560\,\eta^9L^9}$$
$$-\frac{15\,si\,\left(21\,si^4-28\,si^2+8\right)e^3\cos\left(4\,f+g\right)}{256\,\eta^9L^9}+\frac{63\,si^5\left(3\,\eta^2-7\right)e\cos\left(4\,f+5\,g\right)}{512\,\eta^9L^9}$$
$$+\frac{15\,si\,\left(21\,si^4-28\,si^2+8\right)e^3\cos\left(2\,f-g\right)}{128\,\eta^9L^9}+\frac{35\,si^3e^3\left(9\,si^2-8\right)\cos\left(6\,f+3\,g\right)}{768\,\eta^9L^9}$$
$$+\frac{21\,si^5\left(3\,\eta^2-7\right)e\cos\left(6\,f+5\,g\right)}{256\,\eta^9L^9}+\frac{9\,si^5e^2\left(\eta^2-7\right)\cos\left(7\,f+5\,g\right)}{256\,\eta^9L^9}$$
$$+\frac{21\,si^5e^2\left(\eta^2-7\right)\cos\left(3\,f+5\,g\right)}{256\,\eta^9L^9}+\frac{5\,si^3\left(9\,si^2-8\right)e^4\cos\left(7\,f+3\,g\right)}{1024\,\eta^9L^9}$$
$$+\frac{5\,si\,\left(21\,si^4-28\,si^2+8\right)e^4\cos\left(3\,f-g\right)}{512\,\eta^9L^9}-\frac{35\,si^3\left(9\,si^2-8\right)e^4\cos\left(f-3\,g\right)}{1024\,\eta^9L^9}$$
$$-\frac{3\,si\,\left(21\,si^4-28\,si^2+8\right)e^4\cos\left(5\,f+g\right)}{512\,\eta^9L^9}$$
$$+\frac{15\,si\,\left(21\,si^4-28\,si^2+8\right)\left(3\,\eta^2-7\right)e\cos\left(2\,f+g\right)}{128\,\eta^9L^9}$$
$$-\frac{35\,si^3\left(3\,\eta^2-7\right)e\left(9\,si^2-8\right)\cos\left(2\,f+3\,g\right)}{256\,\eta^9L^9}-\frac{35\,si^3\left(3\,\eta^2-7\right)e\left(9\,si^2-8\right)\cos\left(4\,f+3\,g\right)}{512\,\eta^9L^9}$$
$$-\frac{15\,si\,\left(21\,si^4-28\,si^2+8\right)e^2\left(\eta^2-7\right)\cos\left(f-g\right)}{128\,\eta^9L^9}$$
$$-\frac{35\,si^3\left(9\,si^2-8\right)e^2\left(\eta^2-7\right)\cos\left(f+3\,g\right)}{256\,\eta^9L^9}-\frac{35\,si^3\left(f-l\right)e^3\left(9\,si^2-8\right)\sin\left(3\,g\right)}{128\,\eta^9L^9}$$
$$+\frac{5\,si\,\left(21\,si^4-28\,si^2+8\right)e^2\left(\eta^2-7\right)\cos\left(3\,f+g\right)}{128\,\eta^9L^9}-\frac{7\,si^3\left(9\,si^2-8\right)e^2\left(\eta^2-7\right)\cos\left(5\,f+3\,g\right)}{256\,\eta^9L^9}$$
$$+\frac{35\,si^3\left(9\,si^2-8\right)\left(3\,\eta^4-30\,\eta^2+35\right)\cos\left(3\,f+3\,g\right)}{1536\,\eta^9L^9}$$
$$-\frac{15\,si\,\left(21\,si^4-28\,si^2+8\right)\left(3\,\eta^4-30\,\eta^2+35\right)\cos\left(f+g\right)}{256\,\eta^9L^9}\Bigg). \quad \text{(A.10)}$$

$\mathbf{J_6}$ Contribution

$$\mathcal{W}_2 = \frac{{R_e}^6 \mu^6 J_6}{J^2}\left(-\frac{175\,si^2\left(33\,si^4-48\,si^2+16\right)e^4\sin\left(6\,f+2\,g\right)}{8192\,\eta^{11}L^{11}}+\frac{315\,si^4\left(11\,si^2-10\right)e^4\sin\left(8\,f+4\,g\right)}{16384\,\eta^{11}L^{11}}\right.$$
$$-\frac{525\,si^2\left(33\,si^4-48\,si^2+16\right)e^4\sin\left(-2\,g+2\,f\right)}{8192\,\eta^{11}L^{11}}+\frac{1155\,si^6e^2\left(\eta^2-3\right)\sin\left(8\,f+6\,g\right)}{8192\,\eta^{11}L^{11}}$$
$$-\frac{\left(5775\,si^6-9450\,si^4+4200\,si^2-400\right)e^2\left(\eta^2-3\right)\sin\left(2\,f\right)}{512\,\eta^{11}L^{11}}+\frac{1155\,si^6e^2\left(\eta^2-3\right)\sin\left(4\,f+6\,g\right)}{4096\,\eta^{11}L^{11}}$$
$$-\frac{231\,esi^6\left(\eta^4-14\,\eta^2+21\right)\sin\left(5\,f+6\,g\right)}{4096\,\eta^{11}L^{11}}-\frac{165\,esi^6\left(\eta^4-14\,\eta^2+21\right)\sin\left(7\,f+6\,g\right)}{4096\,\eta^{11}L^{11}}$$
$$+\frac{25\,e\left(231\,si^6-378\,si^4+168\,si^2-16\right)\left(\eta^4-14\,\eta^2+21\right)\sin\left(f\right)}{1024\,\eta^{11}L^{11}}$$
$$-\frac{15\,e^5si^2\left(33\,si^4-48\,si^2+16\right)\sin\left(7\,f+2\,g\right)}{8192\,\eta^{11}L^{11}}+\frac{7\,e^5si^4\left(11\,si^2-10\right)\sin\left(9\,f+4\,g\right)}{4096\,\eta^{11}L^{11}}$$
$$+\frac{63\,e^5si^4\left(11\,si^2-10\right)\sin\left(-4\,g+f\right)}{4096\,\eta^{11}L^{11}}-\frac{35\,e^5si^2\left(33\,si^4-48\,si^2+16\right)\sin\left(3\,f-2\,g\right)}{8192\,\eta^{11}L^{11}}$$
$$-\frac{77\,si^6\left(15\,\eta^4-70\,\eta^2+63\right)\sin\left(6\,f+6\,g\right)}{4096\,\eta^{11}L^{11}}+\frac{525\,si^2\left(33\,si^4-48\,si^2+16\right)e^2\left(\eta^2-3\right)\left(f-l\right)\cos\left(2\,g\right)}{1024\,\eta^{11}L^{11}}$$
$$-\frac{45\,e^3si^4\left(11\,si^2-10\right)\left(\eta+3\right)\left(\eta-3\right)\sin\left(7\,f+4\,g\right)}{4096\,\eta^{11}L^{11}}$$
$$+\frac{525\,e^3si^2\left(33\,si^4-48\,si^2+16\right)\left(\eta+3\right)\left(\eta-3\right)\sin\left(-2\,g+f\right)}{8192\,\eta^{11}L^{11}}$$
$$-\frac{315\,e^3si^4\left(11\,si^2-10\right)\left(\eta+3\right)\left(\eta-3\right)\sin\left(f+4\,g\right)}{4096\,\eta^{11}L^{11}}$$
$$+\frac{105\,e^3si^2\left(33\,si^4-48\,si^2+16\right)\left(\eta+3\right)\left(\eta-3\right)\sin\left(5\,f+2\,g\right)}{8192\,\eta^{11}L^{11}}$$
$$+\frac{e^5\left(231\,si^6-378\,si^4+168\,si^2-16\right)\sin\left(5\,f\right)}{2048\,\eta^{11}L^{11}}-\frac{21\,e^5si^6\sin\left(11\,f+6\,g\right)}{8192\,\eta^{11}L^{11}}-\frac{1155\,si^6e^4\sin\left(2\,f+6\,g\right)}{8192\,\eta^{11}L^{11}}$$
$$-\frac{231\,e^5si^6\sin\left(f+6\,g\right)}{8192\,\eta^{11}L^{11}}+\frac{\left(5775\,si^6-9450\,si^4+4200\,si^2-400\right)e^4\sin\left(4\,f\right)}{4096\,\eta^{11}L^{11}}-\frac{231\,si^6e^4\sin\left(10\,f+6\,g\right)}{8192\,\eta^{11}L^{11}}$$
$$-\frac{105\,si^2\left(33\,si^4-48\,si^2+16\right)\left(15\,\eta^4-70\,\eta^2+63\right)\sin\left(2\,g+2\,f\right)}{4096\,\eta^{11}L^{11}}$$
$$+\frac{\left(1155\,si^6-1890\,si^4+840\,si^2-80\right)\left(15\,\eta^4-70\,\eta^2+63\right)\left(f-l\right)}{1024\,\eta^{11}L^{11}}$$
$$+\frac{525\,si^2\left(33\,si^4-48\,si^2+16\right)e^2\left(\eta^2-3\right)\sin\left(2\,g+4\,f\right)}{4096\,\eta^{11}L^{11}}-\frac{105\,si^4\left(11\,si^2-10\right)e^2\left(\eta^2-3\right)\sin\left(6\,f+4\,g\right)}{1024\,\eta^{11}L^{11}}$$
$$-\frac{315\,si^4\left(11\,si^2-10\right)e^2\left(\eta^2-3\right)\sin\left(2\,f+4\,g\right)}{1024\,\eta^{11}L^{11}}$$
$$-\frac{525\,esi^2\left(33\,si^4-48\,si^2+16\right)\left(\eta^4-14\,\eta^2+21\right)\sin\left(f+2\,g\right)}{4096\,\eta^{11}L^{11}}$$

$$
\begin{aligned}
&- \frac{175\, esi^2 \left(33\, si^4 - 48\, si^2 + 16\right) \left(\eta^4 - 14\,\eta^2 + 21\right) \sin\left(3\, f + 2\, g\right)}{4096\, \eta^{11} L^{11}} \\
&+ \frac{105\, esi^4 \left(11\, si^2 - 10\right) \left(\eta^4 - 14\,\eta^2 + 21\right) \sin\left(3\, f + 4\, g\right)}{2048\, \eta^{11} L^{11}} \\
&- \frac{25\, e^3 \left(231\, si^6 - 378\, si^4 + 168\, si^2 - 16\right) (\eta + 3)\, (\eta - 3) \sin\left(3\, f\right)}{6144\, \eta^{11} L^{11}} + \frac{385\, e^3 si^6\, (\eta + 3)\, (\eta - 3) \sin\left(3\, f + 6\, g\right)}{8192\, \eta^{11} L^{11}} \\
&+ \frac{385\, e^3 si^6\, (\eta + 3)\, (\eta - 3) \sin\left(9\, f + 6\, g\right)}{24576\, \eta^{11} L^{11}} + \frac{315\, si^4 \left(11\, si^2 - 10\right) e^4\, (f - l) \cos\left(4\, g\right)}{2048\, \eta^{11} L^{11}} \\
&+ \frac{63\, esi^4 \left(11\, si^2 - 10\right) \left(\eta^4 - 14\,\eta^2 + 21\right) \sin\left(5\, f + 4\, g\right)}{2048\, \eta^{11} L^{11}} \\
&+ \frac{63\, si^4 \left(11\, si^2 - 10\right) \left(15\,\eta^4 - 70\,\eta^2 + 63\right) \sin\left(4\, f + 4\, g\right)}{4096\, \eta^{11} L^{11}} \Bigg). \qquad \text{(A.11)}
\end{aligned}
$$

A.4 First-Order Long-Period Generating Function

$\mathbf{J_2}$ Contribution

$$
\bar{\mathcal{W}}_1 = -1/32\, \frac{\left(G^2 - 15\, H^2\right) \left(G^2 - L^2\right) \left(G^2 - H^2\right) \sin\left(2\, g\right) {R_e}^2 \mu^2}{G^5 L^2 \left(G^2 - 5\, H^2\right)}. \qquad \text{(A.12)}
$$

$\mathbf{J_3}$ Contribution

$$
\bar{\mathcal{W}}_1 = 1/2\, \frac{\sqrt{-G^2 + L^2} \sqrt{G^2 - H^2} \cos\left(g\right) R_e\, \mu\, J_3}{G^2 L J^2}. \qquad \text{(A.13)}
$$

$\mathbf{J_4}$ Contribution

$$
\bar{\mathcal{W}}_1 = -\frac{\left(5\, G^2 - 35\, H^2\right) \left(G^2 - L^2\right) \left(G^2 - H^2\right) \sin\left(2\, g\right) {R_e}^2 \mu^2 J_4}{32\, L^2 G^5 J^2 \left(G^2 - 5\, H^2\right)}. \qquad \text{(A.14)}
$$

$\mathbf{J_5}$ Contribution

$$\bar{\mathcal{W}}_1 = \left(-\frac{5\sqrt{-G^2+L^2}\sqrt{G^2-H^2}\left(G^4-14\,G^2H^2+21\,H^4\right)\left(3\,G^2-7\,L^2\right)\cos\left(g\right)}{32\,L^3G^8J^2\left(G^2-5\,H^2\right)} \right.$$
$$\left. -\frac{35\,\left(-G^2+L^2\right)^{3/2}\left(G^2-H^2\right)^{3/2}\left(G^2-9\,H^2\right)\cos\left(3\,g\right)}{576\,L^3G^8J^2\left(G^2-5\,H^2\right)} \right) {R_e}^3\mu^3J_5. \quad \text{(A.15)}$$

$\mathbf{J_6}$ Contribution

$$\bar{\mathcal{W}}_1 = \left(\frac{\left(175\,G^4-3150\,G^2H^2+5775\,H^4\right)\left(G^4-4\,G^2L^2+3\,L^4\right)\left(G^2-H^2\right)\sin\left(2\,g\right)}{1024\,L^4G^{11}J^2\left(G^2-5\,H^2\right)} \right.$$
$$\left. -\frac{\left(105\,G^2-1155\,H^2\right)\left(-H+G\right)^2\left(H+G\right)^2\left(G^4-2\,G^2L^2+L^4\right)\sin\left(4\,g\right)}{4096\,L^4G^{11}J^2\left(G^2-5\,H^2\right)} \right) {R_e}^4\mu^4J_6. \quad \text{(A.16)}$$

A.5 Second-Order Long-Period Generating Function

$\mathbf{J_2}$ Contribution

$$\bar{\mathcal{W}}_2 = \frac{\mu^4{R_e}^4}{L^7}\left(-\frac{\left(\eta-1\right)}{1536\,\left(5\,si^2-4\right)^2\left(1+\eta\right)\eta^7}\left(2025\,\eta^4si^6-13950\,\eta^3si^6-270\,\eta^4si^4 \right.\right.$$
$$-23700\,\eta^2si^6+53700\,\eta^3si^4-6050\,\eta\,si^6-4032\,\eta^4si^2+68940\,\eta^2si^4-11125\,si^6$$
$$-60096\,\eta^3si^2-4700\,\eta\,si^4+2352\,\eta^4-63984\,\eta^2si^2+16010\,si^4+20832\,\eta^3+21536\,\eta\,si^2$$
$$\left.\left.+19200\,\eta^2-3056\,si^2-11104\,\eta-2096\right)si^2\sin\left(2\,g\right)$$
$$+\frac{si^4\left(\eta-1\right)^2}{3072\,\eta^7\left(5\,si^2-4\right)^3\left(1+\eta\right)^2}\left(10125\,\eta^4si^6+70500\,\eta^3si^6-27675\,\eta^4si^4+173250\,\eta^2si^6 \right.$$
$$-187500\,\eta^3si^4+142500\,\eta\,si^6+25200\,\eta^4si^2-450850\,\eta^2si^4+35625\,si^6+166080\,\eta^3si^2$$
$$-368300\,\eta\,si^4-7644\,\eta^4+390880\,\eta^2si^2-92075\,si^4-49008\,\eta^3+317120\,\eta\,si^2$$
$$\left.\left.-112936\,\eta^2+79280\,si^2-90992\,\eta-22748\right)\sin\left(4\,g\right)\right). \quad \text{(A.17)}$$

$\mathbf{J_3}$ Contribution

$$\bar{\mathcal{W}}_2 = \left(\frac{e\, si\, J_3\, \cos(g)}{384\, \left(5\, si^2-4\right)^2 (1+\eta)\, \eta^5 L^5 J^2} \left(3075\, \eta^3 si^6 + 11075\, \eta^2 si^6 - 4170\, \eta^3 si^4 \right.\right.$$
$$+ 4025\, \eta\, si^6 - 16010\, \eta^2 si^4 + 4025\, si^6 + 540\, \eta^3 si^2 - 9710\, \eta\, si^4 + 3612\, \eta^2 si^2 - 9710\, si^4$$
$$\left. + 672\, \eta^3 + 6660\, \eta\, si^2 + 1696\, \eta^2 + 6660\, si^2 - 1184\, \eta - 1184 \right)$$
$$- \frac{e\, si^3\, (\eta-1)\, J_3\, \cos(3\, g)}{1152\, \eta^5 \left(5\, si^2-4\right)^2 (1+\eta)^2 L^5 J^2} \left(1425\, \eta^3 si^4 + 13875\, \eta^2 si^4 - 2690\, \eta^3 si^2 + 19275\, \eta\, si^4 \right.$$
$$\left.\left. - 24070\, \eta^2 si^2 + 6425\, si^4 + 1276\, \eta^3 - 33030\, \eta\, si^2 + 10484\, \eta^2 - 11010\, si^2 + 14196\, \eta + 4732 \right) \right) {R_e}^3 \mu^3$$
$$+ 1/8\, \frac{si^2 \left(15\, si^2 - 13\right) (\eta-1)\, (1+\eta) \sin(2\, g)\, {J_3}^2 {R_e}^2 \mu^2}{L^3 \eta^3 \left(5\, si^2-4\right) J^4}. \quad \text{(A.18)}$$

$\mathbf{J_4}$ Contribution

$$\bar{\mathcal{W}}_2 = \left(\left(\frac{25 \left(7\, si^2-6\right) e^2 \left(189\, \eta^2 si^4 - 252\, \eta^2 si^2 - 385\, si^4 + 72\, \eta^2 + 500\, si^2 - 136\right) si^2 {J_4}^2}{512\, \eta^7 L^7 J^4 \left(5\, si^2-4\right)^2} \right.\right.$$
$$- \frac{(\eta-1)\, si^2 J_4}{1536\, J^2 L^7 \eta^7 \left(5\, si^2-4\right)^2 (1+\eta)} \left(19425\, \eta^4 si^6 + 86450\, \eta^3 si^6 - 34800\, \eta^4 si^4 + 79450\, \eta^2 si^6 \right.$$
$$- 163200\, \eta^3 si^4 - 59150\, \eta\, si^6 + 15120\, \eta^4 si^2 - 176220\, \eta^2 si^4 - 29575\, si^6 + 85216\, \eta^3 si^2 + 80040\, \eta\, si^4$$
$$+ 480\, \eta^4 + 127232\, \eta^2 si^2 + 40020\, si^4 - 7488\, \eta^3 - 1952\, \eta\, si^2 - 29952\, \eta^2 - 976\, si^2 - 20416\, \eta$$
$$\left.\left. - 10208 \right) \right) \sin(2\, g) + \left(\frac{\left(375\, si^2 - 325\right) \left(7\, si^2-6\right)^2 e^4\, si^4 {J_4}^2}{1024\, J^4 L^7 \eta^7 \left(5\, si^2-4\right)^3} \right.$$
$$+ \frac{si^4\, (\eta-1)^2\, J_4}{6144\, J^2 L^7 \eta^7 \left(5\, si^2-4\right)^3 (1+\eta)^2} \left(49875\, \eta^4 si^6 + 355500\, \eta^3 si^6 - 136950\, \eta^4 si^4 + 720250\, \eta^2 si^6 \right.$$
$$- 938200\, \eta^3 si^4 + 555500\, \eta\, si^6 + 125280\, \eta^4 si^2 - 1874500\, \eta^2 si^4 + 138875\, si^6 + 826240\, \eta^3 si^2$$
$$- 1437400\, \eta\, si^4 - 38160\, \eta^4 + 1627840\, \eta^2 si^2 - 359350\, si^4 - 242752\, \eta^3 + 1240960\, \eta\, si^2 - 471648\, \eta^2$$
$$\left.\left.\left. + 310240\, si^2 - 357440\, \eta - 89360 \right) \right) \sin(4\, g) \right) {R_e}^4 \mu^4$$

$$+\left(\frac{esi\ J_3\ J_4\ \cos(g)}{128\,J^4L^5\eta^5\left(5\,si^2-4\right)^2}\left(25725\,\eta^2si^6-53950\,\eta^2si^4-47425\,si^6+35700\,\eta^2si^2+97910\,si^4\right.\right.$$
$$\left.\left.-7200\,\eta^2-63380\,si^2+12320\right)+\frac{\left(4375\,si^4-7510\,si^2+3220\right)e^3\,si^3J_3\ J_4\ \cos(3\,g)}{384\,J^4L^5\eta^5\left(5\,si^2-4\right)^2}\right){R_e}^3\mu^3. \quad \text{(A.19)}$$

$\mathbf{J_5}$ Contribution

$$\bar{\mathcal{W}}_2=\left(\frac{-25e^2si^2{J_5}^2\sin(2\,g)}{4608\ \left(5\,si^2-4\right)^3\eta^{11}L^{11}J^4}\left(277830\,\eta^4si^{10}-953883\,\eta^4si^8-1203930\,\eta^2si^{10}\right.\right.$$
$$+1262709\,\eta^4si^6+4110561\,\eta^2si^8+1203930\,si^{10}-796110\,\eta^4si^4-5407206\,\eta^2si^6$$
$$-4118058\,si^8+234480\,\eta^4si^2+3386180\,\eta^2si^4+5432385\,si^6-24912\,\eta^4-991648\,\eta^2si^2$$
$$\left.\left.-3419318\,si^4+105504\,\eta^2+1012144\,si^2-110544\right)-\frac{175\,e^4si^4{J_5}^2\sin(4\,g)}{36864\ \left(5\,si^2-4\right)^3\eta^{11}L^{11}J^4}\left(11340\,\eta^2si^8\right.\right.$$
$$-31752\,\eta^2si^6-6615\,si^8+30456\,\eta^2si^4+14112\,si^6-10704\,\eta^2si^2-4704\,si^4+672\,\eta^2-6608\,si^2$$
$$\left.\left.+3808\right)-\frac{\left(18375\,si^2-15925\right)\left(9\,si^2-8\right)^2e^6\,si^6{J_5}^2\sin(6\,g)}{221184\ \left(5\,si^2-4\right)^3\eta^{11}L^{11}J^4}\right){R_e}^6\mu^6$$
$$+\left(\left(-\frac{e\,si\,J_4}{36864\,\eta^9\left(5\,si^2-4\right)^3L^9J^4}\left(178880625\,\eta^4si^{10}-603967350\,\eta^4si^8-738123750\,\eta^2si^{10}\right.\right.\right.$$
$$+787003700\,\eta^4si^6+2482277700\,\eta^2si^8+723295125\,si^{10}-489928800\,\eta^4si^4-3219802600\,\eta^2si^6$$
$$-2429383950\,si^8+143668800\,\eta^4si^2+1994251200\,\eta^2si^4+3147672500\,si^6-15552000\,\eta^4$$
$$\left.\left.\left.-581961600\,\eta^2si^2-1948648800\,si^4+62899200\,\eta^2+569620800\,si^2-62092800\right)\right.\right.$$
$$-\frac{e\,si}{36864\,\eta^9\left(5\,si^2-4\right)^3(1+\eta)\,L^9J^2}\left(24782625\,\eta^5si^{10}+54518625\,\eta^4si^{10}-77480550\,\eta^5si^8\right.$$
$$-35232750\,\eta^3si^{10}-161413350\,\eta^4si^8-122424750\,\eta^2si^{10}+91089780\,\eta^5si^6+139736100\,\eta^3si^8$$
$$+79246125\,\eta\,si^{10}+173626740\,\eta^4si^6+399195300\,\eta^2si^8+79246125\,si^{10}-48959840\,\eta^5si^4$$
$$-229482600\,\eta^3si^6-320874750\,\eta\,si^8-78232928\,\eta^4si^4-511192680\,\eta^2si^6-320874750\,si^8$$
$$+11403840\,\eta^5si^2+195593152\,\eta^3si^4+532534260\,\eta\,si^6+10764864\,\eta^4si^2+324816832\,\eta^2si^4$$
$$+532534260\,si^6-806400\,\eta^5-86564736\,\eta^3si^2-451822688\,\eta\,si^4+815616\,\eta^4-105242496\,\eta^2si^2$$
$$\left.-451822688\,si^4+15860736\,\eta^3+195503424\,\eta\,si^2+14631936\,\eta^2+195503424\,si^2-34420224\,\eta\right.$$

$$
- 34420224\Bigg)\Bigg) J_5\ \cos(g) + \Bigg(\frac{-25e^3\ si^3 J_4}{18432\,\eta^9\left(5\,si^2-4\right)^3 L^9 J^4}\Bigg(231525\,\eta^2 si^8 - 693630\,\eta^2 si^6
$$

$$
- 443205\,si^8 + 755244\,\eta^2 si^4 + 1318814\,si^6 - 349056\,\eta^2 si^2 - 1421084\,si^4 + 56160\,\eta^2 + 645568\,si^2
$$

$$
- 100576\Bigg) + \frac{(\eta-1)\,e\,si^3}{9216\,\eta^9\left(5\,si^2-4\right)^3(1+\eta)^2 L^9 J^2}\Bigg(63000\,\eta^5 si^8 + 1755000\,\eta^4 si^8 + 77175\,\eta^5 si^6
$$

$$
+ 5564250\,\eta^3 si^8 - 4473675\,\eta^4 si^6 + 3384750\,\eta^2 si^8 - 513210\,\eta^5 si^4 - 17039850\,\eta^3 si^6 - 956250\,\eta\,si^8
$$

$$
+ 3657170\,\eta^4 si^4 - 13076550\,\eta^2 si^6 - 318750\,si^8 + 554080\,\eta^5 si^2 + 19253300\,\eta^3 si^4 - 230925\,\eta\,si^6
$$

$$
- 825824\,\eta^4 si^2 + 18848620\,\eta^2 si^4 - 76975\,si^6 - 180560\,\eta^5 - 9475872\,\eta^3 si^2 + 4963110\,\eta\,si^4
$$

$$
- 109552\,\eta^4 - 12038496\,\eta^2 si^2 + 1654370\,si^4 + 1703584\,\eta^3 - 5605056\,\eta\,si^2 + 2879072\,\eta^2
$$

$$
- 1868352\,si^2 + 1820592\,\eta + 606864\Bigg)\Bigg) J_5\ \cos(3\,g) + \Bigg(\frac{-e^5\ si^5 J_4}{36864\,\eta^9\left(5\,si^2-4\right)^3 L^9 J^4}\Bigg(804825\,si^6
$$

$$
- 2101890\,si^4 + 1829660\,si^2 - 530880\Bigg) - \frac{e\,si^5(\eta-1)^2}{184320\,\eta^9\left(5\,si^2-4\right)^3(1+\eta)^3 L^9 J^2}\Bigg(1185975\,\eta^5 si^6
$$

$$
+ 8641875\,\eta^4 si^6 - 3267810\,\eta^5 si^4 + 22301250\,\eta^3 si^6 - 23183850\,\eta^4 si^4 + 26363250\,\eta^2 si^6
$$

$$
+ 2999724\,\eta^5 si^2 - 59014500\,\eta^3 si^4 + 14382375\,\eta\,si^6 + 20743260\,\eta^4 si^2 - 69233700\,\eta^2 si^4
$$

$$
+ 2876475\,si^6 - 917056\,\eta^5 + 52087800\,\eta^3 si^2 - 37633050\,\eta\,si^4 - 6188864\,\eta^4 + 60639480\,\eta^2 si^2
$$

$$
- 7526610\,si^4 - 15333760\,\eta^3 + 32840220\,\eta\,si^2 - 17714560\,\eta^2 + 6568044\,si^2 - 9558080\,\eta
$$

$$
- 1911616\Bigg)\Bigg) J_5\ \cos(5\,g)\Bigg) {R_e}^5 \mu^5
$$

$$
+ \Bigg(\frac{5e^2\ si^2 J_3\ J_5\ \sin(2\,g)}{1152\,\eta^7 L^7 J^4\left(5\,si^2-4\right)^2}\Bigg(22365\,\eta^2 si^6 - 48489\,\eta^2 si^4 - 46935\,si^6 + 33248\,\eta^2 si^2
$$

$$
+ 101577\,si^4 - 6960\,\eta^2 - 69440\,si^2 + 14448\Bigg) + \frac{\left(2625\,si^2-2380\right)\left(6\,si^2-5\right)e^4\ si^4 J_3\ J_5\ \sin(4\,g)}{2304\,\eta^7 L^7 J^4\left(5\,si^2-4\right)^2}\Bigg) {R_e}^4 \mu^4. \tag{A.20}
$$

$\mathbf{J_6}$ Contribution

$$
\bar{\mathcal{W}}_2 = \Bigg(\frac{6125e^2\ si^2 {J_6}^2 \sin(2\,g)}{4194304\ \left(5\,si^2-4\right)^3 \eta^{15} L^{15} J^4}\Bigg(6136515\,\eta^6 si^{12} - 24878502\,\eta^6 si^{10} - 50175675\,\eta^4 si^{12}
$$

$$
+ 40846164\,si^8\eta^6 + 203168790\,\eta^4 si^{10} + 126808605\,\eta^2 si^{12} - 34573728\,\eta^6 si^6 - 333049860\,\eta^4 si^8
$$

$$
- 513054234\,\eta^2 si^{10} - 95314725\,si^{12} + 15792960\,\eta^6 si^4 + 281327520\,\eta^4 si^6 + 840066444\,\eta^2 si^8 + 384843690\,si^{10}
$$

$$
\begin{aligned}
&- 3650560\,\eta^6 si^2 - 128129600\,\eta^4 si^4 - 708375648\,\eta^2 si^6 - 628496604\,si^8 + 327680\,\eta^6 + 29475840\,\eta^4 si^2 \\
&+ 321735360\,\eta^2 si^4 + 528149088\,si^6 - 2621440\,\eta^4 - 73657344\,\eta^2 si^2 - 238726080\,si^4 + 6488064\,\eta^2 + 54254592\,si^2 \\
&- 4718592\Bigg) + \frac{1225\,e^4\,si^4 {J_6}^2 \sin(4\,g)}{1048576\,\left(5\,si^2-4\right)^3 \eta^{15} L^{15} J^4}\Bigg(762300\,\eta^4 si^{10} - 2800215\,\eta^4 si^8 - 4356000\,\eta^2 si^{10} + 4020120\,\eta^4 si^6 \\
&+ 15973650\,\eta^2 si^8 + 5619240\,si^{10} - 2805120\,\eta^4 si^4 - 22893600\,\eta^2 si^6 - 20692287\,si^8 + 944640\,\eta^4 si^2 + 15950400\,\eta^2 si^4 \\
&+ 29819016\,si^6 - 121600\,\eta^4 - 5366400\,\eta^2 si^2 - 20932416\,si^4 + 691200\,\eta^2 + 7120512\,si^2 - 933120\Bigg) \\
&+ \frac{6125\,e^6\,si^6 {J_6}^2 \sin(6\,g)}{4194304\,\left(5\,si^2-4\right)^3 \eta^{15} L^{15} J^4}\Bigg(30855\,\eta^2 si^8 - 97614\,\eta^2 si^6 - 70785\,si^8 + 113140\,\eta^2 si^4 + 223938\,si^6 \\
&- 56416\,\eta^2 si^2 - 258876\,si^4 + 10048\,\eta^2 + 128160\,si^2 - 22464\Bigg) \\
&+ \frac{\left(165375\,si^2 - 143325\right)\left(11\,si^2-10\right)^2 e^8 si^8 {J_6}^2 \sin(8\,g)}{8388608\,\left(5\,si^2-4\right)^3 \eta^{15} L^{15} J^4}\Bigg) {R_e}^8 \mu^8 \\
&+ \Bigg(\frac{e\,si\,J_5\,J_6\,\cos(g)}{4718592\,\eta^{13}\left(5\,si^2-4\right)^3 L^{13} J^4}\Bigg(126267285375\,\eta^6 si^{12} - 492163519050\,\eta^6 si^{10} - 924117319125\,\eta^4 si^{12} \\
&+ 770924013300\,si^8 \eta^6 + 3590301635550\,\eta^4 si^{10} + 2066163994125\,\eta^2 si^{12} - 615854148000\,\eta^6 si^6 \\
&- 5602149644700\,\eta^4 si^8 - 8008345475550\,\eta^2 si^{10} - 1389860616375\,si^{12} + 261287488000\,\eta^6 si^4 \\
&+ 4454554188000\,\eta^4 si^6 + 12460342379100\,\eta^2 si^8 + 5374751819850\,si^{10} - 54700800000\,\eta^6 si^2 \\
&- 1879193792000\,\eta^4 si^4 - 9873304140000\,\eta^2 si^6 - 8339790616500\,si^8 + 4257792000\,\eta^6 + 390528768000\,\eta^4 si^2 \\
&+ 4146807078400\,\eta^2 si^4 + 6586246212000\,si^6 - 30062592000\,\eta^4 - 856655923200\,\eta^2 si^2 - 2754795993600\,si^4 \\
&+ 65311948800\,\eta^2 + 566037964800\,si^2 - 42810163200\Bigg) + \frac{175\,e^2\,e\,si^3 J_5\,J_6\,\cos(3\,g)}{2359296\,\eta^{13}\left(5\,si^2-4\right)^3 L^{13} J^4}\Bigg(29615355\,\eta^4 si^{10} \\
&- 104732166\,\eta^4 si^8 - 149168250\,\eta^2 si^{10} + 143436948\,\eta^4 si^6 + 525578340\,\eta^2 si^8 + 161465535\,si^{10} - 94128768\,\eta^4 si^4 \\
&- 716684760\,\eta^2 si^6 - 569086686\,si^8 + 29106080\,\eta^4 si^2 + 467904640\,\eta^2 si^4 + 776187972\,si^6 - 3289600\,\eta^4 \\
&- 143835840\,\eta^2 si^2 - 506903040\,si^4 + 16163840\,\eta^2 + 155982624\,si^2 - 17601024\Bigg) \\
&+ \frac{35\,e^5\,si^5 J_5\,J_6\,\cos(5\,g)}{2359296\,\eta^{13}\left(5\,si^2-4\right)^3 L^{13} J^4}\Bigg(7182945\,\eta^2 si^8 - 21930930\,\eta^2 si^6 - 13877325\,si^8 + 24200340\,\eta^2 si^4 \\
&+ 42803586\,si^6 - 11206080\,\eta^2 si^2 - 47657988\,si^4 + 1758112\,\eta^2 + 22212288\,si^2 - 3487008\Bigg) \\
&+ \frac{\left(12560625\,si^6 - 33468750\,si^4 + 29722700\,si^2 - 8797600\right) e^7\,si^7 J_5\,J_6\,\cos(7\,g)}{1572864\,\eta^{13}\left(5\,si^2-4\right)^3 L^{13} J^4}\Bigg) {R_e}^7 \mu^7 \\
&+ \Bigg(\Bigg(\frac{-175\,e^2\,si^2 J_4}{131072\,\left(5\,si^2-4\right)^3 \eta^{11} L^{11} J^4}\Bigg(2521365\,\eta^4 si^{10} - 8898432\,\eta^4 si^8 - 12924450\,\eta^2 si^{10} + 12220440\,\eta^4 si^6
\end{aligned}
$$

$$+ 45434400\,\eta^2 si^8 + 14320845\,si^{10} - 8107480\,\eta^4 si^4 - 62088208\,\eta^2 si^6 - 50159136\,si^8 + 2572160\,\eta^4 si^2$$

$$+ 40923440\,\eta^2 si^4 + 68248056\,si^6 - 307200\,\eta^4 - 12865280\,\eta^2 si^2 - 44749656\,si^4 + 1515520\,\eta^2 + 13979520\,si^2$$

$$- 1634304\Bigg) + \frac{5\,(\eta-1)\,si^2}{393216\,\eta^{11}\left(5\,si^2-4\right)^3(1+\eta)\,L^{11}J^2}\Bigg(43329825\,\eta^6 si^{10} + 150125250\,\eta^5 si^{10} - 144514440\,si^8\eta^6$$

$$+37077975\,\eta^4 si^{10} - 489953040\,\eta^5 si^8 - 486964500\,\eta^3 si^{10} + 183263304\,\eta^6 si^6 - 96856920\,\eta^4 si^8 - 236868225\,\eta^2 si^{10}$$

$$+603322512\,\eta^5 si^6 + 1648679520\,\eta^3 si^8 + 469314450\,\eta\,si^{10} - 107737560\,\eta^6 si^4 + 68785112\,\eta^4 si^6 + 718794120\,\eta^2 si^8$$

$$+ 234657225\,si^{10} - 338654128\,\eta^5 si^4 - 2159522016\,\eta^3 si^6 - 1725994320\,\eta\,si^8 + 27834240\,\eta^6 si^2 + 17277784\,\eta^4 si^4$$

$$- 766899272\,\eta^2 si^6 - 862997160\,si^8 + 79621888\,\eta^5 si^2 + 1356946016\,\eta^3 si^4 + 2550919248\,\eta\,si^6 - 2150400\,\eta^6$$

$$- 37742464\,\eta^4 si^2 + 298365400\,\eta^2 si^4 + 1275459624\,si^6 - 4366336\,\eta^5 - 405126656\,\eta^3 si^2 - 1906837168\,\eta\,si^4$$

$$+11440128\,\eta^4 + 8128640\,\eta^2 si^2 - 953418584\,si^4 + 45596672\,\eta^3 + 728059648\,\eta\,si^2 - 21606400\,\eta^2 + 364029824\,si^2$$

$$- 114958336\,\eta - 57479168\Bigg)\Bigg)J_6\,\sin(2\,g) + \Bigg(\frac{-175\,e^4\,si^4 J_4}{65536\,\left(5\,si^2-4\right)^3\eta^{11}L^{11}J^4}\Bigg(100485\,\eta^2 si^8 - 315138\,\eta^2 si^6$$

$$- 271425\,si^8 + 364464\,\eta^2 si^4 + 851850\,si^6 - 183344\,\eta^2 si^2 - 986160\,si^4 + 33600\,\eta^2 + 496752\,si^2 - 91200\Bigg)$$

$$- \frac{(\eta-1)^2\,si^4}{196608\,\eta^{11}\left(5\,si^2-4\right)^3(1+\eta)^2\,L^{11}J^2}\Bigg(7709625\,si^8\eta^6 + 61418500\,\eta^5 si^8 - 22626450\,\eta^6 si^6 + 155959375\,\eta^4 si^8$$

$$- 186523400\,\eta^5 si^6 + 58993000\,\eta^3 si^8 + 23565360\,\eta^6 si^4 - 492047150\,\eta^4 si^6 - 205236625\,\eta^2 si^8 + 206152000\,\eta^5 si^4$$

$$- 226192400\,\eta^3 si^6 - 216089500\,\eta\,si^8 - 9913008\,\eta^6 si^2 + 575225440\,\eta^4 si^4 + 573764450\,\eta^2 si^6 - 54022375\,si^8$$

$$- 96950976\,\eta^5 si^2 + 326018880\,\eta^3 si^4 + 629463800\,\eta\,si^6 + 1270080\,\eta^6 - 294626736\,\eta^4 si^2 - 560130000\,\eta^2 si^4$$

$$+ 157365950\,si^6 + 15944960\,\eta^5 - 209287424\,\eta^3 si^2 - 658494720\,\eta\,si^4 + 55588160\,\eta^4 + 212520944\,\eta^2 si^2$$

$$- 164623680\,si^4 + 50467840\,\eta^3 + 285891008\,\eta\,si^2 - 21144640\,\eta^2 + 71472752\,si^2 - 40986880\,\eta$$

$$- 10246720\Bigg)\Bigg)J_6\,\sin(4\,g) + \Bigg(\frac{-\left(1684375\,si^6 - 4431000\,si^4 + 3885000\,si^2 - 1135400\right)e^6\,si^6 J_4}{131072\,\left(5\,si^2-4\right)^3\eta^{11}L^{11}J^4}$$

$$+\frac{si^6\,(\eta-1)^3}{1179648\,\eta^{11}\left(5\,si^2-4\right)^3(1+\eta)^3\,L^{11}J^2}\Bigg(5110875\,\eta^6 si^6 + 40417250\,\eta^5 si^6 - 14120400\,\eta^6 si^4 + 125473125\,\eta^4 si^6$$

$$- 109471200\,\eta^5 si^4 + 197053500\,\eta^3 si^6 + 12999000\,\eta^6 si^2 - 335602800\,\eta^4 si^4 + 165395125\,\eta^2 si^6 + 98868240\,\eta^5 si^2$$

$$- 522782400\,\eta^3 si^4 + 70229250\,\eta\,si^6 - 3986472\,\eta^6 + 299344680\,\eta^4 si^2 - 436590000\,\eta^2 si^4 + 11704875\,si^6$$

$$- 29772016\,\eta^5 + 462493920\,\eta^3 si^2 - 184917600\,\eta\,si^4 - 89045592\,\eta^4 + 384273960\,\eta^2 si^2 - 30819600\,si^4$$

$$-136456992\,\eta^3 + 162343440\,\eta\,si^2 - 112797272\,\eta^2 + 27057240\,si^2 - 47530224\,\eta - 7921704\Bigg)\Bigg)J_6\,\sin(6\,g)\Bigg){R_e}^6\mu^6$$

$$+ \Bigg(\frac{-e\,si\,J_3\,J_6\,\cos(g)}{4096\,\eta^9\left(5\,si^2-4\right)^2 L^9 J^4}\Bigg(4475625\,\eta^4 si^8 - 11719050\,\eta^4 si^6 - 22926750\,\eta^2 si^8 + 10844400\,\eta^4 si^4$$

$$+59379600\,\eta^2 si^6+22470525\,si^8-4082400\,\eta^4 si^2-54168800\,\eta^2 si^4-57663270\,si^6+492800\,\eta^4+19980800\,\eta^2 si^2$$
$$+51957360\,si^4-2329600\,\eta^2-18819360\,si^2+2123520\Bigg)+\frac{-35\,e^3\,si^3 J_3\,J_6\,\cos(3\,g)}{49152\,\eta^9\left(5\,si^2-4\right)^2 L^9 J^4}\Bigg(112695\,\eta^2 si^6$$
$$-259314\,\eta^2 si^4-330495\,si^6+193540\,\eta^2 si^2+761874\,si^4-46400\,\eta^2-570180\,si^2+137280\Bigg)$$
$$-\frac{\left(65835\,si^4-115458\,si^2+50484\right)e^5\,si^5 J_3\,J_6\,\cos(5\,g)}{16384\,\eta^9\left(5\,si^2-4\right)^2 L^9 J^4}\Bigg){R_e}^5\mu^5. \quad \text{(A.21)}$$

APPENDIX B

EXPRESSIONS FOR THE EXACT SHORT-PERIOD GENERATING FUNCTION FOR THE TESSERAL AND SECTORIAL HARMONICS

B.1 Partial Derivatives of $\mathcal{W}_2^T$

$$\begin{aligned}\mathcal{W}_{2,gh}^T &= \frac{1}{\sin i}\left(\cos i\frac{\partial \mathcal{W}_2^T}{\partial g} - \frac{\partial \mathcal{W}_2^T}{\partial h}\right), \\ &= -\frac{2!}{C_{20}^2}\frac{\mu R_e^n}{\tilde{n}\, a^{n+1}\eta^{2n-1}}\sum_{p=0}^{p=n} F'_{nmp}(i)\left[CS_1\left\{-\cos(\beta)I_2^{nmp} - \sin(\beta)I_1^{nmp}\right\}\right. \\ &\qquad \left. +CS_2\left\{\cos(\beta)I_1^{nmp} - \sin(\beta)I_2^{nmp}\right\}\right],\end{aligned}$$

$$\text{where } F'_{nmp}(i) = \begin{cases} \frac{-m}{G}\ \tan(i/2)\ F_{nmp}(i) & \text{if } (n-2p) = m \\ \frac{1}{2}\frac{\cos(i)(n-2p)-m}{G\cos(i/2)}\ \left(\frac{1}{\sin(i/2)}F_{nmp}(i)\right) & \text{if } (n-2p) \neq m. \end{cases}$$

$$\begin{aligned}\mathcal{W}_{2,lg}^T &= \frac{1}{e}\left(\frac{\partial \mathcal{W}_2^T}{\partial l} - \frac{1}{\eta}\frac{\partial \mathcal{W}_2^T}{\partial g}\right), \\ &= -\frac{2!}{C_{20}^2}\frac{\mu R_e^n}{\tilde{n}\, a^{n+1}\eta^{2n-1}}\sum_{p=0}^{p=n} F_{nmp}(i)\left[CS_1\left\{\cos(\beta)\left(-(n-2p)I_{2,lga}^{nm} - \frac{n+1}{\eta^3}I_{1,lgb}^{nm}\right)\right.\right. \\ &\qquad \left. +\sin(\beta)\left(-(n-2p)I_{1,lga}^{nm} + \frac{n+1}{\eta^3}I_{2,lgb}^{nm}\right)\right\} \\ &\qquad +CS_2\left\{\cos(\beta)\left((n-2p)I_{1,lga}^{nm} - \frac{n+1}{\eta^3}I_{2,lgb}^{nm}\right)\right. \\ &\qquad \left.\left. +\sin(\beta)\left(-(n-2p)I_{2,lga}^{nm} - \frac{n+1}{\eta^3}I_{1,lgb}^{nm}\right)\right\}\right].\end{aligned}$$

B.2 Partial Derivatives of I_1^{nmp} and I_2^{nmp}

$$\frac{\partial I_1^{nmp}}{\partial a} = m\frac{d\delta}{da}\int l\,\sin((n-2p)f - m\delta\, l)(1+e\cos f)^{n-1}\,\mathrm{d}f,$$
$$\frac{\partial I_2^{nmp}}{\partial a} = -m\frac{d\delta}{da}\int l\,\cos((n-2p)f - m\delta\, l)(1+e\cos f)^{n-1}\,\mathrm{d}f,$$

$$\frac{\partial I_1^{nmp}}{\partial e} = \frac{1}{\eta^2}\int\left(\frac{-3e(n-1)}{2}\cos(\alpha(f)) + \frac{(-(n-1)+4p)}{2}\cos(\alpha(f)-f) + \frac{((3n+1)-4p)}{2}\cos(\alpha(f)+f) + \frac{e(2p+1)}{4}\cos(\alpha(f)-2f) + \frac{e(2n-2p+1)}{4}\cos(\alpha(f)+2f)\right)(1+e\cos f)^{n-1}\,\mathrm{d}f,$$

$$\frac{\partial I_2^{nmp}}{\partial e} = \frac{1}{\eta^2}\int\left(\frac{-3e(n-1)}{2}\sin(\alpha(f)) + \frac{(-(n-1)+4p)}{2}\sin(\alpha(f)-f) + \frac{((3n+1)-4p)}{2}\sin(\alpha(f)+f) + \frac{e(2p+1)}{4}\sin(\alpha(f)-2f) + \frac{e(2n-2p+1)}{4}\sin(\alpha(f)+2f)\right)(1+e\cos f)^{n-1}\,\mathrm{d}f,$$

where $\alpha(f) \equiv (n-2p)f - m\delta\, l$,

$$\frac{\partial I_1^{nmp}}{\partial f} = \cos((n-2p)f - m\delta\, l)(1+e\cos f)^{n-1},$$
$$\frac{\partial I_2^{nmp}}{\partial f} = \sin((n-2p)f - m\delta\, l)(1+e\cos f)^{n-1},$$

$$I_{1,lga}^{nm} = \int\frac{1}{\eta^3}\left(e + 2\cos(f) + e\cos^2(f)\right)\cos((n-2p)f - m\delta\, l)(1+e\cos f)^{n-1}\,\mathrm{d}f,$$

$$I_{2,lga}^{nm} = \int \frac{1}{\eta^3} \left(e + 2\cos(f) + e\cos^2(f)\right) \sin((n-2p)f - m\delta\, l)(1 + e\cos f)^{n-1}\, \mathrm{d}f,$$

$$I_{1,lgb}^{nm} = \int \sin(f)\, \cos((n-2p)f - m\delta\, l)(1 + e\cos f)^{n}\, \mathrm{d}f,$$

$$I_{2,lgb}^{nm} = \int \sin(f)\, \sin((n-2p)f - m\delta\, l)(1 + e\cos f)^{n}\, \mathrm{d}f.$$

APPENDIX C

THE EQUINOCTIAL GEOMETRIC TRANSFORMATION MATRIX

C.1 The Geometric Transformation Matrix Definition

The geometric transformation matrix (Σ) formulated using the osculating equinoctial elements is used to compute the relative position and velocity state vector ($\delta\bar{x}$) in the curvilinear frame using the differential equinoctial element vector ($\delta\bar{e}$) as shown below:

$$\delta\bar{x} = \Sigma\,\delta\bar{e}, \tag{C.1}$$

where

$$\delta\bar{x} = \begin{bmatrix} x & y & z & \dot{x} & \dot{y} & \dot{z} \end{bmatrix}^T,$$

$$\delta\bar{e} = \begin{bmatrix} \delta a & \delta\,\Psi & \delta p1 & \delta p2 & \delta q1 & \delta q2 \end{bmatrix}^T.$$

C.2 The Geometric Transformation Matrix Elements

$$\Sigma_{1,1} = -\frac{\left(q1^2 + q2^2 - 1\right)\sqrt{\mu}}{Vt\,\sqrt{p}}, \tag{C.2}$$

$$\Sigma_{1,2} = \frac{Vr\,\sqrt{\mu}\sqrt{p}}{Vt^2}, \tag{C.3}$$

$$\Sigma_{1,3} = 0, \tag{C.4}$$

$$\Sigma_{1,4} = 0, \tag{C.5}$$

$$\Sigma_{1,5} = -\frac{a\left(\cos\left(\Psi\right) q1^{2} - \cos\left(\Psi\right) q2^{2} + 2\,\sin\left(\Psi\right) q1\; q2 + \cos\left(\Psi\right) + 2\,q1\right)\mu}{Vt^{2}p}, \tag{C.6}$$

$$\Sigma_{1,6} = -\frac{a\left(2\,\cos\left(\Psi\right) q1\; q2 - \sin\left(\Psi\right) q1^{2} + q2^{2}\sin\left(\Psi\right) + \sin\left(\Psi\right) + 2\,q2\right)\mu}{Vt^{2}p}, \tag{C.7}$$

$$\Sigma_{2,1} = 0, \tag{C.8}$$

$$\Sigma_{2,2} = \frac{\sqrt{\mu}\sqrt{p}}{Vt}, \tag{C.9}$$

$$\Sigma_{2,3} = 2\,\frac{\sqrt{p}p2\,\sqrt{\mu}}{\left(p1^{2} + p2^{2} + 1\right)\,Vt}, \tag{C.10}$$

$$\Sigma_{2,4} = -2\,\frac{\sqrt{p}p1\,\sqrt{\mu}}{\left(p1^{2} + p2^{2} + 1\right)\,Vt}, \tag{C.11}$$

$$\Sigma_{2,5} = 0, \tag{C.12}$$

$$\Sigma_{2,6} = 0, \tag{C.13}$$

$$\Sigma_{3,1} = 0, \tag{C.14}$$

$$\Sigma_{3,2} = 0, \tag{C.15}$$

$$\Sigma_{3,3} = 2\,\frac{\sqrt{p}\sin\left(\Psi\right)\sqrt{\mu}}{\left(p1^{\,2} + p2^{\,2} + 1\right)\,Vt}, \tag{C.16}$$

$$\Sigma_{3,4} = -2\,\frac{\sqrt{p}\cos\left(\Psi\right)\sqrt{\mu}}{\left(p1^{\,2} + p2^{\,2} + 1\right)\,Vt}, \tag{C.17}$$

$$\Sigma_{3,5} = 0, \tag{C.18}$$

$$\Sigma_{3,6} = 0, \tag{C.19}$$

$$\Sigma_{4,1} = -1/2\,\frac{Vr}{a}, \tag{C.20}$$

$$\begin{aligned}\Sigma_{4,2} = \frac{\sqrt{\mu}}{\sqrt{p}}\Bigg(&\frac{q1\ \left(p1^{\,4} - 2\,p1^{\,2}{\sigma_1}^{\,2} - p2^{\,4} - 2\,{\sigma_1}^{\,2} - 1\right)\cos\left(\Psi\right)}{\left({\sigma_1}^{\,2} + 1\right)^{2}} \\ &+ \frac{q2\ \left(p1^{\,4} - 2\,p1^{\,2}{\sigma_1}^{\,2} - p2^{\,4} - 2\,{\sigma_1}^{\,2} - 1\right)\sin\left(\Psi\right)}{\left({\sigma_1}^{\,2} + 1\right)^{2}} \\ &+ \frac{p1^{\,4} - 2\,p1^{\,2}{\sigma_1}^{\,2} - p2^{\,4} - {\sigma_1}^{\,4} - 4\,{\sigma_1}^{\,2} - 2}{\left({\sigma_1}^{\,2} + 1\right)^{2}}\Bigg) + 2\ Vt,\end{aligned} \tag{C.21}$$

$$\Sigma_{4,3} = 0, \tag{C.22}$$

$$\Sigma_{4,4} = 0, \tag{C.23}$$

$$\Sigma_{4,5} = \frac{aq1\ Vr}{p} + \frac{\sqrt{\mu}\sin\left(\Psi\right)}{\sqrt{p}}, \tag{C.24}$$

$$\Sigma_{4,6} = \frac{aq2\ Vr}{p} - \frac{\sqrt{\mu}\cos(\Psi)}{\sqrt{p}}, \tag{C.25}$$

$$\Sigma_{5,1} = -3/2\,\frac{Vt}{a}, \tag{C.26}$$

$$\Sigma_{5,2} = -Vr, \tag{C.27}$$

$$\Sigma_{5,3} = 2\,\frac{p2\ Vr}{{\sigma_1}^2 + 1} + 2\,\frac{w_1\sqrt{p}\sin(\Psi)\sqrt{\mu}}{({\sigma_1}^2 + 1)\ Vt}, \tag{C.28}$$

$$\Sigma_{5,4} = -2\,\frac{p1\ Vr}{{\sigma_1}^2 + 1} - 2\,\frac{w_1\sqrt{p}\cos(\Psi)\sqrt{\mu}}{({\sigma_1}^2 + 1)\ Vt}, \tag{C.29}$$

$$\begin{aligned}\Sigma_{5,5} = \frac{\mu^{3/2}}{p^{5/2}}\Bigg(&1/4\,\frac{a\left(3\,{q1}^4 + 2\,{q1}^2{q2}^2 - {q2}^4 + 23\,{q1}^2 - 3\,{q2}^2 + 4\right)\cos(\Psi)}{Vt^2} \\ &+ \frac{aq1\ \left(2\,{q1}^2 - 4\,{q2}^2 + 1\right)\cos(2\,\Psi)}{Vt^2} \\ &+ 1/4\,\frac{a\left({q1}^4 - 6\,{q1}^2{q2}^2 + {q2}^4 + {q1}^2 - {q2}^2\right)\cos(3\,\Psi)}{Vt^2} \\ &+ 1/2\,\frac{aq1\ q2\ \left(2\,{q1}^2 + 2\,{q2}^2 + 13\right)\sin(\Psi)}{Vt^2} + \frac{aq2\ \left(5\,{q1}^2 - {q2}^2 + 1\right)\sin(2\,\Psi)}{Vt^2} \\ &+ 1/2\,\frac{aq1\ q2\ \left(2\,{q1}^2 - 2\,{q2}^2 + 1\right)\sin(3\,\Psi)}{Vt^2} + \frac{aq1\ \left(2\,{q1}^2 + 2\,{q2}^2 + 3\right)}{Vt^2}\Bigg) + \\ &\left(\frac{\cos(\Psi)}{\sqrt{p}} + \frac{\cos(\Psi)\,{aq1}^2 + \sin(\Psi)\,aq1\ q2 + aq1}{p^{3/2}}\right)\sqrt{\mu},\end{aligned} \tag{C.30}$$

$$\Sigma_{5,6} = \frac{\mu^{3/2}}{p^{5/2}}\left(1/2\,\frac{aq1\ q2\ \left(2\,{q1}^2 + 2\,{q2}^2 + 13\right)\cos(\Psi)}{Vt^2}\right.$$

$$+\frac{aq2\ \left(4\,q1^{2}-2\,q2^{2}-1\right)\cos\left(2\,\Psi\right)}{Vt^{2}}+1/2\,\frac{aq1\ q2\ \left(2\,q1^{2}-2\,q2^{2}-1\right)\cos\left(3\,\Psi\right)}{Vt^{2}}$$
$$-1/4\,\frac{a\left(q1^{4}-2\,q1^{2}q2^{2}-3\,q2^{4}+3\,q1^{2}-23\,q2^{2}-4\right)\sin\left(\Psi\right)}{Vt^{2}}$$
$$-\frac{aq1\ \left(q1^{2}-5\,q2^{2}-1\right)\sin\left(2\,\Psi\right)}{Vt^{2}}$$
$$-1/4\,\frac{a\left(q1^{4}-6\,q1^{2}q2^{2}+q2^{4}-q1^{2}+q2^{2}\right)\sin\left(3\,\Psi\right)}{Vt^{2}}+\frac{aq2\ \left(2\,q1^{2}+2\,q2^{2}+3\right)}{Vt^{2}}\Bigg)+$$
$$\left(\frac{\sin\left(\Psi\right)}{\sqrt{p}}+\frac{\cos\left(\Psi\right)aq1\ q2+\sin\left(\Psi\right)aq2^{2}+aq2}{p^{3/2}}\right)\sqrt{\mu}, \quad \text{(C.31)}$$

$$\Sigma_{6,1}=0, \quad \text{(C.32)}$$

$$\Sigma_{6,2}=-\frac{w_1\sqrt{p}\sqrt{\mu}}{Vt}, \quad \text{(C.33)}$$

$$\Sigma_{6,3}=2\,\frac{\sin\left(\Psi\right)\ Vr}{{\sigma_1}^{2}+1}+2\,\frac{\cos\left(\Psi\right)\ Vt}{{\sigma_1}^{2}+1}-2\,\frac{w_1\sqrt{p}p2\ \sqrt{\mu}}{\left({\sigma_1}^{2}+1\right)\ Vt}, \quad \text{(C.34)}$$

$$\Sigma_{6,4}=\Bigg(2\,\frac{p1\ w_1\sqrt{p}}{\left({\sigma_1}^{2}+1\right)\ Vt}$$
$$+\frac{1}{\sqrt{p}}\left(-\frac{q2\ \cos\left(2\,\Psi\right)}{{\sigma_1}^{2}+1}+2\,\frac{\sin\left(\Psi\right)}{{\sigma_1}^{2}+1}+\frac{q1\ \sin\left(2\,\Psi\right)}{{\sigma_1}^{2}+1}+\frac{q2}{{\sigma_1}^{2}+1}\right)\Bigg)\sqrt{\mu}-2\,\frac{\cos\left(\Psi\right)\ Vr}{{\sigma_1}^{2}+1}, \quad \text{(C.35)}$$

$$\Sigma_{6,5}=0, \quad \text{(C.36)}$$

$$\Sigma_{6,6}=0, \quad \text{(C.37)}$$

where

$$p = a\left(1 - q1^2 - q2^2\right),$$

$$Vr = \frac{\sqrt{\mu}}{p}\left(q1\sin\Psi - q2\cos\Psi\right),$$

$$Vt = \frac{\sqrt{\mu}}{p}\left(1 + q1\cos\Psi + q2\ \sin\Psi\right),$$

and w_1 is the radial component of the Hill reference frame of the chief, and $(a, \Psi, p1, p2, q1, q2)$ are the equinoctial element set with Ψ as the true longitude.

C.3 Differential Mean and True Longitude

The geometric transformation matrix depends on the differential true longitude ($\delta\Psi$) to compute relative state vector in the curvilinear frame. In case $\delta\Psi$ is not directly available, then it can be computed from the differential mean longitude ($\delta\Lambda$) using the following relation:

$$\delta\Psi = \frac{\partial\Psi}{\delta\Lambda}\delta\Lambda + \frac{\partial\Psi}{\delta q1}\delta q1 + \frac{\partial\Psi}{\delta q2}\delta q2, \tag{C.38}$$

where

$$\frac{\partial\Psi}{\partial\Lambda} = -2\,\frac{q1\ \cos\left(\Psi\right)}{\eta^3} - 1/2\,\frac{\left(\eta^2 + 2\,q1^2 - 1\right)\cos\left(2\,\Psi\right)}{\eta^3} - 2\,\frac{\sin\left(\Psi\right)\,q2}{\eta^3} - \frac{q1\ q2\ \sin\left(2\,\Psi\right)}{\eta^3} + 1/2\,\frac{\eta^2 - 3}{\eta^3}, \tag{C.39}$$

$$\frac{\partial\Psi}{\partial q1} = 4\,\frac{\cos\left(\Psi\right)\,q1\ q2}{2\,\eta^4 + 2\,\eta^3} + \frac{\left(2\,q1^2 q2 - \eta\,q2 - q2\right)\cos\left(2\,\Psi\right)}{2\,\eta^4 + 2\,\eta^3} + \frac{\left(-4\,q1^2 + 4\,\eta + 4\right)\sin\left(\Psi\right)}{2\,\eta^4 + 2\,\eta^3} + \frac{\left(-q1\,\eta^2 - 2\,q1^3 + \eta\,q1 + 2\,q1\right)\sin\left(2\,\Psi\right)}{2\,\eta^4 + 2\,\eta^3}$$

$$+\frac{2\,\eta^2 q2+3\,\eta\,q2+3\,q2}{2\,\eta^4+2\,\eta^3}, \quad \text{(C.40)}$$

$$\frac{\partial\Psi}{\partial q2}=\frac{\left(-4\,\eta^2-4\,q1^{\,2}-4\,\eta\right)\cos\left(\Psi\right)}{2\,\eta^4+2\,\eta^3}+\frac{\left(-2\,q1\,\eta^2-2\,q1^{\,3}-\eta\,q1+q1\right)\cos\left(2\,\Psi\right)}{2\,\eta^4+2\,\eta^3}$$
$$-4\,\frac{\sin\left(\Psi\right)\,q1\;q2}{2\,\eta^4+2\,\eta^3}+\frac{\left(-\eta^2 q2-2\,q1^{\,2}q2-\eta\,q2\right)\sin\left(2\,\Psi\right)}{2\,\eta^4+2\,\eta^3}$$
$$+\frac{-2\,q1\,\eta^2-3\,\eta\,q1-3\,q1}{2\,\eta^4+2\,\eta^3}. \quad \text{(C.41)}$$

APPENDIX D

SWARM SIMULATION TOOL

The analytic propagator for the absolute and relative motion of artificial satellites using the perturbation theories developed in this work is implemented in a MATLAB tool, referred to as SwARM, and is available in the supplementary files as part of this dissertation. The graphical front-end for SwARM is shown in Figure D.1. To be specific, SwARM implements a second-order analytic propagator for the absolute and relative motion in the presence of the gravitational harmonic perturbations. The J_2 harmonic is considered as the first-order perturbation and the rest of the harmonics as the second-order perturbations. The secular and periodic effects due to the oblateness potential are added up to order three and two, respectively (see Section 3.1). For the higher zonal harmonics, secular and short-periodic effects are included up to order two and the long-periodic effects up to order one (see Section 3.2). For tesseral harmonics, only the short-periodic effects have been included up to order two (see Section 3.6). The theory is completely closed-form in the eccentricity with the tesseral effects computed using numerical quadrature. There is an option to use the eccentricity expansions for computing the tesseral periodic effects with the terms included up to $\mathcal{O}(e^7)$.

A formation can be simulated by specifying the formation parameters that determines the mean elements of a deputy satellite (see Section 5.1). The relative orbit is propagated using the RM-STM (see Sections 4.2 and 4.3). In case of the *Relative State* option for the RM-STM in SwARM, the relative states in the curvilinear frame are generated using a first-order transformation between the mean and true longitudes of the chief satellite. Otherwise, only the differential osculating equinoctial elements are analytically propagated and the results are converted into the relative states using the exact nonlinear transformation. For a given chief orbit, the RM-STM needs to be generated only once and different formations can be propagated using the RM-STM without propagating the chief's orbit again. SwARM also provides a common interface to propagate the

orbits numerically using GMAT or MATLAB, and it can also plot the errors between the numerical and analytical results.

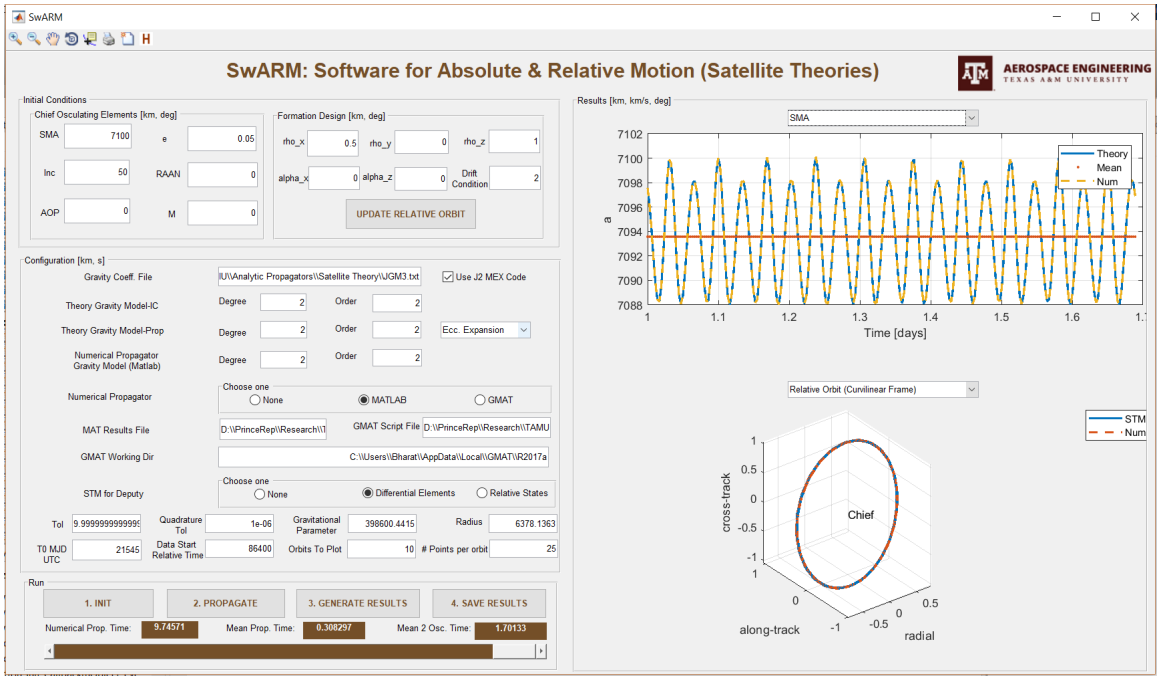

Figure D.1: Frontend for the MATLAB tool SwARM.